The processing and characterisation of recycled glass fibre composites

A thesis in fulfillment of the requirements for the degree of Doctor of Philosophy

By

Ulf Nagel

Department of Mechanical and Aerospace Engineering
University of Strathclyde
Glasgow
Scotland
UK
2016

Declaration of Authenticity and Author's Rights

This thesis is the result of the author's original research. It has been composed by the author and has not been previously submitted for examination which has led to the award of a degree.

Signed:

Date:

Acknowledgement

I would like to express my thanks to my supervisor Professor Dr James Thomason. He provided me invaluable guidance over the course of my studies. Without his advice and patience this thesis would not have been possible. At the same time, he gave me freedom to develop my own science skills and become an independent researcher.

I would also like to take this opportunity to thank the members of the Advanced Composites Group Dr Liu Yang, Dr Chih-Chuan Kao, Dr Durai Raghavalu Thirumalai, Peter Jenkins, Eduardo Sáez Rodriguez, Jose Luis Rudeiros Fernandez, Kerrie Downes, Ross Minty and Kyle Pender who have been a source of friendship, advice and collaboration.

As well as my colleagues in the Advanced Composites Group, I would also like to thank the technicians Dr Fiona Sillars, Chris Cameron, Drew Irvine, James Gillespie, James Kelly and Neil Mc Crindle. Their technical support was essential for my experimental work.

I acknowledge the financial support of the Engineering and Physical Sciences Research Council and I would also like to thank Saudi Basic Industries Cooperation, 3B Fibreglass and PPG Fibreglass Company for providing materials.

Last but not least, I owe also a lot to Laura, my parents, my sister and my brother. Their encouragement and support allowed me to complete this thesis.

Publications

Several results of this thesis have been published over the course of this PhD project in the following journal articles and conference contributions.

Journal articles

Yang L, Sáez Rodriguez E, Nagel U, Thomason JL. Can thermally degraded glass fibre be regenerated for closed-loop recycling of thermosetting composites? Compos Part A Appl Sci Manuf 2015;72:167–74.

Nagel U, Yang L, Kao C-C, Thomason JL. Effects of thermal recycling temperatures on the reinforcement potential of glass fibers. Polym Compos 2016.

Thomason JL, Nagel U, Sáez-Rodríguez E, Yang L. Regenerating the strength of thermally recycled glass fibres using hot sodium hydroxide. Compos Part A Appl Sci Manuf 2016;87:220–7.

Burn DT, Harper LT, Johnson M, Warrior NA, Nagel U, Yang L, Thomason JL. The usability of recycled carbon fibres in short fibre thermoplastics: interfacial properties. J Mater Sci 2016;51:7699–715.

Conference contributions

Nagel U, Kao C-C, Thomason JL. Study on properties of composites reinforced by heat treated glass fibres simulating thermal recycling conditions. 19th International Conference on Composite Materials, Montreal: 2013.

Thomason JL, Yang L, Kao C-C, Jenkins P, Sáez Rodriguez E, Nagel U. The ReCoVeR projects: Regeneration of thermally recycled glass fibre for cost-effective composite recycling. 2nd International Glass Fiber Symposium, Aachen: 2014.

Nagel U, Sáez Rodriguez E, Kao C-C, Thomason JL. Regeneration of thermally recycled glass fibre for cost-effective composite recycling: Performance of composites based on PP and ReCoVeRed glass fibre. 16th European Conference on Composite Materials, Seville: 2014.

Thomason JL, Yang L, Kao C-C, Jenkins P, Sáez Rodriguez E, Nagel U. Composite recycling: Overview of the ReCoVeR projects. 16th European Conference on Composite Materials, Seville: 2014.

Thomason JL, Yang L, Kao C-C, Jenkins P, Saez Rodriguez E, Nagel U. Regeneration of thermally recycled glass fibre for cost-effective composite recycling. CAMX - The Composites and Advanced Materials Exposition, Orlando: 2014.

Nagel U, Thomason JL. Regeneration of thermally recycled glass fibre for cost effective composite recycling: The effect of fibre regeneration and matrix modification. 20th International Conference on Composite Materials, Copenhagen: 2015.

Thomason JL, Sáez Rodriguez E, Kao C-C, Nagel U, Yang L. Regeneration of thermally recycled glass fibre for cost-effective closed-loop composite recycling in automotive. 20th International Conference on Composite Materials, Copenhagen: 2015.

Thomason JL, Yang L, Sáez Rodriguez E, Nagel U. Recover: Regenerating the strength and value of thermally recycled glass fibres. 17th European Conference on Composite Materials, Munich: 2016.

Abstract

The widespread use of glass fibre reinforced polymers (GFRP) over the last decades has led to an increasing amount of waste and a demand for recycling solutions. Mechanical, chemical and thermal GFRP recycling processes have been developed in academia but the commercialisation of GFRP recycling processes has proven to be difficult. The value of recycled glass fibres is low because their strength is usually reduced during recycling processes. Thermal recycling processes involve the exposure of GFRP waste to elevated temperatures to degrade the polymer matrix and extract the glass fibres. The room temperature strength of the glass fibres and organic sizings are degraded during thermal recycling processes which leads to a lower composite performance when the recycled fibres are processed into composites. The main objective of this thesis was to develop composites based on thermally recycled glass fibres that can compete with as received fibre composites. Polypropylene (PP) was chosen as matrix material because of its processability and its widespread use.

First, an understanding of the structure performance relationship of glass fibre PP (GF/PP) composites was established and gaps in existing literature were studied. The addition of maleic anhydride grafted PP (MAPP) to injection moulded GF/PP composites correlated with an increase of the ultimate mechanical properties (tensile strength, strain at break) but too high MAPP contents resulted in a reduction of the ultimate mechanical composite properties and the composite modulus. The optimum MAPP content was observed to depend on the glass fibre content. The composite tensile test data was used to analyse the microstructural composite properties. It was concluded that the analysis of the composite tensile data based on the Kelly-Tyson model can be used as a screening tool to detect general trends of the interfacial adhesion between glass fibres and PP matrix. However, micromechanical tests like the microbond tests are still required for more detailed studies of the interfacial adhesion because the composite tensile properties are often affected by a number of interacting factors.

Glass fibres were thermally degraded before composite processing to simulate a thermal recycling process. Thermal gravimetric analysis and microbond tests showed that all investigated commercial sizings degraded at thermal recycling temperatures. The ultimate mechanical composite properties were reduced when

the glass fibres were thermally degraded. The drop of the composite performance was attributed to a reduction of the glass fibre strength and a low interfacial adhesion between fibres and PP. Most of the interfacial adhesion between thermally degraded glass fibres and PP was recovered when the MAPP content was optimised. However, the composite performance was still low compared to as received glass fibre composites because of the low fibre strength. It was concluded that the post treatment of thermally recycled glass fibres should include the regeneration of the fibre strength and the reactivation of the fibre surface functionality in order to increase the reinforcement potential of the fibres.

Aminopropyltriethoxy silane (APS) and sodium hydroxide (NaOH) were applied to the thermally degraded glass fibres. Approximately 70 % of the tensile strength loss of injection moulded GF/PP composites was recovered when thermally degraded glass fibres were post treated with APS. Micromechanical analysis suggested that the APS regenerated glass fibres experienced similar stresses as the as received fibres. The increase of the glass fibre stress could not solely be explained by an increase of the interfacial adhesion between fibres and matrix. It was proposed that the APS treatment also led to an increase of the maximum glass fibre strength in the injection moulded composites. Thermally degraded glass fibres tend to form a fluffy mat during the NaOH treatment and could not be processed via extrusion compounding and injection moulding. A glass mat thermoplastic (GMT) process was set up over the course of this PhD to process NaOH treated glass fibres. The treatment of the thermally degraded glass fibres with NaOH led to an increase of the composite tensile strength. The increase of the composite tensile strength was correlated with an increase of the glass fibre strength. The APS treatment of the thermally degraded glass fibres also led to an increase of GMT composite tensile strength but the increase was lower compared to the injection moulded GF/PP composites. It was speculated that the effect of APS on the strength of thermally degraded glass fibres might be gauge length dependent. The optimum treatment of thermally recycled glass fibres might therefore depend on the final fibre length in the composite. An APS treatment might be suitable for injection moulded composites with glass fibres shorter than 1 mm while the NaOH treatments might be required for composites with longer fibres. To the author’s knowledge the work presented in this thesis shows for the first time that the reinforcement potential of thermally degraded glass fibres can be regenerated without hydrogen fluoride. Thus, this work might be a step towards the development of an economically viable GFRP recycling process.

Contents

Nomenclature

ε_c	Composite strain
η_l	Fibre length factor
η_{oKr}	Fibre orientation factor (Cox model)
η_{oKT}	Fibre orientation factor (Extended Kelly-Tyson model)
λ_c	Fibre reinforcement efficiency factor (tensile strength)
λ_E	Fibre reinforcement efficiency factor (tensile modulus)
υ	Poisson's ratio
ρ_f	Density fibre
ρ_m	Density matrix
σ_c	Composite tensile stress
σ_{cMax}	Composite tensile strength
σ_f	Fibre tensile strength
σ_m	Matrix tensile strength
τ	Interfacial shear stress
τ_{app}	Apparent interfacial shear strength
τ_{ult}	Interfacial shear strength
APS	AminoPropyltriethoxySilane
d_f	Fibre diameter
DTG	Derivative weight loss curve
E_c	Composite modulus
E_f	Fibre modulus
F_{max}	Maximum force

FE	Finite Element
FRP	Fibre Reinforced Polymers
GFRP	Glass Fibre Reinforced Polymer
GF/PP	Glass Fibre/Polypropylene
GMT	Glass Mat Thermoplastic
G_M	Shear modulus
HCl	Hydrochloric acid
HF	Hydrofluoric acid
IFSS	Interfacial Shear Strength
K	Proportionality factor of Mittal-Gupta analysis
l	Average fibre fibre length
l_c	Critical fibre length (strain dependent)
l_{cFR}	Critical fibre length for fibre failure
L_e	Embedded length
MA	Maleic Anhydride
MAPP	Maleic Anhydride grafted Polypropylene
MPS	MethacryloxyPropyltrimethoxySilane
NaOH	Sodium Hydroxide
PA	Polyamide
PP	Polypropylene
R_{BB}	Ratio of fibre contributions at two different strains based on measurement data

R'_{BB}	Ratio of fibre contributions at two different strains based on model data
$R_{Spacing}$	Mean distance between the centre of fibres
r_f	Fibre radius
SEM	Scanning Electron Microscope
TGA	Thermal Gravimetric Analysis
V_f	Fibre volume fraction
V_i	Volume subfraction of fibres with the length l_i
V_j	Volume subfraction of fibres with the length l_j
W_f	Fibre weight fraction
X	Contribution of subcritical fibres to composite stress
X_i	Fibre packing factor
x_1, x_2, x_3	Polynomial fitting curve parameters
Y	Contribution of supercritical fibres to composite stress
Z	Matrix contribution to composite stress

List of figures

List of tables

1. Introduction

1.1 Background

Fibre reinforcement polymers (FRP) became commercialised on a large scale after the second world war. They are often chosen in engineering applications because of their high specific strength and stiffness [1]. Currently the compound annual growth rate of the FRP market is estimated to be between 7.2 % [2] and 7.5 % [3]. Most of the FRPs are based on glass fibres and carbon fibres. The market for carbon fibres is growing faster than the market for glass fibres. The demand for reinforcement grade glass fibres is growing currently at around 5 % per year [4] while the demand for carbon fibres is growing by more than 10 % per year [5]. However, the demand for glass fibres still far exceeds the demand for carbon fibres. The global demand for carbon fibres was estimated to be 54 Kton in 2014 [5] while the demand for reinforcement grade glass fibres was almost 5000 Kton [4]. Thus, the market for glass fibre reinforcement will be bigger than the market for carbon fibres in the foreseeable future despite the higher growth rate in the demand for carbon fibres.

Figure 1.1 illustrates that glass fibre reinforced polymers (GFRPs) are mainly used in transport, construction, transportation, electricity & electronics and sports applications [5,6].

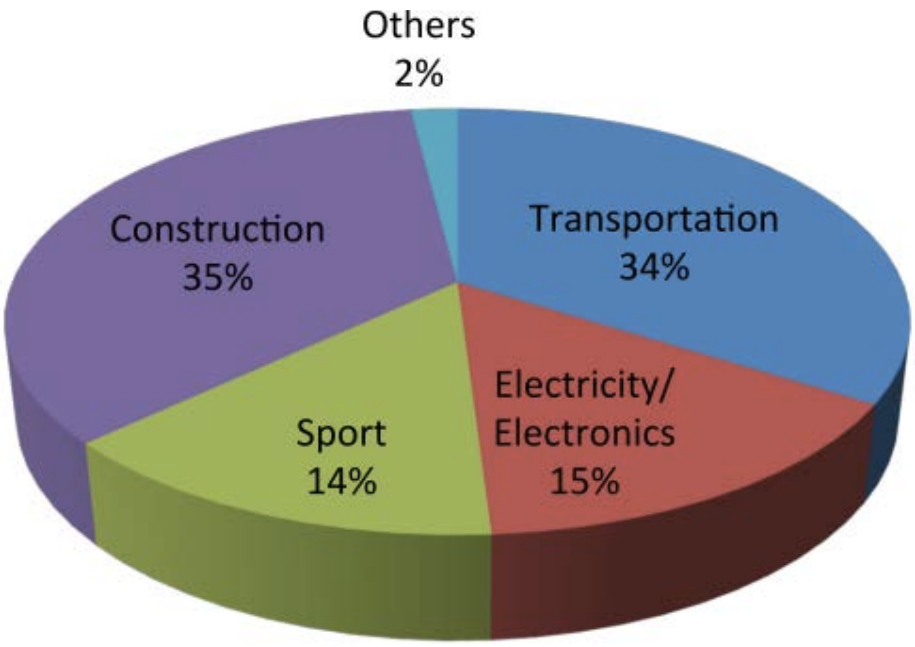

Figure 1.1. Breakdown of GFRP consumption in Europe by application. Reproduced from [6]

The largest fraction of FRPs are based on thermosets which cannot be easily reprocessed and are not intrinsically recyclable like thermoplastics [7–9]. The recycling of GFRPs has not been commercialised to the same extend as the recycling of carbon fibre reinforced composites [10,11]. Different processes have been developed to recycle thermoset based GFRP composites. These can be distinguished between mechanical, chemical and thermal recycling processes. Chapter 3 of this thesis provides an overview of different recycling processes and detailed reviews can be found in literature [7,12,13]. This thesis is focussed on thermally recycled glass fibres. Thermal recycling processes are interesting because they can provide clean and relatively long fibres compared to other recycling processes and they do not involve the use of hazardous chemicals. However, thermally recycled glass fibres have a low reinforcement potential because of their limited tensile strength after exposure to high temperatures. The economic value of thermally recycled glass fibres is therefore low [7,10,12,13].

The challenge to develop commercially viable recycling solutions for end-of-life GFRPs has become important in the recent years because of legislative and economic reasons. Most of the GFRP waste is currently disposed in landfill or used as filler in cement kilns and other downcycling solutions. However, landfilling of GFRP waste has been completely banned in Germany and is becoming more expensive in other countries because of taxes [7,10–12]. Downcycling solutions that involve the use of grinded GFRP waste as filler material in cement kilns or other non-structural applications do not utilise the reinforcement potential of glass fibres. Several companies like ERCOM (Germany), Phoenix (Canada) and Zajon (Germany) specialised in the downcycling of GFRP waste terminated their business because of financial reasons [10,14]. Job [10] concluded that GFRP recycling solutions need to maximise the value of the recyclates to become economically viable.

Figure 1.2 shows that currently up to 50 % of the global demand for reinforcement grade glass fibres could be supplied by recycled glass fibres. The development of composites based on recycled glass fibres that can commercially compete with composites based on new glass fibres would therefore be a major breakthrough. It would help to solve the landfilling problems and potentially reduce the carbon dioxide emissions from the glass fibre industry by 2 Mtonness/annum [15]. The potential saving in carbon dioxide emissions is equivalent to the annual carbon

dioxide emission of more than 400000 cars per year (assuming 4.7 tonnes carbon dioxide per car) [16].

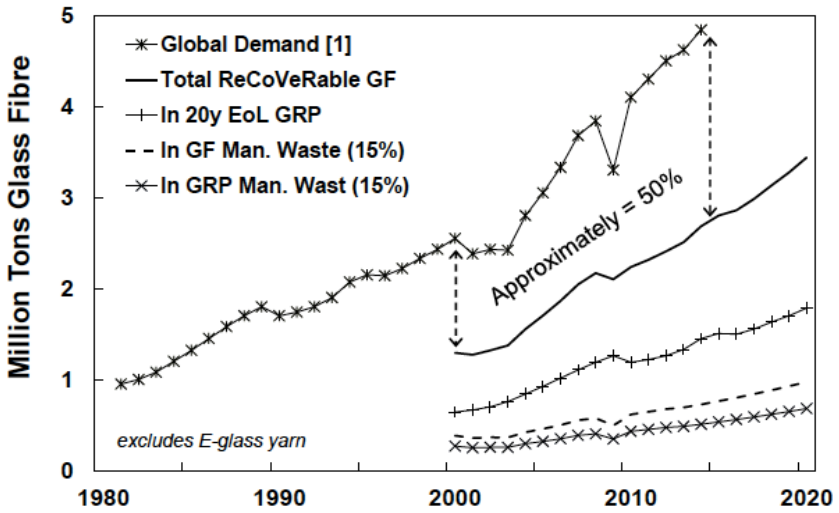

Figure 1.2. Glass fibre global demand and availability for recycling. Reproduced from [15]

1.2 Objective

It was outlined above that the low reinforcement potential of thermally recycled glass fibres is a major obstacle in the commercialisation of GFRP recycling solutions. The goal of this project was to overcome this obstacle and to develop composites based on thermally recycled glass fibres that can compete with composites based on new glass fibres. The composite based on recycled fibres should be a drop in product which means it should be processable without changing existing processing routes. To achieve the principle goal, the following objectives were defined.

(1) Polypropylene (PP) was chosen as matrix material for the composites that were studied in this thesis because of its widespread use and processability. Thus, one objective was to study the structure performance relationship of glass fibre PP (GF/PP) composites.

(2) Another objective was to develop an understanding how the performance of GF/PP composites is effected by the thermal degradation of glass fibres due to thermal recycling

(3) The third objective was to investigate how the post treatment of thermally recycled glass fibres affects the performance of GF/PP composites.

1.3 Outline

This chapter introduces the reader to the background, the objectives and the structure of this thesis. The second chapter reviews existing studies on the structure-performance relationship of GF/PP composites. The second chapter also includes a discussion of previous work on composites based on thermally recycled glass fibres and methods to regenerate thermally recycled fibres. Chapter 3 describes the materials and methods that were used to generate and analyse the data of this thesis. In Chapter 4, experimental results on the structure performance relationship of GF/PP composites are presented and discussed. In Chapter 5 the detrimental effects of thermal recycling on the reinforcement potential of glass fibres in PP composites are investigated. In addition, it is investigated whether composite performance can be recovered only by the modification of the PP matrix with a coupling agent. In Chapter 6, the composite performance is recovered by the post treatment of the glass fibres with different chemicals and the effect of the fibre post treatments on the composite performance is compared with the effect of the matrix modification. The conclusions of this thesis and suggestions for future work can be found in the final chapter. In the appendix, an initial technology assessment was performed to review the costs and energy balance of thermal glass fibre recycling and subsequent regeneration.

1.4 References

[1] Matthews FL, Rawlings RD. Composite materials: Engineering and science. Cambridge (United Kingdom): Woodhead Publishing Limited; 1994.

[2] Advanced Composites Market by Type, by Manufacturing Process, by Resin Type, by Application and by Region - Global Forecast to 2020. 2015. http://www.marketsandmarkets.com/Market-Reports/advanced-composites-market-3930953.html (accessed April 3, 2016).

[3] Hinton M. Advanced Composites – The Engine for Growth 2013. http://www.sampe.org.uk/assets/pdfs/MasterClass2013/MJH SAMPE Masterclass Introduction 021013v1.pdf (accessed April 3, 2016).

[4] Owens Corning Investor Presentation 2015. http://s1.q4cdn.com/942908807/files/doc_presentations/2015/Q3/Q3-Presentation-v9.pdf (accessed April 3, 2016).

[5] Witten E, Kraus T, Kühnel M. Composites Market Report 2015. 2015.

[6] Sirris. Composites : materials of the future Part 2 : Market and market developments 2013. http://www.pluscomposites.eu/sites/default/files/Technical series - Part 2 - Market and market developments_0.pdf (accessed April 3, 2016).

[7] Yang Y, Boom R, Irion B, van Heerden D-J, Kuiper P, de Wit H. Recycling of composite materials. Chem Eng Process Process Intensif 2012;51:53–68.

[8] Lucintel. Opportunities for thermoset resins in the composite industry 2008. http://www.trfa.org/erc/docretrieval/uploadedfiles/Technical Papers/2008 Meeting/Mazumdar-Lucintel_ppt-Composites_industry.pdf (accessed October 20, 2013).

[9] Sirris. Composites : materials of the future Part 1 : Introduction 2013. http://www.pluscomposites.eu/sites/default/files/Technical series - Part 1 - Introduction - English_0.pdf (accessed April 3, 2016).

[10] Job S. Recycling glass fibre reinforced composites – history and progress. ReinforcedPlastics 2013;57:19–23.

[11] Job S. Recycling composites commercially. Reinf Plast 2014;58:32–8.

[12] Oliveux G, Dandy LO, Leeke GA. Current Status of Recycling of Fibre Reinforced Polymers: review of technologies, reuse and resulting properties. Prog Mater Sci 2015;72:61–99.

[13] Pickering SJ. Recycling technologies for thermoset composite materials—current status. Compos Part A Appl Sci Manuf 2006;37:1206–15.

[14] Zajons kämpft ums Überleben. Landeszeitung Für Die Lüneburg Heide GmbH 2014.

[15] Thomason JL, Nagel U, Sáez-Rodríguez E, Yang L. Regenerating the strength of thermally recycled glass fibres using hot sodium hydroxide. Compos Part A Appl Sci Manuf 2016;87:220–7.

[16] U.S. Environmental Protection Agency. Greenhouse Gas Emissions from a Typical Passenger Vehicle 2014:1–5. https://www.epa.gov/sites/production/files/2016-02/documents/420f14040a.pdf (accessed July 11, 2016).

2. Literature Review

In the first four sections of this chapter the structure-performance relationship of glass fibre polypropylene (GF/PP) composites is reviewed. The effects of the microstructure on the uniaxial tensile properties of GF/PP composites are discussed. The residual length of glass fibres in PP composites and the interfacial adhesion between glass fibres and PP are reviewed in detail. Section 2.5 provides an overview of different composite recycling technologies and the detrimental effect of thermal recycling processes on the reinforcement potential of glass fibres. In Section 2.6 the current state of processes to regenerate the reinforcement potential of thermally recycled glass fibres is discussed.

2.1 Residual fibre length in glass fibre Polypropylene composites

The mechanical properties of GF/PP composites and other thermoplastic composites are strongly influenced by the length of the reinforcement fibres. The knowledge of the fibre length in the composite is therefore essential. Numerous studies observed fibre length degradation in GF/PP composites during extrusion or injection moulding [1–9]. The fibre length distributions in extruded or injection moulded composites are usually unimodal and skewed. Figure 2.1 shows the fibre length distribution of GF/PP composites that were compounded with a kneader. At the beginning of the compounding process the fibre length distributions are positively skewed. After a longer compounding time the fibre length distributions are negatively skewed.

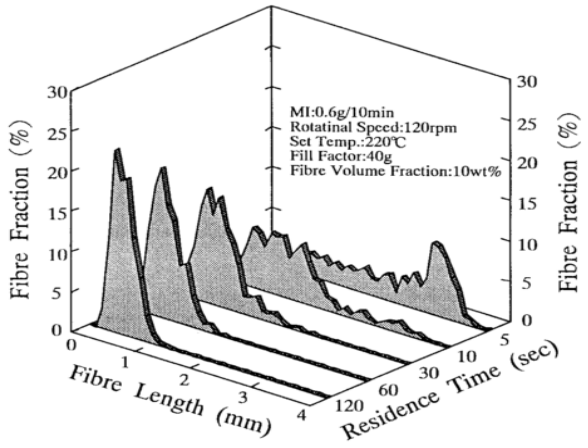

Figure 2.1. Skewness of fibre length distributions in GF/PP composites. Reproduced from [9]

The following sections 2.1.1 - 2.1.3 review different fibre length measurement techniques and discuss mechanisms that govern the length distribution of glass fibres in extruded and injection moulded PP composites. Glass mat thermoplastic (GMT) composites are not included in this review because the GMT processes are regarded as less aggressive to the fibres and to the author's knowledge no literature has reported fibre length degradation in GMT composites.

2.1.1 An overview of fibre length measurement techniques

Different methods have been developed to measure the residual fibre length in discontinuous fibre reinforced thermoplastic composites. In most studies, the fibres were separated from the matrix using an ashing process in air [2,3,5,7,8,10–13], in inert atmosphere [4,14] or a chemical dissolution process [1,15]. The fibres were usually dispersed on a substrate. Magnified images of the dispersed fibres were acquired from a projector or microscope and digitized. More recently scanners were also used to acquire images of fibres. The digitized images were analysed using image analysis software [1,2,4,5,7,8,10–12]. These approaches are usually called manual or semi-automated fibre length measurement techniques and are similar to the method which is specified by the 'ISO 22314' standard [16]. Some of the reviewed papers stated that the fibre length measurement was performed using an automated image analysis software [13–15,17]. In other studies [6,11,12], sieves were used to filter fibres according to their length before they were measured. The sieved fibres of similar length could be measured using the same technique or magnification. Other studies used a particle analyser to measure the fibre length. The fibres were separated from the matrix, dispersed in a suspension and pumped through a particle analyser [3,12].

In addition to the direct methods mentioned above, indirect methods were also used to measure the fibre length in discontinuous fibre composites. In contrast to the direct methods, indirect methods provide only one average value but no fibre length distribution. Sieves were used to determine a weighted mean length of glass fibres. Fibres were suspended in water and the suspension is strained through stacked sieves as illustrated in Figure 2.2 below. Small fibres settle down in fine sieves and large fibres settle down in large sieves. Thus the weight of the fibres on the sieves can be correlated to the length of the fibres [18]. A patent provides a detailed description of this method [19].

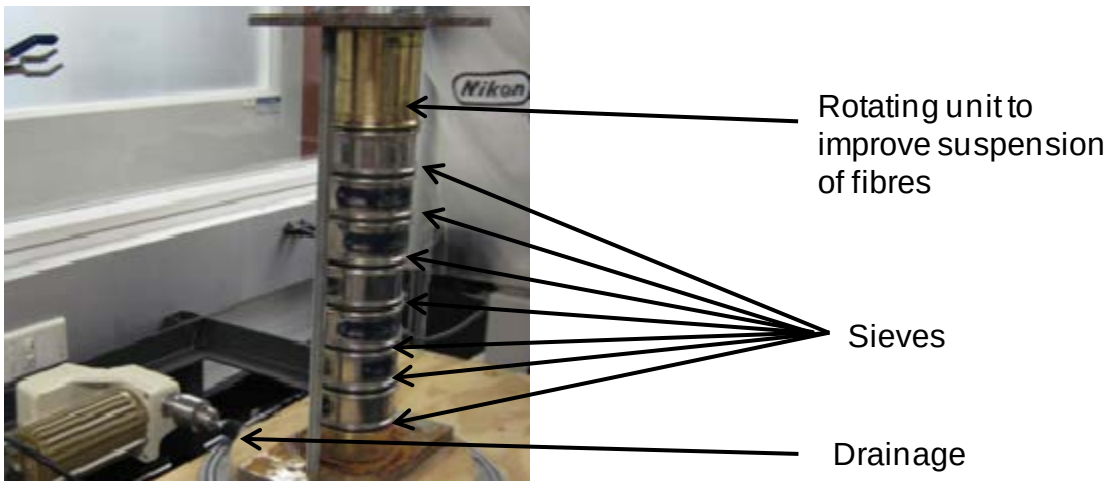

Figure 2.2. Measurement of average fibre length using sieves. Reproduced from [18]

Zhu et al. [20] developed a method to derive the average length of fibres in discontinuous fibre composites from a polished cross-section. The diameter, number and geometry of partly and completely intercepted fibres of one cross-section were used as input parameter. Zak et al. [21] proposed a two-section method to calculate the average fibre length from two parallel cross-sections. The average length was derived from the number of fibres that were intersected by one cross-section, the number of fibres that were intercepted by two cross-sections, the fibre orientation obtained from the geometry of the intercepted fibres and the fibre diameter.

The methods presented above illustrate that the procedures to measure the fibre length in short fibre reinforced thermoplastics vary widely. The question arises which method offers the best ratio between accuracy (as defined in ISO 5725) and time required to perform the measurement.

2.1.2 Accuracy of different fibre length measurement techniques

Most of the presented studies above do not provide information regarding the accuracy of the fibre length measurement technique. It seems reasonable to assume that the trueness of the average fibre length value increases with the number of analysed fibres. Table 2.1 (direct measurement techniques) and Table 2.2 (indirect measurement techniques) compare the number of fibres that were analysed in different studies. Not all studies presented in this chapter state the number of analysed fibres measured per sample and other studies do not provide information if the length measurement was automated or manual. For the sake of simplicity, it will not be distinguished between the arithmetic average and the weighted average in this section.

Table 2.1. Comparison between direct fibre length measurement techniques

Method		Number of fibres analysed/sample	Reference
Direct length measurement, fibres separated from matrix and dispersed on substrate	Manual or semi-automated length measurement using magnified images, digitizer and computer software	40-50	[5]
		400	[1]
		400-600	[2]
		Not stated	[4]
		900	[6]
		Not stated	[7]
		500	[9]
		400-700	[10]
		800	[11]
		1000	[12]
		600-1000	[22]
		400	[23]
		3000-10000	[24]
		Not stated	[25]
	Not clear if automated analysis was used	> 2300	[8]
		1000	[26]
	Automated length measurement using image analysis software	2000	[13]
		> 18000	[14]
		Up to 10000	[15]
		3000	[17]
Direct length measurement, fibres separated from matrix and suspended in water	Suspension with fibres pumped through particle analyser	> 10000	[3]
		5000	[12]
		Not stated	[27]

Table 2.2 Comparison between indirect fibre length measurement techniques

Method		Number of fibres analysed/sample	Reference
Indirect length measurement, fibres separated from matrix and suspended in water	Suspension with fibres drained through a stack of sieves, on each sieve fibres of similar length will settle down, average length calculated from weight fractions	0.9 g and 1.2 g of fibre material equivalent to $4.5x10^6$ and $6.0x10^6$ fibres	[19]
Indirect length measurement, two-section method	Two closely-spaced, parallel cross-sections are cut and then analysed	> 800	[21]

Table 2.1 and Table 2.2 illustrate that the number of analysed fibres varied widely between the reviewed studies. All presented measurement techniques are based on a sufficient number of fibres according to the ISO 22314 standard [16]. However, the standard only specifies the measurement of fibres with an average length shorter than 1 mm. In addition, the standard specifies manual measurement using image analysis software. A low number of analysed fibres might have been chosen to reduce the time required for the measurements. A different study recommends to analyse at least 800 fibres [21]. The required number of analysed fibres might also depend on the shape of the fibre length distribution. Narrow length distributions might require a lower number of measurements to determine an accurate average value for the fibre length. The reviewed studies suggest that automated image analysis, particle analyser and indirect measurements using sieves are more capable of measuring a large number of fibres than manual or semi-automated image analysis as well as the two section method. The analysis of a large number of fibres might be a necessary condition to obtain an accurate average value of the fibre length but it might not be a sufficient condition. Measurement errors might also occur when the length of the individual fibres is determined.

The trueness of fibre length measurement results based on image analysis can be limited by the size or magnification of the image. Short fibres might need a high magnification while long fibres require a low magnification. Thus, the trueness can be compromised if the fibre length varies over a large range. As already mentioned, sieves can be used to classify fibres according to their length before the actual length measurement [6,11,12]. This enables to adjust the magnification of images to the fibre length and to measure the length of fibres accurately even if their length varies over a large range. Fu et al. [22] showed that fibres crossing the edge of images need to be considered. The measured average fibre length was lower when these fibres were not considered. They also developed a method to compensate this error. A different solution was developed by Davidson and Clarke [14]. They developed an algorithm which allowed scanning a large area with a high magnification. Several images of adjacent overlapping areas with high magnification were taken and used to construct one large image with a high magnification. Fibre length measurement techniques based on image analysis also cannot consider very short fibres because of the limited resolution of the images and the presence of dust. Thus, automated image analysis software uses a threshold for the minimum fibre length [13,14]. Automated image analysis software might not be able to

consider crossing fibres or curved fibres [15] which might lead to an underestimation of the fibre length. Long fibres are more likely to be curved and to cross other fibres [14]. Even if the image analysis software considers crossing fibres and curved fibres (Figure 2.3), the algorithms for the analysis of these fibres are based on approximations [14,17,28].

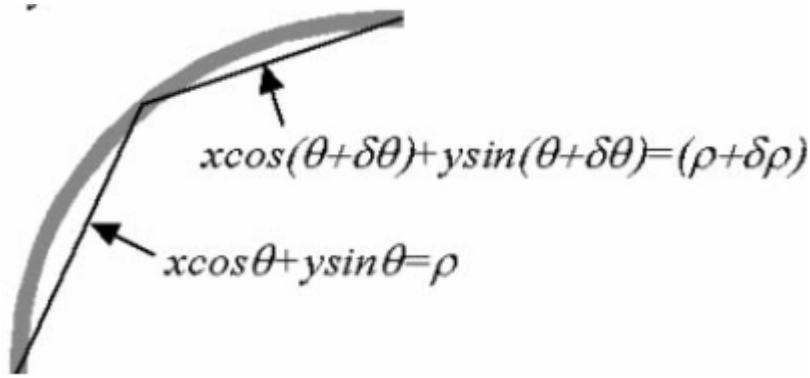

Figure 2.3. Approximation to calculate the length of curved fibres. Reproduced from [14]

Similar to image analysis software, particle analysers usually have a minimum fibre length that can be measured. Particle analyser, based on the light blockage principle, can only perform fibre length measurements with limited trueness because they assume a constant fibre diameter [3]. The trueness of the two-section method [21] might be limited because fibres shorter than the distance between the cross-sections will not be considered if they fall between these cross-sections. Similar other direct length measurement, the trueness of the two-section method is limited by the magnification of the analysed image. A compromise between large sample area and high resolution might be required. The two-section method also assumes that the fibre length distribution of the polished cross-sections is representative of the whole specimen.

Indirect methods like measurement systems using sieves [18,19] do not measure individual fibres but might also not provide a true value of the average fibre length. The trueness of the weight procedure of the fibres on the sieves will limit the trueness of the fibre length measurement. In addition, fibres might pass through all sieves if they are shorter than the mesh size.

The discussion above was focussed on the trueness of fibre length measurements. However, the accuracy might also be affected by the precision of the fibre length measurements. Apart from few exceptions [14,21], results of repeat measurements to assess the precision were not presented in literature [1,2,4,6,7,9–

11,13,22,23,25,26,29]. The absence of repeat measurements might be explained by the fact that most fibre length measurement techniques are time consuming. Automated fibre length measurement techniques based on image analysis allow measurement of fibre length distributions in a relatively short period of time compared to manual techniques. For example, the FASEP fibre length systems allows measurement of more than 3000 fibres in less than 10 min [17]. Algorithms are available to correct potential sources of errors like crossing fibres and curved fibres. These algorithms can be automated since computing capacities have increased rapidly. In contrast to particle analysers, fibre length measurement techniques based on image analysis do not assume that all fibres have the same diameter. A wide range of fibre lengths can be considered. Thus, fibre length measurement techniques based on (automated) image analysis might be the most accurate fibre length measurement techniques and offer a beneficial ratio between accuracy and time.

2.1.3 Factors influencing the residual fibre length

The length degradation of glass fibres during hot melt processing is influenced by processing parameters [3,5,9–13,23,26,30] and parameters related to the constituents of the composites [3–7,24,31]. The investigated parameters are discussed in this section and related to the mechanisms identified by Turkovich [1]. Turkovich distinguished between three different mechanisms that cause fibre length degradations during hot melt processing. These mechanisms are fibre/fibre interactions, fibre/polymer interactions and fibre/processor surface interactions. Different studies investigated parameters that influence the residual length of glass fibres. A number of studies on the length degradation of glass fibres during hot melt processing is based on Polyamide (PA) based composites [10–13,15,23,30]. Thus, studies based on PA composites will also be considered in this section to discuss the length degradation of glass fibres during hot melt processing like extrusion and injection moulding.

Processing parameters and residual fibre length

Several authors investigated the influence of the processing temperature on the fibre length degradation of GF/PP composites [1,3,5,9] and GF/PA composites [11]. It was observed that higher processing temperatures reduce the fibre length degradation. Models explained the length degradation of glass fibres in molten polymer during processing by considering the shear forces within the polymer melt

which can cause buckling and breakage of the glass fibres [8,32]. Higher processing temperature causes a reduction of the polymer melt viscosity and the shear stresses in polymer melts during hot melt processes are proportional to its viscosity [11].

The screw speed is another processing parameter that influences the shear stresses in polymer melts during hot melt processes. An increase of the screw speed was observed to result in a reduction of the residual fibre length in GF/PP composites [3,9] and GF/PA composites [11,13,23,30]. The effect of the screw speed was also investigated in combination with the residence time of the glass fibres in the polymer melt [3,9,23]. Similar to the screw speed, an increase of the residence time caused a reduction of the residual fibre length. Fisa [3] and Shimizu [9] observed that GF/PP systems of identical composition suffer the same level of fibre length degradation as long as the “work of mixing” (product of screw speed and residence time) is constant. A similar study by Inceoglu [23] introduced the term specific mechanical energy to consider the polymer melt viscosity in addition to the screw speed and residence time.

To the author’s knowledge, the role of fibre/processor surface interaction has not been explicitly investigated but wear of processing equipment due to the processing of fibre reinforced thermoplastic was reported [10]. It seems likely that modifications to the processing equipment influence the fibre/processor surface interactions. Turkovich [1] reported that the fibre length in extruded GF/PP was not influenced by the presence or absence of an extrusion die because most fibres were broken before. Lunt et al. [11] observed that the fibre length degradation in extruded PA composites can be reduced by increasing the extrusion die diameter. Lafranche et al [26] demonstrated that the fibre breakage during injection moulding processing of GF/PA composites can be significantly reduced by an optimised design of the screw and the non-return valve. While modifications to the processing equipment can influence the fibre length degradation these modifications might also influence the fibre/fibre interactions and fibre/polymer interactions. The challenge to investigate fibre/processor surface interaction without influencing other mechanisms of fibre length degradation might be one reason for the lack of studies on this mechanism.

Material parameters and residual fibre length

A number of studies reported a reduction of the residual fibre length in GF/PP composites [3–7,25,33] and GF/PA composites [24,31] as a function of the fibre content of the composites. The reduction of the residual fibre length was attributed to fibre/fibre interactions and an increase of the melt viscosity because of the glass fibres. In contrast, Lunt and Shortall [11] and Lafranche et al. [26] reported a more complex relationship between the fibre content and the residual length of glass fibres in PA composites. Lunt and Shortall [11] observed an initial decrease of the residual fibre length but an increase at higher fibre contents. The increase of the residual fibre length at higher fibre contents was attributed to a poor dispersion of the glass fibres in the polymer melt. Lafranche et al. [26] reported an increase of the residual fibre length at the nozzle of the injection moulder when the fibre content was increased. They postulated that the presence of glass fibres enhances the melting of the polymer due to their themal conductivity and reduces shear forces.

Several studies documented the influence of the initial fibre length on the residual fibre length in discontinuous glass fibre composites during hot melt processing. It was observed that the residual fibre length in GF/PP composites [2,6,7] and GF/PA composites [24,26,31] increased with the initial fibre length. Thomason [7] observed that glass fibres that were pre-compounded via a wire coating process are less susceptible to length degradation than pultrusion pre-compounded fibres. He postulated that the fibres pre-compounded via wire coating were better protected against length degradation because they were fed as bundles into the hot melt process.

It has also been suggested that the length degradation of glass fibres in PP composites is influenced by the presence of functional groups like maleic anhydride, which are added to GF/PP composites to enhance the interfacial shear strength between glass fibres and PP. It was postulated that the enhanced interaction between glass fibres and PP might cause more severe fibre length degradation. Figure 2.4 shows the residual length of glass fibres in injection moulded GF/PP composites without added MAPP and with 2 % added MAPP (by matrix weight) as reported by Thomason [25]. The data suggests a reduction of the residual fibre length due to the addition of MAPP to the composites. Roux et al. [34] also observed a reduction of the residual fibre length from 0.59 $\pm$ 0.42 µm to 0.51 $\pm$ 0.37 µm in injection moulded GF/PP composites when MAPP was added to the composites.

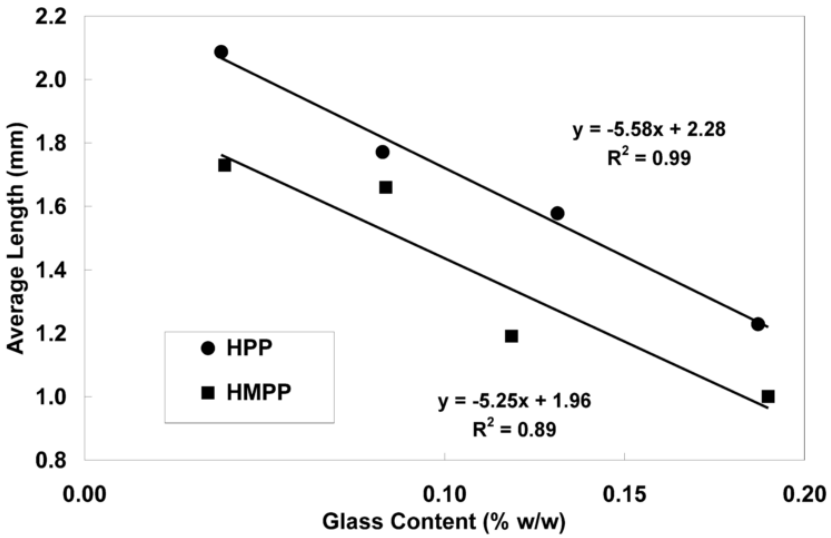

Figure 2.4. Reduction of residual length of glass fibres in injection moulded PP composites with the addition of MAPP. Reproduced from [25]

2.1.4 Summary and Conclusion

It can be concluded that fibre length measurements based on automated image analysis offer the best ratio between accuracy and time required to perform the measurement. Similar to other techniques, fibre length analysis based on automated image analysis has several shortcomings but rapidly increasing computing capacities allow implementation of algorithms that reduce errors. Research agrees that the length of glass fibres in PP is reduced during extrusion and injection moulding. The final fibre length of injection moulded PP composites depends on fibre content, polymer melt viscosity, screw speed, initial fibre length and the design of the processing equipment. Thus, the residual fibre length varied between 4 mm and 0.42 mm amongst the reviewed studies. A final fibre length of 4 mm was reported by Spahr et al. [6] when they processed glass fibres with an initial length of 10 mm. Depending on the factors discussed above other authors reported a clearly lower residual fibre length. Ota et al. [5] observed a fibre length reduction from 0.78 mm to 0.42 mm.

2.2 Interfacial adhesion between glass fibres and Polypropylene

The interfacial adhesion between glass fibres and the PP matrix is one of the parameters that govern the macromechanical properties of GF/PP composites. The mechanisms of interfacial adhesion in fibre reinforced polymer composites have been subject to research and several reviews have been published [35,36]. This section focuses on the review of studies related to the interfacial adhesion between

glass fibres and PP. The factors that influence the interfacial adhesion and methods to assess the interfacial adhesion between glass fibres and PP are reviewed in this section.

2.2.1 Mechanical characterization of the interfacial adhesion

A number of techniques have been developed to mechanically characterise the interfacial shear strength (IFSS) between fibres and polymer matrices. According to the scale these can be distinguished between macromechanical methods and micromechanical methods. The macromechanical methods like the short beam shear test, Iosipescu test, off axis tensile test, in-plane lap-shear test or rail shear test require bulk composites and usually aim to induce shear stresses in the composites. The ability of the composites to withstand shear stresses is regarded as an indirect measure for the IFSS. Usually these tests require long fibre composites with a well defined fibre orientation. In addition, the test results might be affected by other factors that influence the composite properties like voids, manufacturing defects etc. Micromechanical methods usually involve the testing of single fibre composites. Although they allow direct measurement of the IFSS and do not require as much material as the macromechanical methods, they tend to be time consuming. Examples for micromechanical test to determine the IFSS are single fibre compression tests, fibre fragmentation tests, fibre push-out test, fibre pull-out test and microbond test [35,36]. This section will only review the microbond test because of its relevance for this thesis. Comprehensive reviews of other methods to mechanically characterize the interfacial adhesion can be found elsewhere [35,36]. Figure 2.5 below illustrates the set-up of a microbond test. A fibre is partly embedded in a polymer matrix. The polymer matrix usually forms a microdroplet. Shear blades of a microvice are positioned close to the fibre above the polymer droplet. Then a force is applied to the fibre. The fibre moves upwards which causes shear forces in the sample because the droplet is pushed against the shear blades. The test continues at least until the droplet is debonded from the fibre [35,37,38]. The force is constantly recorded. From the recorded force the apparent IFSS can be calculated as the quotient of the maximum force and the embedded fibre interfacial area. The results of microbond tests are influenced by the experimental procedure and the data reduction. According to Zhandarov and Mäder [39] microbond tests can be regarded as a variation of the single fibre pull-out test. Thus, it will not be distinguished between them in this section.

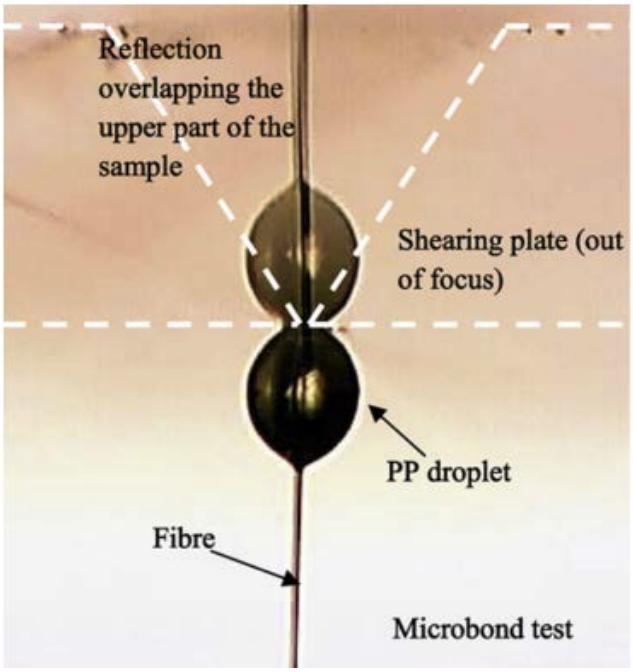

Figure 2.5. Set-up of microbond test. Reproduced from [40]

Influence of experimental procedure

The preparation of thermoplastic microbond samples requires melting of the polymer to form a microdroplet sample or pull-out sample. Thomason and Yang et al. [41] observed that the apparent IFSS of GF/PP samples dropped from 7.9 MPa to 2.1 MPa when the PP was degraded by oxidation. This observation can be explained with a reduction of crystallinity of the PP and residual stresses. The severity of the degradation was found to depend on the droplet volume, sample preparation time and processing temperature [42]. Auvray et al. [43] and Zhandarov and Mäder [39] observed that the apparent IFSS of pull-out samples based on bismaleimide resin and epoxy resin decreases with the embedded length. Auvray et al. observed the apparent IFSS to drop from more than 100 MPa to less than 20 MPa when the embedded length of carbon fibres in BMI resin was increased from less than 0.02 mm to 0.2 mm. In contrast Yang and Thomason [41] reported the apparent IFSS of GF/PP microbond samples to be independent from the embedded length. The dependence of the apparent IFSS on the embedded length is an inherent property of microbond tests or pull-out tests and can be related to the stress distribution at the interface [44]. A further discussion can be found in the next section about the data reduction of microbond test results. To the author's knowledge, the influence of the free fibre length between the clamps and the droplet has not been studied specifically for GF/PP systems. Schüller et al. [45] concluded from finite element

analysis that the free fibre length affects the shape of the stress strain curve because the system becomes more elastic with increasing free fibre length. However, their analysis also shows that the maximum load is not affected. In addition to factors related to the specimen itself, the results of the microbond tests can also be influenced by ambient conditions. Thomason and Yang [41] showed that the IFSS of GF/PP microbond samples is sensitive to the ambient temperature. The IFSS decreased from almost 14 MPa at -40 °C to less than 3 MPa at 100 °C. In contrast to PA [46], GF/PP microbond samples were not reported to be sensitive to moisture which can be explained with their low water absorption rate [36]. The test speed is another parameter that influences the results of microbond tests. Morlin and Czigany [47] varied the test speed when they performed microbond tests on glass fibre polyester samples. The IFSS was observed to depend on the test speed. The measured values for the IFSS dropped between 0.05 mm/min (21 MPa) and 0.2 mm/min (14 MPa) but increased linearly in the range between 0.2 mm/min and 10 mm/min (29 MPa). No change of the IFSS was observed at test speeds higher than 10 mm/min. Another parameter related to the set-up of the microbond test is the distance between the shear blades. Several studies [48–50] agreed that the measured value of the IFSS increases with the separation distance of the shear blades. For example, Chou et al. [50] observed an increase of the measured IFSS of Kevlar/Epon specimens from 33.1 MPa to 37.8 MPa when the gap between the fibre and the shear blades was increased from 0 μm to 22.3 μm.

Influence of data reduction

Different methods have been developed to reduce the data from microbond tests or fibre pull-out tests. The models that can be used to analyse microbond test results can be classified into models based on stress-controlled debonding, energy controlled debonding and adhesional pressure [39]. In this thesis only the stress-controlled models will be discussed since previous work on GF/PP systems is based on this approach. According to the stress based approach, debonding occurs when the interfacial shear stress exceeds the ultimate IFSS. As already mentioned, the apparent interfacial adhesion can be calculated as the quotient of the maximum force F_{max} and the embedded area [51]

Equation 2.1. Apparent interfacial adhesion

$$\tau_{app} = \frac{F_{max}}{\pi * d_f * L_e}$$

where D_f is the fibre diameter and L_e is the embedded length. The apparent IFSS in Equation 2.1 can be regarded as the ultimate IFSS assuming that the interfacial shear stress between fibre and matrix is homogenous along the interface and that fibre and matrix debond simultaneously along the whole interface [51]. Both assumptions have been shown to be inaccurate. Observation of microbond samples [52] and pull-out samples [53] using a microscope revealed that a crack grows at the interface before the maximum load is reached. After the initial debond the load might continue to rise because of frictional forces. Thus, the embedded length in Equation 2.1 is not constant and the failure does not occur simultaneously over the whole length of the interface. The fact that debond occurs before maximum load is reached also means that the interfacial shear stress at the initiation of the debond might be more representative of the interfacial adhesion between fibre and matrix [44,53]. As already mentioned above, the apparent IFSS was observed to depend on the embedded fibre length. Finite element analysis [54], shear lag theory [55] and other analytical approaches [39,44] showed that the shear stresses during microbond tests or pull-out tests are not homogenous along the interface. These models have in common that they predict maximum stresses to be at the point where the fibre enters the matrix. The dependence of the embedded length on the apparent IFSS might therefore be explained with the nonhomogeneous stress distribution along the interface and the apparent IFSS might underestimate the ultimate IFSS [39,44]. However, Meretz et al. [56] and Gonon et al. [57] observed that apparent IFSS was independent from the embedded length when the matrix was ductile. A ductile matrix might compensate local stress concentrations. For GF/PP systems several researchers [27,38,41,58,59] used the apparent IFSS to characterise the interfacial adhesion. Thus, the apparent IFSS might be sufficiently accurate to characterise these systems.

2.2.2 Factors that govern the IFSS between glass fibres and PP

Transcrystallinity

In several studies transcrystallinity was observed in GF/PP systems. Several authors did not observe transcrystallinity in GF/PP homopolymer systems when the samples were cooled down at a rate of 10 °C / min [60–62]. It was found that transcrystalline layers can be formed in GF/PP samples when the cooling rate is high enough [63,64]. Figure 2.6 shows an example for transcrystallinity in a GF/PP system that was cooled down rapidly. Several authors [63,65] also demonstrated

that shear forces between glass fibres and PP enhance the formation of transcrystalline layers. Glass fibres were pulled through PP before the samples were cooled down or during the cooling process. Transcrystalline layers were also observed in injection moulded GF/PP composites [65,66]. Guo et al. [66] varied the shear forces during the injection moulding of GF/PP composites. Based on atomic force microscopy they concluded that high shear forces promoted the formation of transcrystalline layers in the composites. The functionalisation of the fibre surface and the PP matrix can also promote the growth of transcrystalline layers. Wagner et al. [67] demonstrated that the coating of glass fibres with nucleating agents promotes the formation of transcrystalline layers. Aminosilane itself was not correlated to transcrystallinity but the combination of aminosilane and functionalised PP was observed to enhance the formation of transcrystalline layers also at cooling rates below 10 °C / min in quiescent conditions [68,69]. Pompe and Mäder [27] also observed transcrystallinity in composites based on unsized glass fibres and PP that was blended with maleic anhydride grafted PP (MAPP). They observed a higher transcrystallinity content in the unsized fibre samples. Several authors correlated the results of fibre fragmentation tests [68,69], single fibre pull-out tests [27,64] and composite tensile test data [27,66] to transcrystallinity. However, it should be noticed that it is difficult to correlate the property enhancement solely to transcrystallinity. In the study by Guo et al [66] the high shear rates also caused more fibres to align in the melt flow direction. Nagae et al. [68], Mäder et al. [27] and Zheng et al. [69] used functionalised PP which can also enhance the IFSS by other mechanisms like acid basic interactions that are discussed below. However, the consensus between the reviewed publications is that the IFSS and tensile strength of GF/PP composite increased because of the formation of a transcrystalline layer in the interphase.

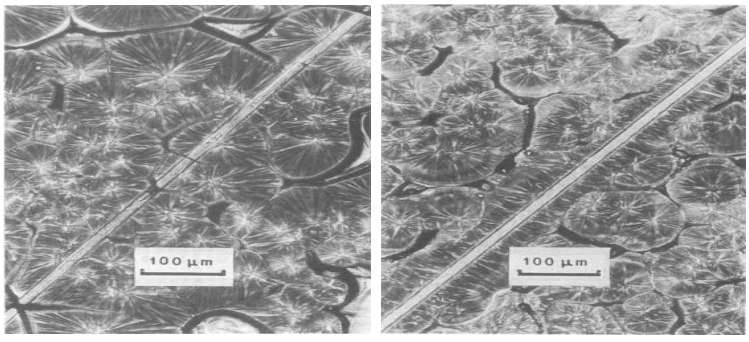

Figure 2.6. Glass fibre PP samples cooled at 10 °C/min without transcrystallinity (left) and 280 °C/min with transcrystallinity (right). Reproduced from [63]

Wettability and Acid basic interaction

Mäder and Pisanova [52] demonstrated that inverse gas chromatography, contact angle measurements based on the capillary rise technique and continuously monitored microbond tests can provide similar values for the work of adhesion of unsized glass fibre PP systems. The wetting kinetics were observed to be modified by organosilane on the glass fibre surface and the introduction of acidic groups into the PP [59]. Figure 2.7 and Figure 2.8 illustrate the mechanism by which organosilanes modify the surface chemistry of glass fibres. After hydrolysis in water the silanol group of the organosilane forms a hydrogen bond with the glass fibre surface. When the fibre is dried, a polysiloxane layer is formed that is covalently bonded to the glass fibre surface [35,70].

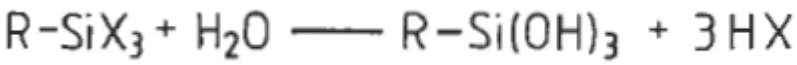

Figure 2.7. Hydrolisis of silane in water after [70]. Reproduced from [35]

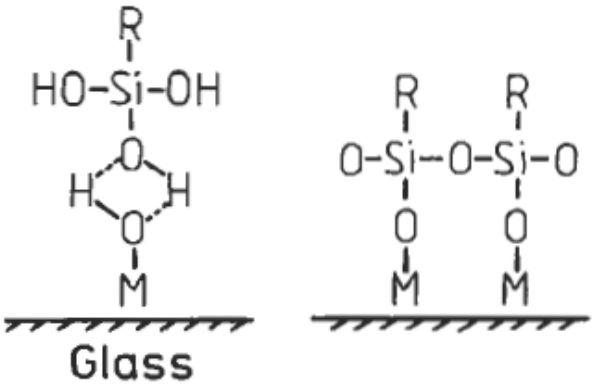

Figure 2.8. Bonding between glass fibres and silanes after [70]. Reproduced from [35]

However, the sizing of the fibres itself does not necessarily lead to an improvement of the IFSS because of the nonpolar nature of PP. Single fibre pullout tests [58,59], microbond tests [52] and single fibre fragmentation tests [71] showed that improvement in the IFSS is only obtained when silane is used in combination with the acidic groups of modified PP. The acidic groups of the modified PP can interact with basic groups of the silane on the glass fibre surface [52,59,71,72]. Figure 2.9 illustrates the acid basic interaction between aminopropyltriethoxy silane on a glass fibre surface and MAPP.

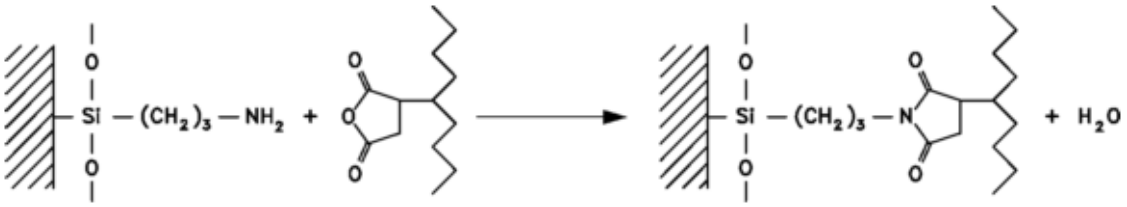

Figure 2.9. Chemical reaction between an amino group and maleic anhydride after [72]. Reproduced from [71]

The same studies [52,58,59] that explained the effect of silane and maleic anhydride groups on the IFSS by acid basic interactions also observed that the reaction of functional groups to PP can also improve the IFSS between unsized glass fibres and PP. Since the surface of unsized glass fibres is acidic [52,59], acid-basic interactions are not possible following Figure 2.9. Thus, the maleic anhydride groups might also directly interact with the OH groups of the glass fibre surface.

Intermolecular entanglement

Intermolecular entanglements in the interphase is another mechanism that was proposed to influence the IFSS between glass fibres and PP. Nygård [71] et al. added MAPP to the PP matrix and coated glass fibres directly with MAPP. In both cases, the IFSS increased when MAPP with a high molecular weight was used. It was proposed that high molecular weight MAPP promotes intermolecular entanglements in the interface regions because of the long entanglement length as shown in Figure 2.10. Similar observations were reported by Mäder and Pisanova [52] when they investigated film formers with a low molecular weight and a high molecular weight. Thomason and Van Royen [63] related the molecular weight of PP to transcrystallinity in the interphase. PP with a high molecular weight was observed to be beneficial for formation of a trancrystalline layer in glass fibre PP systems. It might therefore be speculated that film formers with a high molecular weight promote transcrystallinity in the interphase which leads to an increase of the interphase strength as shown by Mäder et al. [27].

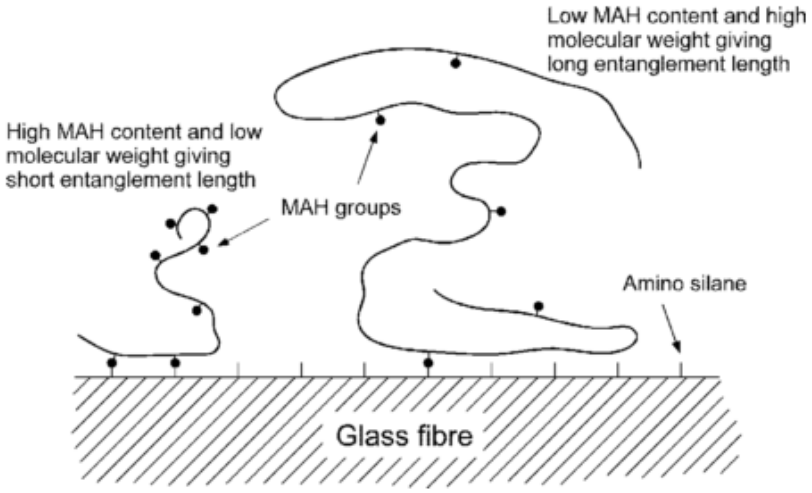

Figure 2.10. Effect of molecular weight of MAPP on entanglement length in glass fibre PP composites. Reproduced from [71]

Residual stresses

Thomason and Yang [41] modified a thermal mechanical analyser to perform microbond tests at different temperatures. They observed that the apparent IFSS decreased when the temperature increased. Further analysis showed that up to 70 % of the IFSS could be attributed to residual stresses caused by different thermal expansions of the unsized glass fibres and the PP.

2.2.3 Summary and Conclusion

The microbond test results are highly dependent on the experimental procedure and the data reduction. Studies from different researchers might not be comparable because of the lack of a standard. However, the factors that affect the microbond test results are well reported in the literature. The apparent IFSS might not always be accurate but several studies showed that it can be used to qualitatively detect differences in GF/PP composites. Despite several publications, no definite conclusion can be drawn regarding the bonding mechanism in GF/PP composites. Residual stresses, acid basic interactions and intermolecular entanglement have been identified in the literature as possible bonding mechanisms in GF/PP composites. The extent to which each mechanism affects the adhesion between fibre and matrix is not completely clarified and might depend on several factors such as the glass fibre sizing or the modification of the PP matrix. It was found that interfacial adhesion can be modified by glass fibre sizings, introduction of acid groups in the PP and the processing history of the composites.

2.3 Tensile properties of GF/PP composites

This section reviews factors that influence the tensile strength, modulus and strain at break of GF/PP composites. The terms are used according to the ISO 527 standard. The Kelly-Tyson model to describe the composite tensile strength and the Cox model to describe the composite modulus are also introduced.

2.3.1 Tensile strength of discontinuous GF/PP composites

Fibre content

Several studies have observed a relationship between the fibre content and the tensile strength of discontinuous GF/PP composites. The tensile strength of injection moulded GF/PP composites [4–7,25,33,73,74] and GMT composites [75–78] was reported to improve with the addition of fibres at fibre contents between 0 wt% and 40 wt% - 50 wt%. Several authors observed a decrease of the reinforcement efficiency with increasing fibre content. The level of strength improvement was higher at low fibre contents than at high fibre contents when the fibre content was increased by the same increment [4,7,25,33,74,75]. The data in Figure 2.11 illustrates this increase of the tensile strength and reduction of the fibre reinforcement efficiency. Fibres contents higher than 40 wt% - 50 wt% led to a reduction of the tensile strength of injection moulded composites [33] and GMT composites [75]. Fu et al. [4] attributed the decrease of fibre reinforcement efficiency in injection moulded composites to enhanced fibre length degradation at high fibre contents. Thomason [25,79] calculated the IFSS in injection moulded GF/PP composites from tensile test data and observed a reduction of the IFSS with increasing fibre content. He explained the reduction of the tensile strength at high fibre contents with a reduction of both the IFSS and the residual fibre length. GMT processes are less susceptible to fibre length degradation during processing. In a study by Thomason et al. [76] the tensile strength increased linearly up to 60 wt% fibre content. However, other issues might limit the use of high fibre contents in GMT composites. Lee and Jang [75] dissolved polypropylene in xylene and poured the solution over glass fibres to produce GMT composites. They attributed the reduction to the tensile strength at high fibre contents to insufficient wetting of the glass fibres. They also postulated that the fibre ends act as failure initiation sides. It should also be noticed that the tensile strength of some types of commercial GMT composites can vary significantly. Stoke [80] demonstrated that the tensile strength within one commercial Azdel GMT laminate can vary between 70 MPa and 120

MPa. He explained his observations with variations in the density and glass fibre contents.

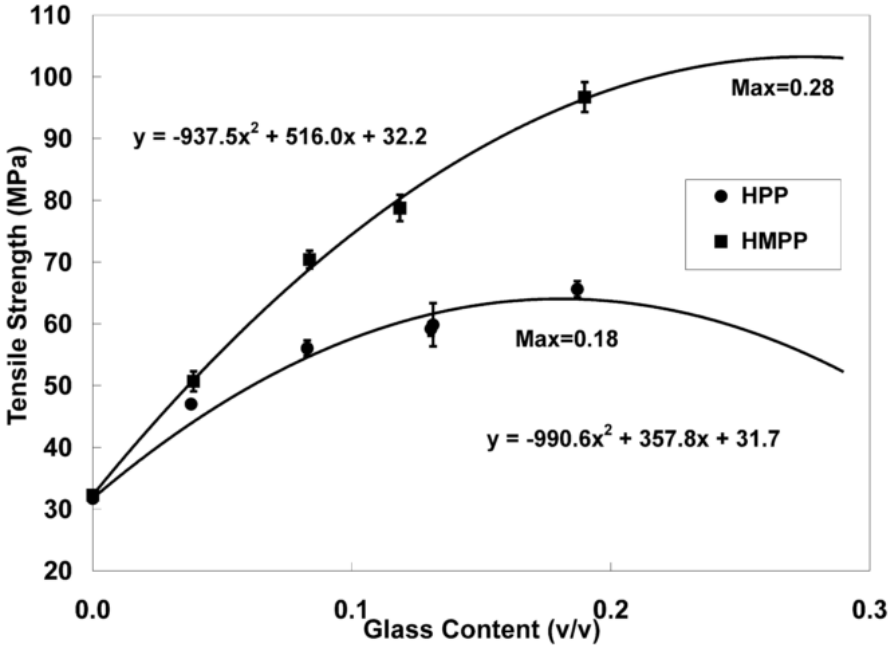

Figure 2.11. Increase of tensile strength of injection moulded GF/PP composites with fibre content - MAPP added (HMPP) and no MAPP added (HPP). Reproduced from [25]

Interfacial shear strength

The IFSS between matrix and glass fibres also strongly influences the tensile strength of discontinuous GF/PP composites. As discussed in section 2.2.2 the interfacial adhesion between glass fibres and PP can be increased by the presence of sizing on the glass fibre surface and the addition of functional groups to the PP matrix. Several authors [27,34,52,58,72,73] observed an increase of the tensile strength of injection moulded GF/PP composites when coupling agents were added to the composites. Mäder et al. [27,52,58] showed in several studies that the increase of the composite tensile strength corresponded to an increase of the IFSS that was obtained from microbond tests and fibre pull-out tests. Similar observations were reported for GMT composites. Cantwell et al. [81] and Zheng et al. [69] observed that the addition MAPP to the PP matrix increased the tensile strength of GMT composites. Thomason and Schoolenberg [82] observed that GMT composites based on fibres with a PP compatible sizing exhibited a higher tensile strength than other GMT composites. Similar observations were reported by Davies et al. [83] when they investigated the influence of functionalized PP on the tensile strength of GMT composites that were based on polyester sized glass fibres. Ericson and

Berglund [78] did not observe an increase of the tensile strength of commercial GMT composite when MAPP was added to the PP matrix. They explained their observation with local variations in the material that predominate the influence of improved interfacial adhesion. They argued that the MAPP might not have reached the glass fibre surface because of a too short processing time [59]. Their argument about the effect of the processing time on the IFSS was supported by Zheng et al. [69] when they varied the processing time of GF/PP single fibre pull-out samples with added MAPP. The IFSS was observed to increase with the processing time until it reached a plateau [69].

Thomason [25] compared the tensile strength of extrusion compounded and injection moulded GF/PP composites with different fibre contents. The addition of MAPP improved the tensile strength significantly despite a slight reduction of the residual fibre length (see Figure 2.11). The IFSS obtained from the tensile test data also increased from less than 8 MPa to approximately 16 MPa due to the addition of the coupling agent. In a more recent study, Thomason [33] also investigated the tensile properties of pultrusion compounded and injection moulded GF/PP composites. The tensile strength and the IFSS obtained from the macromechanical test data increased due to the presence of MAPP. As mentioned above, the reduction of the tensile strength at high fibre contents was explained by a reduction of the IFSS. The IFSS obtained from macromechanical test data dropped from more than 20 MPa to less than 5 MPa. It was proposed that the IFSS mainly decreased with the fibre content because the ratio between coupling agent molecules and fibre surface was reduced. Studies by Bowland [84,85] supported this hypothesis. Bowland demonstrated that the tensile strength of injection moulded GF/PP composites depends on the fibre surface area and the MAPP content (number of maleic anhydride groups) as shown in Figure 2.12. In addition, he showed that the effect of MAPP based coupling agents on the performance of GF/PP composites depends also on the melt flow index. Coupling agents with a high melt flow index improved the flexural strength of the GF/PP composites more than coupling agents with a low melt flow index.

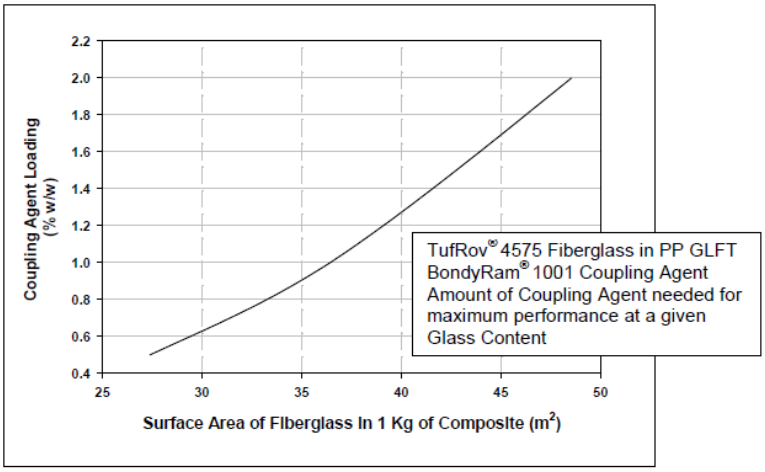

Figure 2.12. Dependence of coupling agent loading on fibre surface area to maximise composite tensile strength. Reproduced from [85]

Conflicting data can be found in literature regarding the effect of high coupling agent concentrations on the performance of GF/PP composites. As described above, research agrees that the addition of MAPP to GF/PP composites improves the composite tensile strength and flexural strength. However, several researchers observed a drop of the composite performance when the MAPP content was increased further beyond the content that is required to reach the maximum composite performance. Bowland [84,85] observed a small (174 MPa to 169 MPa) but continuous decrease of the composite tensile strength at high maleic anhydride contents. In addition, his data indicates a small reduction of the flexural modulus at high coupling agent contents. In contrast, Roux et al. [34] did not observe a reduction of the tensile strength or tensile modulus of injection moulded GF/PP composites. Rijsdijk et al. [86] varied the amount of MAPP in continuous GF/PP composites that were prepared via compression moulding. Their data indicated a single peak (one data point) in the composite flexural strength but apart from that peak the data did not follow a trend. The composite modulus did not change with the MAPP content. Cantwell et al. [81] observed an increase of the tensile strength of GMT composites when the coupling agent content (coupling agent not specified) was increased. No significant reduction of the composite tensile strength was observed and the composite modulus did not change significantly. Zheng et al. [69] observed a reduction of the tensile strength of GMT composites from 92 MPa to 77 MPa when the MAPP content was increased from 5 % to 10 %. In addition, the data of Zheng et al. also suggests a reduction of the composite modulus with the MAPP content. However, in contrast to the tensile strength only three data points are provided, the error bars are missing and the values are low compared to other

values that can be found in literature [77,87,88]. Thus, care should be taken when interpreting that data. Based on the studies by Bowland [84,85] and Thomason [25] it might be expected that the different observations on the effect of high MAPP contents can be explained with the ratios between fibre surface area and coupling agent content. At high fibre contents more MA groups would be required to observe a reduction of the composite performance. However, the data summarised in Table 2.3 does not support such a relationship. The comparability between the studies above is limited because of different manufacturing processes, glass fibres (diameter, sizing), PP grades and MAPP grades. It appears that each GF/PP system has its own optimum coupling agent content and maleic anhydride content which is required for maximum composite performance.

Table 2.3. Optimum MAPP content observed in different studies

Reference	Maleic anhydride grafting level	Fibre content	Fibre diameter	Optimum MAPP content	Property
[86]	1 %	58 vol%	unknown	10 wt%	Flexure strength
[81]	unknown	25 wt%	unknown	7 wt%	Tensile strength
[69]	1.2 %	30 wt%	25 µm	5 wt%	Tensile strength
[34]	0.8 %	25 wt%	unknown	10 wt%	Tensile strength
[84,85]	1 %	30 wt%	17 µm	1-2 wt%	Tensile strength

Rijsdijk et al. [86] discussed potential causes for the drop of the composite performance at high coupling agent contents. They suggested that the interphase was weakened due to large quantities of MAPP. This would agree with the hypothesis of Qiu et al. [89]. They observed that MAPP can also contain maleic anhydride (MA) monomers. The tensile strength of compression moulded cellulose fibre PP composites decreased with the concentration of MA monomers in the matrix. The drop of the composite performance was explained with a reduction of

the IFSS because the MA monomers reacted with the fibre surface. Thus the MAPP could not react with the fibre surface. Other systems also exhibited a drop of the interfacial adhesion when the concentration of functional groups like MA exceeded an optimum. Schultz et al. [90] observed a reduction of the peel strength between aluminium and PP by up to 50 % when the optimum MAPP content was exceeded. They explained the existence of an optimum MAPP content with two competing mechanisms. MAPP migrates to the aluminium surface where the MA groups chemically interact the hydroxyl groups of the aluminium surface. The interfacial adhesion increases because of the interaction between the aluminium surface and the MA groups. MAPP has a lower molecular weight than PP. The increased concentration of low molecular weight MAPP close to the aluminium surface weakens the interphase close to the aluminium surface. Higher MAPP contents promote the formation of a weak interphase because more MAPP can migrate to the aluminium surface. Above the optimum MAPP content the negative effect of a weak interphase predominates the positive effect of chemical interactions between MA groups and aluminium. Thus, high MAPP concentrations lead to cohesive failure because of a weak interphase close to the aluminium polymer interface. Gong et al. [91] studied the interfacial adhesion between aluminium and polybutadiene that was functionalised with carboxyl groups. They also observed a decrease of the interfacial adhesion above an optimum concentration of functionalised groups and correlated it to cohesive failure of the interphase. In contrast to Schultz et al. [90], they did not relate the drop of the interfacial adhesion between polymer and metal to the molecular weight of the functionalised polymer. They suggested that a high concentration of functionalised groups leads to a dense attachment of the functionalised polymer chains to the aluminium surface. The functionalised polymer chains wrap the aluminium and do not interact with the bulk polymer which leads to cohesive failure of the interphase. A similar explanation was proposed by Beck Tan et al. [92] when they observed a drop of the adhesion between polystyrene and poly(2-vinylpyridine) above an optimum content of functional sulfonic acid groups. Gangster et al. [93] observed a reduction of the tensile strength of injection moulded cellulose fibre PP composites with the MAPP content beyond an initial improvement. They speculated that the matrix properties were affected by large quantities of MAPP with a low molecular weight compared to PP. However, Roux et al. [34] and Rijsdijk et al. [86] observed that the tensile strength of PP was not degraded by the addition of MAPP. Zheng et al. [69] explained the detrimental effect of high MAPP

contents with a brittle failure of the composites. A high IFSS would lead to the reduction of fibre pull-out as an energy absorbing mechanism. A single fibre fracture would lead to the formation of crevices and the failure of the surrounding fibres and the matrix. Their explanation is based on observations of the PP matrix of single fibre fragmentation test samples and is a common explanation why too strong interfaces might reduce the tensile strength of unidirectional continuous fibre composites [94]. It might be questionable whether a continuous single fibre composite or a 'normal' unidirectional continuous fibre composite behaves similar to discontinuous GF/PP composites. Zheng et al. [69] used heat cleaned glass fibres. The exposure of glass fibre to elevated temperatures reduces their strength which will be discussed later. Thus, fibre failure was more likely compared to other studies on GF/PP composites that were reviewed in this section. It appears, that there is currently no consensus about the cause for the detrimental effect of high MAPP contents on the performance of GF/PP composites.

Fibre aspect ratio

The fibre aspect ratio is another important parameter that determines the tensile strength of discontinuous GF/PP composites. As mentioned above, the fibre reinforcement efficiency was observed to decrease with increasing fibre content [4]. This can at least partially be attributed to the enhanced fibre length degradation and lower aspect ratio. As discussed in section 2.1.3, high fibre contents promote fibre length degradation during extrusion and injection moulding of GF/PP composites. The result is a reduction of the residual fibre length and aspect ratio with increasing fibre content [3–7]. Thomason [7] and Spahr et al. [6] studied the properties of extrusion compounded and pultrusion compounded GF/PP composites that were injection moulded. The pultrusion compounded composites with relatively long fibres in the final composites exhibited a higher tensile strength than the extrusion compounded composites. To study the effect of the fibre length on the mechanical properties, Thomason et al. [76] prepared GMT composites with different fibre lengths using a wet deposition technique which minimizes uncontrolled fibre length degradation. The tensile strength increased almost linearly with the fibre length until a fibre length of 3-6 mm. Further increase of the fibre length improved the tensile strength only slightly. Ericson and Berglund [77] compared the mechanical properties of GMT composites that were prepared via the papermaking process with GMT composites that were prepared using a melt impregnation process. They

observed that the papermaking process provided composites with a higher tensile strength than the melt impregnation process. In contrast to the papermaking process, the fibres were not well dispersed when the composites were prepared via melt impregnation. The fibre bundles were acting like single fibres with a low aspect ratio which led to composites with a low tensile strength.

The tensile strength of glass fibre PP composites is closely related to the concept of the critical fibre length L_C which was developed by Kelly and Tyson [95]. That concept describes the fibre stress when the fibre is embedded in a ductile matrix. Depending on the fibre length, stress builds up along the fibre until it reaches a plateau and the stress in the fibre is equal to the fibre strength σ_f as illustrated in Figure 2.13.

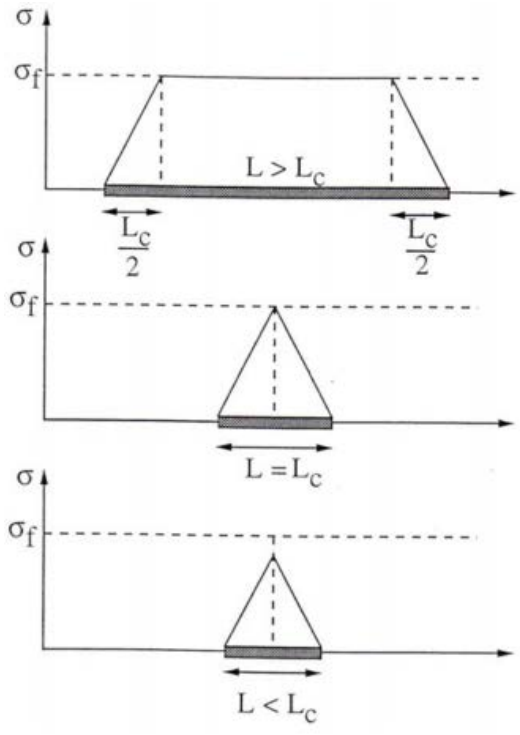

Figure 2.13. Fibre stress and critical fibre length after Kelly and Tyson [95]. Reproduced from [96]

The composite tensile strength, composite modulus and composite impact strength all increase with the fibre length in composites but Figure 2.14 shows that optimum fibre length depends on the composite property. Relatively short fibres are required to optimise the composite modulus compared to the composite tensile strength and impact strength. The tensile strength of GF/PP composites was reported to level off beyond a fibre length of 3 mm while the modulus of GF/PP composites was not influenced by the fibre length if the fibres were longer than 0.5 mm.

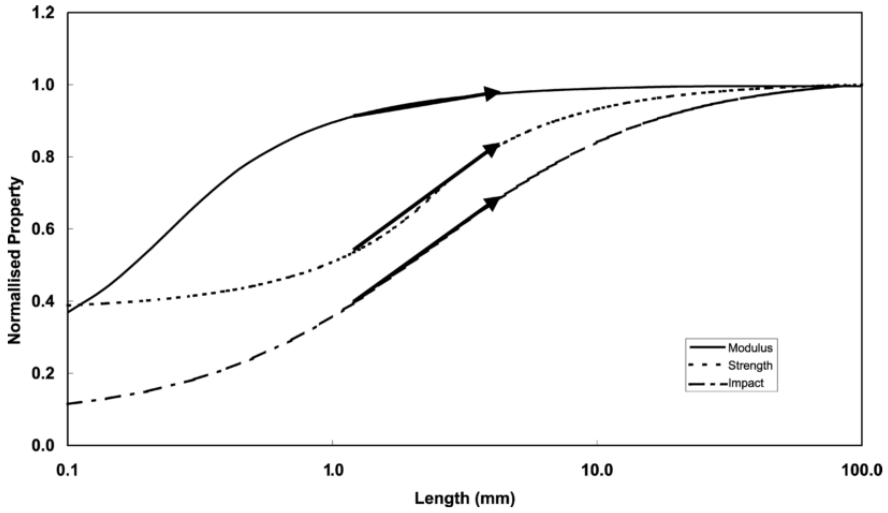

Figure 2.14. Dependence of critical fibre length on mechanical properties. Reproduced from [7]

Fibre orientation

The orientation of the glass fibres in the PP also influences the composite tensile strength. Mittal et al. [97] demonstrated the influence of the fibre orientation on the tensile strength. GF/PP sheets with an almost unidirectional fibre orientation were extruded and tensile tested. The highest strength (67.6 MPa) was measured when the fibres were aligned parallel with the loading axis. The tensile strength dropped to 38.6 MPa when the angle between fibre axis and loading axis was 45 deg. Spahr et al. [6] investigated the tensile strength of injection moulded GF/PP composites. Samples were tested parallel and transverse to the flow direction of the polymer melt. A higher tensile strength was measured parallel to the flow direction. This behaviour was explained with fibres predominantly aligned in the melt flow direction. Similar to injection moulded GF/PP composites, the tensile strength of GMT composites rises when the fibres are aligned parallel to the applied load. The melt flow during compression moulding can induce fibre alignment transverse to the melt flow direction which can cause an increase of the composite tensile strength in that direction [88,98].

In summary, the fibre content, fibre length, fibre orientation and IFSS are all important parameters that influence the tensile strength of discontinuous GF/PP composites. Generally, the tensile strength increases with the fibre length and the IFSS. High fibre contents are also desirable to improve the tensile strength. The fibres should be orientated parallel with the loading axis to utilize the strength of the fibres. The interaction between the micromechanical parameters mentioned above also needs also to be considered.

2.3.2 Extended Kelly-Tyson to describe discontinuous GF/PP composites

The fibre content, fibre length, fibre orientation and IFSS are considered in models which can be applied to discontinuous GF/PP composites. According to Fu et al. [4], the tensile strength σ_{cMax} of a discontinuous GF/PP composite can be calculated with Equation 2.2.

Equation 2.2. Tensile strength of discontinuous fibre composites

$$\sigma_{cMax} = \lambda_C * \sigma_f * V_f + \sigma_m * (1 - V_{f)})$$

where V_f is the fibre volume fraction, σ_f is the fibre tensile strength and σ_m is the tensile strength of the PP matrix. λ_C is the reinforcement efficiency factor which considers the influence of the fibre length, fibre orientation and IFSS [4]. A similar approach was used by Templeton [99] to predict the strength of injection moulded GF/PP composites. Similar to Fu et al [4], he had to introduce empirical factors to account for the IFSS and fibre orientation. The equation above provides only a simplified description of the composite strength. As shown in Figure 2.11 above, the relationship between fibre content and tensile strength is not linear.

The extended Kelly-Tyson model [100] is a more sophisticated model to describe the tensile strength of discontinuous fibre composites. It is based on the assumption that the critical fibre length changes with the stress in the composite. The critical fibre length l_c at a strain ε_c can be described with Equation 2.3.

Equation 2.3. Critical fibre length

$$l_C = \frac{E_f * r_f * \varepsilon_c}{\tau_{ult}}$$

where E_f is the modulus of the fibre, r_f is the fibre radius and τ_{ult} is the interfacial shear strength. A fibre that is shorter than the critical length is called subcritical fibre and is subjected to a stress $(\sigma_f)_{sub}$.

Equation 2.4. Tensile stress of subcritical fibres

$$(\sigma_f)_{sub} = \frac{l * \tau_{ult}}{2 * r_f}$$

where l is the fibre length. Fibres longer than the critical fibre length are also called supercritical fibres and experience the stress $(\sigma_f)_{sup}$.

Equation 2.5. Tensile stress of supercritical fibres

$$(\sigma_f)_{sup} = E_f * \varepsilon_C * \left(1 - \frac{E_f * \varepsilon_c * r_f}{2 * l * \tau_{ult}}\right)$$

Thus, the contribution X of all subcritical fibres with the volume subfraction V_i and length l_i can be described with

Equation 2.6. Contribution of subcritical fibres to composite tensile stress

$$X = \sum \frac{\tau * l_i * V_i}{2 * r_f}$$

The contribution Y of the supercritical fibres with a volume subfraction V_j and length l_j can be described with

Equation 2.7. Contribution of supercritical fibres to composite tensile stress

$$Y = \sum E_f * \varepsilon_c * \left(1 - \frac{E_f * \varepsilon_c * r_f}{2 * l_j * \tau_{ult}}\right) * V_j$$

The stress Z in the matrix with a modulus E_M can be calculated from

Equation 2.8. Contribution of matrix to composite tensile stress

$$Z = E_M * \varepsilon_c * (1 - V_f)$$

where V_f is the fibre volume fraction.

The terms above can be combined to calculate the composite tensile stress σ_C where η_{oKT} describes the fibre orientation.

Equation 2.9. Composite tensile stress

$$\sigma_C = \eta_{oKT} * (X + Y) + Z$$

Thomason et al. [76] demonstrated that the extended Kelly-Tyson model can predict the strength of GMT composites with randomly orientated glass fibres. The modified Kelly-Tyson model matched the experimental data if the orientation factor η_{oKT} is fitted to the experimental data. In other studies, Thomason [33,79] used the Kelly-Tyson model to describe the tensile strength of pultrusion compounded and injection moulded GF/PP composites. An excellent agreement between the Kelly-Tyson model and experimental results was achieved when modified input parameters were used. The IFSS was calculated from tensile test data using an algorithm developed by Bowyer and Bader [100] which will be discussed later in section 2.4.1. The fibre stress at composite failure was calculated and it was concluded that the fibres are unlikely to break. It was suggested that a strain based failure criterion is more suitable than a stress based failure criterion. Consequently, the fibre stress at composite failure was recalculated from the composite strain at failure and used to predict the composite tensile strength. The results matched the experimental data.

In conclusion, the extended Kelly-Tyson model described above seems to be suitable to predict the tensile strength of discontinuous GF/PP composites. The quality of the model data depends not only on the input parameters but also on an understanding of the failure process. The modified Kelly-Tyson model is based on several assumptions. It is assumed that a fibre orientation distribution can be described with a single factor. This assumption was questioned and the rule of mixture was modified [101,102] to account for the fibre orientation distribution. Piggott [103] developed a fracture based model specifically for brittle composites. Although these models aim to overcome some of the limitations of the Kelly-Tyson model, only the Kelly-Tyson model and the simple rule of mixture have been applied to discontinuous GF/PP composites. This might be explained by the mathematical simplicity of the Kelly-Tyson model. In this thesis the Kelly-Tyson model will be used similar to previous work of Thomason et al. [76,79] which showed an agreement between model data and experimental data.

2.3.3 The modulus of discontinuous GF/PP composites

The effect of the glass fibre content on the modulus of injection moulded GF/PP composites [4–7,33,74,104] and GMT composites [73,75,77,87] is well documented. Several authors reported a linear or almost linear increase of the modulus with fibre content by weight fraction [87] or volume fraction [7,33,75]. At high fibre contents, a further increase of the fibre content improved the modulus only slightly [4,33,75,87]. This was explained by the presence of voids [75,87] or a reduction of the residual fibre length due to enhanced fibre length degradation at high fibre contents [4]. The modulus of GF/PP composites depends also on the length of the glass fibres in the composites. Thomason and Vlug [87] documented an increase of the modulus with fibre length. However, they also reported that fibres longer than 0.5 mm did not lead to a further improvement of the modulus. The orientation of the glass fibres in the composite is another important parameter that influences the modulus. Mittal and Gupta [104] extruded GF/PP sheets with almost unidirectional fibre alignment. The highest modulus was measured when the fibres were aligned parallel to the loading axis. A similar effect was observed by Spahr et al [6]. Samples were cut from injection moulded material. The samples cut parallel to the flow direction exhibited a higher stiffness because the fibres were predominantly aligned in the melt flow direction. Similar to the tensile strength, the modulus of GMT composites was observed to vary within moulded laminates. Specimens cut from the edge of moulded laminates exhibited a higher modulus than specimens cut from the centre

of laminates which can be attributed to melt flow induced fibre alignment [88,98]. Manufacturing defects like voids [87] or local variations in the fibre content were also reported to affect the modulus [105].

In conclusion, the modulus of discontinuous GF/PP composites depends mainly on the fibre content and fibre orientation. The length of the glass fibres also influences the modulus but relatively short fibres (0.5 mm) are sufficient to reach a maximum stiffness level. Manufacturing defects also affect the modulus and need to be considered.

2.3.4 Cox model to predict the modulus of discontinuous GF/PP composites

Fu et al. [4] used the rule of mixture to calculate the reinforcement efficiency factor for the composite modulus. The rule of mixture can be used to estimate the composite modulus E_c.

Equation 2.10. Modulus of composites according to the rule of mixture

$$E_c = \lambda_E * E_f * V_f + E_m * (1 - V_f)$$

where λ_E is the reinforcement efficiency factor for the composite modulus which depends on the fibre orientation and fibre length.

A combination of the rule of mixture and the Cox model [106] can be used to describe the modulus [77,87] of GMT composites. The reinforcement efficiency factor λ_E was replaced by the product of the fibre orientation factor η_{oKr} and the fibre length efficiency factor η_l. The value of the orientation factor was assumed to be 0.375 [107] and the fibre length efficiency factor of fibres with an average length L was calculated from

Equation 2.11 Length efficiency factor

$$\eta_l = 1 - \frac{tanh\left(\beta * \frac{L}{2}\right)}{\beta * \frac{L}{2}}$$

The factor β can be calculated with

Equation 2.12. β factor

$$\beta = \frac{2}{d_f} \sqrt{\left[\frac{2 * G_M}{E_f * \ln\left(\sqrt{\frac{r_f}{R}}\right)}\right]}$$

where the factor r_f/R and the shear modulus G_M can be calculated with the equations below

Equation 2.13. Shear modulus

$$G_M = \frac{E_M}{2 * (1 + \upsilon)}$$

where υ is the Poisson's ratio of the matrix.

Equation 2.14. Factor $r/R_{Spacing}$

$$\ln\left(\sqrt{\frac{r_f}{R_{Spacing}}}\right) = \ln\left(\sqrt{\frac{\pi}{X_i * V_f}}\right)$$

X_i depends on the geometrical packing of the fibres. The value of X_i depends on the arrangement of the fibres in the composites (Square packing X_i = 1, Hexagonal packing X_i = 0.866). There is a disagreement in literature about the use of $R_{Spacing}$. Ericson and Berglund [77] assumed $R_{Spacing}$ to be the mean distance between the centre of the fibres. In contrast, Thomason and Vlug [87] assumed that 2 $R_{Spacing}$ represent the mean distance between the centre of the fibres. Depending on the assumed value for $R_{Spacing}$ the calculated value for β in Equation 2.12 changes especially at short fibre lengths.

Other approaches such as the Halpin-Tsai model or models based on Eshelby's equivalent inclusions [36,108] can also be used to calculate the stiffness of discontinuous GF/PP composites. Lusti et al. [109] demonstrated that finite element analysis can predict the stiffness of injection moulded GF/PP composites with high accuracy. Tucker and Liang [108] compared the Halpin-Tsai model, models based on Eshelby's equivalent inclusions with the modified Cox model and finite element (FE) analysis for discontinuous fibre composites with unidirectional aligned fibres. They found that models based on Eshelby's equivalent inclusions provided results close the FE analysis. However, models based on Eshelby's equivalent inclusions involve more mathematical complexity than the Halpin-Tsai model or the modified Cox model. The Halpin-Tsai model deviated significantly from the FE model when the aspect ratio of the fibres was higher than 10. The Cox model provided results similar to the FE analysis when the aspect ratio of the fibres was higher than 10. In this thesis, only the modified Cox model will be used. It has been shown to be sufficiently accurate to predict the stiffness of discontinuous GF/PP composites with a moderate or long fibre length [77,87].

2.3.5 Strain at break

Similar to the modulus and tensile strength, the strain at break and yield strain of discontinuous GF/PP composites are influenced by the fibre content. Research agrees that the strain at break of injection moulded GF/PP composites [6,33,4,74,110] and GMT composites [75–77] decreases with fibre content. A common explanation is that the fibre ends act as failure initiation sites [4,75,76,110]. This was confirmed by Sato et al. [111] when they observed the tensile fracture of polyamide glass fibre composites in an SEM (see Figure 2.15). They observed a four stage fracture process. First microvoids grew at fibre ends. Then cracks were formed along the fibre matrix interfaces. Between the fibres the matrix yielded until a crack opened which resulted in catastrophic failure of the composite. In addition, Hassan et al. [110] proposed that the fibres prevent the molecular rearrangement in the PP matrix which would lead to a more brittle behaviour of the PP matrix.

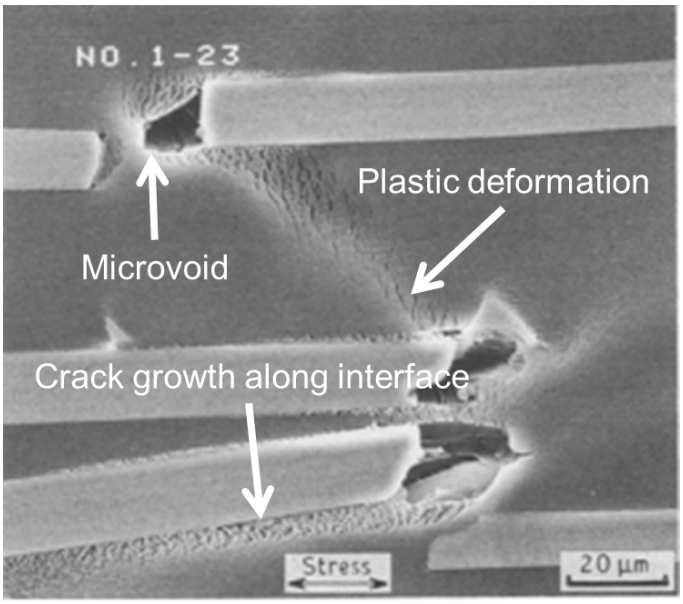

Figure 2.15. Failure process of glass fibre polyamide composites initiated at the fibre ends. Reproduced from [111]

Conflicting observations were reported regarding the influence of the IFSS on the strain at break of discontinuous GF/PP composites. Hassan et al. [110] observed a reduction of the strain at break of injection moulded GF/PP composites when 5 wt% MAPP were added to the PP matrix. Only limited information about the IFSS is available because the authors did not provide information regarding the glass fibre sizing. However, dynamic mechanical analysis and composite tensile tests indicated that the IFSS increased due to the addition of MAPP. Thus that study suggests that the improvement of the IFSS can be detrimental for the strain at break of GF/PP

composites. Mäder et al. [27] observed that the coating of AminoPropyltriethoxySilane (APS) sized glass fibres with a PP film former leads to higher IFSS in GF/PP systems than the coating of APS sized glass fibres with Polyurethane (PU). At room temperature the composites with the PP film former exhibited a lower strain at break than composites with a PU film former. However, it should be noted that no error bars were provided for the strain at break in that publication. Thus, it is not clear to which extent the reported trends were significant. Nevertheless, the trend of the strain at break at room temperature agrees with the observation of Hassan et al. [110] who observed a reduction of the strain at break with increasing IFSS. Bikiaris et al. [112] observed an increase of the strain at break when MAPP was added to the PP matrix. Similar to Hassan et al. [110], the IFSS was not measured directly but tensile data and dynamic mechanical analysis indicated that the addition of MAPP caused a rise of the IFSS. Care must be taken again when interpreting results from that study because no error bars were provided. Thomason [25] also reported an increase of the strain at break due to the addition of MAPP to injection moulded PP composites with different glass fibre contents. Micromechanical modelling showed that the addition of MAPP also increased the IFSS. Cantwell et al. [81] and Davies et al. [83] characterized the tensile properties of GMT composites with modified PP as coupling agent. No increase of the strain at break due to the addition of modified PP was observed. However, in both studies the MAPP was added to the preform. It might therefore be questioned if the MAPP actually reached the fibre matrix interphase.

Spahr et al. [6] reported a reduction of the strain at break of injection moulded GF/PP composites with fibre length. The influence of the fibre length on the strain at break of GMT composites was investigated by Thomason et al. [76]. They observed a decrease of the strain at break with fibre length at fibre contents below 30 wt%. The authors suggested that the reduction of the composite strain at break with fibre length might have been caused by increasing stresses at the fibre ends. A similar hypothesis was proposed by Curtis et al. [113]. Based on the Kelly-Tyson model, they suggested that cracks in the polymer matrix are more likely to be formed at the fibres ends when the fibres are longer than the critical fibre length. The shear stresses at the fibre ends caused by different moduli of fibre and matrix would be lower when the fibres are shorter than the critical fibre length. The relationship between shear stresses and fibre length according to the Kelly-Tyson model is

illustrated in Figure 2.16. The shear stress at the fibre end reaches a maximum when the fibres are equal or longer than the critical fibre length l_c.

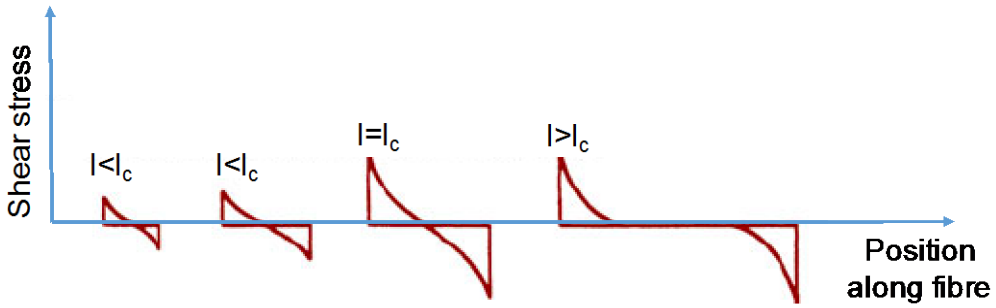

Figure 2.16. Increase of the shear stress at the fibre end with fibre length after [95]. Adapted from [114]

Few studies provide results regarding the influence of the fibre alignment on the strain at break. Spahr et al. [6] showed that the strain at break of injection moulded GF/PP composites decreases when most fibres are aligned in the loading direction. Ericson and Berglund [115] demonstrated in a study on GMT composites based on polyethylene that the strain at break of GMT composites is reduced when the fibres are predominantly aligned in the loading direction. Mittal et al. [97] demonstrated that the stress transfer between fibres and matrix is reduced when the fibres are not aligned in the loading direction. Fibres that are aligned in the loading direction carry the highest stresses [116]. Thus, matrix cracks are more likely to be formed at fibres that are aligned in the loading direction [113]. The growth of cracks at the fibre ends could initiate a composite failure as described by Sato et al. [111].

In conclusion, the strain at break of GF/PP composites depends on the residual fibre length, fibre orientation and fibre content. Research agrees that the strain at break decreases as a function of the fibre content and fibre length. Few studies related the strain at break to fibre orientation. A high degree of fibre alignment in loading direction was reported to reduce the composite strain at break because of enhanced stress transfer between fibre and matrix which might lead to higher stresses at the fibre ends and the formation of cracks in the matrix. Conflicting results were found regarding the influence of the IFSS and MAPP on the strain at break.

2.3.6 Summary and Conclusion

The relationships of the composite microstructure with the tensile properties of discontinuous GF/PP composites are well documented. Several researchers showed that the tensile strength and modulus increase with fibre content and fibre

length until a plateau is reached. A high degree of fibre orientation parallel to the load axis improved the strength and stiffness of the composites. The IFSS between glass fibres and PP also influences the composite tensile strength. In the reviewed studies the composite tensile strength increased with the IFSS until a plateau was reached. It was also demonstrated in several studies that the Cox model and the Kelly-Tyson model can be used to describe the modulus and tensile strength of GF/PP composites. The strain at break was found to be less well investigated. Research agrees that the strain at break decreases with increasing fibre content and fibre length. A high degree of fibre alignment was found to reduce the strain at break. However, contradicting studies were found regarding the effect of the IFSS on the strain at break.

2.4 Micromechanical properties from macromechanical data

As discussed in Section 2.2, microbond tests are a suitable tool to assess the IFSS between glass fibres and PP. Similar to other techniques that involve handling of single fibres, the microbond test is time consuming. In contrast, macroscopic tensile tests are a rapid and widely used method to assess the performance of GF/PP composites. To further utilize the data obtained from tensile tests, different approaches have been developed to derive micromechanical properties like the IFSS from composite tensile test data. Three different approaches were found in the literature which will be reviewed in this section.

2.4.1 Bowyer-Bader analysis

Bowyer and Bader [100] developed an algorithm to obtain the IFSS from tensile test data of injection moulded GF/PP composites. The algorithm is based on the Kelly-Tyson model.

(1) First the ratio R_{BB} was determined. R_{BB} represents the fibre contributions at two chosen strains ε_1 and ε_2 ($\varepsilon_2=2\varepsilon_1$) where σ_1 and σ_2 are the corresponding measured tensile stresses. Z_1 and Z_2 are the matrix contributions which were calculated using Equation 2.8.

Equation 2.15. Bowyer-Bader analysis - Factor R_{BB}

$$R_{BB} = \frac{\sigma_1 - Z_1}{\sigma_2 - Z_2}$$

(2) In the next step, a value for the IFSS was chosen and the critical fibre length at the strains ε_1 and ε_2 calculated with Equation 2.3.

(3) Then the contributions X_1, X_2 of the subcritical fibres and the contributions of the supercritical fibres Y_1, Y_2 at the chosen strains ε_1 and ε_2 were calculated with Equation 2.6 and Equation 2.7. The length of the glass fibres was measured and the value for the modulus of the fibres was taken from literature.

(4) The theoretical value of the ratio of the fibre contribution R'_{BB} at the chosen strains ε_1 and ε_2 was calculated and compared with the measured value R_{BB}.

Equation 2.16. Bowyer-Bader analysis - Factor R'_{BB}

$$R'_{BB} = \frac{X_1 + Y_1}{X_2 + Y_2}$$

(5) The value of the IFSS was adjusted until the theoretical value R'_{BB} matched the experimental value R_{BB}. The adjusted value for the IFSS was regarded as the true value. After the determination of the IFSS, the fibre orientation factor could be determined by rearranging Equation 2.9.

Bowyer and Bader [100] used the algorithm described above to calculate the IFSS of GF/PP composites with coupling agent and without coupling agent. The calculated value of the IFSS increased from 16 MPa to 25 MPa when coupling agent was added to the GF/PP composites. Thomason [25,79] improved the accuracy of the method described above. He used a polynomial to describe the stress-strain curve of the PP matrix which is more accurate than the assumed linear relationship between stress and strain in Equation 2.8. In addition, he calculated the fibre stress at composite failure using the Kelly-Tyson model. Thomason used the improved analysis to calculate the IFSS of GF/PP composites that were prepared via extrusion compounding/injection moulding [25] and pultrusion compounding/injection moulding [79]. The calculated IFSS was used to predict the tensile strength. Agreement between predicted results and measurement data was reported [79].

2.4.2 Mittal-Gupta analysis

Load applied parallel to fibre orientation axis

Mittal and Gupta [104] developed a slightly different method to calculate the IFSS from composite tensile test data. They argued that the approach of Bowyer and Bader is based on the assumption that the interfacial shear stress is constant at all composite strains. Thus, even at low composite strains a maximum stress would act in the interface which might not be realistic. An alternative approach was suggested. It was suggested that the interfacial shear stress τ increases linearly with the

composite tensile stress. K is a proportionality factor that was determined as described below.

Equation 2.17. Mittal-Gupta analysis – Interfacial shear stress vs. composite tensile stress

$$\tau = K * \sigma_C$$

The critical fibre length was calculated with

Equation 2.18. Mittal-Gupta analysis - Critical fibre length

$$l_C = \left(\frac{E_f * r_f}{K}\right) * \left(\frac{\varepsilon_c}{\sigma_c}\right)$$

To assess the proposed relationship in Equation 2.17, extruded GF/PP sheets with almost unidirectional fibre alignment were tensile tested and analysed. The load was applied parallel to the fibre orientation axis. Thus the orientation factor η_{oKT} was assumed to be approximately 1. Equation 2.19 was derived from Equation 2.3 and Equation 2.17. The fibre contributions X and Y were calculated with Equation 2.6 and Equation 2.7 under consideration of the relationship in Equation 2.17. K was adjusted to fulfil the criterion in Equation 2.19.

Equation 2.19. Mittal-Gupta analysis - Fibre orientation factor criterion

$$\frac{\sigma_c - (1 - V_f) * \sigma_m}{X + Y} = \eta_{oKT} \approx 1$$

After the determination of K the interfacial shear stress at composite failure was calculated using Equation 2.17.

Fibres inclined to load axis

In a second study [97], the IFSS of the same GF/PP sheets with unidirectional fibre alignment was calculated. In contrast to the first study, the fibres were inclined to the load axis when the composite was tensile tested. Based on geometrical considerations the stress $\sigma_{\theta C}$ and strain $\varepsilon_{\theta C}$ that act in fibre direction were calculated.

Equation 2.20. Mittal-Gupta analysis - Stresses in fibre direction

$$\sigma_{\theta C} = \sigma_C * cos^2\theta$$

Equation 2.21. Mittal-Gupta analysis - Strains in fibre direction

$$\varepsilon_{\theta C} = \varepsilon_C(\cos^2\theta - \nu(\theta)\sin^2\theta)$$

θ is the angle between loading axis and fibre direction. After the calculation of the stress and strain in fibre axis, the procedure outlined above was followed. The value

for K was adjusted until the criterion in Equation 2.19 was fulfilled and the interfacial stress at composite failure was calculated with Equation 2.17.

2.4.3 Ramsteiner-Theysohn analysis

Ramsteiner and Theyson [117] performed tensile tests on injection moulded GF/PP composites and other glass fibre reinforced thermoplastics. The fibre alignment in the composites was shown to be almost unidirectional. The tensile strength of the composites was plotted as a function of the fibre content. An almost linear increase of the tensile strength with the fibre content was reported at intermediate fibre volume fractions. The slope $d\sigma_{cMax}/dV_f$ of the graph was described with

Equation 2.22. Ramsteiner-Theysohn analysis to determine the IFSS

$$\frac{d\sigma_{cMax}}{dV_f} = \frac{1}{2} * \frac{\tau}{r_f} * \sum z_i * l_i - \sigma'_m$$

where z_i stands for the fraction of the fibres with the length l_i and σ'_m is the matrix stress at composite failure.

2.4.4 Comparison between the different approaches to calculate the IFSS

All three approaches were shown to be sensitive enough to detect the influence of modified PP on the IFSS in GF/PP composites [73,100,117]. Ramsteiner and Theysohn [117] and Gupta et al. [73] also demonstrated that their methods can detect the influence of ambient temperature on the IFSS.

The inherent limitation of the Ramsteiner-Theyson approach is the assumption of a linear relationship between tensile strength and fibre volume fraction. However, the results of several studies failed to support the assumption of a linear relationship between fibre volume fraction and tensile strength [33,75]. In addition, the Ramsteiner-Theyson analysis assumes the IFSS to be independent from the fibre content but a reduction of the IFSS with increasing fibre content was reported by Thomason [25,79]. The simplicity of the analysis is a clear advantage of the Ramsteiner-Theyson analysis. The Bowyer-Bader analysis is based on the questionable assumption that the stress at the interface is independent from the tensile stress in the composite. In addition, it was shown that the calculated fibre orientation factor varies with the strain of the composite [97]. Despite these limitations, Thomason [79] reported excellent agreement between experiment and model if the calculated IFSS was used to predict the composite tensile strength. In contrast to the Ramsteiner-Theyson analysis, only one specimen is required to

determine the IFSS. The Bowyer-Bader analysis is more complex than the Ramsteiner-Theyson analysis. The Mittal-Gupta analysis [97,104] is based on the assumption that the stress in the interface increases with the tensile stress in the composite. One major disadvantage of that approach is that it requires the knowledge of the fibre orientation. In terms of complexity, the Mittal-Gupta analysis is comparable to the Bowyer-Bader analysis.

2.4.5 Summary and Conclusion

All presented approaches were shown to detect differences between GF/PP composites and detected the influence of modified PP on the IFSS. The Ramsteiner-Theyson method and the Bowyer-Bader also detected the influence of ambient temperature on the IFSS. No study has systematically compared micromechanical test results with the IFSS values that were obtained from one of the methods described above. Only Mäder and Freitag [58] briefly compared fibre pullout results with values that were obtained from the Mittal-Gupta method. Both methods detected the increase of the IFSS due to the addition of modified PP to the PP matrix but the comparison is limited to two data points.

2.5 Composites based on recycled glass fibres

This section provides an overview of different recycling processes that have been used for glass fibre reinforced plastic (GFRP) waste. Only the recycling of thermoset based composites is discussed since thermoplastics are intrinsically recyclable. The reinforcement potential of thermally recycled glass fibres is discussed in detail.

2.5.1 An overview of recycling processes

Mechanical recycling

Mechanical recycling involves the size reduction of composite waste by cutting or crushing. This process usually involves several stages. In the first stage the composite material is cut or crushed in a low speed process. In a second step the recyclates are further reduced in size by a high speed milling process or hammer milling process. The final size of the particle is typically between 10 mm and 50 µm. Then cyclones and sieves can be used to separate fibrous fractions of the recyclates from finer particles of the recyclates. The mechanically recycled glass fibres have a lower reinforcement potential than new glass fibres. Composites based on these fibres have relatively low mechanical properties. This can be explained

with a reduced fibre length, a reduction of the fibre strength and the lack of interfacial bonding between glass fibres and the polymer matrix. Yang et al. [118] and Pickering [119] published articles that review mechanical recycling processes of GFRP waste. Despite their limitations, several companies have commercialised mechanical recycling processes. Reprocover (Belgium) [120] incorporates grinded GFRP waste into moulded composites which can be used for non-structural applications. Zajon Logistik (Germany) used ground GFRP waste as feedstock in cement kilns. However, their businesses terminated in 2014 because of financial problems [121]. A number of other companies use mechanical recycling processes to recycle their own GFRP waste and several businesses are about to start their glass fibre composite recycling operations [122,123].

Chemical recycling

Chemical recycling processes use supercritical water, glycols, basic solutions or acids to depolymerise and remove the thermoset matrix. Several studies showed that carbon fibres can retain more than 90% of their tensile strength after chemical recycling processes [124,125]. However, a study on the recycling of glass fibres using supercritical water reported a strength reduction of more than 40% [126,127]. Chemical recycling processes are interesting because they allow recycling of both the matrix and the fibres. However, these processes are highly dependent on the matrix composition and chemicals like glycols or acids might be consumed [118,122,128]. To the author's knowledge no chemical recycling process has been commercialised for glass fibre composite waste.

Thermal recycling

Thermal recycling processes can be classified into combustion processes and pyrolysis processes. Pyrolysis recycling processes involve the separation of the glass fibres from the matrix at high temperatures in the absence of oxygen. The polymer matrix is depolymerised into lower weight molecules like oil, gas or solid char. The depolymerised matrix residues can be used for further processing. The solid and liquid can be used as feedstock for polymers and the gas can be used for combustion processes. However, the strength of the glass fibres is reduced due to the exposure to high temperatures. Thus the fibres cannot replace pristine fibres without reducing the properties of the composite. The pyrolysis process has not

been commercialised for GFRP waste because of a disadvantageous ratio between the recycling costs and the value of the recyclates [118,119].

Combustion recycling processes are recycling processes in the presence of oxygen. The combustion process is exothermic and can be used as an energy source. The combustion of GFRP waste in cement kilns has been commercialised. The incombustible components of the composites like glass fibres are used as filler material in cement and the heat released by the exothermic combustion process helps to reduce the fuel consumption of the kiln [119,122]. A fluidised bed process at the University of Nottingham was used to recycle glass fibre composite waste. The process is illustrated in Figure 2.17 below. The GFRP waste is cut to a size of around 25 mm and fed into the fluidised bed. The fluidised bed contains silica sand that is heated by a stream of hot air. The matrix is combusted and the fibres and filler materials are carried by the stream of hot air and gas. The gas is introduced into a secondary combustion chamber after the fibres and filler materials were separated from the gas. The combustion process in the second chamber is used as an energy source. Similar to the pyrolysis process, the strength of the glass fibres was severely reduced due to the exposure to high temperatures [119].

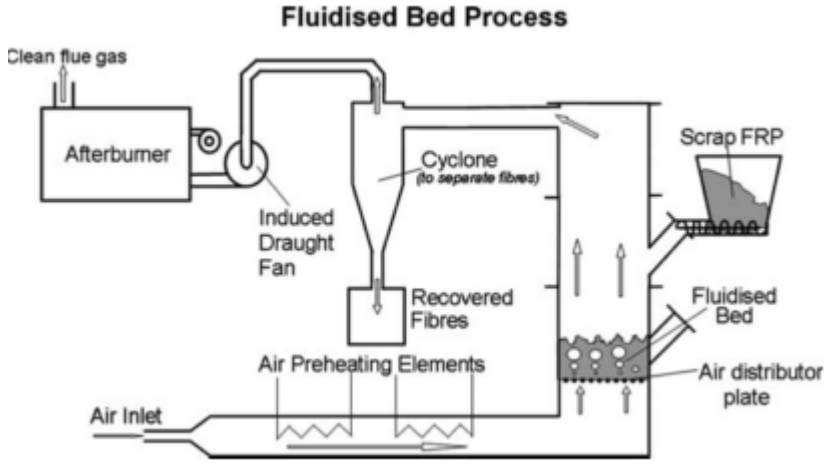

Figure 2.17. Set-up of a fluidised bed process to recycle composites. Reproduced from [119]

The fluidised bed process has not been commercialised for GFRP waste. A study by Pickering et al. [129] showed that a commercial fluidised bed recycling process could reach a break-even point at a scrap capacity of around 9000 t/year. Figure 1.2 in Chapter 2 illustrates that the global production of reinforcement grade glass fibres already exceeded 1 million tonnes in 1980 and reached approximately 5 million tonne in 2014 [130]. In 2013 more than 1 million tonnes of GFRP were produced in

Europe alone [122]. More than 50 % of the GFRPs are based on thermosets [118]. Thus, there would be a sufficient amount of GFRP waste available to run a fluidised bed plant.

Although thermal recycling processes of GFRP waste have not been commercialised they appear to be interesting. In contrast to mechanical recycling processes, thermally recycled glass fibres are relatively clean which improves their reinforcement potential. In addition, thermal recycling processes are already developed and used for carbon fibre composite waste [119,123]. Pickering et al. [129] analysed the economic aspects of the fluidised bed process but they did not discuss the energy balance. The appendix contains a technology assessment with a review of the energy balance.

2.5.2 Properties of composites based on thermally degraded glass fibres

The properties of composites based on thermally recycled glass fibres have been investigated in several studies [131–136]. Other authors investigated the properties of composites based on thermally conditioned glass fibres. The thermal conditioning was performed to imitate thermal recycling conditions [137–139] or to clean the fibres from organic residues [34,112,140]. The mechanical testing data is summarised in Table 2.4. It shows the tensile strength or flexural strength of composites based on thermally recycled or thermally conditioned glass fibres. For comparison the strength of composites based on new glass fibres is also shown (reference composite). Table 2.4 also provides information about the maximum temperature and the time that the fibres were exposed to that temperature. Several processes also involve a heating up and cooling down which is not shown in Table 2.4 for the sake of brevity. It should also be mentioned that the reference material in [34] has a fibre weight fraction of 25% while the composites based on thermally conditioned fibres have a fibre weight fraction of 20%.

Table 2.4. Properties of composites based on thermally recycled or conditioned glass fibres

Matrix	Strength Reference composite [MPa]	Thermal history of glass fibres	Strength composite based on recycled/ conditioned fibres [MPa]	Ref
PP	51-52 (tensile)	500 °C, 12 h	28-29 (tensile)	[34]
Polyester	250-350 (tensile)	500 °C, 20 min	100-150 (tensile)	[137]
Epoxy	220 (tensile)	500 °C, 30 min	85 (tensile)	[138]
Vinylester	100 % (tensile)	550 °C, 2 h	20 % (tensile)	[139]
Polyester	96 (flexure)	450 °C, 1.5 h	89 (flexure)	[131]
Polyester	188.8 (flexure)	Max 400 °C, no isothermal section	61.1 (flexure)	[132]
Polyester	20-27 (tensile)	450 °C, time not stated	14-16 (tensile)	[133]
Polyester	22.9 (tensile)	500 °C, 1.5 h	24 (tensile)	[134]
Polyester	500 (Flexure)	370 °C, 30 min	100 (flexure)	[136]

The data in Table 2.4 shows clearly that the tensile strength and flexural strength of composites based on thermally recycled or conditioned glass fibres is inferior to composites based on new glass fibres. Cunliffe and Williams [131] reported only a slight decrease of the flexural strength. However, that value of the flexural strength was measured when only 25 % of new glass fibres were replaced by recycled fibres. They also produced composites based only on recycled glass fibres but the flexural properties are not reported. It is likely that a higher fraction of recycled fibres caused a larger drop of the flexural strength. Marco et al. [134] reported no significant change of the tensile strength but they also replaced the new glass fibres only partly with recycled glass fibres. In addition, the standard deviation of 30 % might have masked the effect of recycled fibres on the composite properties. Most of the studies in Table 2.4 were based on Polyester. PP might be particularly interesting as matrix

for composites based on thermally recycled fibres because of its beneficial cost to performance ratio and the widespread use. As discussed in Chapter 2.3, the tensile properties of GF/PP composites are dependent on the fibre length and fibre orientation. Different composite manufacturing processes result in different fibre length distributions and fibre orientation distributions. To assess the effect of thermal recycling processes or thermal conditioning on the reinforcement potential of glass fibres it is therefore essential to have a reference composite. The reference composite should be processed in the same way with the same polymer matrix like the recycled glass fibre composite but with new glass fibres. Only one study [34] was found that provides reference data for PP based composites but the reference composite was based on a higher fibre volume fraction.

The reduction of the composite performance in Table 2.4 can be attributed to a reduction of the glass fibre strength and a low interfacial adhesion between fibres and matrix. Feih et al. [139] demonstrated that the tensile strength of continuous glass fibre vinylester composites is solely governed by the fibre strength. However, in discontinuous glass fibre composites the composite performance is also dependent on the interfacial adhesion between glass fibres and matrix. According to the Kelly-Tyson model the shorter the fibres the larger the effect of the IFSS on the composite performance. The degradation of the fibre strength due to exposure to high temperatures and the interfacial adhesion between thermally degraded fibres and the matrix are discussed in the following paragraphs.

2.5.3 Effect of thermal recycling temperatures on glass fibre strength

A number of authors observed a reduction of the fibre strength when reinforcement grade glass fibres were thermally recycled [132,137] or thermally conditioned [133,137–139,141–144]. The level of reduction of the tensile strength is dependent on the temperature and time. Higher temperatures were observed to cause a more severe reduction of the fibre strength. This observation applies to thermally conditioned [139,141–143] and thermally recycled fibres [133,137]. For the sake of simplicity, thermally recycled and thermally conditioned fibres will be referred as thermally degraded fibres. The degradation is in both cases caused by the exposure of the glass fibres to elevated temperatures. Thomas [145] and Feih et al. [139] observed that the tensile strength decreased as a function of time to an asymptotic minimum value. Other studies observed differences between sized fibres and unsized fibres [141–143]. The results of a study by Jenkins et al. [141] in Figure 2.18

show that APS sized glass fibres retained a higher tensile strength than unsized fibres up to a thermal conditioning temperature of 450 °C. Figure 2.18 also shows that a higher fibre strength was retained when the unsized fibres were thermally conditioned as single fibres which was explained with a reduction of mechanical handling damage. Fibre damage due to fibre-fibre interactions was reduced when the unsized fibres were extracted from bundles before the thermal conditioning. The strength of the sized fibres behaved different to the strength of unsized fibres. No difference was observed between single fibres and fibre bundles up to 300 °C conditioning temperature which was explained with the protective effect of the fibre sizing. Above 300 °C conditioning temperature the sizing degraded and the fibres were no longer protected from additional damage due to fibre-fibre interactions when they were thermally conditioned in bundles. Thus, the data in Figure 2.18 demonstrates that fibre-fibre interaction can cause a strength loss of the fibres. The data in Figure 1.16 also shows that the fibre strength dropped at conditioning temperatures higher than 300 °C when the fibres were conditioned as single fibres. Thus, the strength of the glass fibres is also reduced by a fundamental mechanism apart from mechanical damage due to fibre-fibre interactions. The nature of this mechanism is still subject to discussion in literature. The formation of additional surface flaws and changes in the bulk glass were proposed as mechanisms to explain the strength loss of thermally degraded glass fibres. Both mechanisms will be reviewed in the following three paragraphs.

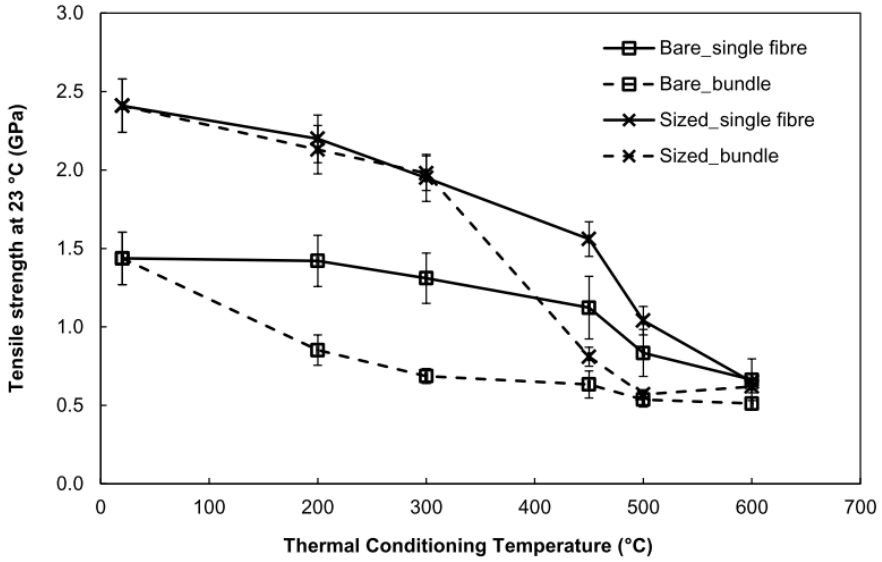

Figure 2.18. Reduction of the tensile strength of bare and APS sized glass fibres after thermal conditioning in air. Fibres treated individually or in bundles. Reproduced from [141]

Early work of Otto [146] suggested that the structure of the glass fibres is affected by thermal conditioning. He reported an increase of the fibre modulus by up to 15 % and a length contraction of approximately 0.23 %. The observations of Otto were recently confirmed by Yang and Thomason [147] who observed similar changes in the fibre modulus and fibre length. The authors explained their findings with enthalpy relaxation and a reorganisation of the hyperquenched glass network which requires temperatures of at least 300 °C. The theory of enthalpy relaxation agrees with a study by Ya et al. [148] who observed an exothermic signal between 300 °C and approximately 700 °C when they performed differential scanning calorimetry (DSC) on glass fibres. The exothermic signal was explained with excess enthalpy that was released during the DSC scan when the glass network went to a lower energy state. Based on birefringence measurements, Ya et al. proposed that the thermal conditioning of glass fibres also leads to anisotropy relaxation. Optical microscopy showed that the birefringence of glass fibres started to drop between 250 °C and 300 °C conditioning temperature. No birefringence was observed when the fibres were conditioned at 550 °C for 3 h. Similar results were reported by Lund and Yue [144] who related anisotropy relaxation to the reduced strength of thermally conditioned glass fibres. They argued that defects like microbubbles are aligned in reinforcement grade glass fibres because of the drawing of the glass melt during the glass fibre manufacturing process. The defects would lose their alignment when they are exposed to elevated temperatures which would result in a drop of the fibre strength.

The theory of structural relaxation was challenged by a recent publication of Feih et al. [149]. They used an ion beam to create flaws in silane sized glass fibres. They demonstrated that glass fibres with artificial surface flaws created by an ion beam have similar tensile properties to thermally degraded fibres. Based on fracture surface analysis and fracture toughness modelling they concluded that the bulk properties of the glass fibres did not change when glass fibres were exposed to thermal recycling temperatures. It was concluded that the strength degradation is solely controlled by surface flaws. The growth of surface flaws at thermal recycling temperatures was attributed to water from the fibre sizing or atmosphere that reacts with siloxane bonds. Figure 2.19 shows an SEM micrograph of a surface flaw on an untested fibre. The surface flaw was produced by the ion beam.

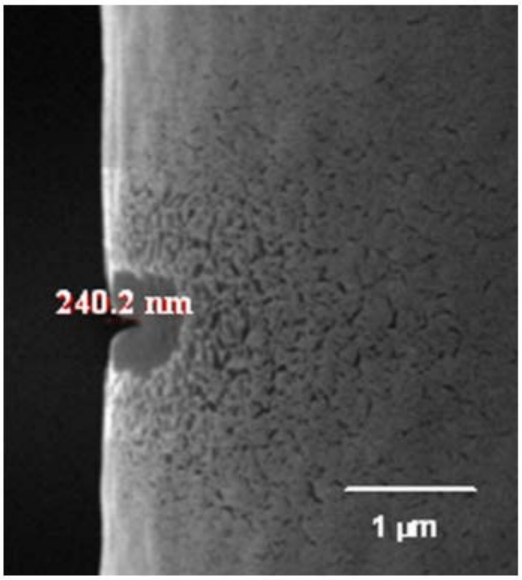

Figure 2.19. SEM image of an E-glass fibre containing notch created by ion beam milling. Reproduced from [149]

The surface flaw theory is further supported by studies on the regeneration of thermally degraded glass fibres which will be discussed in Section 2.6. Etching of thermally degraded fibres using hydrofluoric acid was shown to lead to a reduction of the fibre diameter and an increase of the fibre strength. The main weakness of the surface flaw theory presented by Feih et al. [149] is that no direct observation of surface flaws was reported. Surface flaws similar to the artificial one in Figure 2.19 should have been detected by SEM or atomic force microscopy. A final proof for the surface flaw theory is therefore still required. The role of the water is also not clear. According to Feih et al. atmospheric water and water from the fibre sizing cause the growth of surface flaws. However, it was shown that the immersion of silica rods in hot water (88 °C) can increase their tensile strength [150,151]. That effect was explained by crack blunting [150] and compressive forces [151]. It was proposed that water penetrates the glass network which would lead to a swelling and compressive forces at the crack tips of the silica rods. If reinforcement grade glass fibres behave similar to silica rods their strength loss might be explained with a dehydration due to exposure to elevated temperatures. The dehydration of glass fibres would lead to a lower fracture toughness of the glass fibre because of the absence of compressive forces at the crack tips. However, there is currently no experimental evidence for this speculation [152].

2.5.4 Effect of the thermal recycling temperatures on the IFSS

The strength of composites based on thermally degraded glass fibres is limited due to the lack of interfacial adhesion between glass fibre and polymer matrix [112,132,135,136,138,140]. Fracture surfaces were used as a proof of low interfacial adhesion [112,132] and only a few authors [34,138] have actually measured the IFSS using micromechanical tests. Yang et al. [138] used microbond tests to show that APS on glass fibres lost its functionality after exposure to 500 °C. The IFSS was observed to drop from almost 16 MPa to less than 8 MPa. Roux et al. [34] performed fibre fragmentation tests on GF/PP samples but only the critical fibre length was reported. The fibre diameter and fibre strength were not reported. In addition, error bars were not stated. It is therefore difficult to draw any conclusions about the IFSS. Feih et al. [139] and Kennerley et al. [137] stated that the composite tensile strength was solely dependent on the fibre strength. The influence of the IFSS was not discussed. In contrast to other authors, they used fabrics with continuous glass fibres as reinforcement. Thus, the composite properties will have been less affected by the IFSS. Depending on the polymer matrix composite manufacturer might choose different glass fibre sizings. Thus a large variety of glass fibre sizings is in use and their composition might be confidential. However, most sizings contain an organosilane and a film former [36,153]. Rudzinski et al. [154] performed thermal gravimetric analysis (TGA) on combinations of APS and different film formers. Most of the mass loss was observed between 250 °C and 450 °C. Gao and Su [155] performed isothermal TGA of two different commercial glass fibre sizing. Both sizings degraded completely within 15 min. In a combined TGA Differential scanning calorimetry (DSC) experiment Jenkins et al. [141] observed that APS lost most of its mass between 300 °C and 600 °C. The DSC analysis showed a large exothermic peak between 400 °C and 450 °C. In addition, another exothermic peak and a small mass loss was observed between 200 °C and 250 °C. In addition to APS, Pham and Chern [156] analysed the thermal degradation of several other organosilanes. All of them degraded between 300 °C and 600 °C and the highest rate of mass loss was observed between 400 °C and 450 °C. Based on thermal analysis results and micromechanical testing presented above it appears unlikely that commercial glass fibres sizing can withstand thermal recycling processes without degradation.

2.5.5 Processability of thermally degraded glass fibres

New glass fibres are usually provided by the glass manufacturers in the form of rovings, chopped bundles, mats and yarns. The glass fibres are usually held together by the glass fibre sizing [157]. As discussed above the sizing is degraded by the exposure to thermal recycling temperatures and the fibres might move during the recycling process. Thus, the fibre architecture of the recycled composites might not be retained in thermal recycling processes. In addition, thermal recycling processes might involve some size reduction of the composite waste for the ease of transport and to use the volume of the recycling reactor effectively [131–135]. Thus, the recycled fibres might also be discontinuous. Figure 2.20 shows an example of fibres that were recycled using the fluidized bed process developed at the University of Nottingham [129].

Figure 2.20. Discontinuous and fluffy fibres recovered from SMC sheet using a fluidised bed process. Reproduced from [129]

The fibres in Figure 2.20 are discontinuous and fluffy. Discontinuous fibres composites might be a more likely application for thermally recycled fibres because of the size reduction before the thermal recycling process. Studies by Feih et al. [139], Kennerley et al. [137] and Shi et al. [136] on thermally conditioned continuous glass fibre fabrics are interesting regarding the strength loss of glass fibres but they might not represent future commercial composites based on recycled fibres. Table 2.4 shows that several studies on thermally conditioned or thermally recycled glass fibres were based on unsaturated polyester matrix material. In different studies [131,133,134] discontinuous, thermally recycled glass fibres were processed into polyester based dough moulding compounds. Akesson et al. [132] prepared mats of randomly aligned thermally recycled fibres and impregnated them with polyester in a heated press. To compound thermally conditioned glass fibres with PP, researchers

used twin-screw extruders [34,135] and torque rheometer [112]. Nee and Yang [140] used a papermaking process to incorporate thermally conditioned glass fibres into GMT composites. Thus, DMC processes, extrusion and the papermaking process have been shown to be suitable for thermally recycled or thermally conditioned glass fibres. These processes appear to be suitable because they do not require continuous glass fibres with a specific fibre alignment.

2.5.6 Summary and Conclusion

The main challenges for glass fibre composite recycling is currently the lack of markets and the low profitability due to the low value of the recyclates [118,122]. Mechanical recycling processes have already been commercialised on a small scale. However, mechanically recycled fibres can only be used as low value reinforcement or filler. In contrast to mechanical recycling processes, thermal recycling can provide clean fibres and they do not require the use of chemicals like chemical recycling processes. In addition, they have already been commercialised for carbon fibre composites. The major disadvantages of thermal recycling processes are the reduction of the glass fibre strength and the low interfacial adhesion between thermally recycled fibres and the polymer matrix. The low interfacial adhesion can be explained with a degradation of the fibre sizing. The fibre strength reduction was explained by partly competing theories like the growth of surface flaws and structural changes of the glass. Due to the thermal degradation of the glass fibres the performance of composites based on thermally recycled glass fibres is relatively low. Several authors studied thermoset composites based on thermally recycled glass fibres. Less systematic work was found on the reinforcement potential of thermally recycled glass fibres in PP composites. It can be concluded that a regeneration of thermally recycled glass fibres is necessary to increase the reinforcement potential of thermally recycled glass fibres.

2.6 Regeneration of glass fibres and its effect on composites performance

It was concluded in the previous section that thermally recycled glass fibres need to be regenerated to act as an effective reinforcement in composites. This section reviews approaches to regenerate thermally degraded glass fibres and the effect of fibre regeneration on the mechanical properties of the composites.

2.6.1 Regeneration of fibre strength

Different potential approaches can be found in the literature to regenerate the strength of thermally recycled or thermally conditioned glass fibres. Several studies [27,158,159] showed that the treatment of new glass fibres with APS and film formers can lead to an increase of the measured fibre strength. That effect was explained with a flaw healing theory. It was postulated that particles in APS solutions and films formers can fill flaws in the surface of glass fibres as schematically shown in Figure 2.21. Solutions with smaller particles were found to be more effective than solutions with larger particles because only small particles would fit into the surface flaws. Fracture mechanics has shown that the flaw dimensions are in the range between 200 nm and 400 nm (in z-direction) without sizing and decreased to 75 nm when the fibres were sized with APS and a PP film former [159]. It should be noted that no direct observation of surface flaws as shown in Figure 2.21 could be found in literature. It is likely that surface flaws as shown in Figure 2.21 would have been detected by SEM or atomic force microscopy. The absence of such a proof indicates that the geometry of the surface flaws is different to the one in Figure 2.21.

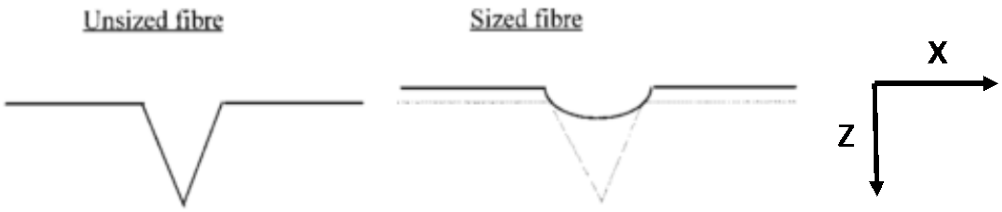

Figure 2.21. Flaw healing theory - effect of glass fibre sizing. Reproduced from [158]

Feih et al. [149] proposed that the low strength of glass fibres after exposure to thermal recycling temperatures can be explained with surface flaws. Based on fracture mechanics and the mechanical testing of glass fibres with artificially created surface flaws they predicted the flaw size. Depending on its shape, the flaw size of new glass fibres was estimated to be between 40 nm and 95 nm as shown in Figure 2.22. After heat treatment at 500 °C the flaw size increased from 200 nm to 600 nm. The surface flaws reported by Feih et al. [149] were larger than the surface flaws determined by Zinck et al. [159] when they explained the beneficial effect of APS and film formers on the measured single fibre strength with the flaw healing theory. The particles of the APS solution should therefore repair surface flaws of thermally degraded glass fibres and the fibres strength should increase. However, there is no clear experimental data that supports this speculation. Sáez et al. [160] and Thomason et al. [143] attempted to regenerate the strength of thermally conditioned

fibres with APS and MethacryloxyPropyltrimethoxySilane (MPS). The treatment with APS and MPS were combined with hydrochloric acid (HCl) treatments. Although the average values of the fibre strength increased the authors stated that the increase of the fibre strength was not significant at 95 % confidence. On the other hand Yang et al. [138] reported in a recent study a significant increase of the tensile strength of thermally degraded fibres fibres after an APS treatment. The reason for these conflicting observations between studies by Zinck et al. [158,159], Mäder et al. [27] and Sáez et al. [160] and Thomason et al. [143] cannot be explained in this review. Yang and Thomason [161] argued against the existence of the flaw healing mechanism and suggested that APS might only increase the measured fibre strength because it protects the fibres from damage. According to their hypothesis, the treatment of glass fibres with APS maintains the fibre strength but it does not lead to an increase of the fibre strength. Thus, the post treatment of thermally degraded fibres with APS might have a beneficial effect on the fibre strength even if the flaw healing theory does not apply. All the studies mentioned above prepared APS at room temperature. Sáez et al. [162] filed a patent which claims that APS can be used to regenerate thermally degraded glass fibres when the APS is hydrolysed at 83 °C. It was proposed that the hydrolysis at 83 °C promotes the formation of crosslinks in the APS. The crosslinked structures in the APS would be able to heal flaws of thermally degraded glass fibres [163].

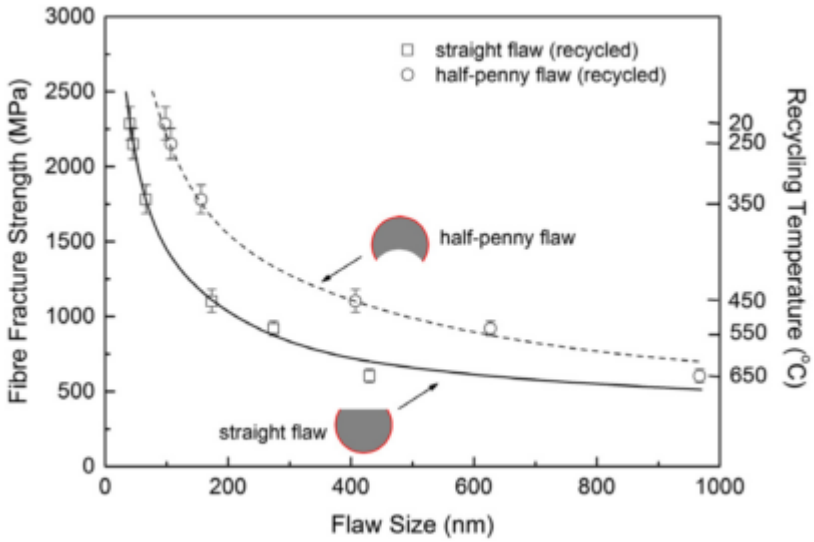

Figure 2.22. Reduction of fibre fracture stress as a function of flaw size and recycling temperature. Reproduced from [149]

While the treatment of thermally degraded glass fibres with silane aims to repair the fibre surface, other studies showed that etching can lead to an increase of the

tensile strength of thermally degraded fibres. Early work by Aslanova [164] and Sakka [165] showed that the strength of glass fibres can be increased by treatment in hydrofluoric acid (HF). This was confirmed in a more recent study [138] which showed that the strength improvement of the glass fibres was dependent on the treatment time and the concentration of the HF solution. The authors explained the strength regeneration with the etching of damaged surface layers and the modification of existing cracks. In that study thermally degraded and regenerated fibres were incorporated into epoxy composites [138]. The tensile strength and the tensile strain at break of the composites improved when the thermally degraded glass fibres were regenerated with HF. In contrast, the unnotched impact strength and notched impact strength did not increase which was explained with the lack of energy dissipation in the interphase. While HF is proven to be effective in the regeneration of the glass fibre strength, it is also highly toxic. The same patent mentioned above [162] also describes how the strength of thermally degraded glass fibres can be regenerated using a sodium hydroxide (NaOH) solution. In contrast to the HF treatment, no significant reduction of the fibre diameter was observed when the fibres were treated with NaOH. However, it is commonly known that NaOH dissolves glass. It is likely that the NaOH treatment of glass fibres as reported in [162,163] causes a small fibre diameter reduction. The changes might not have detected because the fibre diameter was measured with an optical microscope which might not be sensitive enough to detect the diameter changes. Further details of the NaOH treatment can be found in [163]. In a recently published work [166] the properties of composites based on NaOH regenerated glass fibres are presented. These results are part of this thesis and are discussed in Chapter 6.

2.6.2 Regeneration of the surface functionality

As discussed in section 2.5.4 the organic coating on glass fibres is degraded due to thermal recycling temperatures which limits the interfacial adhesion between fibre and matrix and reduces the composite performance. Yang et al. [138] performed microbond tests to demonstrate that the surface functionality of thermally degraded fibres can be regenerated. The interfacial adhesion between glass fibres and PP was completely regenerated when the thermally degraded fibres were treated with APS. The tensile properties and impact properties of epoxy based glass fibre composites also improved significantly when the thermally degraded fibres were resized with APS. Figure 2.23 shows that the largest improvement of the composite tensile strength was observed for a combination of treatments. The fibre strength

was regenerated by etching in HF and APS was applied after the etching. Bikiaris et al. [112] observed that the treatment of thermally degraded glass fibres with aminopropyltrimethoxysilane and APS caused changes in the morphology of the composite fracture surfaces. The silane treated fibres on the fracture surface were observed to be covered in the PP matrix. In contrast, the surface of the untreated fibres were not covered with PP residues. Lee and Jang [140] applied vinylbenzylaminoethyl-aminopropyltrimethoxy silane on thermally degraded glass fibres. Fibre fragmentation tests on single fibre PP composites showed an improvement of the IFSS due to the silane treatment. Kennerley et al. [133] did not observe an improvement in the performance of polyester based composites when the thermally degraded fibres were resized with MPS. The absence of any effect of the MPS might be explained with the large deviations between the samples which might have masked the effect of the MPS.

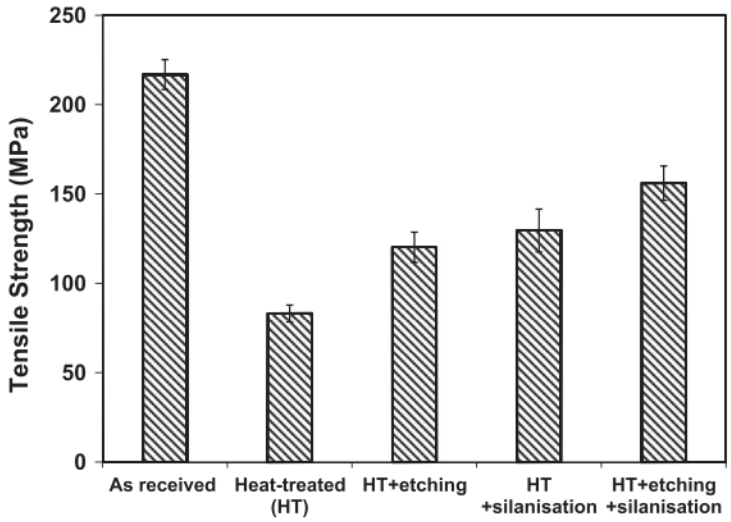

Figure 2.23. Recovery of the tensile strength of glass fibre epoxy composites due to the regeneration of thermally degraded glass fibres. Reproduced from [138]

2.6.3 Summary and Conclusion

Different methods are available to regenerate the strength of thermally degraded glass fibres. These methods can be classified according to their mechanism of action. The treatment of fibres with acid solutions or basic solutions aims to remove or modify surface flaws. It has been known for more than fifty years that HF can increase the strength of glass fibres. It was recently confirmed that HF can also regenerate thermally degraded glass fibres and the tensile strength of the composites increased when the fibres were regenerated. The use of NaOH is a new method to regenerate the strength of thermally degraded glass fibres. The major

advantage of NaOH is its relatively low toxicity compared to HF. No data has been published on the performance of composites based on NaOH regenerated glass fibres apart from data that was generated as part of this thesis [166]. The application of silanes might help to repair surface flaws of thermally degraded glass fibres. In addition, the surface functionality of thermally degraded glass fibres can be regenerated by the application of silanes. The regeneration of the fibre surface functionality improved the interfacial adhesion between fibre and matrix, the tensile strength and impact strength of composites. In conclusion, the regeneration of thermally degraded glass fibres can increase the reinforcement potential of thermally degraded glass fibres. To maximise the reinforcement potential both the fibre strength and the surface functionality must be regenerated.

2.7 Summary and Conclusion

This review shows that the microstructural and macromechanical properties of discontinuous GF/PP composites are well researched and methods to characterise these properties are developed. Nevertheless, some gaps in published literature were found which will be addressed in this thesis:

- It is well known that MAPP can lead to an increase of the composite performance. Less work has been done on the relationship between fibre content and the amount of coupling agent that is required to optimise composite performance. The correlation between fibre content and optimum MAPP content in long fibre thermoplastic composites has been investigated. However, no such systematic data on short fibre composites could be found in literature.
- Different methods were developed to derive the IFSS from composite tensile test data but no comprehensive comparison exists between these methods and single fibre test methods like the microbond test.

The review of published literature showed that composites based on thermally recycled glass fibres have lower mechanical properties than composites based on new glass fibres. The reduced mechanical properties were explained with a degradation of the glass fibres during thermal recycling processes. Thermally degraded glass fibres have a lower tensile strength than new glass fibres and degradation of the sizing leads to a low IFSS in the composites. A recent study showed that the regeneration of the fibre strength with HF and the reactivation of the

fibre surface with APS can improve the mechanical properties of composites significantly. The following areas require further research and will be investigated in this thesis:

- Despite widespread use of PP, little work has been done on the reinforcement potential of thermally degraded glass fibres in PP composites. A more comprehensive study [167] was published based on data that is presented in Chapter 5 of this thesis.
- Recently it was demonstrated that the strength of glass fibres can be regenerated without the use of hazardous HF. The performance of composites based on these fibres has not been reported in literature apart from work [166] that is part of Chapter 6 of this thesis.

2.8 References

[1] Turkovich R, Erwin L. Fiber fracture in reinforced thermoplastic processing. Polym Eng Sci 1983;23:743–9.

[2] Gupta VB, Mittal RK, Sharma PK, Mennig G, Wolters J. Some studies on glass fiber-reinforced polypropylene. Part 1: Reduction in fiber length during processing. Polym Compos 1989;10:8–15.

[3] Fisa B. Mechanical degradation of glass fibers during compounding with polypropylene. Polym Compos 1985;6:232–41.

[4] Fu S-Y, Lauke B, Mäder E, Yue C-Y, Hu X. Tensile properties of short-glass-fiber- and short-carbon-fiber-reinforced polypropylene composites. Compos Part A Appl Sci Manuf 2000;31:1117–25.

[5] Ota WN, Amico SC, Satyanarayana KG. Studies on the combined effect of injection temperature and fiber content on the properties of polypropylene-glass fiber composites. Compos Sci Technol 2005;65:873–81.

[6] Spahr DE, Friedrich K, Schultz JM, Bailey RS. Microstructure and fracture behaviour of short and long fibre-reinforced polypropylene composites. J Mater Sci 1990;25:4427–39.

[7] Thomason JL. The influence of fibre length and concentration on the properties of glass fibre reinforced polypropylene: 5. Injection moulded long and short fibre PP. Compos Part A Appl Sci Manuf 2002;33:1641–52.

[8] Phelps JH, Abd El-Rahman AI, Kunc V, Tucker CL. A model for fiber length attrition in injection-molded long-fiber composites. Compos Part A Appl Sci Manuf 2013;51:11–21.

[9] Shimizu Y, Arai S, Kawamoto H. Experimental analysis of the kneading disk region in a co-rotating twin screw extruder: Part 2. glass-fiber degradation during compounding. Adv Polym Technol 1997;16:25–32.

[10] Franz BN, Klason C, Kuba JT, Kitano T. Fibre degradation during processing of short fibre reinforced thermoplastics. Composites 1989;20:65–76.

[11] Lunt JM, Shortall JB. The effect of extrusion compounding on fibre degradation and strength properties in short glass-fibre-reinforced nylon 6.6. Plast Rubber Process 1979;4:108–14.

[12] Vu-Khanh T, Denault J, Habib P, Low A. The effects of injection molding on the mechanical behavior of long-fiber reinforced PBT/PET blends. Compos Sci Technol 1991;40:423–35.

[13] Yilmazer U, Cansever M. Effects of processing conditions on the fiber length distribution and mechanical properties of glass fiber reinforced nylon-6. Polym Compos 2002;23:61–71.

[14] Davidson N, Clarke A. Extending the dynamic range of fibre length and fibre aspect ratios by automated image analysis. J Microsc 1999;196:266–72.

[15] Chinga-Carrasco G, Solheim O, Lenes M, Larsen A. A method for estimating the fibre length in fibre-PLA composites. J Microsc 2013;250:15–20.

[16] International Organization for Standardization. Plastics —Glass-fibre-reinforced products — Determination of fibre length BS ISO 22314 2006;3.

[17] Hartwich MR, Höhn N, Mayr H, Sandau K, Stengler R. FASEP ultra-automated analysis of fibre length distribution in glass-fibre-reinforced products. Opt. Meas. Syst. Ind. Insp. VI, 2009.

[18] Dahl J, Blanchard P, Latimer T, Sudrla J, Henshaw J. A method for characterizing fiber length distribution in random fiber composites 2011. http://www.speautomotive.com/SPEA_CD/SPEA2011/pdf/VPT/VPT1.pdf (accessed January 12, 2016).

[19] Weber C, Rannenberg C. Method of determining an average length of reinforcing fiber in a sample of reinforcing fibers US 6925857 B2, 2005.

[20] Zhu YT, Blumenthal WR, Lowe TC. Determination of non-symmetric 3-D fiber-orientation distribution and average fiber length in short-fiber composites. J Compos Mater 1997;31:1287–301.

[21] Zak G, Haberer M, Park CB, Benhabib B. Estimation of average fibre length in short-fibre composites by a two-section method. Compos Sci Technol 2000;60:1763–72.

[22] Fu S, Mai Y, Ching EC, Li RKY. Correction of the measurement of fiber length of short fiber reinforced thermoplastics. Compos Part A Appl Sci Manuf 2006;33:1549–55.

[23] Inceoglu F, Ville J, Ghamri N, Pradel JL, Durin A, Valette R, Vergnes, B. Correlation between processing conditions and fiber breakage during compounding of glass fiber-reinforced polyamide. Polym Polym Compos 2008;16:101–13.

[24] Thomason JL. The influence of fibre length, diameter and concentration on the modulus of glass-fibre reinforced polyamide 6,6. Compos Part A Appl Sci Manuf 2009;40:114–24.

[25] Thomason JL. Micromechanical parameters from macromechanical measurements on glass reinforced polypropylene. Compos Sci Technol 2002;62:1455–68.

[26] Lafranche E, Krawczak P, Ciolczyk JP, Maugey J. Injection moulding of long glass fibre reinforced polyamide 6-6: Guidelines to improve flexural properties. Express Polym Lett 2007;1:456–66.

[27] Mäder E, Moos E, Karger-Kocsis J. Role of film formers in glass fibre reinforced polypropylene - new insights and relation to mechanical properties. Compos Part A Appl Sci Manuf 2001;32:631–9.

[28] Sandau K, Ohser J. The chord length transform and the segmentation of crossing fibres. J Microsc 2007;226:43–53.

[29] Thomason JL. The influence of fibre length, diameter and concentration on the impact performance of long glass-fibre reinforced polyamide 6,6. Compos Part A Appl Sci Manuf 2009;40:114–24.

[30] Wall D. The processing of fiber reinforced thermoplastics using co-rotating twin screw extruders. Polym Compos 1989;10:98–102.

[31] Thomason JL. Structure-Property Relationship in Glass-Reinforced Polyamide, Part 1: The effects of fibre content. Polym Compos 2006;16:101–13.

[32] Mittal RK, Gupta VB, Sharma PK. Theoretical and experimental study of fibre attrition during extrusion of glass-fibre-reinforced polypropylene. Compos Sci Technol 1988;31:295–313.

[33] Thomason JL. The influence of fibre length and concentration on the properties of glass fibre reinforced polypropylene. 6. The properties of injection moulded long fibre PP at high fibre content. Compos Part A Appl Sci Manuf 2005;36:995–1003.

[34] Roux C, Denault J, Champagne MF. Parameters regulating interfacial and mechanical properties of short glass fiber reinforced polypropylene. J Appl Polym Sci 2000;78:2047–60.

[35] Kim Y-K, Mai Y-W. Engineered interfaces in fibre reinforced composites. Amsterdam: Elsevier Ltd; 1998.

[36] Clyne DHTW. An introduction to composite materials. Second Edi. Cambridge (United Kingdom): Cambridge University Press; 1996.

[37] Sockalingam S, Nilakantan G. Fiber-matrix interface characterization through the microbond test. Int J Aeronaut Sp Sci 2012;13:282–95.

[38] Yang L, Thomason JL. Interface strength in glass fibre–polypropylene measured using the fibre pull-out and microbond methods. Compos Part A Appl Sci Manuf 2010;41:1077–83.

[39] Zhandarov S, Mäder E. Characterization of fiber/matrix interface strength: applicability of different tests, approaches and parameters. Compos Sci Technol 2005;65:149–60.

[40] Yang L, Thomason JL. Development and application of micromechanical techniques for characterising interfacial shear strength in fibre-thermoplastic composites. Polym Test 2012;31:895–903.

[41] Thomason JL, Yang L. Temperature dependence of the interfacial shear strength in glass–fibre polypropylene composites. Compos Sci Technol 2011;71:1600–5.

[42] Yang L, Thomason JL, Zhu W. The influence of thermo-oxidative degradation on the measured interface strength of glass fibre-polypropylene. Compos Part A Appl Sci Manuf 2011;42:1293–300.

[43] Auvray MH, Chéneau-Henry P, Leroy FH, Favre JP. Pull-out testing of carbon/bismaleimide systems in the temperature range 20–250°C. Composites 1994;25:776–80.

[44] Zhandarov S, Mader E, Yurkevich OR. Indirect estimation of fiber/polymer bond strength and interfacial friction from maximum load values recorded in the microbond and pull-out tests. Part 1: local bond strength. J Adhes Sci Technol 2002;16:1171–200.

[45] Schüller T, Bahr U, Beckert W, Lauke B. Fracture mechanics analysis of the microbond test. Compos Part A Appl Sci Manuf 1998;29:1083–9.

[46] Downes KA, Thomason JL. A method to measure the influence of humidity and temperature on the interfacial adhesion in polyamide composites. Compos Interfaces 2015;22:757–66.

[47] Morlin B, Czigany T. Cylinder test: Development of a new microbond method. Polym Test 2012;31:164–70.

[48] Nishikawa M, Okabe T, Hemmi K, Takeda N. Micromechanical modeling of the microbond test to quantify the interfacial properties of fiber-reinforced composites. Int J Solids Struct 2008;45:4098–113.

[49] Miller B, Gaur U, Hirt D. Measurement and mechanical aspects of the microbond pull-out technique for obtaining fiber/resin interfacial shear strength. Compos Sci Technol 1991;42:207–19.

[50] Chou C., Gaur U, Miller B. The effect of microvise gap width on microbond pull-out test results. Compos Sci Technol 1994;51:111–6.

[51] Miller B, Muri P, Rebenfeld L. A microbond method for determination of the shear strength of a fiber/resin interface. Compos Sci Technol 1987;28:17–32.

[52] Mäder E, Pisanova E. Characterization and design of interphases in glass fiber reinforced polyproplyene. Polym Compos 2000;21:361–8.

[53] Hampe A, Marotzke C. The energy release rate of the fiber/polymer matrix interface: Measurement and theoretical analysis. J Reinf Plast Compos March 1997;16:341–52.

[54] Marotzke C. Influence of fiber length on the stress transfer from glass and carbon fibers into a thermoplastic matrix in the pull-out test. Compos Interfaces 1993;1:153–66.

[55] Gray RJ. Analysis of the effect of embedded fibre length on fibre debonding and pull-out from an elastic matrix - Part 2 Application to a steel fibre-cementitious matrix composite system. J Mater Sci 1984;19:1680–91.

[56] Meretz S, Auersch W, Marotzke C, Schulz E, Hampe A. Investigation of morphology-dependent fracture behaviour with the single-fibre pull-out test. Compos Sci Technol 1993;48:285–90.

[57] Gonon L, Momtaz A, Van Hoyweghen D, Chabert B, Gérard JF, Gaertner R. Physico-Chemical and micromechanical analysis of the interface in a poly(phenylene sulfide)/glass fiber composite—a microbond study. Polym Compos 1996;17:265–74.

[58] Mäder E, Freitag K-H. Interface properties and their influence on short fibre composites. Composites 1990;21:397–402.

[59] Mäder E, Jacobasch HJ, Grundke K, Gietzelt T. Influence of an optimized interphase on the properties of polypropylene/glass fibre composites. Compos Part A Appl Sci Manuf 1996;27:907–12.

[60] Thomason JL, Van Royen AA. Transcrystallized interphase in thermoplastic composites: Part I Influence of fibre type and crystallization temperature. J Mater Sci 1992;27:889–96.

[61] Arroyo M, Lopez-Manchado MA, Avalos F. Crystallization kinetics of polypropylene: II. Effect of the addition of short glass fibres. Polymer (Guildf) 1997;38:5587–93.

[62] Avalos F, Lopez-Manchado MA, Arroyo M. Crystallization kinetics of polypropylene III. Ternary composites based on polypropylene/low density polyethylene blend matrices and short glass fibres. Polymer (Guildf) 1998;39:6173–8.

[63] Thomason JL, Van Royen AA. Transcrystallized interphase in thermoplastic composites: Part II Influence of interfacial stress, cooling rate, fibre properties and polymer molecular weight. J Mater Sci 1992;27:897–907.

[64] Yue CY, Cheung WL. The morphology, character and strength of the interface in glass fibre-polypropylene composites. J Mater Sci 1991;26:870–80.

[65] Misra A, Deopura BL, Xavier SF, Hartley FD, Peters RH. Transcrystallinity in injection molded polypropylene glass fibre composites. Appl Macromol Chem Sci 1982;113:113–20.

[66] Guo M, Yang H, Tan H, Wang C, Zhang Q, Du R, Fu, Q. Shear enhanced fiber orientation and adhesion in PP/glass fiber composites. Macromol Mater Eng 2006;291:239–46.

[67] Wagner HD, Lustiger A, Marzinsky CN, Mueller RR. Interlamellar failure at transcrystalline interfaces in glass/polypropylene composites. Compos Sci Technol 1993;48:181–4.

[68] Nagae S, Otsuka Y, Nishida M, Shimizu T, Takeda T, Yumitori S. Transcrystallization at glass fibre/polypropylene interface and its effect on the improvement of mechanical properties of the composites. J Mater Sci Lett 1995;14:1234–6.

[69] Zheng A, Wang H, Zhu X, Masuda S. Studies on the interface of glass fiber-reinforced polypropylene composite. Compos Interfaces 2002;9:319–33.

[70] Plueddemann EP. Mechanism of adhesion through silane coupling agents. Compos. Mater. Vol. 6 Interfaces Polym. Matrix Compos., Academic Press Incorporated; 1974, p. 173–216.

[71] Nygård P, Redford K, Gustafson C-G. Interfacial strength in glass fibre-polypropylene composites: influence of chemical bonding and physical entanglement. Compos Interfaces 2002;9:365–88.

[72] Su D-T, Chang G-Y, Lee M-S. A study of interfacial phenomena in the glass-fiber/PP composite. ANTEC, 1989, p. 531–4.

[73] Gupta VB, Mittal RK, Sharma PK. Some studies on Glass Fiber-Reinforced Polypropylene. Part II: Mechanical Properties and Their Dependence on Fiber Length, Interfacial Adhesion, and Fiber Dispersion. Polym Compos 1989;10:16–27.

[74] Xavier SF, Misra A. Influence of glass fiber content on the morphology and mechanical properties in injection molded polypropylene composites. Polym Compos 1985;6:93–9.

[75] Lee N-J, Jang J. The effect of fibre content on the mechanical properties of glass fibre mat/polypropylene composites. Compos Part A Appl Sci Manuf 1999;30:815–22.

[76] Thomason JL, Vlug MA, Schipper G, Krikort HGLT. Influence of fibre length and concentration on the properties of glass fibre-reinforced polypropylene Part 3 Strength and strain at failure. Compos Part A Appl Sci Manuf 1996;27A:1075–84.

[77] Ericson M, Berglund L. Deformation and fracture of glass-mat- reinforced polypropylene. Compos Sci Technol 1992;43:269–81.

[78] Ericson ML, Berglund LA. Effect of microstructure on the elastic modulus and strength of preformed and commercial GMTs. Polym Compos 1993;14:35–41.

[79] Thomason JL. The influence of fibre length and concentration on the properties of glass fibre reinforced polypropylene: 7. Interface strength and fibre strain in injection moulded long fibre PP at high fibre content. Compos Part A Appl Sci Manuf 2007;38:210–6.

[80] Stokes VK. Random glass mat reinforced thermoplastic composites Part IV: Characterization of the tensile strength. Polym Compos 1990;11:354–67.

[81] Cantwell WJ, Tato W, Kausch HH, Jacquemet R. The Influence of a Fiber-Matrix Coupling Agent on the Properties of a Glass Fiber / Polypropylene GMT. J Thermoplast Compos Mater 1992;5:304–17.

[82] Thomason JL, Schoolenberg GE. An investigation of glass fibre/polypropylene interface strength and its effect on composite properties. Composites 1994;25:197–203.

[83] Davies P, Månson J-A, Roulin M, Kausch HH, Echalier B, Jacquemet R. Structure and properties of a stampable thermoplastic composite. J Thermoplast Compos Mater 1991;4:285–98.

[84] Bowland C. A formulation study of long fiber thermoplastic polypropylene (Part1): The effects of coupling agent, glass content & resin properties on mechanical properties. Automot. Compos. Conf. Expo., 2008.

[85] Bowland C. A formulation study of long fiber thermoplastic polypropylene (Part 2): The effects of coupling agent type and properties. Automot. Compos. Conf. Expo., 2009.

[86] Rijsdijk HA, Contant M, Polymers C, Box PO, Eindhoven MB. Continuous-glass-fibre-reinforced polypropylene composites: 1. Influence of maleic-anhydride-modified polypropylne on mechanical properties. Compos Sci Technol 1993;48:161–72.

[87] Thomason JL, Vlug MA. The influence of fibre length and concentration on the properties of glass fibres reinforced polypropylene: 1. Tensile and flexural modulus. Compos Part A Appl Sci Manuf 1996;27:477–84.

[88] Gayle D, Tomkinson-Walles. Performance of random glass mat reinforced thermoplastics. J Thermoplast Compos Mater 1988;1:94–106.

[89] Qiu W, Endo T, Hirotsu T. Interfacial interaction, morphology, and tensile Properties of a composite of highly crystalline cellulose and maleated polypropylene. Eur Polym J 2006;42:1059–68.

[90] Schultz J, Lavielle L, Carre A, Comien P. Surface properties and adhesion mechanisms of graft polypropylenes. J Mater Process Technol 1989;24:4363–9.

[91] Gong L, Friend AD, Wool RP. Polymer-solid interfaces: Influence of sticker groups on structure and strength. Macromolecules 1998;31:3706–14.

[92] Tan Beck NC, Peiffer DG, Briber RM. Reactive reinforcement of polystyrene/poly(2-vinylpyridine) interfaces. Macromolecules 1996;29:4969–75.

[93] Ganster J, Fink HP, Pinnow M. High-tenacity man-made cellulose fibre reinforced thermoplastics - Injection moulding compounds with polypropylene and alternative matrices. Compos Part A Appl Sci Manuf 2006;37:1796–804.

[94] Goda K, Miwa Y, Kodama H. Effect of IFSS on tensile strength of unidirectional fiber composites using 3D-FEM simulation. Adv Compos Mater 2003;12:73–89.

[95] Kelly A, Tyson WR. Tensile properties of fibre-reinforced metals: Copper/tungsten and copper/molybdenum. J Mech Phys Solids 1965;13:329–50.

[96] Matikas TE. Analysis of load transfer behaviour and determination of interfacial shear strength in single-fibre reinforced titanium alloys. Adv Compos Lett 2007;15:181–92.

[97] Mittal RK, Gupta VB, Sharma P. The effect of fibre orientation on the interfacial shear stress in short fibre-reinforced polypropylene. J Mater Sci 1987;22:1949–55.

[98] Nilson G, Ericson ML, Holmberg JA. Flow induced fiber orientation in compression molded glass mat thermoplastics. Polym Compos 2000;21:1007–13.

[99] Templeton PA. Strength predictions of injection molding compounds. J Reinf Plast Compos 1990;9:210–25.

[100] Bowyer WH, Bader MG. On the re-inforcement of thermoplastics by imperfectly aligned discontinuous fibres. J Mater Sci 1972;7:1315–21.

[101] Fu SY, Lauke B. Effects of fiber length and fiber orientation distributions on the tensile strength of short-fiber-reinforced polymers. Compos Sci Technol 1996;56:1179–90.

[102] Fukuda H, Chou TW. A probabilistic theory of the strength of short-fibre composites with variable fibre length and orientation. J Mater Sci 1982;17:1003–11.

[103] Piggott R. Short Fibre Polymer Composites : A fracture-based theory of fibre reinforcement 1994.

[104] Mittal RK, Gupta VB. The strength of the fibre-polymer interface in short glass fibre-reinforced polypropylene. J Mater Sci 1982;17:3179–88.

[105] Stokes VK. Random glass mat reinforced thermoplastic composites. Part I: Phenomenology of tensile modulus variations. Polym Compos 1990;11:32–44.

[106] Cox HL. The elasticity and strength of paper and other fibrous materials. Br J Appl Phys 2002;3:72–9.

[107] Krenchel H. Theoretical investigations of the elasticity and strength of fibre-cement. Fibre Reinf., Alademisk forlag; 1964, p. 11–38.

[108] Tucker CL, Liang E. Stiffness predictions for unidirectional short-fiber composites : Review and evaluation. Compos Sci Technol 1999;59:655–71.

[109] Lusti HR, Hine PJ, Gusev A a. Direct numerical predictions for the elastic and thermoelastic properties of short fibre composites. Compos Sci Technol 2002;62:1927–34.

[110] Hassan A, Rahman NA, Yahya R. Extrusion and injection-molding of glass fiber/MAPP/polypropylene: effect of coupling agent on DSC, DMA, and mechanical properties. J Reinf Plast Compos 2011;30:1223–32.

[111] Sato N, Kurauchi T, Sato S, Kamigaito O. Microfailure behaviour of randomly dispersed short fibre reinforced thermoplastic composites obtained by direct SEM observation. J Mater Sci 1991;26:3891–8.

[112] Bikiaris D, Matzinos P, Larena A, Flaris V, Panayiotou C. Use of silane agents and poly(propylene-g-maleic anhydride) copolymer as adhesion promoters in glass fiber/polypropylene composites. J Appl Polym Sci 2001;81:701–9.

[113] Curtis PT, Bader MG, Bailey JE. The stiffness and strength of a polyamide thermoplastic reinforced with glass and carbon fibres. J Mater Sci 1978;13:377–90.

[114] Chawla KK. Micromechanics of composites. Compos. Mater. Sci. Eng., Springer; 2011, p. 337–83.

[115] Ericson ML, Berglund LA. Processing and mechanical properties of orientated preformed glass-mat-reinforced thermoplastics. Compos Sci Technol 1993;49:121–30.

[116] Gupta VB, Mittal RK, Goel M. Energy absorbing mechanisms in short-glass-fibre-reinforced polypropylene 1990;37:353–69.

[117] Ramsteiner F, Theysohn R. Tensile and impact strengths of unidirectional, short fibre-reinforced thermoplastics. Composites 1979;10:111–9.

[118] Yang Y, Boom R, Irion B, van Heerden D-J, Kuiper P, de Wit H. Recycling of composite materials. Chem Eng Process Process Intensif 2012;51:53–68.

[119] Pickering SJ. Recycling technologies for thermoset composite materials—current status. Compos Part A Appl Sci Manuf 2006;37:1206–15.

[120] Reprocover SA. Company Website Reprocover SA n.d. http://www.reprocover.com/en/company (accessed December 7, 2015).

[121] Zajons kämpft ums Überleben. Landeszeitung Für Die Lüneburg Heide GmbH 2014.

[122] Job S. Recycling glass fibre reinforced composites – history and progress. ReinforcedPlastics 2013;57:19–23.

[123] Job S. Recycling composites commercially. Reinf Plast 2014;58:32–8.

[124] Piñero-Hernanz R, García-Serna J, Dodds C, Hyde J, Poliakoff M, Cocero MJ, Kingman S, Pickering S, Lester E. Chemical recycling of carbon fibre composites using alcohols under subcritical and supercritical conditions. J Supercrit Fluids 2008;46:83–92.

[125] Liu Y, Meng L, Huang Y, Du J. Recycling of carbon/epoxy composites. J Appl Polym Sci 2004;94:1912–6.

[126] Kao CC, Ghita OR, Hallam KR, Heard PJ, Evans KE. Mechanical studies of single glass fibres recycled from hydrolysis process using sub-critical water. Compos Part A Appl Sci Manuf 2012;43:398–406.

[127] Oliveux G, Bailleul J-L, Salle ELG La. Chemical recycling of glass fibre reinforced composites using subcritical water. Compos Part A Appl Sci Manuf 2012;43:1809–18.

[128] Asmatulu E, Twomey J, Overcash M. Recycling of fiber-reinforced composites and direct structural composite recycling concept. J Compos Mater 2014;48:593–608.

[129] Pickering SJ, Kelly RM, Kennerley JR, Rudd CD, Fenwick NJ. A fluidised-bed process for the recovery of glass fibres from scrap thermoset composites bundles. Compos Sci Technol 2000;60:509–23.

[130] Owens Corning Investor Presentation 2015. http://s1.q4cdn.com/942908807/files/doc_presentations/2015/Q3/Q3-Presentation-v9.pdf (accessed April 3, 2016).

[131] Cunliffe AM, Williams PT. Characterisation of products from the recycling of glass fibre reinforced polyester waste by pyrolysis. Fuel 2003;82:2223–30.

[132] Akesson D, Foltynowicz Z, Christeen J, Skrifvars M. Microwave pyrolysis as a method of recycling glass fibre from used blades of wind turbines. J Reinf Plast Compos 2012;31:1136–42.

[133] Kennerley JR, Kelly RM, Fenwick NJ, Pickering SJ, Rudd CD. The characterisation and reuse of glass fibres recycled from scrap composites by the action of a fluidised bed process. Compos Part A Appl Sci Manuf 1998;29:839–45.

[134] Marco I De, Legarreta JA, Laresgoiti MF, Torres A, Cambra JF, Jesu M, Caballero, B. Recycling of the products obtained in the pyrolysis of fibre-glass polyester SMC 1997;50:187–92.

[135] Li S, Sun S, Liang H, Zhong S, Yang F. Production and characterization of polypropylene composites filled with glass fibre recycled from pyrolysed waste printed circuit board. Environ Technol 2014;35:2743–51.

[136] Shi J, Bao L, Kobayashi R, Kato J, Kemmochi K. Reusing recycled fibers in high-value fiber-reinforced polymer composites: Improving bending strength by surface cleaning. Compos Sci Technol 2012;72:1298–303.

[137] Kennerley JR, Fenwick NJ, Pickering SJ, Rudd CD. The properties of glass fibers recycled from the thermal processing of scrap thermoset composites. J Vinyl Addit Technol 1997;3:58–63.

[138] Yang L, Sáez Rodríguez E, Nagel U, Thomason JL. Can thermally degraded glass fibre be regenerated for closed-loop recycling of thermosetting composites? Compos Part A Appl Sci Manuf 2015;72:167–74.

[139] Feih S, Boiocchi E, Mathys G, Mathys Z, Gibson AG, Mouritz AP. Mechanical properties of thermally-treated and recycled glass fibres. Compos Part B Eng 2011;42:350–8.

[140] Lee N-J, Jang J. The use of a mixed coupling agent system to improve the performance of polypropylene-based composites reinforced with short-glass-fibre mat. Compos Sci Technol 1998;57:1559–69.

[141] Jenkins PG, Yang L, Liggat J., Thomason JL. Investigation of the strength loss of glass fibre after thermal conditioning. J Mater Sci 2014;50:1050–7.

[142] Thomason JL, Kao CC, Ure J, Yang L. The strength of glass fibre reinforcement after exposure to elevated composite processing temperatures. J Mater Sci 2013;49:153–62.

[143] Thomason JL, Yang L, Meier R. The properties of glass fibres after conditioning at composite recycling temperatures. Compos Part A Appl Sci Manuf 2014;61:201–8.

[144] Lund MD, Yue Y. Impact of drawing stress on the tensile strength of oxide glass fibers. J Am Ceram Soc 2010;93:3236–43.

[145] Thomas WF. An investigation of the factors likely to affect the strength and properties of glass fibres. Phys Chem Glas 1960;1:4–18.

[146] Otto H. Compaction effects in glass fibers. J Am Ceram Soc 1961;44:68–72.

[147] Yang L, Thomason JL. The thermal behaviour of glass fibre investigated by thermomechanical analysis. J Mater Sci 2013;48:5768–75.

[148] Ya M, Deubener J, Yue Y. Enthalpy and anisotropy relaxation of glass fibers. J Am Ceram Soc 2008;91:745–52.

[149] Feih S, Mouritz AP, Case SW. Determining the mechanism controlling glass fibre strength loss during thermal recycling of waste composites. Compos Part A Appl Sci Manuf 2015;76:255–61.

[150] Ito S, Tomozawa M. Crack blunting of high-silica glass. J Am Ceram Soc 1982;65:368–71.

[151] Wiederhorn SM, Fett T, Rizzi G, Fünfschilling S, Hoffmann MJ, Guin JP. Effect of water penetration on the strength and toughness of silica glass. J Am Ceram Soc 2011;94:196–203.

[152] Thomason J, Jenkins P, Yang L. Glass fibre strength - A Review with relation to composite recycling. Fibers 2016;4:18.

[153] Thomason JL, Adzima LJ. Sizing up the interphase: An insider's guide to the science of sizing. Compos Part A Appl Sci Manuf 2001;32:313–21.

[154] Rudzinski S, Häussler L, Harnisch CH, Mäder E, Heinrich G. Glass fibre reinforced polyamide composites: Thermal behaviour of sizings. Compos Part A Appl Sci Manuf 2011;42:157–64.

[155] Gao P, Su KB. Effects of chemical composition and thermal stability and high melting temperature thermoplastics. Polym Compos 2000;21:312–21.

[156] Pham QT, Chern CS. Thermal stability of organofunctional polysiloxanes. Thermochim Acta 2013;565:114–23.

[157] Wallenberger FT, Watson JC, Li H. ASM Handbook Volume 21: Composites. In: Miracle DB, Donaldson SL, editors. Composites. 21st ed., ASM International; 2001, p. 77–92.

[158] Zinck P, Pays MF, Rezakhanlou R, Gerard JF. Mechanical characterisation of glass fibres as an indirect analysis of the effect of surface treatment. J Mater Sci 1999;34:2121–33.

[159] Zinck P, Mäder E, Gerard JF. Role of silane coupling agent and polymeric film former for tailoring glass fiber sizings from tensile strength measurements. J Mater Sci 2001;36:5245–52.

[160] Sáez Rodríguez E, Yang L, Thomason JL. IInvestigation of strength recovery of recycled heat treated glass fibres through chemical treatments. 19th Int. Conf. Compos. Mater., Montreal: 2013, p. 1166–77.

[161] Yang L, Thomason JL. Effect of silane coupling agent on mechanical performance of glass fibre. J Mater Sci 2012;48:1947–54.

[162] Thomason JL, Sáez Rodríguez E, Yang L. Patent Glass Fibre Recovery. WO2015011490 A1, 2015.

[163] Sáez Rodríguez E. Regenerating the strength of thermally recycled glass fibres using chemical treatments. University of Strathclyde, 2016.

[164] Aslanova MS. The effect of different factors on the mechanical properties of glass fibres. Transl from Steklo I Keramika 1960;17:10–5.

[165] Sakka S. Effects of reheating on strength of glass fibres. Bull Inst Chem Res 1957;34:316–20.

[166] Thomason JL, Nagel U, Sáez Rodríguez E, Yang L. Regenerating the strength of thermally recycled glass fibres using hot sodium hydroxide. Compos Part A Appl Sci Manuf 2016;87:220–7.

[167] Nagel U, Yang L, Kao C-C, Thomason JL. Effects of thermal recycling temperatures on the reinforcement potential of glass fibers. Polym Compos 2016.

3. Materials and Methods

In this chapter the materials and methods are described that were used for the experimental work of this thesis. The first section describes the materials that were processed. In this thesis glass fibres were processed and incorporated into composites. A description of these processes can be found in Section 3.2 and Section 3.3. Section 3.4 – 3.7 provide information about the methods that were used for the characterisation of the composites and the glass fibres.

3.1 Materials

Depending on the manufacturing process different Polypropylene (PP) products and glass fibre products were processed into composites.

Table 3.1. Commercial names of materials that were processed into composites

Composite	Matrix	Glass fibre
Injection moulded	SABIC® PP 579 S Polybond 3200	3B DS2200-13P
Glass mat thermoplastic	DA3/60 PP fibres	PPG 8069

SABIC® PP 579 S PP was supplied by Saudi Basic Industries Coporation (SABIC). Polybond 3200 maleic anhydride-grafted polypropylene (MAPP) was added to the injection moulded composites to improve the interfacial adhesion between glass fibre and the PP matrix. Polybond 3200 and SABIC® PP 579 S were received as pellets. DA3/6 PP fibres were purchased from Goonvean Fibres Limited. The PP fibres were received chopped with a nominal length of 6 mm and a nominal linear mass of 3.3 dtex.

Chopped 3B DS2200-13P Advantex glass fibres were supplied by 3B Fibreglass The fibres had a nominal diameter of 13 µm and a nominal length of 4 mm. The actual fibre diameter was measured to be 12.7 ± 0.1 µm using optical microscopy. Fibre length measurements as described in section 3.4.3 showed that the actual arithmetic mean length of the fibres was 3.33 ± 0.04 mm. The sizing of the glass fibres was optimized for PP composites. PPG 8069 chopped glass fibres were supplied by PPG Fibreglass Company. The fibres were received non-dried with a

sizing that is optimized for the dispersion in aqueous media. The nominal fibre diameter was 10 µm and the nominal fibre length 9 mm. The actual fibre diameter was measured to be 10.5 ± 0.1 µm and the actual arithmetic mean fibre length was determined to 8.6 ± 0.5 mm.

3.2 Glass fibre processing

3.2.1 Pre-wash

It was shown by Sáez [1] that the treatments to recover the strength of thermally degraded glass fibres can be improved by a pre-washing step. In this thesis, the pre-washing step was only applied to the chopped PPG 8069 glass fibres. A SNOL 60/300 oven was used to treat 100 g of wet PPG 8069 glass fibres in 5 l of demineralised water at 70 °C. After 4 h the fibres were drained and dried for 6 h at 105°C in a Sanyo Convection MOV 212 oven.

3.2.2 Thermal preconditioning

To imitate a thermal recycling process the glass fibres were thermally conditioned in air before composite processing. A Carbolite CWF 12/13 furnace was preheated to 500 °C for 1 h. 310 g of chopped 3B DS2200-13P glass fibres were placed in an aluminium foil container. The container was placed in the preheated furnace. After 25 min the container was taken out of the furnace and the fibres were allowed to cool down at room temperature. A similar procedure was used to thermally condition chopped PPG 8069 glass fibres. The PPG 8069 glass fibres occupied a larger volume than the 3B DS2200-13P glass fibres because they were filamentized due to the prewashing step. Thus, only approximately 93 g of dried PPG 8069 glass fibres (equivalent to 100 g wet fibres) were placed in one aluminium foil container.

3.2.3 Sodium hydroxide treatment

To regenerate the fibre strength, the thermally preconditioned glass fibres were treated in a sodium hydroxide (NaOH) solution. Sodium hydroxide pellets were dissolved in deionised water to prepare a solution with a concentration of 3 mol. 5 l solution were prepared to treat approximately 93 g of chopped PPG 8069 glass fibres. The effect of the ratio between glass fibre surface area and volume of the solution was not investigated in this thesis. 5 l solution were used because that volume was found to be sufficient to immerse the fibres completely in the solution. The solution was prepared in a polypropylene storage container. The container was closed with a lid and placed in an AX60 carbolite oven. The temperature of the oven

was set to 90 °C. After 4 h the solution was taken out of the oven and poured over the glass fibres. The fibres were left for 10 min in the solution. To maintain the temperature, the solution with the glass fibres was returned to the oven. After 10 min, the fibres were drained using a nylon sieve and rinsed in hydrochloric acid. To remove residues of the chemical treatments the fibres were rinsed once in 5 l hot deionised water (90 °C) and twice in 5 l cold deionised water. The NaOH treated fibres were dried at 105 °C for approximately 6 h. Further information about the NaOH treatment can be found in a recently filed patent [2]. The development of the NaOH treatment was described by Sáez [1].

Apart from initial trials the NaOH treatment was only applied to chopped PPG 8069 glass fibres. The chopped 3B DS2200-13P glass fibres were received in bundles as shown in Figure 3.1. Figure 3.1 also shows that thermally conditioned glass fibre bundles disintegrated when they were treated with NaOH solution. The fibres formed a fluffy mat which was not suitable for further processing via extrusion compounding and injection moulding.

Figure 3.1. Chopped 3B DS2200-13P glass fibres as received, after thermal conditioning at 500 °C and regenerated

3.2.4 Aminopropyltriethoxysilane treatment

The glass fibres were treated with AminoPropyltriethoxySilane (APS) to improve the compatibility between fibre and matrix. APS purchased from Sigma Aldrich was added to deionised water to prepare a 1 vol% solution. Then the solution was left for 24 h at ambient temperature to fully hydrolyse.

To treat chopped PPG 8069 glass fibres, 5 l of APS solution were prepared in a 10 l polypropylene storage container. The glass fibres were dispersed in smaller polypropylene storage containers and the solution was poured over the fibres. 1 l solution was used to treat 13.44 g of glass fibres. The containers were closed with a lid and left at room temperature. After 15 min the fibres were drained and directly processed into composites without drying. It was found that the APS treated fibres

are more difficult to disperse when they were dried. To control the composite fibre content the fibres were weighed to the required quantities (13.44 g / layer) before the APS treatment. 3B DS2200-13P glass fibres were APS treated with a similar procedure. However, the fibres occupied a smaller volume. Thus, 2 l solution were sufficient to immerse 310 g of fibres. After treatment, all fibres were dried at 110 °C for 8 h in a SNOL 60/300 oven.

3.3 Composite processing

3.3.1 Extrusion compounding

A Betol BC25 single screw extruder was used to compound SABIC® PP 579 S PP and Polybond 3200 MAPP with chopped 3B DS2200-13P glass fibres. The processing barrel zone temperatures are listed in Table 3.2 and the speed of the screw was set to 80 rpm. The extruded material was drawn through a water bath and cut into pellets using a rotary cutter.

Table 3.2. Extrusion processing temperatures

Barrel Zone 1 (next to the hopper)	190 °C
Barrel Zone 2	205 °C
Barrel Zone 3	215 °C
Barrel Zone 4 (next to the extrusion die)	220 °C
Extrusion die	175 °C

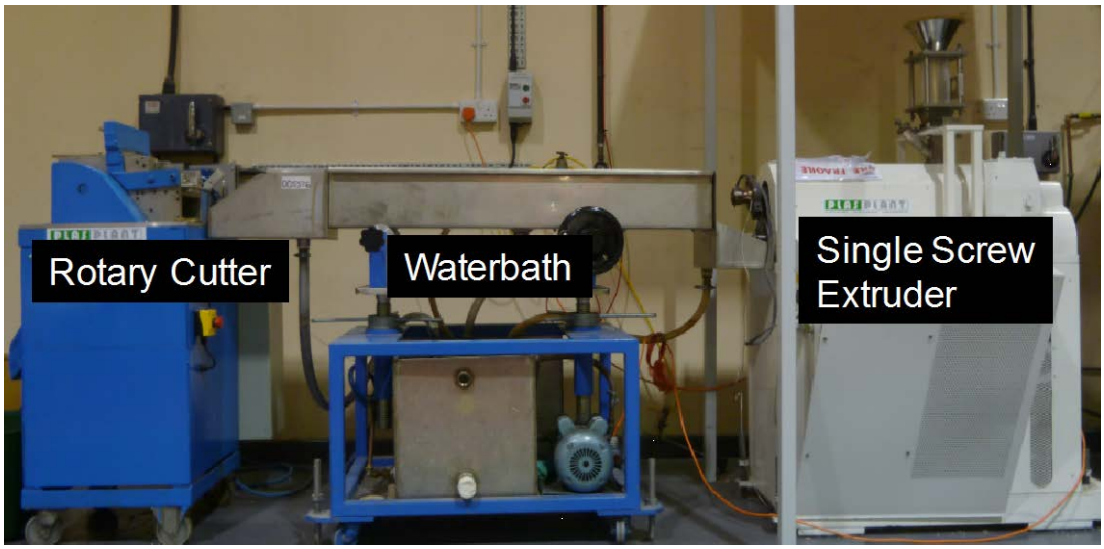

Figure 3.2. Extrusion line

3.3.2 Injection moulding

The pelletized glass fibre PP compound was fed into an Arburg 170-90/200 injection moulding machine that was used to produce dog-bone shaped specimens. The dimensions of the specimens were as specified in the ISO 527 standard. The processing parameters are listed in Table 3.3 and were used for all composites. Figure 3.3 shows the injection moulding machine and the mould that were used. In addition to the tensile test specimens, the mould had two other cavities to produce impact test specimens and hardness test specimens. The moulded impact specimens were not used for impact tests. They were flatwise notched because of the cavity but not according to the ISO 179 standard. The impact test specimens were cut from the centre of the injection moulded tensile test specimens.

Table 3.3. Injection moulding processing parameters

Barrel Rear Temperature	200 °C
Barrel Centre Temperature	215 °C
Barrel Front Temperature	220 °C
Nozzle Temperature	230 °C
Mould temperature	40 °C

Figure 3.3. Injection moulding machine (left) and mould (right)

3.3.3 Glass mat thermoplastic processing

31.36 g of Goonvean DA3/60 PP fibres and 13.44 g of PPG 8069 glass fibres were dispersed in a Premier International KCL type hand sheet former to prepare one GMT mat. The sheet former was filled with 20 l water and an electrical stirrer was used to agitate the dispersion at a stirring speed of 1200 rpm. After 6 min, the

dispersion was rapidly strained through the nylon sieve of the sheet former. The wet mat of glass fibres and PP fibres (200 mm x 200 mm) was dried for 8 h in a Sanyo Convection MOV 212 oven at 105 °C. The weight loss was monitored to control the moisture content. A Polystat 400S heated press was used to preconsolidate the mats at a pressure of 6.8 bar and a temperature of 200 °C for 1 min. The preconsolidated material was cooled down outside of the press and a weight of 15 kg was placed on the preconsolidated material. After cooling down, the preconsolidated sheets were trimmed to squares with dimensions identical to the mould in Figure 3.4 (165 mm x 165 mm) using a laminate cutter. Four preconsolidated sheets were stacked in the mould to prepare one laminate. The compression moulding was performed at 200 °C. A pressure of 20 bar was applied for 4 min. Then the mould was transferred to a second press and the material was quenched cooled at the same pressure. The final dimensions of the laminates were approximately 165 mm x 165 mm x 4 mm. A water jet cutter was used to cut dog bone shaped tensile test specimens according to the ISO 527 standard out of the moulded laminate. Figure 3.5 shows a cut laminate. Six tensile test specimens were cut out of one laminate. A similar procedure was followed to prepare samples of unreinforced PP but 36.2 g PP fibres were used to prepare one mat.

To prevent the composite from sticking to the mould a PTFE glass fibre fabric (Biscor Fluorofab® Fabric 100-6) was placed in the mould (Figure 3.4). In addition, Chemlease 2203 W release agent was applied to the lid and walls of the mould.

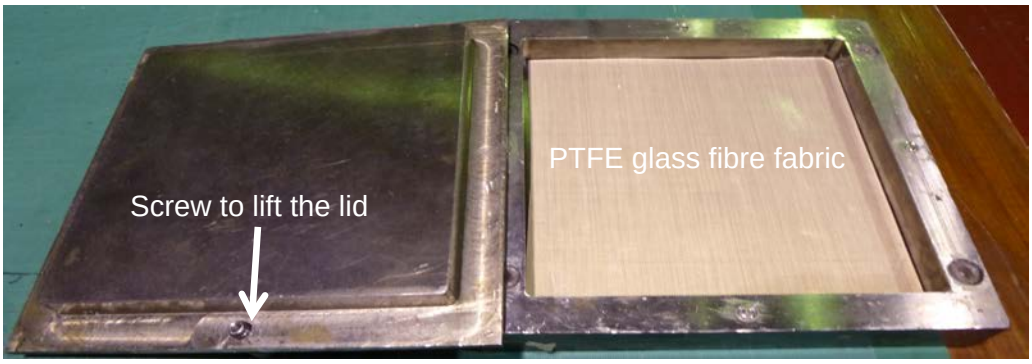

Figure 3.4. Mould used to prepare GMT laminates

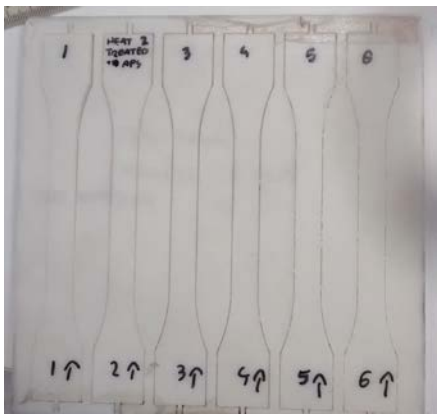

Figure 3.5. GMT laminate

3.4 Composite characterisation

3.4.1 Tensile testing

The uniaxial tensile tests of the composites and the unreinforced PP were guided by the ISO 527 standard. An Instron 5969 testing machine equipped with a 50 kN load cell was used to perform the tensile test. The displacement rate was set to 1 mm/min and the strain was recorded with an Instron 2663-821 video extensometer. An Instron humidity and temperature probe was used to control the temperature (23 ± 2 °C) and humidity (50 ±10 RH%) when the tests were performed at room temperature.

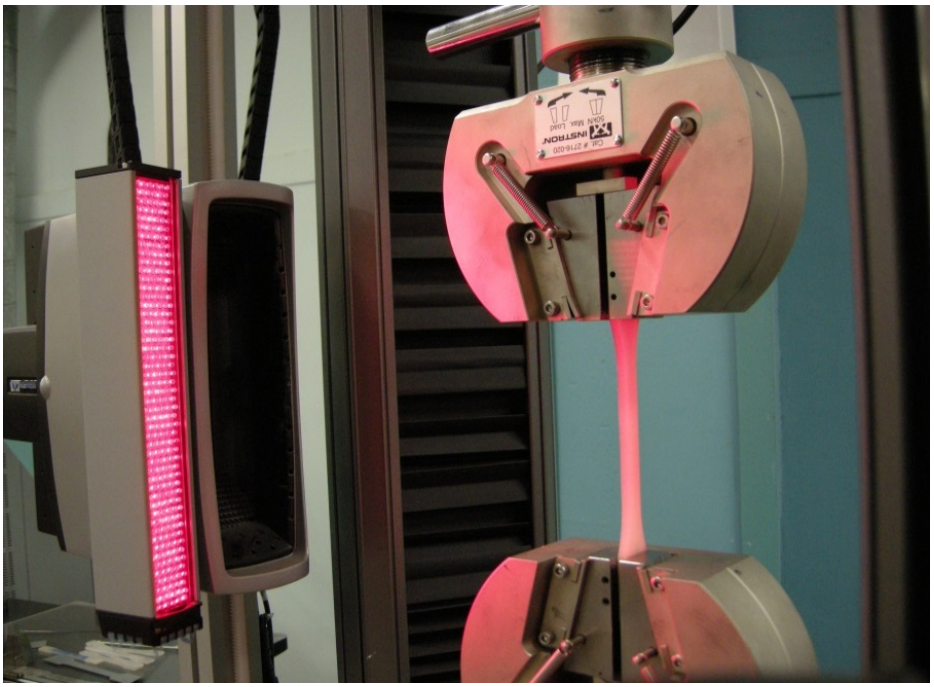

Figure 3.6. Instron 5969 tensile test set-up

3.4.2 Unnotched impact testing

Unnotched impact test specimens were cut from the injection moulded tensile bars and the GMT laminates using a waterjet cutter. The dimensions of the impact test specimens (80 mm x 10 mm x 4 mm) followed the ISO 179 standard. All specimens were tested edgewise using a Tinius Olsen Impact 503 impact tester with a 25 J hammer.

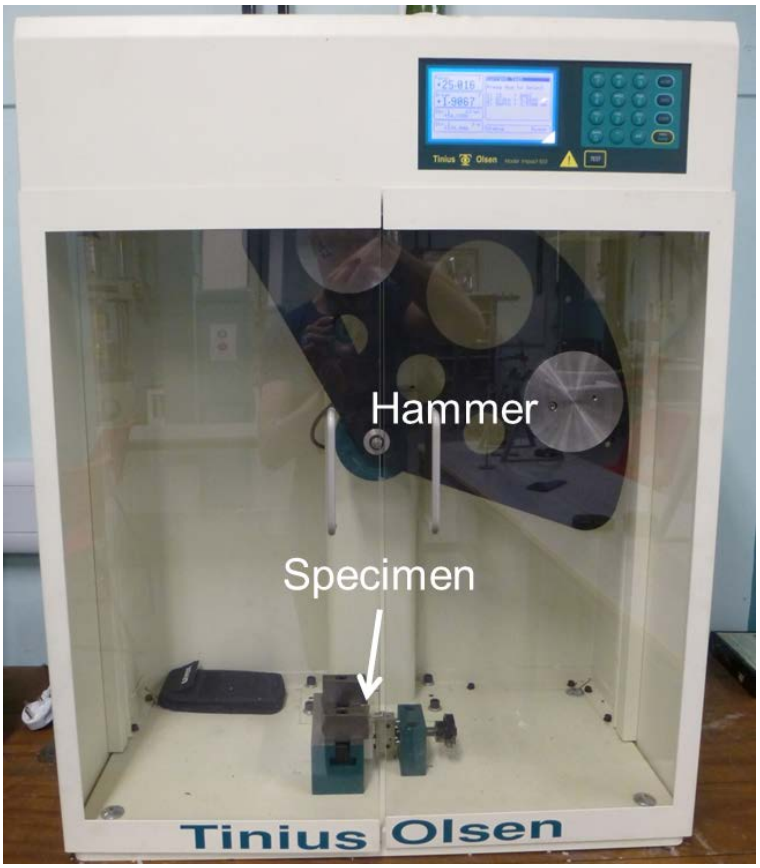

Figure 3.7. Impact tester

3.4.3 Fibre length measurements

A procedure similar to Hartwich et al. [18] was used to determine the length of the glass fibres in the composites. Glass fibres were extracted from the tensile bars using an ashing process. The PP matrix was burned off in a programmable Carbolite CWF 12/13 furnace using a 6 hour ashing process with temperatures up to 550 °C. The temperature profile of the ashing program is plotted in Figure 3.8.

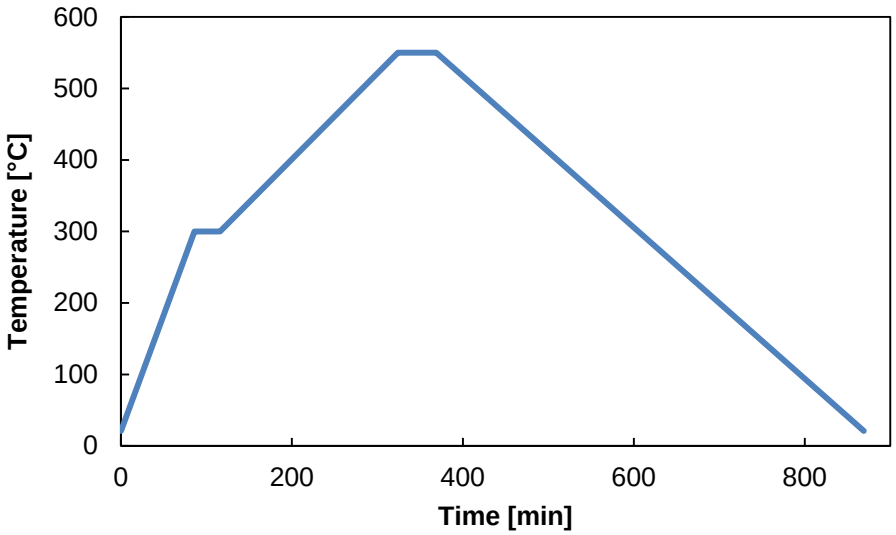

Figure 3.8. Temperature profile of ashing process

Approximately 25 mg of the extracted fibres from the centre of the tensile bar were dispersed in 500 ml distilled water. Then, 250 ml of the dispersion were poured into another receptacle and diluted with another 250 ml of distilled water. 2 drops (approximately 0.1 ml) of glycerine were added to reduce surface tension of the water. The dispersion was prepared immediately before the analysis and manually stirred. Approximately 0.5 ml of a domestic window cleaning agent were poured into each petri-dish to reduce the surface tension. Then, a small quantity of the glass fibre suspension was poured into at least four different petri-dishes. The petri-dishes were placed in the dark field box of an IDM FASEP fibre length measurement system (Figure 3.9). The dark field box was placed on a Canon ScanoScan 9000F high resolution scanner with a resolution of 10.52 µm per pixel. The dark field box was illuminated to improve the contrast between fibres and the black background.

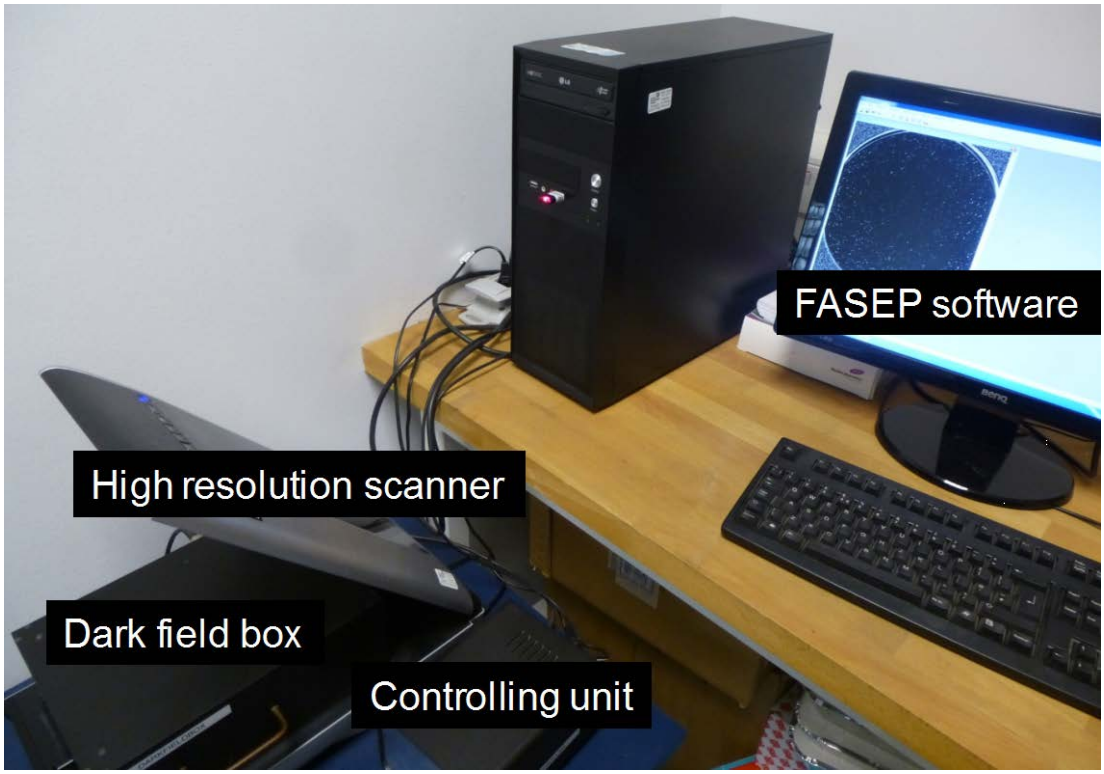

Figure 3.9. FASEP fibre length measurement system set-up

The scanned images were analysed using the Image Pro macro of the IDM FASEP fibre length measurement system. Depending on their width, the detected objects were classified into dust, single fibres and crossing or curved fibres as shown in Figure 3.10.

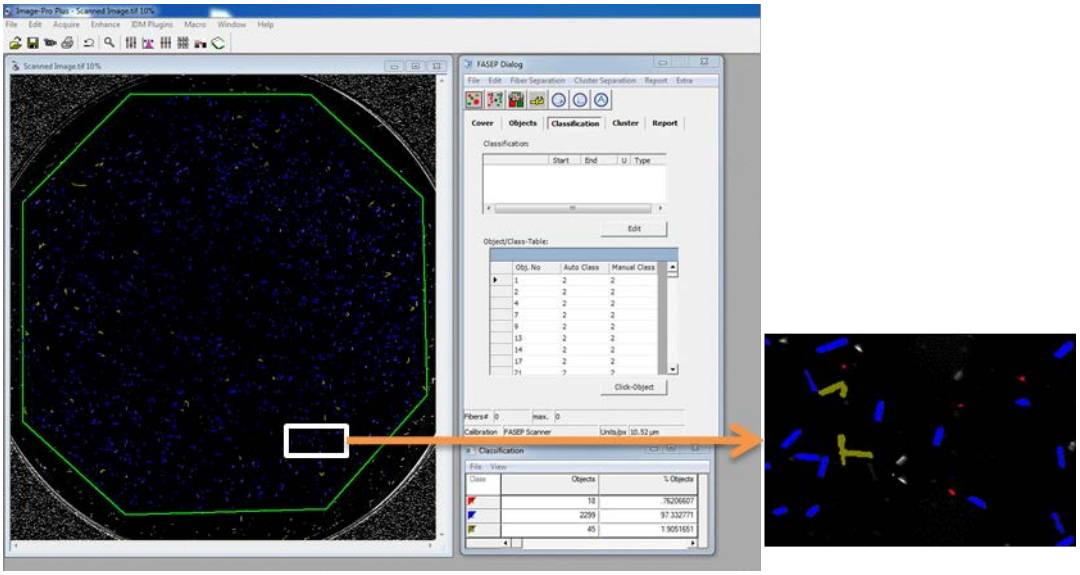

Figure 3.10. Object classified by the IDM FASEP fibre length measurement system (dust=red, fibre=blue, crossing and curved fibres=green)

The classified objects were measured by the FASEP software. The FASEP software used an algorithm based on the Hough Transformation to analyse crossing and curved fibres. Figure 3.11 below shows an example of crossing fibres that were separated by the FASEP software.

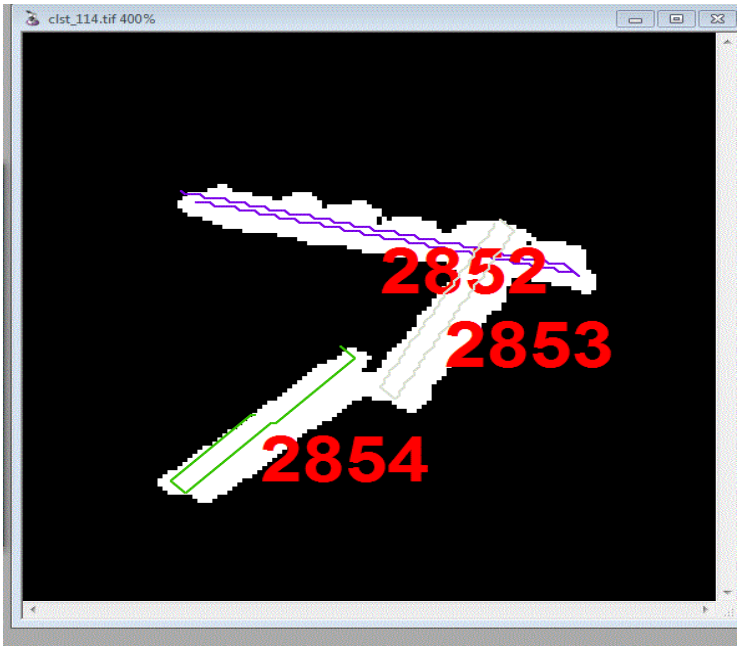

Figure 3.11. Crossing fibres separated by the FASEP software

3.4.4 Fibre content measurements

The tensile test specimens were ashed to assess the fibre content of the composites. An ashing process as described in the previous paragraph was used to separate the glass fibres from the PP matrix. The samples were weighed before and after the ashing process. The ratio between the weight after the ashing process and before the ashing process was regarded as the fibre weight fraction. A Sartorius AX224 analytical balance was used to weigh the samples.

3.4.5 Microbond sample preparation and testing

Microbond tests were performed to assess the interfacial shear strength (IFSS) between glass fibres and PP. The microbond tests were performed on the same glass fibres and PP that was used to prepare composite samples. The PP was prepared by extrusion or by compression moulding. A Prism TSE twin screw extruder was used to blend SABIC® PP 579 S PP and Polybond 3200 MAPP. The barrel temperatures were set to 170 °C - 230 °C and the screw speed was set to 100 rpm. 36.2 g Goonvean DA3/60 PP fibres were preconsolidated as described in section 3.3.3. The compression moulded material and the extrudates were cut into

pellets. The pellets were heated to 200 °C on a glass slide which was placed on a hot plate. After 45 s the PP pellets were molten and drawn to form fibres. Figure 3.12 illustrates the procedure of the microbond sample preparation. Tweezers were used to extract single fibres from fibre bundles. Great care was taken not to touch the centre of the glass fibres. A single glass fibre was suspended on double sided sticky tape next to a bright desk light and a PP fibre was knotted around the suspended glass fibre. Then the free ends of the PP fibre were trimmed. It was necessary to trim the PP fibre close to the knot to reduce the droplet size of the microbond samples. Glass fibres that were exposed to high temperatures have a low tensile strength and might break during the microbond test. A small microbond droplet debonds at lower loads than a large droplet and reduces the probability of fibre breakage. To cut the PP fibre close to the knot the movement of the PP fibre was restrained by sticking the fibre ends to double sided sticky tape. Vanna's-Type microscissors (straight 80 mm, purchased from Agar scientific) enabled high precision cutting of the PP fibre.

After cutting the PP fibre, the glass fibre with the PP knot was glued onto a washer. Two component Araldite epoxy adhesive was applied on top of the sticky tape and glass fibres. The glue was allowed to cure for at least 8 h at room temperature. The samples were suspended on metal frames and placed in an OV-11 vacuum oven that was purged with nitrogen. The samples were heated up to 220 °C and cooled down to room temperature in the oven. The temperature profile is plotted in Figure 3.13.

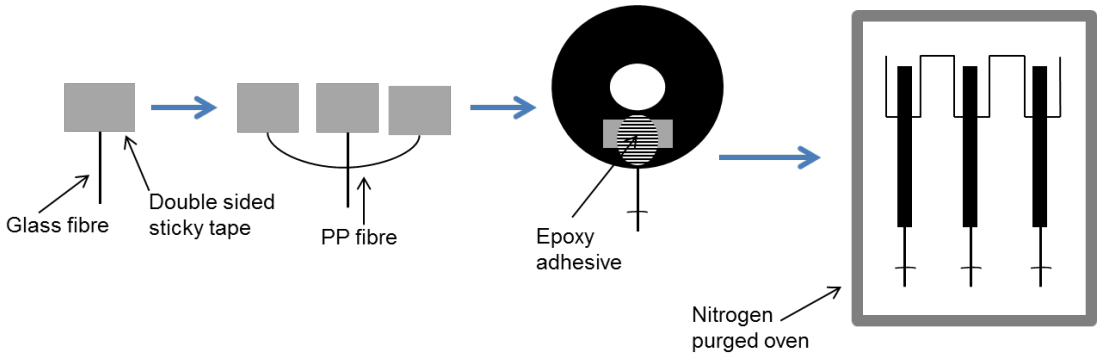

Figure 3.12. Microbond sample preparation

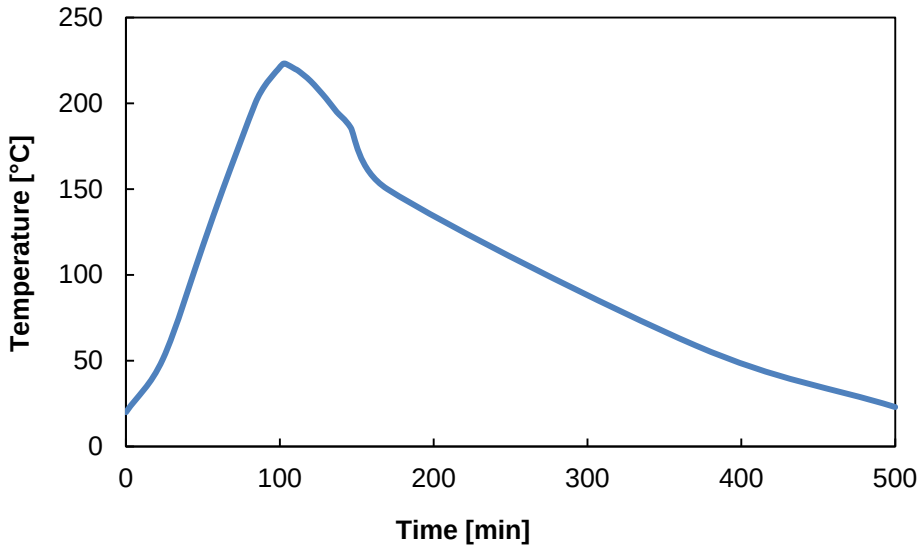

Figure 3.13. Temperature profile of vacuum oven used to prepare microbond samples

The fibre diameter, droplet diameter and the embedded fibre length of the microbond samples were determined using a Nikon Epiphot Inverted optical microscope and ImageJ image analysis software. Only samples with symmetric droplets were tested. A procedure as described by Yang and Thomason [3,4] was used to test the microbond samples using washers instead of card frames as sample holders. Figure 3.15 illustrates the microbond test set-up. An Instron 3342 universal testing machine equipped with a 10 N load cell was used apply load to the microbond samples. The microbond samples were hooked as shown in Figure 3.15 and the shear blades of the microvice were moved close to the fibre. Then the fibre was moved until the microbond droplet was below the shear blades. A stereo microscope (45x magnification) connected with a DCM130 video camera was used to observe the microbond samples and the shear blades. The test speed was set to 0.1 mm/min and all tests were performed at room temperature (22 ± 2 °C). The Instron Bluehill 2 software recorded the load as a function of the displacement. The test was stopped after the load reached a maximum value and dropped to a plateau. Figure 3.14 shows example of two load-extension. One sample debonded at a low load (low IFSS) and the other one debonded at a high load (high IFSS).

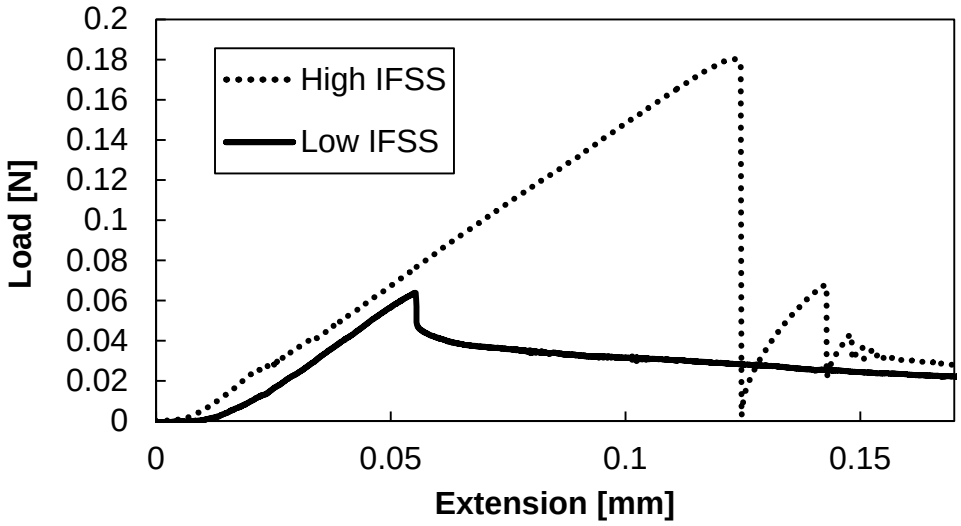

Figure 3.14. Typical load extension curves of microbond tests

Equation 2.1 (see Chapter 2) was used to calculate the apparent interfacial shear strength from the maximum load and the fibre surface area that is embedded in the PP matrix.

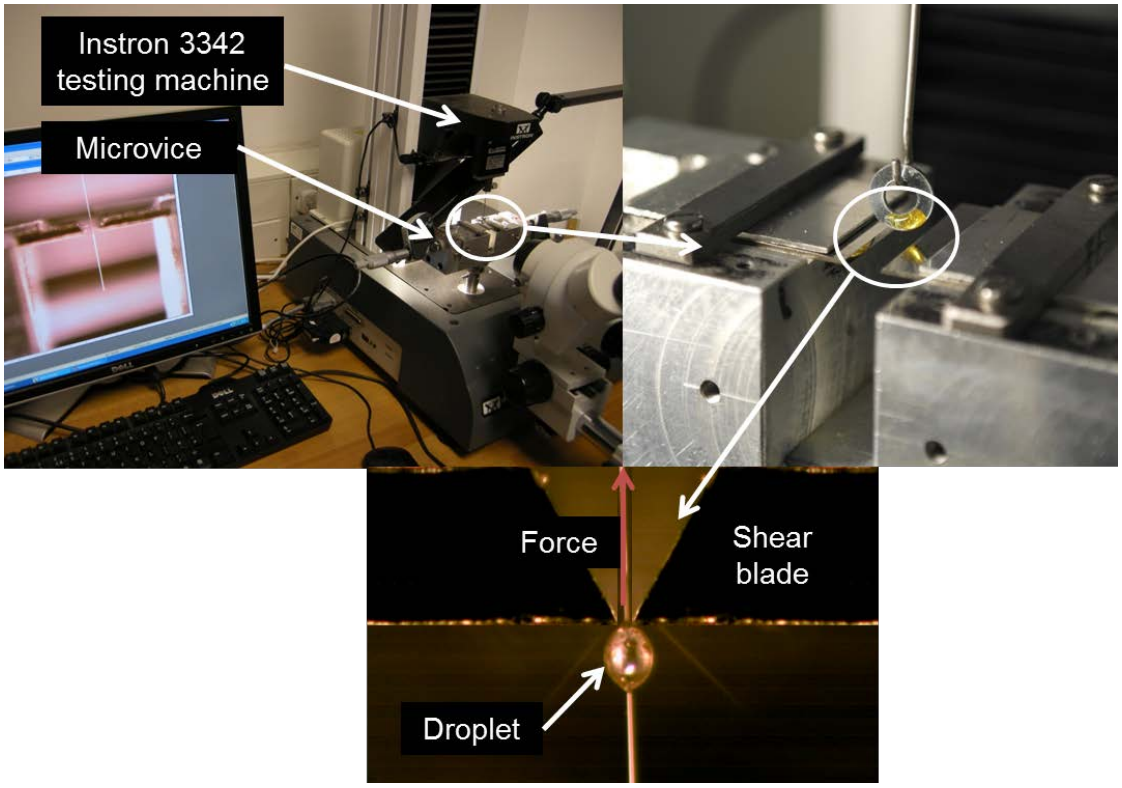

Figure 3.15. Microbond test set-up

3.5 SEM

A Hitachi SU6600 scanning electron microscope (SEM) was used to analyse the fracture surfaces of microbond samples, injection moulded composites and GMT composites. Carbon adhesives discs were used to glue the specimens on aluminium stubs. In addition, silver painting was used to secure composite samples. The samples were gold coated to prevent charging when they were analysed in the SEM.

3.6 Single fibre tensile testing

The PPG 8069 glass fibres were tensile tested according to the standard ASTM C1557-03 with a gauge length of 5 mm. Card tabs were cut out of 250 g/m^2 grade paper card. Double sided tape was placed on the paper tab approximately 1 mm away from the window. The fibres were placed on top of the double sided tape and Loctite Gel Superglue was applied on the fibres up to the edge of the window. The diameter of the fibres was determined before the test using a Nikon Epiphot inverted optical microscope and ImageJ image analysis software. An Instron 3342 universal testing machine equipped with a 10 N load cell was used to perform the tensile tests. The crosshead displacement rate was set to 0.3 mm/min and the tests were performed at room temperature (22 ± 2 °C). The Bluehill 2 software recorded the load as a function of the displacement.

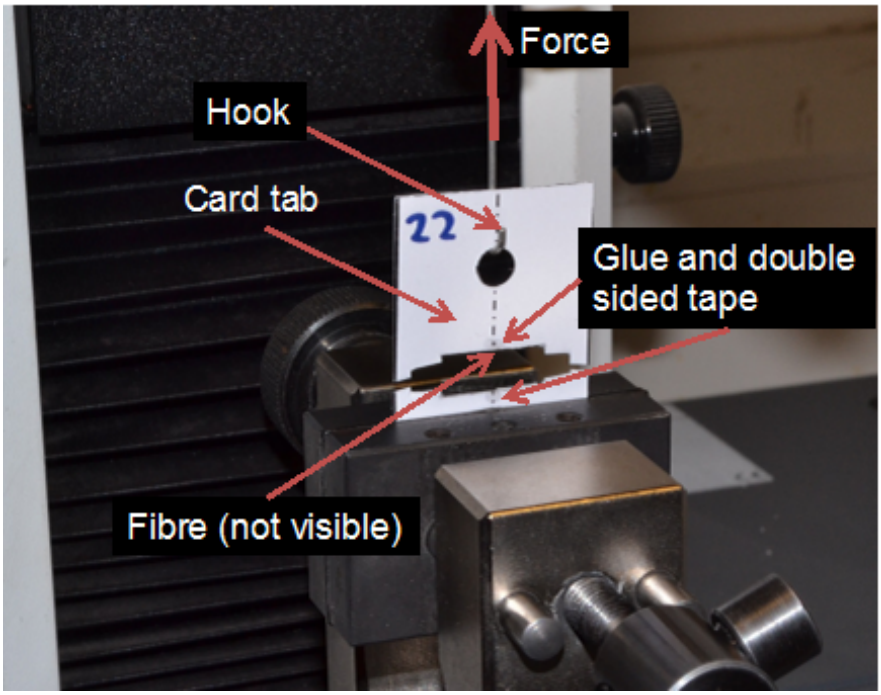

Figure 3.16. Single fibre tensile test set-up

3.7 Thermal gravimetric analysis

Temperature scans with a heating rate of 10 °C/min were performed using a Netzsch STA 449 F1 Jupiter thermogravimetric analyser. The weight loss of glass fibres with different sizings, PP, MAPP and dried APS film was recorded as a function of the temperature in both air and a nitrogen atmosphere. Figure 3.17 shows the configuration that was used. The weight of the sizings is relatively small which might lead to scatter in the TGA signal. The relatively large volume of the beaker allowed to place 250 mg of glass fibres in the beaker and obtain a clear TGA signal.

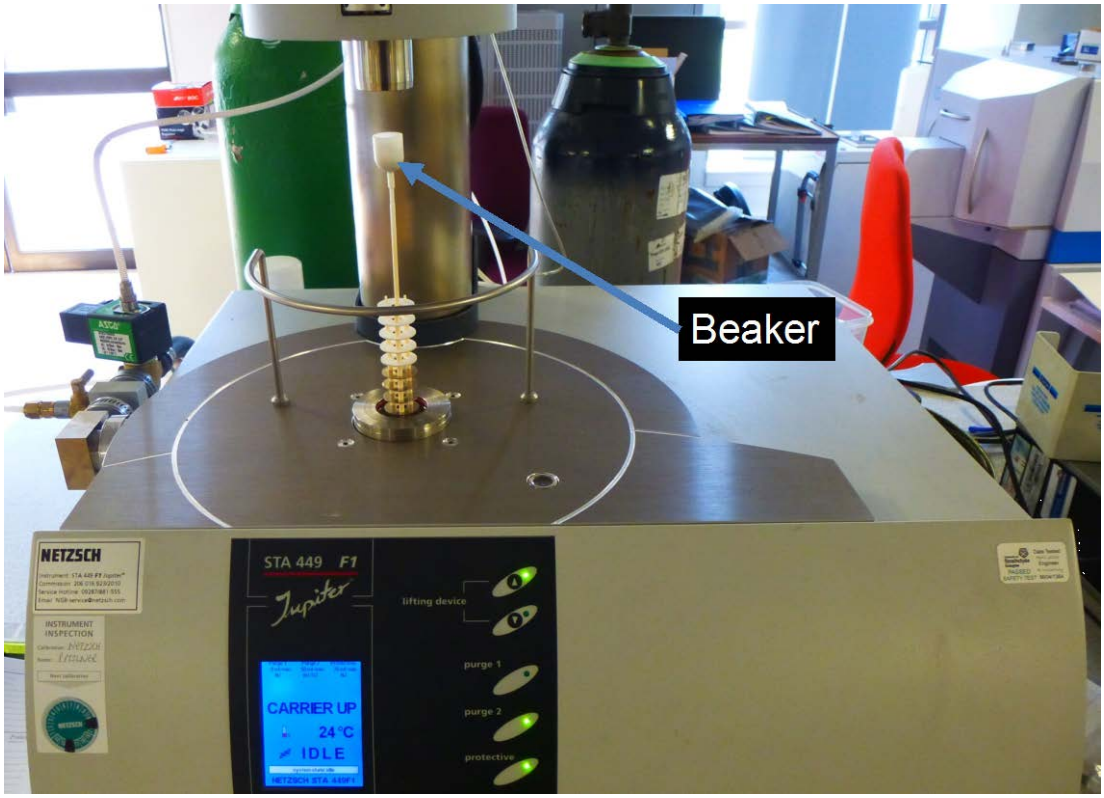

Figure 3.17. Thermal gravimetric analyser

3.8 References

[1] Sáez Rodríguez E. Regenerating the strength of thermally recycled glass fibres using chemical treatments. PhD thesis. University of Strathclyde, 2016.

[2] Thomason JL, Sáez Rodríguez E, Yang L. Patent Glass Fibre Recovery. WO2015011490 A1, 2015.

[3] Yang L, Thomason JL. Development and application of micromechanical techniques for characterising interfacial shear strength in fibre-thermoplastic composites. Polym Test 2012;31:895–903.

[4] Yang L, Thomason JL. Interface strength in glass fibre–polypropylene measured using the fibre pull-out and microbond methods. Compos Part A Appl Sci Manuf 2010;41:1077–83.

4. Structure-Performance Relationship of Glass Fibre Polypropylene Composites

The aim of the work reported in this chapter was to develop an understanding of the structure performance relationship of injection moulded glass fibre Polypropylene (GF/PP) composites and the characterisation techniques that are also used in Chapter 5 and Chapter 6. The effect of maleic anhydride grafted PP (MAPP) on the composite performance is discussed. Tensile tests and unnotched charpy impact tests were performed to assess the macromechanical performance of the composites. In addition, a comparison between the apparent interfacial shear strength (IFSS) obtained from microbond tests and the IFSS of the Bowyer-Bader analysis is provided. The error bars in all plots represent 95 % confidence intervals. T-tests (p=0.05) were performed to further assess the significance of observed trends.

The glass fibres and the polymer were compounded according to their weight fraction but micromechanical models like the Kelly-Tyson model and the Cox model use the fibre volume fraction as input parameter. The fibre volume fraction V_f was calculated from the fibre weight fraction W_f using Equation 4.1 [1]. Based on the data sheet of the supplier the density of the PP was assumed to be 0.905 g/cm^3 and the density of the glass fibres was assumed to be 2.62 g/cm^3 [2].

Equation 4.1. Conversion from fibre weight fraction to fibre volume fraction

$$V_f = \frac{1}{1 + \frac{\rho_f}{\rho_M} * \left(\frac{1}{W_f} - 1\right)}$$

The coupling agent Polybond 3200 was added to the composites to vary the MAPP content of the composites. The term MAPP content will be used to refer to the amount of Polybond 3200 that was added to the composites. It should be noted that the actual MAPP content of the composites was probably higher because of the MAPP in the sizing of the glass fibres. The added MAPP content was measured as a percentage of the PP matrix weight. The weight of the polymer matrix (combined weight of the PP and MAPP) was kept constant at 707 g (12.8 vol% glass fibre content) or 505 g (25.5 vol% glass fibre content). For example, to process a composite with 12.8 vol% glass fibre content and 6 % added MAPP content 300 g glass fibres, 664.58 g PP and 42.42 g Polybond 3200 were blended.

4.1 Precision of the fibre length measurements

The procedure to measure the residual length of glass fibres in PP composites is described in Chapter 3. Usually, the glass fibres were extracted from one tensile bar of each composite and four different samples were analysed. To assess the precision (as defined in ISO 5725) of the fibre length measurements, glass fibres were extracted from three different tensile bars and analysed. The tensile bars were injection moulded at the same date. 1 % MAPP was added to the composites. The results of the measurements are plotted in Figure 4.1 and Figure 4.2. Figure 4.1 shows the arithmetic means of the measurements. Figure 4.2 shows the weighted means of the measurements. The means were calculated according to the ISO 22314 standard. 12 samples were taken from tensile bar 37 to assess the precision of samples taken from the same tensile bar. Four samples were taken from tensile bar 16 and tensile bar 17 to assess the precision of samples taken from different tensile bars that were produced at the same date.

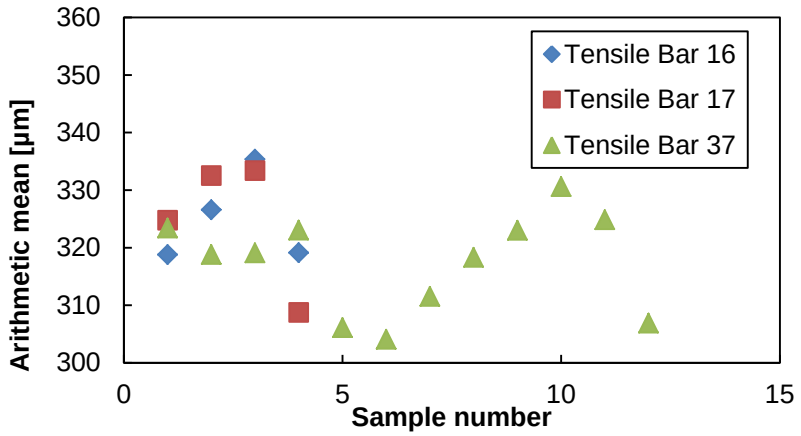

Figure 4.1. Arithmetic mean values of repeated fibre length measurements

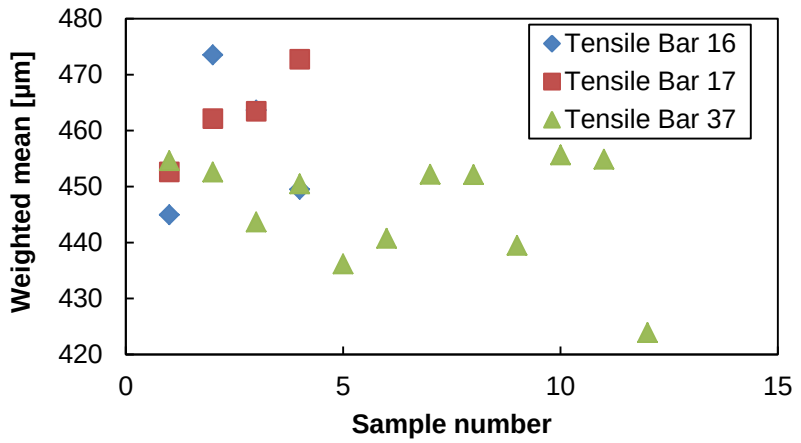

Figure 4.2. Weighted mean values of repeated fibre length measurements

The values for the fibre length in Figure 4.1 and Figure 4.2 of the samples taken from different tensile bars fell in the same range. This indicates that the variation of the residual fibre length between the injection moulded samples is relatively small compared to the means. Thus, the analysis of one tensile bar is sufficient to assess the residual fibre length of a composite when the processing conditions were kept constant. This is further supported by t-tests which showed that there was no significant difference at 95 % confidence limit between the means of tensile bar 16, tensile bar 17 and tensile bar 37. However, the variation between samples taken from the same tensile bar suggests that at least three samples should be analysed of each tensile bar. It was decided to prepare at least four samples of each material in this thesis. Thus, at least three samples were available for analysis when one sample was affected by dirt or scratches on the surface of the petri-dish.

The values in Table 4.1 are based on Figure 4.1. Table 4.1 shows the arithmetic means of the fibre length distributions of each tensile bar. All individual fibre length values of the repeat measurements were combined to one single fibre length distribution for each tensile bar. As specified in the ISO 22314 standard, Table 4.1 shows the corresponding standard deviations that were calculated from the individual fibre length values for each tensile bar. For comparison Table 4.1 also shows the arithmetic means and standard deviations that are based on the values of the repeat measurements in Figure 4.1.

Table 4.1. Difference between arithmetic mean values and standard deviations of repeated fibre length measurements

Tensile bar	Arithmetic mean length distribution	Standard deviation length distribution	Arithmetic mean repeat measurements	Standard deviation repeat measurements
16 (2nd batch]	327 µm	209 µm	325 µm	11 µm
17 (2nd batch]	320 µm	217 µm	325 µm	8 µm
37 (2nd batch]	318 µm	202 µm	318 µm	8 µm

The arithmetic means calculated from of the individual fibre length values in Table 4.1 deviate only marginally from the arithmetic means of the repeat measurements. The standard deviations of the individual fibre length values are large compared to the means. Different fibre length distributions might have overlapping error bars

when only the standard deviations of the fibre length distributions are considered. This might be misleading because the standard deviations are often used as error bars and overlapping error bars might be associated with nonsignificant differences. However, the standard deviations of the fibre length distributions calculated from the individual fibre length values describe rather the shape of the fibre length distribution than the repeatability of the measurement. The values for the standard deviations between the repeat measurements in Table 4.1 are in the same size of magnitude like the resolution of the scanner (10.52 µm / pixel) that was connected to the FASEP fibre length measurements system. Thus, the precision of the FASEP system is higher than the standard deviations calculated from the individual fibre length values suggest. In addition, the length distributions of the fibres in the injection moulded composites are skewed towards higher values as shown in Figure 4.3. Skewed length distributions of glass fibres in injection moulded polypropylene composites were also reported by other authors [3–6]. The skewness of the fibre length distributions explains the difference between the arithmetic means and weighted means in Figure 4.1 and Figure 4.2 because the weighted mean is more influenced by the long fibre fraction than the arithmetic mean. In this thesis, both means are reported for all analysed composite samples.

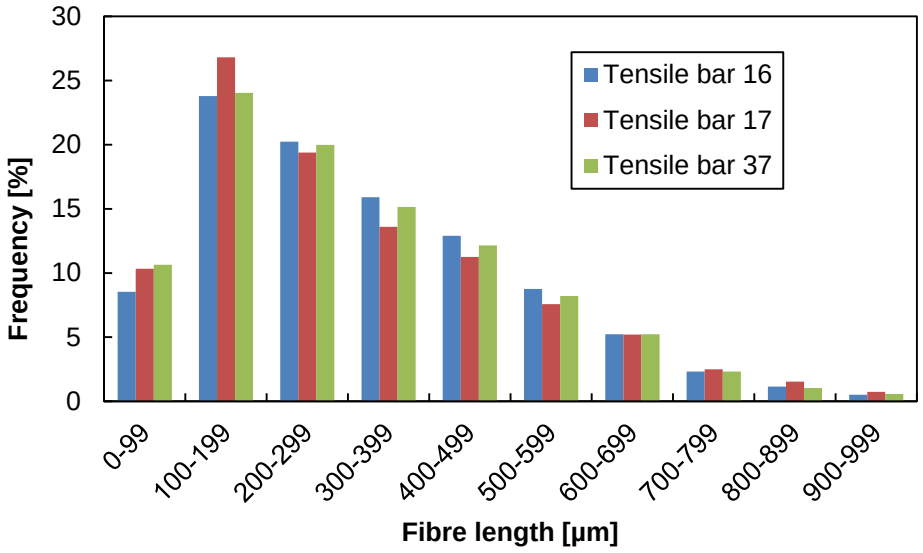

Figure 4.3. Fibre length distributions of different tensile bars moulded from the same material

4.2 Effect of fibre content and MAPP content on residual fibre length

Figure 4.4 shows the weighted mean length and arithmetic mean length of the glass fibres in the injection moulded GF/PP composites as a function of the MAPP content. Similar to Table 4.1, Table 4.2 and Table 4.3 show two different sets of standard deviations. One set of standard deviations was calculated from the individual values of the fibre length measurements and provides information about the shape of the fibre length distribution. The other set of standard deviations was calculated from the arithmetic means of the repeat measurements.

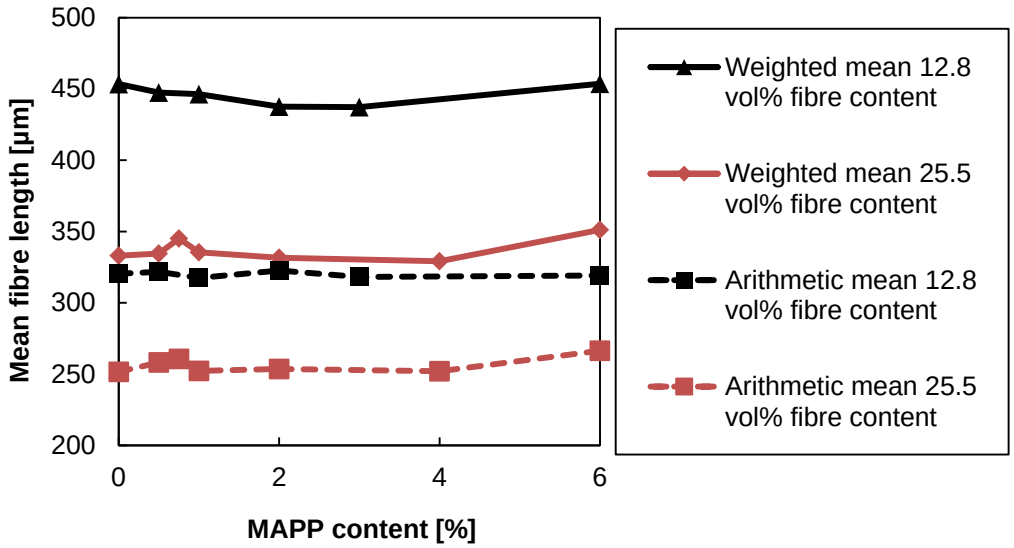

Figure 4.4. Absence of a correlation between the residual fibre length and MAPP content

Table 4.2. Difference between standard deviations of fibre length distributions and repeat measurements vs. MAPP content (12.8 vol% fibre content)

MAPP content	Standard deviation of length distribution	Standard deviation between repeat measurements
0 %	206 µm	9 µm
0.5 %	201 µm	6 µm
1 %	202 µm	8 µm
2 %	193 µm	16 µm
6 %	208 µm	9 µm

Table 4.3. Diference between standard deviations of fibre length distributions and repeat measurements vs. MAPP content (25.5 vol% fibre content)

MAPP content	Standard deviation of length distribution	Standard deviation between repeat measurements
0 %	144 µm	8 µm
0.5 %	140 µm	8 µm
0.75 %	148 µm	4 µm
2 %	140 µm	17 µm
4 %	140 µm	8 µm
6 %	150 µm	10 µm

The standard deviations of the fibre length distributions in Table 4.2 and in Table 4.3 do not exhibit a clear trend which indicates that the shape of the fibre length distribution did not change with the addition of MAPP. The data in Figure 4.4 suggests that the means of the residual fibre length were not influenced by the addition of MAPP. Thomason [1] suggested that MAPP promotes the length degradation of glass fibres in injection moulded PP composites due to enhanced fibre/polymer interactions. Similar observations were reported by Roux et al. [7]. The reason for the absence of this effect in this thesis is not clear. Thomason [1] and Roux et al. [7] used similar processing temperatures but other processing parameters like the back pressure [8] and the design of the injection moulder [9] can also affect the residual fibre length. The injection moulding processing conditions were kept constant and the design of the injection moulding machine was not changed when the specimens for this thesis were produced. However, the processing parameters and injection moulder design that were used in this thesis might have promoted the fibre/polymer interactions, fibre/fibre interactions and fibre/processor surface interactions which might have masked the effects of the MAPP. Thus, a more detailed comparison between the present data and the studies mentioned above [1,7] would require detailed knowledge of the processing conditions and injection moulder design.

4.3 Composite tensile modulus vs. fibre content and MAPP content

4.3.1 Influence of fibre content on the composite modulus

Figure 4.5 shows the modulus of injection moulded GF/PP composites as a function of the fibre volume fraction. The modulus increased with the fibre content which was also observed in several other studies [1,5,7,10–13].

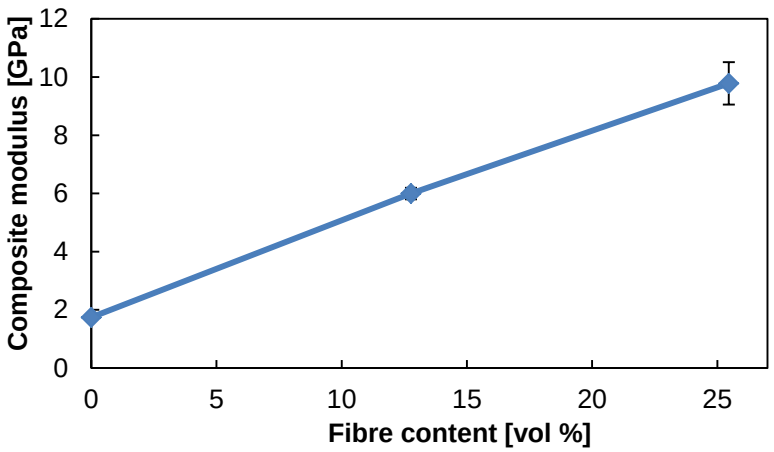

Figure 4.5. Increase of the composite modulus with fibre content

4.3.2 Influence of MAPP on the composite modulus

Figure 4.6 shows the modulus of the injection moulded GF/PP composites as a function of the MAPP content. The modulus of the composites with 25.5 vol% fibre content did not follow a clear trend. It appears that the modulus increased slightly between 0.5 % and 0.75 % MAPP. However, t-tests did not support a significant difference between 0 % and 0.75 % MAPP. The relatively low modulus at 0.5 % MAPP might be an outlier.

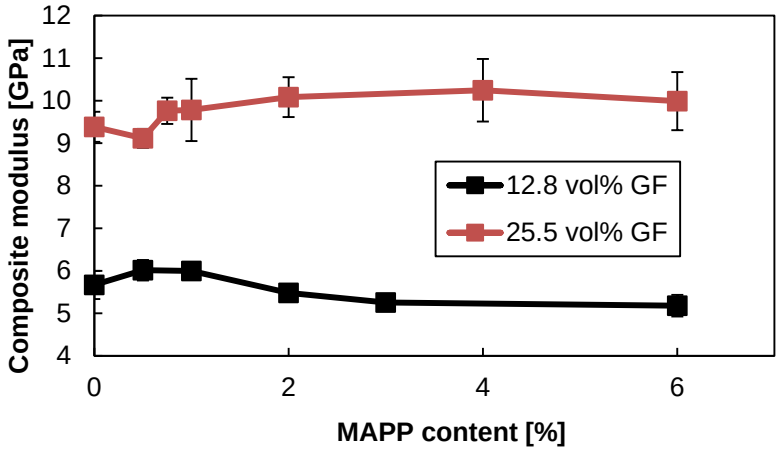

Figure 4.6. Effect of fibre content and MAPP content on the composite modulus

The data in Figure 4.6 suggests that the modulus of composites reinforced with 12.8 vol% fibre content decreased between 1 % MAPP and 6 % MAPP which was confirmed by t-tests. It was concluded in Chapter 2 that the modulus of GF/PP composites depends on the fibre length [5,14], fibre content [5,10–13,15,16] and fibre orientation [5,15]. The data in Figure 4.4 indicates that the residual fibre length was not affected by the addition of MAPP to the composites. The ashing and weighing of tensile bars showed that the fibre content of the composites with a nominal fibre content of 12.8 vol% varied between 12.2 vol% and 12.6 vol%. The Cox model was used to estimate the effect of the fibre content variations on the composite modulus. The use of the Cox model to calculate the composite modulus requires the fibre orientation factor as input parameter. Equation 4.2 and the input parameters in Table 4.4 were used to calculate the fibre orientation factor η_{oKr} from the measured modulus of composites with 1 % MAPP and a nominal fibre content of 12.8 vol%. Equation 4.2 can be derived from the Cox model and requires knowledge of several parameters that are listed in in Table 4.4. A value of 0.64 was obtained for η_{oKr} and used to calculate the values in Figure 4.8.

Equation 4.2. Calculation of fibre orientation factor using the Cox model

$$\eta_{\mathrm{oKr}} = \frac{E_C - \left(1 - V_f\right) * E_M}{E_F * V_f * \eta_L}$$

Table 4.4. Input parameter for Cox model to estimate the influence of the fibre content

Fibre volume fraction V_f	Calculated from the fibre weight fraction (see Equation 4.1) density of glass fibres 2.62 g/cm^3 [2], density of PP 0.905 g/cm^3 (manufacturer data)
Poison's ratio υ	Calculated using rule of mixture, Poisons ratio of glass fibre 0.2 and PP 0.4 [17]
Fibre packing factor X_i	4 [14]
Matrix modulus E_M	1.71 GPa (measured)
Fibre modulus E_f	78.7 GPa [18]
Arithmetic mean fibre length l	Measured (see Figure 4.4)
Fibre length factor η_L	Calculated (see Chapter 2 and [14])
Fibre orientation factor η_{oKr}	0.64 (calculated with Equation 4.2)

Equation 4.3 was published by Krenchel [19] and allows to calculate η_{oKr} from visually observed fibre orientations where a_i is the volume fraction of fibres with an angle θ_i between fibre axis and loading axis. Figure 4.7 shows the fibre orientation factor η_{oKr} based on the assumption that all fibres are aligned in the same direction.

Equation 4.3. Fibre orientation factor according to Krenchel

$$\eta_{oKr} = \Sigma a_i * cos^4\theta_i$$

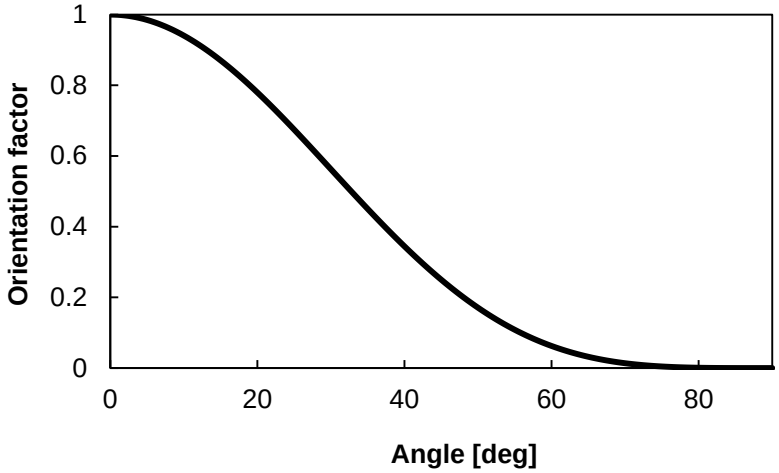

Figure 4.7. Orientation factor according to Krenchel as a function of the fibre orientation angle

An orientation factor of 0.64 would therefore mean that all fibres are aligned at an angle of 26.5 deg between the fibre axis and the loading axis. However, fibres are often orientated in multiple directions in composites. It was shown that η_{oKr} has a value of 0.375 when the fibres are randomly orientated in plane [19]. This value was used to model the stiffness of GMT composites and an agreement between model data and experimental data was reported [14,20,21]. In injection moulded composites glass fibres are aligned because of shear flow and extensional flow. The glass fibres tend to align in the melt flow direction close to the walls of the cavities because of shear forces. Compressive forces act in the centre of the cavity and the fibres tend to align transverse to the melt flow direction [22,23]. The shear flow and extensional flow lead to a formation of a three layer shell-core-shell structure which was reported by several authors [5,22,24]. The fibres in the shell are mainly aligned in the melt flow direction and the fibres in the core tend to be aligned transversely to the melt flow direction. It is therefore difficult to relate η_{oKr} to one orientation angle because the fibre orientation in injection moulded composites is a distribution. The value of 26.5 deg stated above for the angle between fibre axis and loading axis

might therefore be regarded as an average value for the fibre orientation but it does not consider the layered structure of the injection moulded composites.

Figure 4.8 shows the measured values of the composite modulus as a function of the measured fibre content. In addition, Figure 4.8 shows the composite modulus predicted by the Cox model [25] as described in Chapter 2 [14,20]. The results in Figure 4.8 are based on the input parameters in Table 4.4.

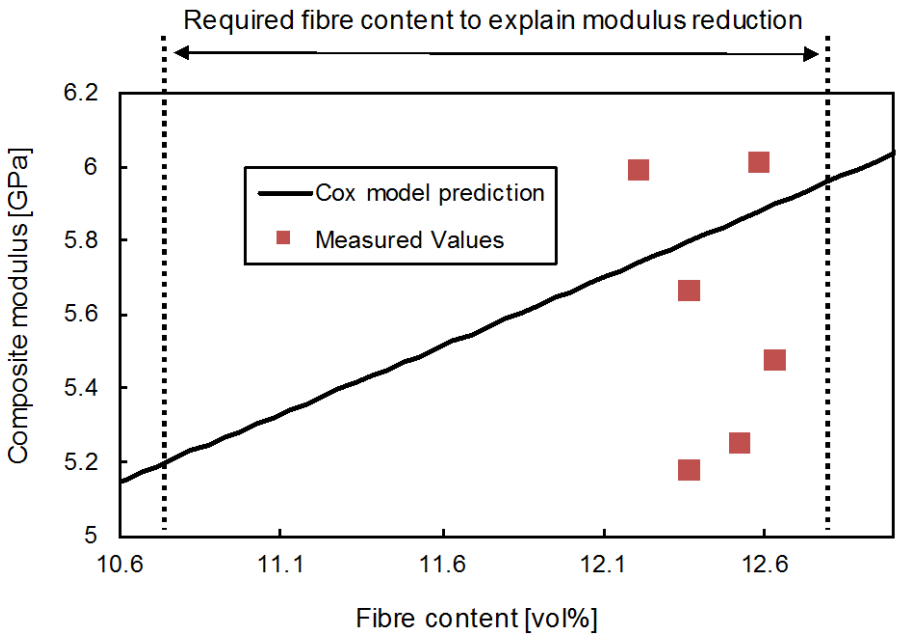

Figure 4.8. Comparison between measured fibre content variation and fibre content required to explain the composite modulus reduction

The data in Figure 4.8 suggests that the variation of the fibre content cannot explain the measured variation of the composite modulus. The fibre content would need to decrease by approximately 2 vol% to cause the measured drop of the composite modulus.

The PP modulus was observed to drop with the molecular weight [26,27]. It might be expected that the addition of MAPP to PP leads to an increase of the modulus because of its lower molecular weight. Experimental data did not support this suggestion. Similar to data published by Roux et al. [7] and Rijsdijk [28], the data in Figure 4.9 shows that the addition of MAPP did not affect the modulus of unreinforced PP. Thus, it is unlikely that the modulus of the PP matrix was affected by the addition of MAPP.

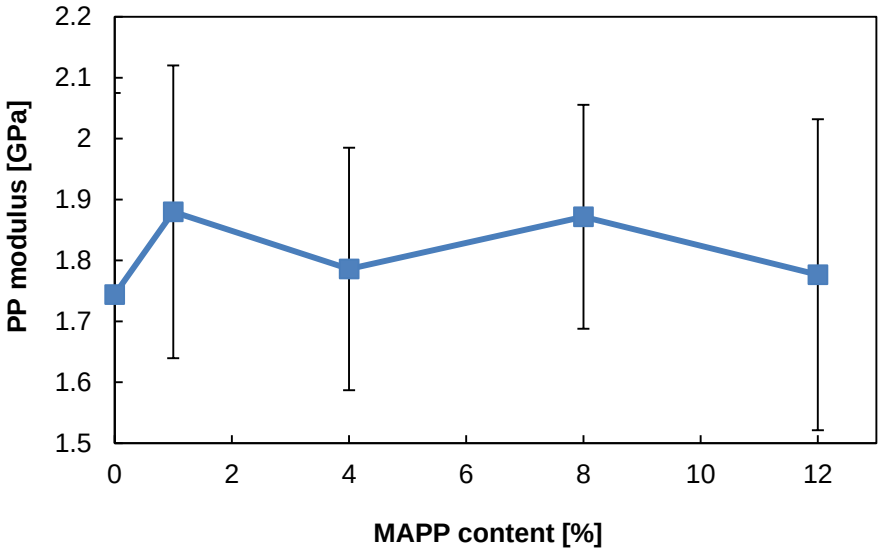

Figure 4.9. Independence of the PP modulus from the MAPP content

The fibre orientation is another parameter that might have affected the composite modulus at high MAPP contents. The data in Figure 4.6 was analysed using Equation 4.2 to determine the fibre orientation factor as a function of the MAPP content. The input parameters are summarised in Table 4.5 and the results are plotted in Figure 4.10.

Table 4.5. Input parameter for Cox model to determine fibre orientation factor

Fibre volume fraction V_f	Calculated from the fibre weight fraction (see Equation 4.1) density of glass fibres 2.62 g/cm^3 [2], density of PP 0.905 g/cm^3 (manufacturer data)
Poison's ratio υ	Calculated using rule of mixture, Poisons ratio of glass fibre 0.2 and PP 0.4 [17]
Packing factor X_i	4 [14]
Matrix modulus E_M	1.71 GPa (measured average)
Fibre modulus E_f	78.7 GPa [18]
Composite modulus E_c	Measured (see Figure 4.6)
Arithmetic mean fibre length l	Measured (Figure 4.4)
Fibre length factor η_l	Calculated (see Chapter 2 and [14])

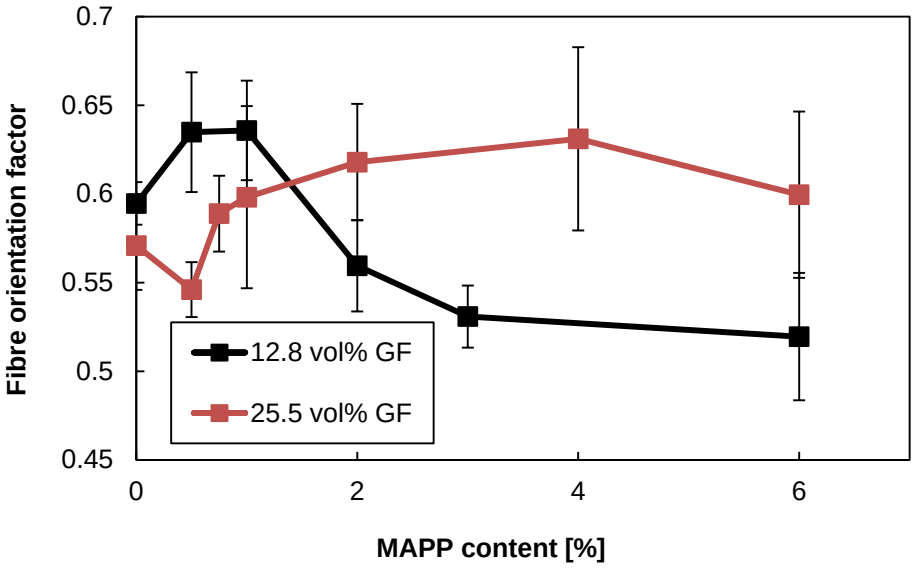

Figure 4.10. Partial reduction of the fibre orientation factor with MAPP content based on the Cox model

Above 2 % MAPP content, composites with 25.5 vol% fibre content had a higher fibre orientation factor than composites with 12.8 vol% fibre content. The right hand side of the plot in Figure 4.10 suggests that more fibres were aligned in the melt flow direction/loading direction when the fibre content increased. It was reported by Ota et al. [13] that the melt viscosity of GF/PP composites increased with the fibre content. In the same study a reduction of the modulus of injection moulded GF/PP composites with increasing barrel temperatures was observed. The drop of the composite modulus was related to changes in the melt flow properties at higher processing temperatures. Several other studies [29–31] also indicated a correlation between melt viscosity and fibre alignment in injection moulded glass fibre thermoplastics. The fibre alignment in the melt flow direction was reduced with melt temperature. It was suggested that an increase of the melt temperature leads to a reduction of the melt viscosity and lower shear forces which would result in a lower degree of fibre alignment in the melt flow direction. Akay and Barkley [31] correlated a reduction of the composite tensile strength and composite modulus with the melt temperature and a lower degree of fibre alignment. Based on the studies mentioned above it might be expected that composites with a higher fibre content exhibit a higher degree of fibre orientation because of a higher melt viscosity. Such observations were reported by several authors [11,30,32,33] when they analysed polished cross-sections of injection moulded composites using optical microscopy. The data in Figure 4.10 partially agrees with the studies cited above because the

composites with 25.5 vol% fibre content had a higher fibre orientation factor than the composites with 12.8 vol% fibre content when more than 2% MAPP was added. However, Figure 4.10 also suggests that below 2 % MAPP the composites with 12.8 vol% had a higher fibre orientation factor than the composites with 25.5 vol% fibre content. The data in Figure 4.10 is therefore not completely conclusive regarding the relationship between fibre content and fibre orientation. It should be mentioned that not all reviewed studies reported an increase of the degree of fibre orientation in the melt flow direction with the fibre content. In a different study on injection moulded GF/PP composites Thomason [1] did not find a correlation between fibre content and the fibre orientation factor obtained from optical microscopy. Other studies [5,16] based on optical microscopy reported that the thickness of the core in injection moulded GF/PP composites increased with the fibre content. The fibre orientation factor might therefore have decreased because the fibres in the core of injection moulded composites tend to align transverse to the melt flow direction. A reduction of the degree of fibre orientation in the melt flow direction with the fibre content was also reported by Thomason [11] when he calculated the fibre orientation factor from composite tensile test data using micromechanical models. Thus, the reviewed studies and the experimental data in Figure 4.10 do not allow to draw a final conclusion about the effect of fibre content on fibre orientation in injection moulded GF/PP composites.

The fibre orientation factor of composites reinforced with 12.8 vol% nominal glass fibre content appears to decrease between 1 % MAPP and 6 % MAPP. It might be speculated that the orientation of the glass fibres was affected by the addition of MAPP. The MAPP content was varied by adding Polybond 3200 coupling agent to the composites. Polybond 3200 has different rheological properties than the PP homopolymer. A melt flow index of 47 g / 10 min was cited by the manufacturer for the PP homopolymer that was used as matrix material. This value is based on measurements according to the ISO 1133 standard (230 °C, 2.16 kg). Measurements according to the ASTM 1238 standard (190 °C, 2.16 kg) showed that Polybond 3200 has a melt flow index of 104 g / 10 min [34]. The melt flow index of polyolefins like PP increases with temperature [35] although the effect of the temperature on the melt viscosity becomes smaller at high shear rates [36]. It can therefore be expected that Polybond 3200 has a higher MFI at 230 °C than PP. Thus, a reduction of the viscosity of the composite melt due to the addition of Polybond 3200 might explain the data Figure 4.10. The reduction of the melt

viscosity led to lower shear forces and a reduced degree of fibre alignment in the melt flow direction. The reduction of the fibre orientation factor was not observed in composites with 25.5 vol% fibre content. Reasons for the absence of this effect are relatively large error bars that could mask trends and the lower amount of Polybond 3200 compared to composites reinforced with 12.8 vol% glass fibres. As already mentioned above, the MAPP content was measured as weight fraction of the PP matrix. Thus a composite reinforced with 25.5 vol% glass fibre and 6 % MAPP contained 30.3 g Polybond 3200. A composite reinforced with 12.8 vol% glass fibres and 6 % MAPP contained 42.42 g Polybond 3200.

Coupling agents like Polybond 3200 based on MAPP are the most expensive components of GF/PP composites. It is therefore aimed to minimise the amount of coupling agent that is required for optimised composite performance [37,38]. Thus, few studies have added quantities of coupling agents to GF/PP composites that are comparable to the present study. It was found in Chapter 2 that there is conflicting data in the literature regarding the detrimental effect of high MAPP contents on the tensile strength of GF/PP composites. Most of the reviewed studies did not suggest a detrimental effect of high MAPP contents on the composite modulus [7,28,39,40]. The data of Bowland [37,38] indicated a small reduction of the flexural modulus of injection moulded GF/PP composites. It might be speculated that most authors did not observe a reduction of the composite modulus because they processed composites via compression moulding [28,39,40] which does not involve as much melt flow as injection moulding. The glass fibre orientation is therefore less affected by melt flow properties of the polymer compared to injection moulding processes which might explain the absence of a correlation between coupling agent content and composite modulus. Roux et al. [7] did not observe a reduction of the modulus of injection moulded GF/PP composites. However, their data exhibits relatively large error bars that might have masked trends. In addition, they used Polybond 3001 and Polybond 3150 MAPP coupling agents which have a lower melt flow index than the Polybond 3200 coupling agent that was used in this thesis [34]. Thus, changes of the fibre orientation are a possible explanation for the observed reduction of the composite modulus in Figure 4.6. An extensive study of the fibre orientation using computer tomography [41] or optical microscopy [42] are required to confirm this hypothesis. The behaviour of the composite tensile strength and strain at break might also partially be explained with changes in the fibre orientation and will be discussed in the following sections.

4.4 Influence of fibre content and MAPP content on composite tensile strength

Figure 4.11 shows the tensile strength of the injection moulded GF/PP composites as a function of the fibre content and MAPP content. As expected from studies that were reviewed in Chapter 2 [1,5,10–13,16,43], the composite tensile strength increased with the fibre content. The addition of MAPP to the composites enhanced the composite tensile strength. The results in Figure 4.11 agree with the hypothesis of Thomason [44] and Bowland [37,38] that the performance of GF/PP composites depends on the ratio between the glass fibre surface and the number of MAPP molecules in the matrix. 2 % MAPP was required to optimise the tensile strength of composites with 25.5 vol% glass fibre content and 0.5 % MAPP was required to optimise the tensile strength of composites with 12.8 vol% glass fibre content. The glass fibre surface area increased with the fibre content. Thus, a higher concentration of MAPP in the matrix is required to 'cover' the fibre surfaces. The relationship between composite tensile strength, MAPP concentration and IFSS will be discussed in this section.

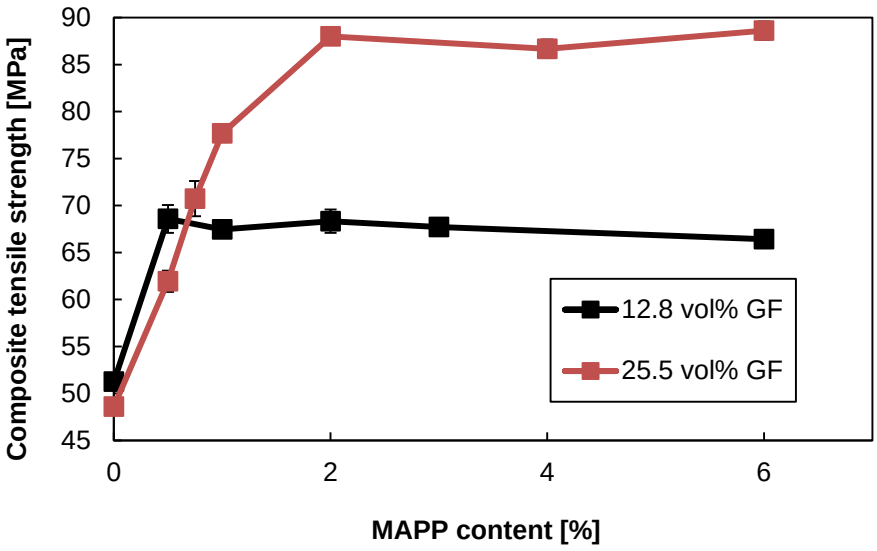

Figure 4.11. Increase of the composite tensile strength with fibre content and MAPP content

The data in Figure 4.11 also indicates a reduction of the tensile strength of composites reinforced with 12.8 vol% fibre content between 2 % MAPP and 6 % MAPP. A reduction of the performance of GF/PP composite at high MAPP contents was also observed by Zheng et al. [40] and Bowland [37,38]. It was speculated in the previous section, that the addition of MAPP to the composites affected the orientation of the glass fibres in the composites. This might at least partially also

explain the reduction of the tensile strength of composites with 12.8 vol% fibre content. It is well known that the tensile strength of composites is affected by the fibre orientation [5,15]. On the other hand, Zheng et al. [40] processed composites via compression moulding. Compression moulding does not involve as much melt flow as injection moulding. Thus, it is less likely that their results were affected by changes of the fibre orientation. They explained the reduction of the composite tensile strength at high MAPP contents with an embrittlement of the composites. The IFSS increased with the MAPP content and less energy was absorbed by fibre pull-out. When a fibre broke the released energy created crevices and surrounding fibres failed as well which led to the formation of cracks and composite failure. The Bowyer-Bader analysis and microbond tests were performed to further investigate the structure performance relationship of the composites that were studied for this thesis. The results are discussed in this section.

4.4.1 Fibre stress and matrix stress from Bowyer-Bader analysis

The Bowyer-Bader analysis [1,45,46] as described in Chapter 2 was used to analyse the microstructural properties of the composites. The input parameters are summarised in Table 4.6. The polynomial fitting curve parameters x_1, x_2, and x_3 were obtained from the recorded stress strain curves of unreinforced PP. The polynomial fitting curve parameters were calculated for five different tensile test samples of five different MAPP concentrations in the range between 0 % and 3 % strain. Then the averages were calculated for each parameter. The stress strain curves based on the polynomial fitting curve parameters are plotted in Figure 4.12 for different MAPP concentrations.

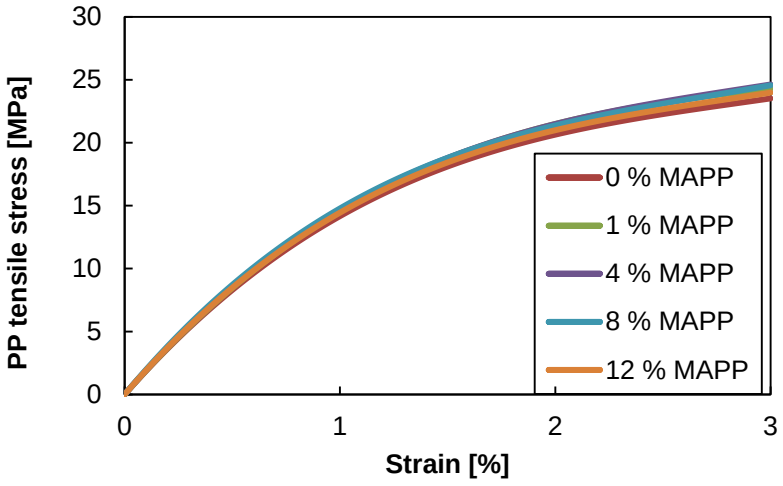

Figure 4.12. Polynomial fitting curves for different MAPP concentrations

The plots in Figure 4.12 and the data in Figure 4.9 indicate that the tensile behaviour of PP below the 3 % strain was not affected by the addition of MAPP. Thus, the polynomial fitting curve parameters in Table 4.6 were used throughout this thesis.

Table 4.6. Input parameters for Bowyer-Bader analysis

Fibre volume fraction V_f	Calculated from nominal fibre weight content (see Equation 4.1)
Fibre modulus E_f	78.7 GPa taken from [18]
Average fibre radius r_f	6.4 µm (measured)
Composite strain 1 ε_1	1/3 of strain at break
Composite strain 2 ε_1	2/3 of strain at break
Composite tensile stress 1 σ_1	Composite tensile stress at ε_1
Composite tensile stress 2 σ_2	Composite tensile stress at ε_1
Composite tensile strength σ_{cMax}	Measured (see Figure 4.11)
Fibre length distribution	Measured as described in Chapter 3
Matrix stress Z	Calculated from strain using a polynomial fitting curve [1]
Polynomial fitting curve parameter x_1	0.68 obtained from tensile tests
Polynomial fitting curve parameter x_2	-5.98 obtained from tensile tests
Polynomial fitting curve parameter x_3	19.79 obtained from tensile tests

Figure 4.13 shows the maximum fibres stress obtained from the Bowyer-Bader analysis as a function of the MAPP content. It should be noted that in this thesis the maximum fibre stress was calculated. The maximum fibre stress was observed at maximum composite tensile stress when the composite yield strain was reached. In contrast, Thomason [1,46] calculated the fibre stress at composite failure. The maximum fibre stress was calculated in this thesis to assess the possibility of fibre failure. The maximum fibre stress in Figure 4.13 increased with the addition of MAPP to the composites which can be explained with an improved stress transfer between matrix and fibres. The fibres in composites with 25.5 vol% fibre content experienced lower stresses than fibres in composites with 12.8 vol% fibre content.

This can be explained with the larger number of fibres in composites with 25.5 vol% fibre content. The load was shared between a larger number of fibres. The data in Figure 4.13 suggests that the fibre stress reached a maximum between 2 % MAPP and 6 % MAPP in composites with 25.5 vol% fibre content. In contrast, the fibre stress in composites with 12.8 vol% MAPP decreased between 2 % MAPP and 6 % MAPP. It appears unlikely that this reduction was caused by a reduction of the fibre strength and it will be shown in section 4.4.5 that more than 75 % of the fibres were shorter than the critical fibre length for fibre failure. Most of the fibres were therefore unlikely to fail. Thus, the microstructure of the composites might have been changed between 2 % MAPP and 6 % MAPP.

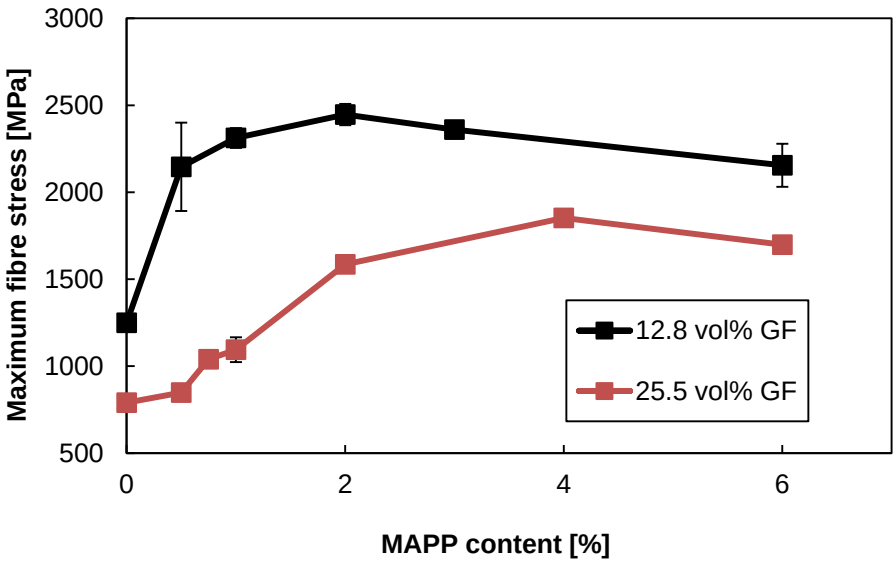

Figure 4.13. Effect of MAPP content and fibre content on the maximum fibre stress

Figure 4.14 shows the fibre strain that was calculated from the fibre stress in Figure 4.13. A linear stress-strain relationship and a fibre modulus of 78.7 GPa [18] were assumed. Figure 4.14 also shows the yield strain of the composites. The data shows a qualitative agreement between composite yield strain and maximum fibre strain at maximum composite stress similar to the agreement between strain at break and fibre stress at composite failure that was reported by Thomason [1,46]. A t-test confirmed that the composite yield strain decreased significantly between 3 % MAPP and 6 % MAPP similar to the fibre strain and maximum fibre stress. The reduction of the fibre stress and fibre strain correlates with a reduction of the composite tensile strength in Figure 4.11. It appears that the mechanisms that

caused the reduction of the tensile strength of composites with 12.8 vol% fibre content did not affect the tensile strength of composites with 25.5 vol% fibre content.

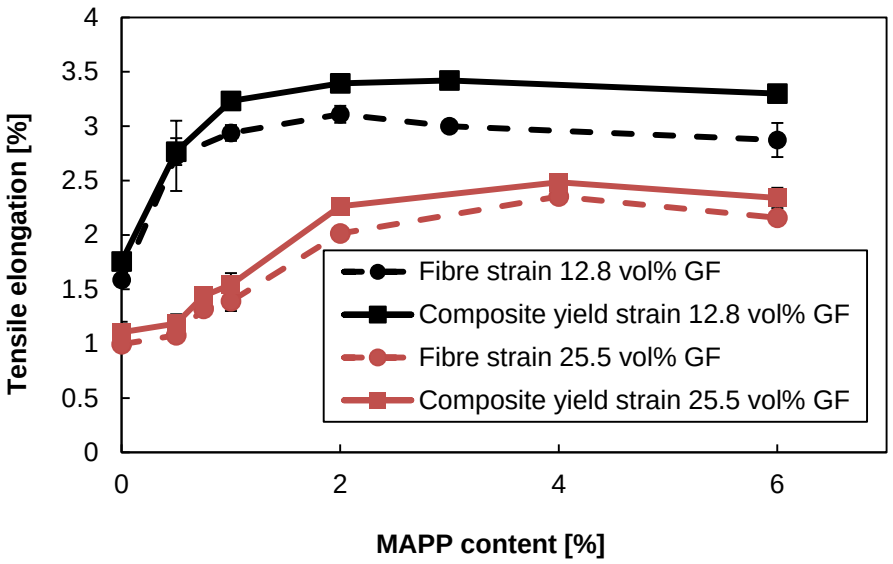

Figure 4.14. Agreement between the Bowyer-Bader fibre strain and the composite yield strain

The properties of composites with 25.5 vol% fibre content were more controlled by the glass fibres than the properties of composites with 12.8 vol% fibre content. It might therefore be speculated that the composite tensile strength was affected by changes of the PP matrix properties. Similar to the modulus, the tensile strength of PP decreases with the molecular weight [26,27]. It might therefore not be expected that the addition of MAPP leads to a reduction of the tensile strength of PP. However, the tensile data in a study by Qiu et al. [47] suggested that MAPP reduces the strength of unreinforced PP. Their results are conflicting to the observations of Roux et al. [7] who did not observe a significant change of the PP tensile strength with the addition of MAPP. Rijsdijk et al. [28] even observed an increase of the tensile strength of unreinforced PP with the MAPP content. The data in Figure 4.15 shows that the yield strength of unreinforced PP decreased slightly between 1 % MAPP and 12 % MAPP but increased between 0% MAPP and 1 % MAPP.

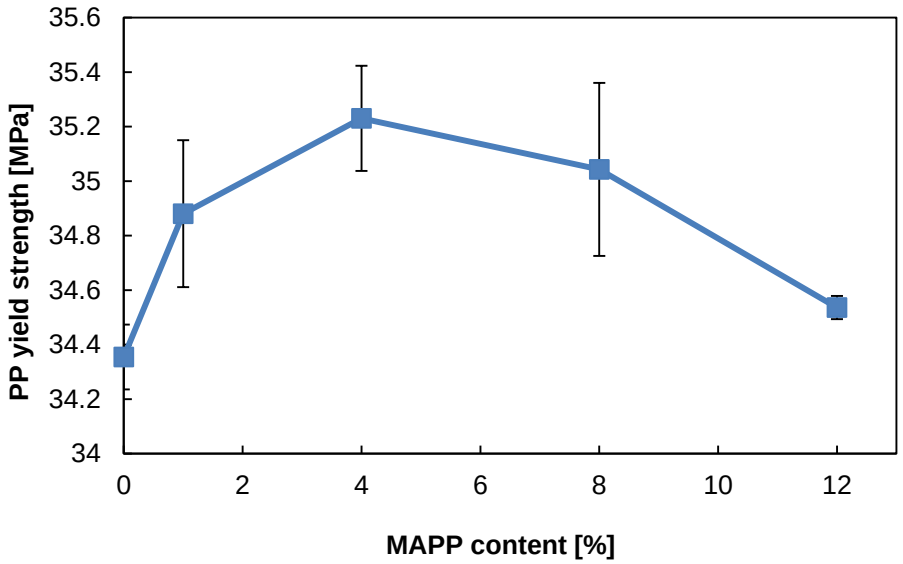

Figure 4.15. Polypropylene yield strength as a function of the MAPP content

As already mentioned in Chapter 3 the PP was tested at two different speeds to reduce the testing time. Below 5 % strain a test speed of 1 mm/min was used. At 5 % strain the test speed was increased from 1 mm/min to 5 mm/min. It is well known that the tensile strength of PP increases with the test speed [48–50]. For comparison, five PP specimens with 1 % MAPP were tested at a constant speed of 1 mm/min. The maximum tensile stress dropped slightly from 34.9 ± 0.3 MPa to 32 ± 0.1 MPa when a constant test speed of 1 mm/min was used. Thus the PP tensile strength at a test speed of 1 mm/min is slightly lower than shown in Figure 4.15. However, it is unlikely that the composite tensile strength was significantly affected by variations of the PP yield strength. The results of the Bowyer-Bader analysis in Figure 4.16 indicate that the PP matrix was not subjected to average stresses above 26 MPa before composite failure and the data in Figure 4.15 shows only small variations of the PP yield strength with the MAPP content. It was concluded in Chapter 2 that the tensile strength of GF/PP composites is influenced by the fibre content, fibre length, fibre orientation and IFSS. Based on the data in Figure 4.4 and Figure 4.8 the first two parameters can be excluded as factors that might explain the behaviour of the composite tensile strength in Figure 4.11. The following sections will focus on the fibre orientation and the IFSS.

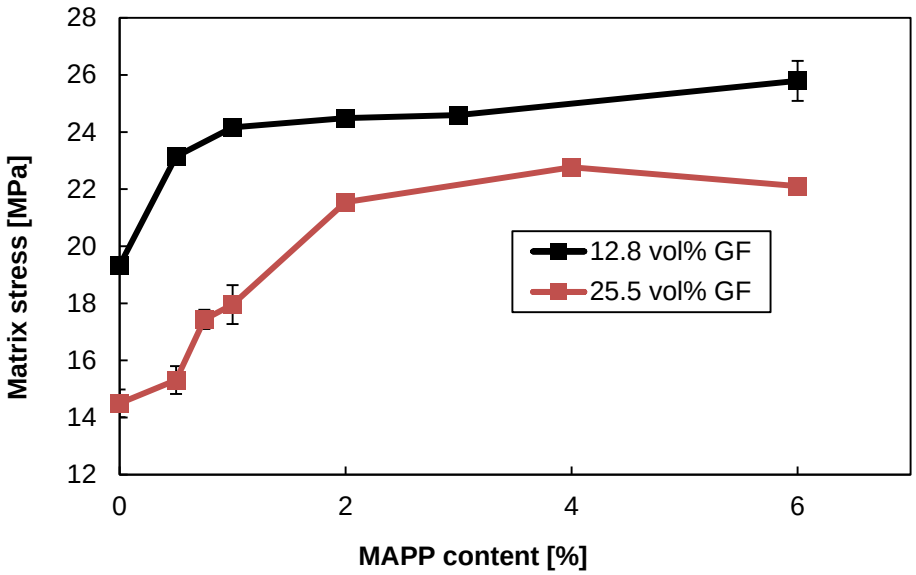

Figure 4.16. Matrix contribution to the composite tensile stress as a function of the MAPP content

4.4.2 Fibre orientation factor from Bowyer-Bader analysis

Figure 4.17 shows the fibre orientation factor obtained from the Bowyer-Bader analysis as a function of the MAPP content.

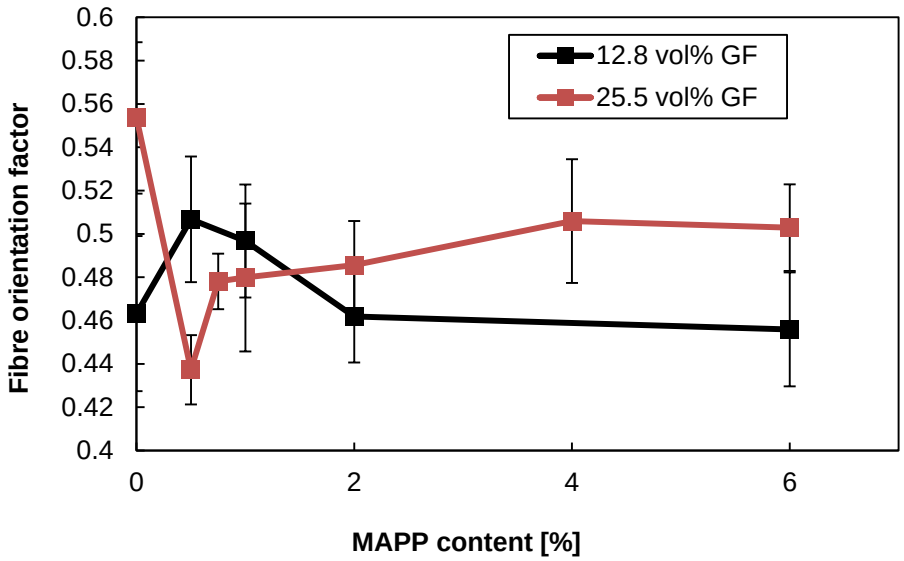

Figure 4.17. Partial reduction of the fibre orientation factor with MAPP content based on the Bowyer-Bader analysis

The trends of the fibre orientation factor in Figure 4.17 are less clear than the trends in Figure 4.10 for the fibre orientation factor obtained from the composite modulus. There is no difference between 0 % MAPP and 6 % MAPP for composites with 12.8 vol% fibre content. In addition, the fibre orientation factor for composites with 25.5

vol% glass fibre content and 0 % MAPP is quite high compared to the other values at higher MAPP contents. Similar to Figure 4.10 and the literature reviewed in section 4.3.2, the data in Figure 4.17 is not conclusive regarding the relationship between fibre content and fibre orientation. However, the data in Figure 4.17 suggest a reduction of the fibre orientation factor between 1 % MAPP and 6 % MAPP for composites with 12.8 vol% glass fibre content which agrees with the data in Figure 4.10.

4.4.3 IFSS from from Bowyer-Bader analysis

In addition to the maximum fibre stress, the Bowyer-Bader analysis can also be used to calculate the IFSS. For the sake of brevity, the IFSS obtained from the Bowyer-Bader analysis will be called Bowyer-Bader IFSS. Figure 4.18 shows Bowyer-Bader IFSS as a function of the MAPP content.

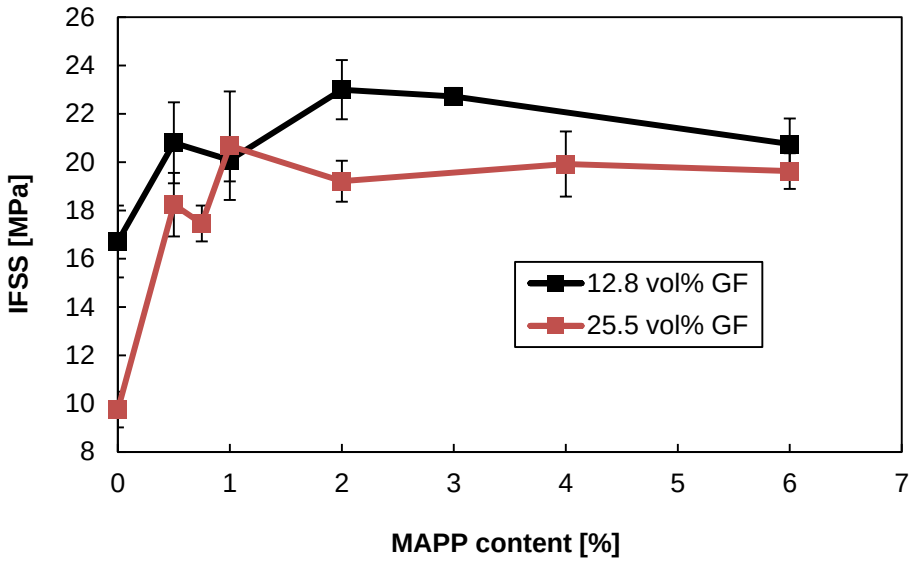

Figure 4.18. Increase of the Bowyer-Bader IFSS with the MAPP content

Apart from one data point the Bowyer-Bader IFSS of composites with 12.8 vol% fibre content is higher than the Bowyer-Bader IFSS of composites with 25.5 vol% fibre content. Similar observations were reported by Thomason [1] on injection moulded GF/PP composites. He suggested that residual stresses in composites decrease with the fibre content which also leads to a reduction of the IFSS.

As expected from the literature review in Chapter 2, the Bowyer-Bader IFSS of composites increased with the MAPP content. The data in Figure 4.18 suggests that the IFSS of composites with 12.8 vol% fibre content increased between 0 % MAPP

and 2 % MAPP and decreased between 3 % MAPP and 6 % MAPP. However, further statistical analysis using t-tests indicated that the Bowyer-Bader IFSS reached a plateau between 0.5 % MAPP and 3 % MAPP. The reduction of the Bowyer-Bader IFSS between 3 % MAPP and 6 % MAPP was confirmed to be significant. The initial increase, plateau and reduction of the Bowyer-Bader IFSS in Figure 4.18 correlates with the behaviour of the composite tensile strength in Figure 4.11. The observed behaviour of the Bowyer-Bader IFSS of composites with 12.8 vol% glass fibre content supports the conclusions of Bowland [37,38]. The Bowyer-Bader IFSS increased initially with the MAPP content. The increase of the Bowyer-Bader IFSS with the MAPP content can be attributed to chemical interactions between aminosilane and the maleic anhydride groups of the MAPP [51,52]. In addition, MAPP might also have improved the wetting of the glass fibres during the composite processing because of acid-basic interactions [53] and a higher melt flow index compared to PP [37]. Several authors [54,55] suggested that MAPP also improves the dispersion of natural fibres in PP composites. The improved dispersion of the fibres was related to an increase of the tensile properties. The glass fibres of the present study were sized with a PP compatible coating and the manufacturer emphasizes the good dispersion ability of the fibres [56]. The sizing of the glass fibres is likely to contain MAPP [57]. In addition, the modulus of composites correlates inversely to the fibre diameter according to the Cox model [25] but the data in Figure 4.6 does not indicate an increase of the composite modulus with the addition of MAPP. It appears therefore unlikely that the addition of MAPP to the composites influenced the dispersion of the glass fibres in the present study.

At higher MAPP contents the Bowyer-Bader IFSS of composites with 12.8 vol% fibre content levelled off because the fibre surfaces were saturated with maleic anhydride groups. The reduction of the Bowyer-Bader IFSS between 3 % MAPP and 6 % MAPP agrees with the composite tensile test data in Figure 4.11. A reduction of the Bowyer-Bader IFSS might be explained with an increasing number of monomers in the MAPP which block reactive sites of the glass fibre surface [47]. This hypothesis will be assessed in the next section when the microbond test results are being discussed. The Bowyer-Bader IFSS of composites with 25.5 vol% also increased with the MAPP content. The values for the Bowyer-Bader IFSS in Figure 4.18 reached a plateau between 0.5% MAPP and 1% MAPP. In contrast to the Bowyer-Bader IFSS, the tensile strength of composites with 25.5 vol% in Figure 4.11 continued to increase between 0.5 % MAPP and 2 % MAPP. As already mentioned,

the tensile strength of GF/PP is mainly controlled by the fibre content, fibre orientation and the IFSS. The fibre content did not show large variations and the data in Figure 4.10 indicates that the fibre orientation of composites with 25.5 vol% did not vary significantly between 0.5 % MAPP and 2 % MAPP. Thus, changes of the IFSS due to higher MAPP contents are the most likely explanation for the increase of the composite tensile strength between 1 % MAPP and 2 % MAPP. The results of the Bowyer-Bader analysis might therefore be subject to further discussion.

Mittal and Gupta [6,15] showed that the values for the fibre orientation factor of the Bowyer-Bader analysis depend on the chosen composite strains ε_1 and ε_2. They modified the Bowyer-Bader analysis and assumed a linear relationship between interfacial shear stress and composite tensile stress. Details can be found in their publications and in Chapter 2. To assess the effect of the chosen composite strains ε_1 and ε_2 on the results of the Bowyer-Bader analysis, four different strain ranges were chosen. The stress strain curves of composites with 12.8 vol% fibre content and composites with 25.5 vol% fibre content (both 2 % MAPP) were analysed for the four chosen strain ranges. The strain ranges are illustrated in Figure 4.19 and Figure 4.20 where the chosen composite strains ε_1 and ε_2 are the left and right values of the four boxes. The results of the Bowyer-Bader analysis are summarised in Table 4.7 and Table 4.8.

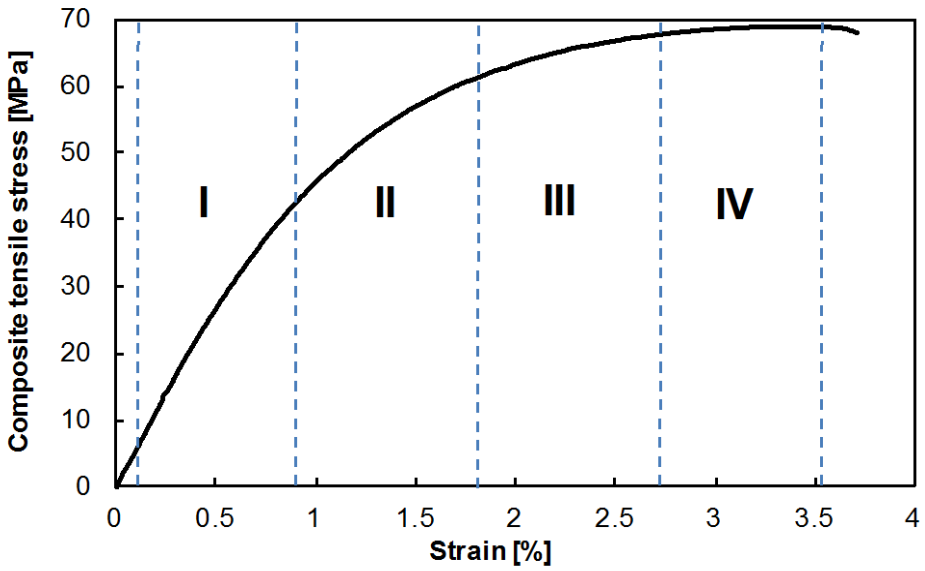

Figure 4.19. Stress-strain curve of a composite with 12.8 vol% fibre and 2 % MAPP content

Table 4.7. Dependence of Bowyer-Bader analysis on strain range (composite with 12.8 vol% fibre content, 2 % MAPP)

	12.8 vol% fibre content, 2 % MAPP content			
Property	Section I	Section II	Section III	Section IV
Fibre orientation factor	0.39 ± 0.04	0.45 ± 0.01	0.46 ± 0.01	1 ± 0.27
IFSS [MPa]	54.3 ± 33.4	23.5 ± 1.3	23.1 ± 0.5	10.2 ± 3.4
Fibre stress [MPa]	1524 ± 205	2402 ± 86	2449 ± 22	2660 ± 27

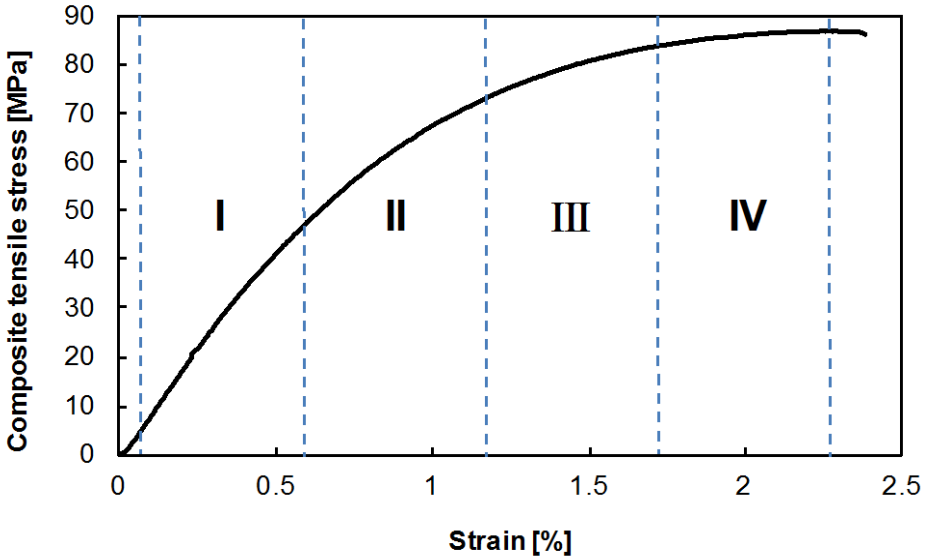

Figure 4.20. Stress-strain curve of composite with 25.5 vol% fibre content and 2 % MAPP

Table 4.8. Dependence of Bowyer-Bader analysis on strain range (composite with 25.5 vol% fibre content, 2 % MAPP)

	25.5 vol% fibre content, 2 % MAPP content			
Property	Section 1	Section 2	Section 3	Section 4
Fibre orientation factor	0.49 ± 0.02	0.5 ± 0.02	0.49 ± 0.01	0.8 ± 0.35
IFSS [MPa]	19.4 ± 2.1	18.7 ± 0.8	18.9 ± 0.4	12.9 ± 3.4
Fibre stress [MPa]	1870 ± 1004	1686 ± 110	1630 ± 41	1782 ± 42

The results in Table 4.7 and Table 4.8 confirm the conclusion of Mittal and Gupta [6,15] that the results of the Bowyer-Bader analysis are dependent on the chosen strain range. For both composites the fibre orientation factor increased between section I and section IV. The IFSS decreased between section I and section IV. For

composites with 12.8 vol% fibre content the maximum fibre stress decreased between section I and section IV. For composites with 25.5 vol% fibre content no clear trend was observed. The results in Table 4.7 and Table 4.8 also indicate that the results of the Bowyer-Bader analysis in section II and section III are almost constant when the error bars are considered. The strain range chosen in this thesis (1/3 and 2/3 of the strain at break) fall into section II and section III of Figure 4.19 and Figure 4.20.

Thus, the Bowyer-Bader analysis can provide precise results as long as the strain values are chosen properly. However, the results of this section also showed that the Bowyer-Bader analysis might not always detect differences between different GF/PP composites. Based on the discussion above, it appears likely that the increase of the tensile strength of composites with 25.5 vol% glass fibre content between 0.5 % MAPP and 2 % MAPP was caused by an increase of the IFSS. This increase of the IFSS was not detected by the Bowyer-Bader analysis. However, the Bowyer-Bader analysis detected that MAPP improves the IFSS. It is therefore a useful screening tool to detect general trends but it is worth comparing the results of the Bowyer-Bader analysis with micromechanical test data.

4.4.4 Microbond IFSS and the correlation to composite tensile data

Similar to the Bowyer-Bader analysis, the microbond data in Figure 4.21 shows that the IFSS between the glass fibres and the PP increased with the addition of MAPP. In contrast to the microbond test data in Figure 4.21, the Bowyer-Bader analysis did not show a significant increase of the IFSS of the composites between 0.5 % MAPP and 2 % MAPP. As discussed above, the Bowyer-Bader analysis did not always detect differences between composites with different MAPP content. The trend of the tensile strength of the composites with 25.5 vol% glass fibre content can be explained by the microbond data. The IFSS of the microbond samples reached a plateau at 1 % MAPP. The tensile strength of the composites with 25.5 vol% fibre content reached a plateau at 2 % MAPP. The microbond samples had a fibre volume fraction of approximately 2.3 $\pm$ 0.3 vol%. Thus, the microbond samples had a higher ratio between number of MAPP molecules and fibre surface area than the injection moulded composites. A lower amount of MAPP was required to saturate the glass fibre surface of the microbond samples with MAPP molecules. The injection moulded GF/PP composites with a higher fibre volume fraction and larger fibre surface area required more MAPP than the microbond samples to reach a

maximum IFSS. Thus, the tensile strength of the composites continued to increase between 1 % MAPP and 2 % MAPP while the microbond IFSS did not change significantly.

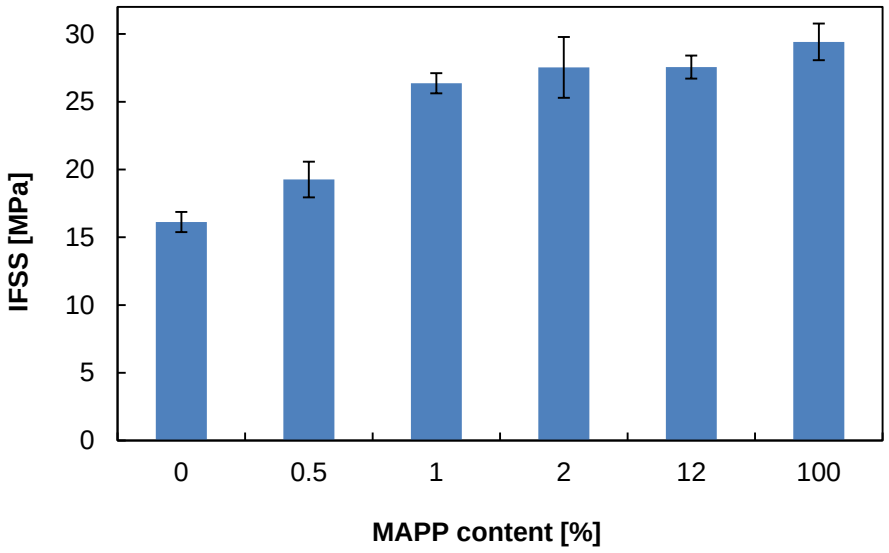

Figure 4.21. Increase of the microbond IFSS with MAPP content

The different trends of the tensile strength of composites with 12.8 vol% fibre content and microbond IFSS cannot be explained with the ratio between fibre surface area and number of MAPP molecules. The tensile strength and the Bowyer-Bader IFSS of composites with 12.8 vol% reached a plateau at 0.5 % MAPP but the IFSS of the microbond samples increased further with the addition of MAPP. The fact that the microbond IFSS did not decrease even at 100 % MAPP indicates that the hypothesis of Qiu et al. [47] does not apply to the materials that were used for this thesis. The microbond data does not support the hypothesis that high MAPP concentrations reduce the IFSS because monomers in the MAPP block reactive sites on the fibre surface. In addition, the data in Figure 4.21 also does not indicate a formation of a weak interphase at high MAPP contents as suggested by Schultz et al. [58] when they worked on PP aluminium interfaces. In contrast to the microbond IFSS, the composite tensile strength and the Bowyer-Bader IFSS dropped between 3 % MAPP and 6 % MAPP. Thus, the tensile strength and the Bowyer-Bader IFSS of composite with 12.8 vol% glass fibre content did not follow the trend of the microbond test results. This suggests that the tensile strength of the composites was affected by at least one other mechanism apart from the IFSS.

Based on the analysis of the composite modulus and the Bowyer-Bader analysis it was speculated that the addition of MAPP also affected the melt flow properties of the composites during the injection moulding process and reduced the degree of fibre alignment. A reduction of the degree of fibre alignment would also have affected the composite tensile strength. Another mechanism by which high MAPP contents could affect the tensile strength of GF/PP composites was proposed by Zheng et al. [40]. They explained the strength reduction of GF/PP composites at high MAPP contents with an embrittlement of the composites. If the IFSS of a GF/PP composite is high enough the fibres would not debond from the PP matrix. No energy would be absorbed by fibre pull-out. The sudden release of energy into the PP matrix would lead to crevices, breakage of adjacent fibres and composite failure.

4.4.5 Influence of MAPP on the critical fibre length for fibre fracture

The concept of the critical fibre length has already been used in the previous section for the Bowyer-Bader analysis. The Bowyer-Bader analysis is based on the assumption that the critical fibre length depends on the composite strain. The critical fibre length is calculated as a function of the composite strain. It is also possible to calculate the critical fibre length for fibre failure l_{CFr}.

Equation 4.4. Critical fibre length for fibre failure

$$l_{CFr} = \frac{\sigma_f * r_f}{\tau_{ult}}$$

where σ_f is the tensile strength of the glass fibre, τ_{ult} stands for the IFSS and r_f the fibre radius. The value of σ_f is not known and can only be estimated. Recent studies reported the strength of continuous E-glass fibres to be in the range between 2.2 GPa and 2.4 GPa when samples with 20 mm gauge length were tested [59,60]. At a gauge length of 5 mm or less values between 2.5 GPa and 2.7 GPa were measured [18,61]. There is an inverse correlation between the tensile strength of glass fibres and the gauge length [18]. Chopped fibres might therefore be expected to have a higher tensile strength. However, chopped glass fibres might be damaged during the chopping process. Values of approximately 2 GPa were previously obtained when chopped fibre were tensile tested with a gauge length between 180 µm and 380 µm [62]. Further damaged might have been caused to the glass fibres in the present study during extrusion and injection moulding of the composites. On the other hand it might be argued that the fibres in the composite are stronger than as received

chopped fibres because the weak fibres are likely to break into shorter and stronger fibres. To the author's knowledge the strength of glass fibres extracted from injection moulded composites has not been reported in the literature. The values for the critical fibre length for fibre failure obtained from Equation 4.3 are therefore only an indication of trends because of the uncertainty around the value for σ_f.

In this section two different sets of data were calculated for l_{CFr}. One set of data is based on an assumed value of 2 GPa for σ_f. The value of 2 GPa was taken from a study on chopped fibres as mentioned above [18]. The second set of data is based on a value of 2.36 GPa for σ_f. The value of 2.36 GPa was taken from Chapter 6 of this thesis. It is the strength of the chopped fibres that were processed into GMT composites measured at 5 mm gauge length [63].

The fibre length measurement data and the calculated values of l_{CFr} were used to calculate the fraction of fibres that are shorter than the critical fibre length and longer than the critical fibre length for fibre failure. Figure 4.22 shows the perdentage of fibres that are longer than l_{CFr} (supercritical fibres).

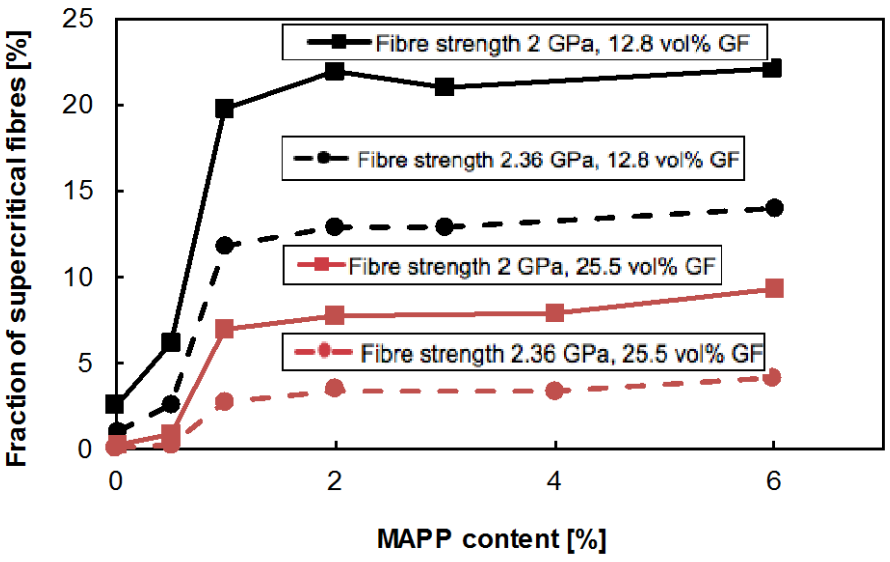

Figure 4.22. Increase of the fraction of supercritical fibres with MAPP content (12.8 vol% glass fibre content)

Figure 4.22 shows that in all composites most of the fibres were shorter than the critical fibre length. The percentage of supercritical fibres decreased with the σ_f but the qualitative trends in Figure 4.22 are independent from the assumed value of σ_f. As discussed in Section 4.2, composites with 25.5 vol% fibre content had a shorter residual fibre length than composites with 12.8 vol%. A smaller percentage of fibres

was longer than the critical fibre length. The percentage of fibres longer than the critical fibre length increased with the MAPP content. The IFSS increased and shorter fibres could contribute to the composite stress. However, the majority of the fibres was shorter than the critical fibre even when the MAPP content was optimised and the plateau for the IFSS was reached. Thus, it is likely that the strength of most of the fibres was not utilized in the composites. It might therefore be expected that the composites failed because of interfacial failure and microcracks in the matrix [32,64] rather than fibre fracture.

4.5 Strain at break

According to the studies reviewed in Chapter 2 the strain at break of GF/PP composites depends on the fibre content [5,11,12,16,65], fibre length [66], fibre alignment [5,67] and the IFSS [65,68,69]. It was suggested in the previous sections that the addition of MAPP to the composites increased the IFSS and possibly reduced the degree of the fibre alignment.

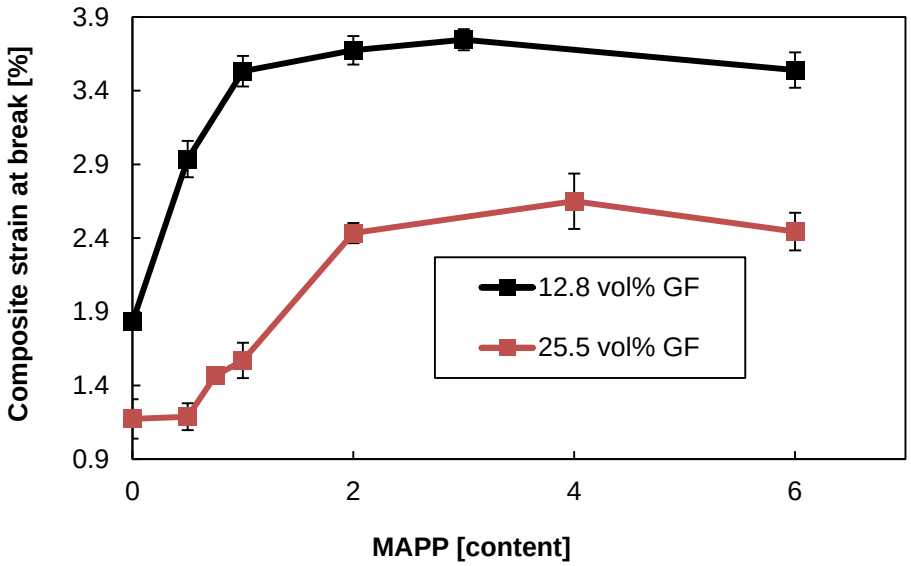

Figure 4.23. Effect of MAPP content on the composite strain at break

A comparison between Figure 4.14 and Figure 4.23 reveals that the strain at break followed the yield strain. The strain at break of composites with 25.5 vol% glass fibre content in Figure 4.23 increased sharply between 0 % MAPP and 2 % MAPP. T-tests showed that the strain at break of composites with 25.5 vol% glass fibre content reached a plateau between 2 % MAPP and 6 % MAPP. The strain at break of composites with 12.8 vol% glass fibre content increased between 0 % MAPP and

1 % MAPP and dropped between 3 % MAPP and 6 % MAPP. The observed trends in Figure 4.23 are similar to the trends of the composite tensile strength in Figure 4.11. Similar to the composite tensile strength, the strain at break of the composites increased with the addition of MAPP to the composites. This might be explained with an increase of the IFSS. When short fibre thermoplastics are subjected to a tensile stress the highest stress concentrations are at the fibre ends. The fibre ends might debond from the matrix which leads to the growth of microvoids at the fibre ends and subsequent growth of cracks along the interface and in the matrix [64]. A higher IFSS might therefore delay this process and lead to an increase of the strain at break. Composites with 25.5 vol% fibre content required a higher MAPP concentration than composites with 12.8 vol% fibre content because of the larger fibre surface area. According to Zheng et al. [40], high MAPP contents and a high IFSS reduce the strain at break of GF/PP composites because less energy can be dissipated via fibre pull-out. The high IFSS might also explain the plateau and decrease of the strain at break in Figure 4.23. Based on the analysis of the composite modulus it was suggested in this chapter that the fibre orientation factor decreased with the addition of MAPP to the composites. A lower degree of fibre alignment in the load direction usually causes an increase of the composite strain at break [5,67]. The absence of this effect means that either the fibre orientation was not affected by the MAPP content or the lack of energy dissipation by fibre pull-out masked the effect of the fibre orientation. Following this argument, the strain at break might increase when the MAPP content is increased beyond 6 %. The IFSS would reach a plateau but the increasing amount of MAPP changes the flow properties of the composite during the injection moulding process. Thus, the degree of fibre orientation will continue to decrease while the IFSS reaches a plateau. The data in Chapter 5 shows indeed an increase of the strain at break when more than 6 % MAPP were added to the composites.

Figure 4.24 shows the strain at break and yield strain of unreinforced PP as a function of the MAPP content. The yield strain of the PP did not exhibit a clear correlation with the MAPP content. In contrast to the yield strain, the strain at break decreased with the MAPP content. Pure PP without MAPP was not tested to failure.

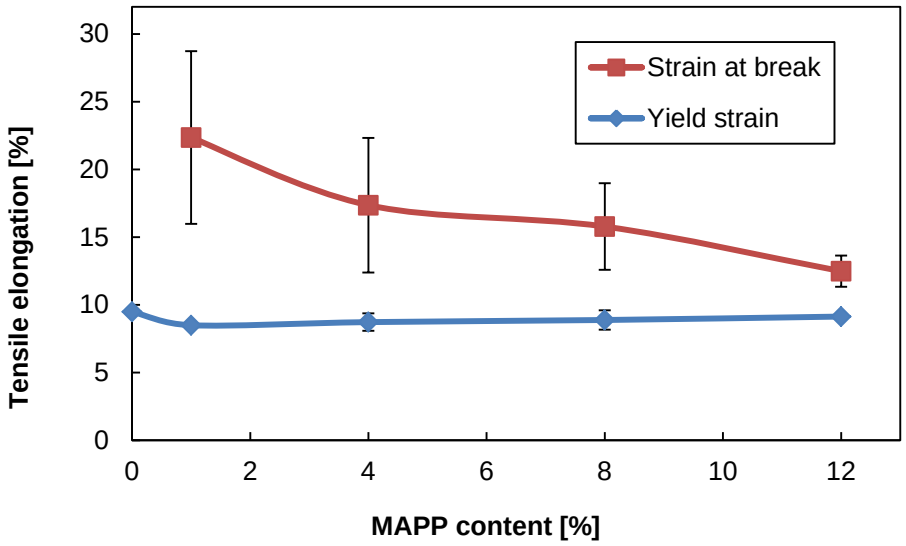

Figure 4.24. Effect of MAPP content on the strain at break of PP

The strain at break of unreinforced PP was reported to decrease when the molecular weight of the PP decreases [26]. Thus, the reduction of the strain at break in Figure 4.24 could be explained with the lower molecular weight of MAPP compared to PP. The strains at break and the yield strains of the unreinforced PP were significantly higher than the composite strain at break. However, the composite strain at break is a global average strain. The local strains of short fibre at the fibre ends are higher than the composite strain at break [64,70]. Thus, the drop of the strain at break of the PP in Figure 4.24 might also have contributed to the reduction of the strain at break of the composites.

4.6 Unnotched charpy impact strength

The impact properties of composites are not the main focus of this thesis and they were not reviewed in Chapter 2. The unnotched impact strength of GF/PP composites was observed to depend on the fibre length [10], fibre content [10,11,16,38] and the IFSS [38,68,71]. The data in Figure 4.25 shows that the addition of MAPP improved the unnotched charpy impact strength. Similar observations were reported by Bowland [38]. Bowland also observed a decrease of the unnotched impact strength when an optimum MAPP content was exceeded. The data in Figure 4.25 suggests a reduction of the unnotched impact strength between 3 % MAPP and 6 % MAPP but a t-test showed that this difference is not significant. Matrix deformation, matrix fracture, fibre pull-out (debond and friction) and fibre fracture were identified as energy dissipation mechanisms in impact tests of GF/PP

composites [10,72,73]. In the present study the contributions of the energy mechanisms were affected by the addition of MAPP to the composites. It was shown in Figure 4.22 that the fraction of supercritical fibres (fibres longer than the critical length for fibre failure) increased with the addition of MAPP which was attributed to an increase of the IFSS. Despite the increase of the MAPP content, more than 75 % of the fibres were shorter than the critical fibre length. Energy dissipation by fibre debond and pull-out was therefore more frequent than energy dissipation by fibre fracture. The work of fracture of short fibre composites correlates with the IFSS [74] and it can be concluded that the energy absorbed by fibre pull-out increased with the IFSS when the fibres were subcritical. The increase of the impact strength in Figure 4.25 can therefore be explained with an increase of the work of fracture by fibre debond and fibre pull-out.

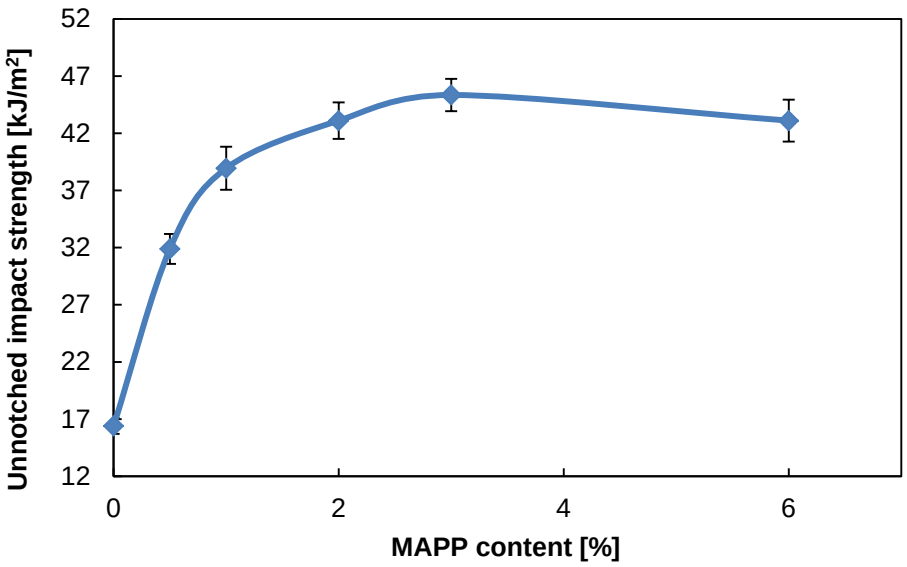

Figure 4.25. Increase of the unnotched charpy impact strength with MAPP content (composites with 12.8 vol% fibre content)

4.7 Summary and Conclusions

In this chapter the structure performance relationships of injection moulded GF/PP were investigated. Similar to the study by Bowland [37,38] on long fibre thermoplastics, the tensile strength, strain at break and unnotched charpy impact strength increased with the addition of MAPP to the composites. The MAPP content to achieve maximum composites performance depended on the glass fibre content. Micromechanical analysis and microbond tests showed that MAPP can improve the IFSS in GF/PP composites. At high MAPP contents a reduction of the composite

tensile strength, strain at break and composite modulus were observed. Two different mechanisms were proposed to explain these observations. Based on micromechanical analysis it was suggested that the reduction of the composite modulus and composite tensile strength could be attributed to a lower degree of fibre alignment parallel to the load axis. It was hypothesized that MAPP changes the melt flow properties of the composites because of its lower viscosity compared to PP. A high IFSS might have reduced the energy absorbed by fibre pull-out which led to a reduction of the composite tensile strength and strain at break. The addition of MAPP also led to a reduction of the strain at break of unreinforced PP. Thus, the composite strain at break might also have been affected by a reduction of the strain at break of the PP matrix.

The Bowyer-Bader analysis of the composite tensile test data provided precise results when the strain range was chosen between one quarter and three quarter of the composite yield strain. It was also found that the Bowyer-Bader analysis might not always provide results that agree with microbond data. For example, the Bowyer-Bader analysis indicated a reduction of the IFSS between 3 % MAPP and 6 % MAPP for composites with 12.8 vol% fibre content. The microbond data did not suggest a reduction of the IFSS with the MAPP content. It is likely that the IFSS obtained from the Bowyer-Bader analysis was affected by the same mechanisms that reduced the composite tensile strength. It can be concluded from the data of this chapter that the Bowyer-Bader analysis is a useful screening tool but micromechanical tests like microbond tests are still essential to obtain information about the adhesion between fibre and matrix of discontinuous GF/PP composites.

4.8 References

[1] Thomason JL. Micromechanical parameters from macromechanical measurements on glass reinforced polypropylene. Compos Sci Technol 2002;62:1455–68.

[2] Wallenberger FT, Watson JC, Hong L. Glass Fibers. ASM Handb 2001;21:27–34.

[3] Gupta VB, Mittal RK, Sharma PK, Mennig G, Wolters J. Some studies on glass fiber-reinforced polypropylene. Part 1: Reduction in fiber length during processing. Polym Compos 1989;10:8–15.

[4] Phelps JH, Abd El-Rahman AI, Kunc V, Tucker CL. A model for fiber length attrition in injection-molded long-fiber composites. Compos Part A Appl Sci Manuf 2013;51:11–21.

[5] Spahr DE, Friedrich K, Schultz JM, Bailey RS. Microstructure and fracture behaviour of short and long fibre-reinforced polypropylene composites. J Mater Sci 1990;25:4427–39.

[6] Mittal RK, Gupta VB, Sharma P. The effect of fibre orientation on the interfacial shear stress in short fibre-reinforced polypropylene. J Mater Sci 1987;22:1949–55.

[7] Roux C, Denault J, Champagne MF. Parameters regulating interfacial and mechanical properties of short glass fiber reinforced polypropylene. J Appl Polym Sci 2000;78:2047–60.

[8] Rohde M, Ebel A, Wolf-Fabris F, Altstädt V. Influence of processing parameters on the fiber length and impact properties of injection molded long glass fiber reinforced polypropylene. Int Polym Process 2001;26:292–303.

[9] Lafranche E, Krawczak P, Ciolczyk JP, Maugey J. Injection moulding of long glass fibre reinforced polyamide 6-6: Guidelines to improve flexural properties. Express Polym Lett 2007;1:456–66.

[10] Thomason JL. The influence of fibre length and concentration on the properties of glass fibre reinforced polypropylene: 5. Injection moulded long and short fibre PP. Compos Part A Appl Sci Manuf 2002;33:1641–52.

[11] Thomason JL. The influence of fibre length and concentration on the properties of glass fibre reinforced polypropylene. 6. The properties of injection moulded long fibre PP at high fibre content. Compos Part A Appl Sci Manuf 2005;36:995–1003.

[12] Fu S-Y, Lauke B, Mäder E, Yue C-Y, Hu X. Tensile properties of short-glass-fiber- and short-carbon-fiber-reinforced polypropylene composites. Compos Part A Appl Sci Manuf 2000;31:1117–25.

[13] Ota WN, Amico SC, Satyanarayana KG. Studies on the combined effect of injection temperature and fiber content on the properties of polypropylene-glass fiber composites. Compos Sci Technol 2005;65:873–81.

[14] Thomason JL, Vlug MA. The influence of fibre length and concentration on the properties of glass fibres reinforced polypropylene: 1. Tensile and flexural modulus. Compos Part A Appl Sci Manuf 1996;27:477–84.

[15] Mittal RK, Gupta VB. The strength of the fibre-polymer interface in short glass fibre-reinforced polypropylene. J Mater Sci 1982;17:3179–88.

[16] Xavier SF, Misra A. Influence of glass fiber content on the morphology and mechanical properties in injection molded polypropylene composites. Polym Compos 1985;6:93–9.

[17] Lee N-J, Jang J. The effect of fibre-content gradient on the mechanical properties of glass-fibre-mat/polypropylene composite. Compos Sci Technol 2000;60:209–17.

[18] Yang L, Thomason JL. Effect of silane coupling agent on mechanical performance of glass fibre. J Mater Sci 2012;48:1947–54.

[19] Krenchel H. Theoretical investigations of the elasticity and strength of fibre-cement. Fibre Reinf., Alademisk forlag; 1964, p. 11–38.

[20] Ericson M, Berglund L. Deformation and fracture of glass-mat- reinforced polypropylene. Compos Sci Technol 1992;43:269–81.

[21] Garkhail SK, Heijenrath RWH, Peijs T. Mechanical properties of natural-fibre-mat-reinforced thermoplastics based on flax fibres and polypropylene. Appl Compos Mater 2000;7:351–72.

[22] Bright PF, Crowson RJ, Folkes MJ. A study of the effect of injection speed on fibre orientation in simple mouldings of short glass fibre-filled polypropylene. J Mater Sci 1978;13:2497–506.

[23] Vincent M, Giroud T, Clarke A, Eberhardt C. Description and modeling of fiber orientation in injection molding of fiber reinforced thermoplastics. Polymer (Guildf) 2005;46:6719–25.

[24] Gupta l VB, Mittal RK, Sharma PK. Some studies on Glass Fiber-Reinforced Polypropyelen. Part II: Mechanical Properties and Their Dependence on Fiber Length, Interfacial Adhesion, and Fiber Adhesion. Polym Compos 1989;10:16–27.

[25] Cox HL. The elasticity and strength of paper and other fibrous materials. Br J Appl Phys 2002;3:72–9.

[26] Qiu W, Endo T, Hirotsu T. Structure and properties of composites of highly crystalline cellulose with polypropylene: Effects of polypropylene molecular weight. Eur Polym J 2006;42:1059–68.

[27] Tripathi D. Practical Guide to Polypropylene. Rapra Technology Ltd; 2002.

[28] Rijsdijk HA, Contant M, Polymers C, Box PO, Eindhoven MB. Continuous-glass-fibre-reinforced polypropylene composites: 1. Influence of maleic-anhydride-modified polypropylne on mechanical properties. Compos Sci Technol 1993;48:161–72.

[29] Bailey R, Rzepka B. Fibre orientation mechanisms for injection molding of long fibre composites. Int Polym Process 1991;6:35–41.

[30] Sanou M, Chung B, Cohen C. Glass fiber-filled thermoplastics. II. Cavity filling and fiber orientation in injection molding. Polym Eng Sci 1985;25:1008–16.

[31] Akay M, Barkley D. Fibre orientation and mechanical behaviour in reinforced thermoplastic injection mouldings. J Mater Sci 1991;26:2731–42.

[32] Curtis PT, Bader MG, Bailey JE. The stiffness and strength of a polyamide thermoplastic reinforced with glass and carbon fibres. J Mater Sci 1978;13:377–90.

[33] Neves NM, Pontes AJ, Pouzada AS. Fiber content effect on the fiber orientation in injection molded GF/PP composite plates. SPE ANTEC, San Francisco: 2002.

[34] Kim H-S, Lee B-H, Choi S-W, Kim S, Kim H-J. The effect of types of maleic anhydride-grafted polypropylene (MAPP) on the interfacial adhesion properties of bio-flour-filled polypropylene composites. Compos Part A Appl Sci Manuf 2007;38:1473–82.

[35] Liang JZ, Tang CY, Man HC. Flow and mechanical properties of polypropylene/low density polyethylene blends. J Mater Process Technol 1997;66:158–64.

[36] Nanguneri SR, Rao NS, Subramanian N. Rheological characteristics of glass-fibre-filled polypropylene melts. Rheol Acta 1987;26:301–7.

[37] Bowland C. A formulation study of long fiber thermoplastic polypropylene (Part1): The effects of coupling agent, glass content & resin properties on mechanical properties. Automot. Compos. Conf. Expo., 2008.

[38] Bowland C. A formulation study of long fiber thermoplastic polypropylene (Part 2): The effects of coupling agent type and properties. Automot. Compos. Conf. Expo., 2009.

[39] Cantwell WJ, Tato W, Kausch HH, Jacquemet R. The influence of a fiber-matrix coupling agent on the properties of a glass fber / polypropylene GMT. J Thermoplast Compos Mater 1992;5:304–17.

[40] Zheng A, Wang H, Zhu X, Masuda S. Studies on the interface of glass fiber-reinforced polypropylene composite. Compos Interfaces 2002;9:319–33.

[41] Bernasconi A, Cosmi F, Hine PJ. Analysis of fibre orientation distribution in short fibre reinforced polymers: A comparison between optical and tomographic methods. Compos Sci Technol 2012;72:2002–8.

[42] Mlekusch B. Fibre orientation in short- fibre-reinforced thermoplastics II . Quantitative measurements by image analysis. Compos Sci Technol 1999;59:547–60.

[43] Gupta VB, Mittal RK, Sharma PK. Some studies on glass fiber-reinforced polypropylene. Part II: Mechanical properties and their dependence on fiber length, interfacial adhesion, and fiber dispersion. Polym Compos 1989;10:16–27.

[44] Thomason JL. The influence of fibre length and concentration on the properties of glass fibre reinforced polypropylene: 7. Interface strength and fibre strain in injection moulded long fibre PP at high fibre content. Compos Part A Appl Sci Manuf 2007;38:210–6.

[45] Bowyer WH, Bader MG. On the re-inforcement of thermoplastics by imperfectly aligned discontinuous fibres. J Mater Sci 1972;7:1315–21.

[46] Thomason JL. Interfacial strength in thermoplastic composites - at last an industry friendly measurement method? Compos Part A Appl Sci Manuf 2002;33:1283–8.

[47] Qiu W, Endo T, Hirotsu T. Interfacial interaction, morphology, and tensile Properties of a composite of highly crystalline cellulose and maleated polypropylene. Eur Polym J 2006;42:1059–68.

[48] Zhou Y, Mallick PK. Effects of temperature and strain rate on the tensile behavior of unfilled and talc-filled polypropylene. Part I: Experiments. Polym Eng Sci 2002;42:2449–60.

[49] Zrida M, Laurent H, Grolleau V, Rio G, Khlif M, Guines D, et al. High-speed tensile tests on a polypropylene material. Polym Test 2010;29:685–92.

[50] Schossig M, Bieroegel C, Grellmann W, Bardenheier R, Mecklenburg T. Effect of strain rate on mechanical properties of reinforced polyolefins. In: Gdoutos EE, editor. 16th Eur. Conf. Fract., Dordrecht: Springer Netherlands; 2006, p. 507–8.

[51] Su D-T, Chang G-Y, Lee M-S. A study of interfacial phenomena in the glass-fiber/PP composite. ANTEC, 1989, p. 531–4.

[52] Nygård P, Redford K, Gustafson C-G. Interfacial strength in glass fibre-polypropylene composites: influence of chemical bonding and physical entanglement. Compos Interfaces 2002;9:365–88.

[53] Mäder E, Jacobasch HJ, Grundke K, Gietzelt T. Influence of an optimized interphase on the properties of polypropylene/glass fibre composites. Compos Part A Appl Sci Manuf 1996;27:907–12.

[54] Pracella M, Chionna D, Anguillesi I, Kulinski Z, Piorkowska E. Functionalization, compatibilization and properties of polypropylene composites with hemp fibres. Compos Sci Technol 2006;66:2218–30.

[55] Kazayawoko M, Balatinecz JJ, Woodhams RT, Law S. Effect of ester linkages on the mechanical properties of wood fiber-polypropylene composites. J Reinf Plast Compos 1997;16:1383–406.

[56] 3B Fibreglass. DS 2200-13P Chopped Strand for PP & PE n.d. http://www.3b-fibreglass.com/wp-content/themes/3b/pdf/Datasheets/CS_2200-13P.pdf (accessed August 8, 2016).

[57] Thomason JL. Glass Fibre Sizing A Review of Size Formulation Patents. 2015.

[58] Schultz J, Lavielle L, Carre A, Comien P. Surface properties and adhesion mechanisms of graft polypropylenes. J Mater Process Technol 1989;24:4363–9.

[59] Yang L, Sáez Rodríguez E, Nagel U, Thomason JL. Can thermally degraded glass fibre be regenerated for closed-loop recycling of thermosetting composites? Compos Part A Appl Sci Manuf 2015;72:167–74.

[60] Feih S, Mouritz AP, Case SW. Determining the mechanism controlling glass fibre strength loss during thermal recycling of waste composites. Compos Part A Appl Sci Manuf 2015;76:255–61.

[61] Lund MD, Yue Y. Impact of drawing stress on the tensile strength of oxide glass fibers. J Am Ceram Soc 2010;93:3236–43.

[62] Thomason JL, Kalinka G. Technique for the measurement of reinforcement fibre tensile strength at sub-millimetre gauge lengths. Compos Part A Appl Sci Manuf 2001;32:85–90.

[63] Thomason JL, Nagel U, Sáez Rodríguez E, Yang L. Regenerating the strength of thermally recycled glass fibres using hot sodium hydroxide. Compos Part A Appl Sci Manuf 2016;87:220–7.

[64] Sato N, Kurauchi T, Sato S, Kamigaito O. Microfailure behaviour of randomly dispersed short fibre reinforced thermoplastic composites obtained by direct SEM observation. J Mater Sci 1991;26:3891–8.

[65] Hassan A, Rahman NA, Yahya R. Extrusion and injection-molding of glass fiber/MAPP/polypropylene: effect of coupling agent on DSC, DMA, and mechanical properties. J Reinf Plast Compos 2011;30:1223–32.

[66] Thomason JL, Vlug MA, Schipper G, Krikort HGLT. Influence of fibre length and concentration on the properties of glass fibre-reinforced polypropylene Part 3 Strength and strain at failure. Compos Part A Appl Sci Manuf 1996;27A:1075–84.

[67] Ericson ML, Berglund LA. Processing and mechanical properties of orientated preformed glass-mat-reinforced thermoplastics. Compos Sci Technol 1993;49:121–30.

[68] Mäder E, Moos E, Karger-Kocsis J. Role of film formers in glass fibre reinforced polypropylene - new insights and relation to mechanical properties. Compos Part A Appl Sci Manuf 2001;32:631–9.

[69] Bikiaris D, Matzinos P, Larena A, Flaris V, Panayiotou C. Use of silane agents and poly(propylene-g-maleic anhydride) copolymer as adhesion promoters in glass fiber/polypropylene composites. J Appl Polym Sci 2001;81:701–9.

[70] Geers MGD, Peijs T, Brekelmans WAM, De Borst R. Experimental monitoring of strain localization and failure behaviour of composite materials. Compos Sci Technol 1996;56:1283–90.

[71] Mäder E, Pisanova E. Characterization and design of interphases in glass fiber reinforced polyproplyene. Polym Compos 2000;21:361–8.

[72] Thomason JL, A. VM. Influence of fibre length and concentration on the properties of glass fibre reinforced polypropylene: 4. Impact properties. Compos Part A Appl Sci Manuf 1997;28A:277–88.

[73] Cottrell AH. Strong Solids. Proc. R. Soc. London. Ser. A, London: 1964, p. 2–9.

[74] Friedrich K. Microstructural efficiency and fracture toughness of short fiber/thermoplastic matrix composites. Compos Sci Technol 1985;22:43–74.

5. Polypropylene composites based on thermally degraded glass fibres

In this chapter the effect of elevated temperatures on the reinforcement potential of glass fibres is investigated. In Section 5.1 the effect of the atmosphere and temperature on the degradation of glass fibre sizings is discussed. One result of the literature review in Chapter 2 was that little systematic work has been done on the reinforcement potential of thermally recycled glass fibres in glass fibre Polypropylene (GF/PP) composites. In Section 5.2 the effects of thermal glass fibre degradation on the performance of injection moulded GF/PP composites are investigated. In Section 5.3 results are presented on how the performance of PP composites based on thermally recycled glass fibres can be improved by the addition of maleic anhydride grafted Polypropylene (MAPP) to the PP matrix.

Tensile tests and unnotched charpy impact tests were performed to assess the performance of the injection moulded composites. Microbond tests were performed to determine the apparent interfacial shear strength (IFSS) between the glass fibres and the PP. The error bars in all plots represent 95 % confidence intervals. T-tests (p=0.05) were performed to further assess the significance of observed trends.

All composites had a nominal fibre content of 30 wt% (12.8 vol%). Polybond 3200 was used to modify the PP matrix and vary the IFSS of the composites. Similar to Chapter 4, the term MAPP content is used in this chapter to refer to the amount of Polybond 3200 that was added to the composites as a weight fraction of the PP matrix. For example, 300 g glass fibre, 14.14 g Polybond 3200 and 692.86 g PP were blended to produce a composite with 2 % MAPP.

5.1 Degradation of glass fibre sizings due to exposure to elevated temperatures

In this section, results on the thermal degradation of glass fibres are presented. Thermal gravimetric analysis (TGA) was used to record the weight loss of sized glass fibres as a function of temperature and atmosphere. A description of the TGA can be found in Chapter 3. Microbond tests as described in Chapter 3 were performed to assess the effect of thermal degradation on the compatibility between glass fibres and PP. Four different commercial glass fibres were analysed. Owens Corning SE1500 and PPG Hybon 2002 are continuous glass fibres with thermoset compatible sizing. 3B DS2200-13P chopped glass fibres and PPG 4575 continuous glass fibres are coated with a thermoplastic compatible sizing.

5.1.1 Thermal gravimetric analysis of thermoset compatible sizings

Figure 5.1 and Figure 5.2 show the weight loss curves of Owens Corning SE1500 glass fibres and PPG Hybon 2002 glass fibres. The experiments were performed in air and in a nitrogen rich atmosphere. Figure 5.1 shows the weight loss curves as a function of the temperature. Figure 5.2 shows the derivative of the weight loss curves (DTG).

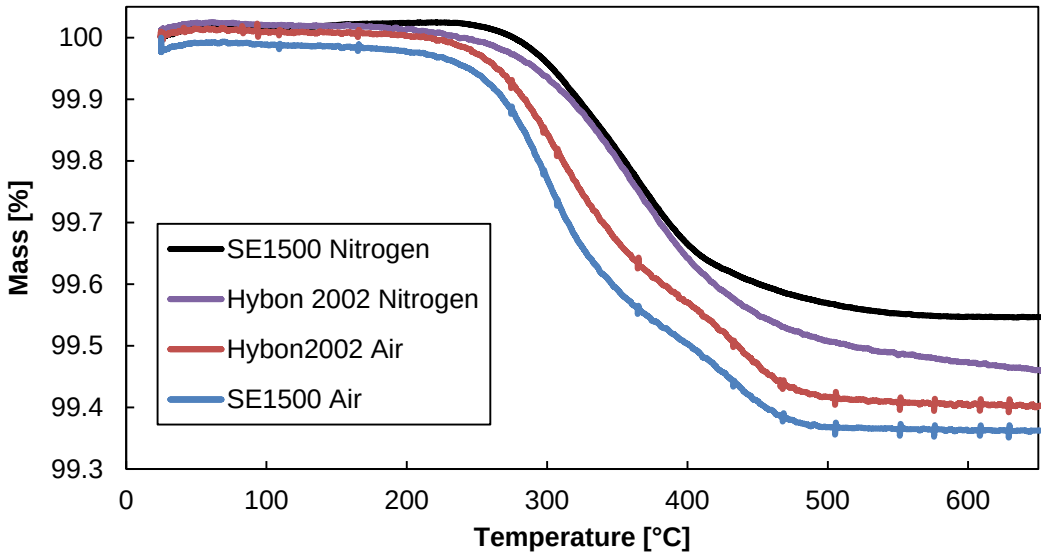

Figure 5.1. TGA weight loss curves of thermoset compatible sizings

Both glass fibres exhibited a similar mass loss which can be explained with a similar glass fibre sizing formulation [1]. Figure 5.1 reveals that the total weight loss due to the degradation of the glass fibre sizing was marginally higher when the TGA was performed in air. This phenomena was also observed by others [2] and can be

explained with the formation of char on the fibre surface when the TGA was performed in a nitrogen rich atmosphere. The onset of degradation was at around 250 °C and did not depend on the atmosphere. The DTG curves in Figure 5.2 show that the characteristics of the sizing degradation depended on the atmosphere. The main peak was shifted higher by around 50 °C when the TGA was performed in a nitrogen rich atmosphere. It might be speculated that the first peak of the DTG curves was caused by the degradation of the film former. The second peak might have been caused by the oxidation of char. The majority of the reviewed studies in Chapter 2 used temperatures of around 500 °C to thermally recycle glass fibre composites. Thus, the data in Figure 5.1 and Figure 5.2 confirm the conclusion in Chapter 2 that commercial glass fibre sizing cannot withstand the temperatures of thermal recycling processes without severe degradation.

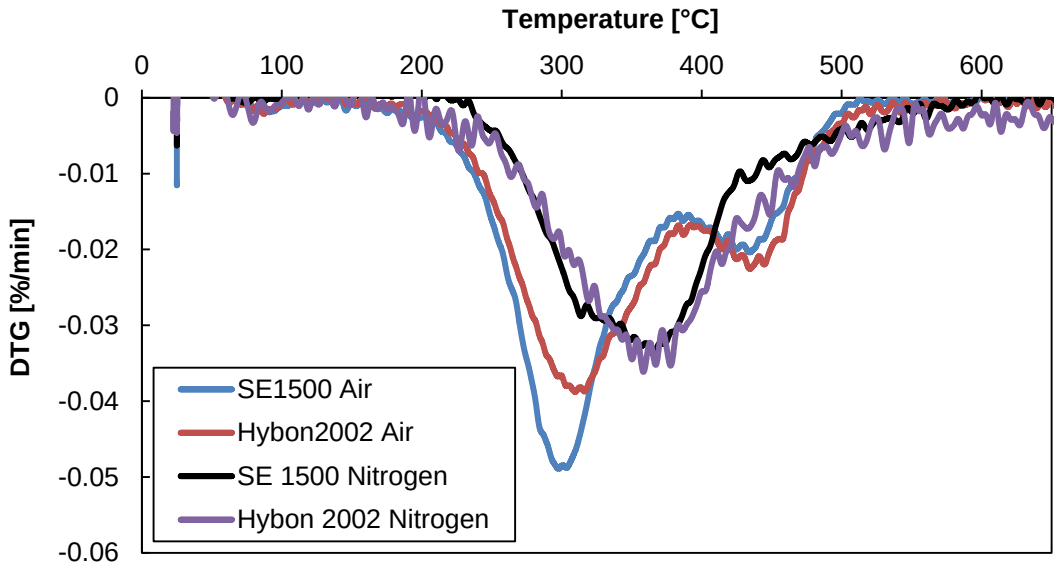

Figure 5.2. DTG curves of thermoset compatible sizings

5.1.2 Thermal gravimetric analysis of thermoplastic compatible sizings

The weight loss curves of 3B DS2200-13P glass fibres and PPG 4575 glass fibres are plotted in Figure 5.3. Figure 5.4 shows the derivatives of the weight loss curves.

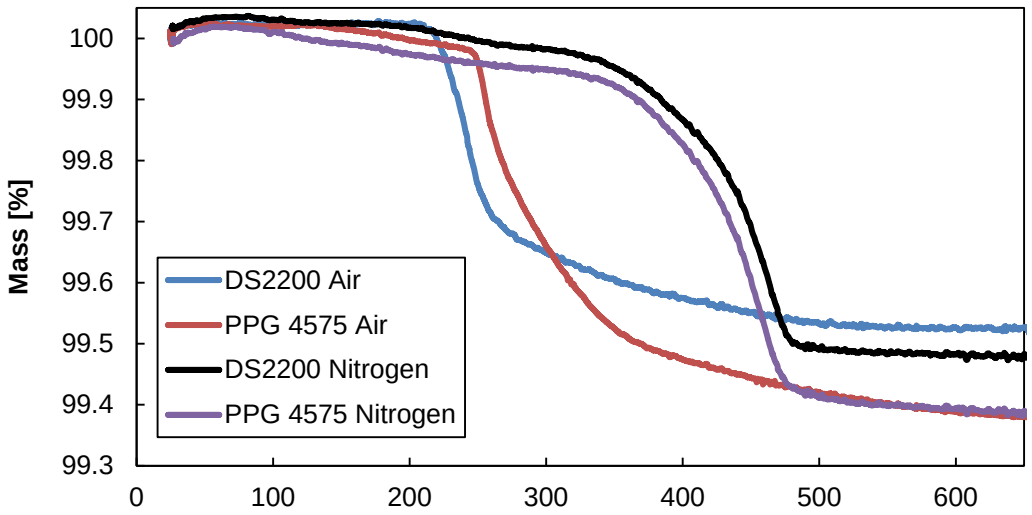

Figure 5.3. TGA weight loss curves of PP compatible sizings

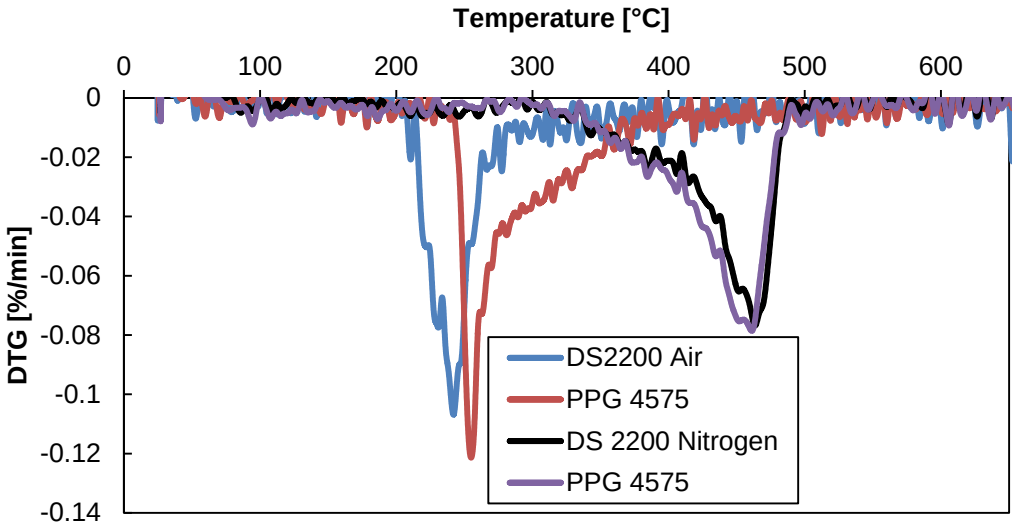

Figure 5.4. DTG curves of PP compatible sizings

The weight loss curves of the 3B DS 2200-13P fibres and the PPG 4575 fibres in Figure 5.3 have a similar profile which suggests similar sizing formulations. A review of glass fibre sizing patents by Thomason [1] also suggested that both sizings have a similar formulation, consisting of more than 50 % MAPP film former by weight. Thus, the weight losses in Figure 5.3 can partly be explained by the degradation of the MAPP film former. Figure 5.3 and Figure 5.4 suggest that the degradation

characteristics depended strongly on the atmosphere. A sharp weight loss was observed around 250 °C when the TGA was performed in air. In contrast, almost no weight loss was observed up to 350 °C when the TGA was performed in a nitrogen rich atmosphere. This is in agreement with literature. It was observed in different studies that the thermal degradation of PP is accelerated by the presence of oxygen [3,4] and the thermal behaviour of MAPP is similar to thermal behaviour of PP [5].

To further investigate the degradation of the MAPP film former an initial TGA experiment was performed. 50 ml of FGLASS X35 Michelmann MAPP film former were dried at 105 °C for 8 h in an open container (10 cm x 30 cm). The dried film former was powderised and the TGA was performed in air and in nitrogen rich atmosphere. For comparison, pellets of Polybond 3200 MAPP were also analysed. The results are plotted in Figure 5.5 and Figure 5.6.

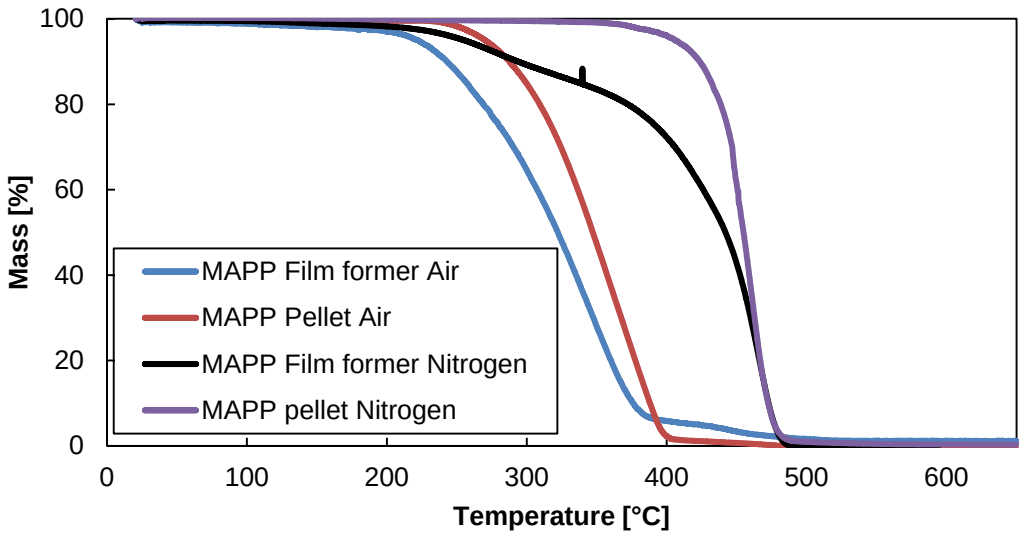

Figure 5.5. TGA weight loss curves of MAPP pellets and MAPP film former

The MAPP film former was slightly more susceptible to thermal degradation in air than the MAPP pellets. This might be explained with the absence of antioxidants in the film former or the surface/volume ratio. A large surface/volume ratio usually enhances the degradation of polymeric materials in TGA experiments [6]. The film former was powderised and had a large surface/volume ratio compared to the pellets. Similar to the PP compatible glass fibre sizings in Figure 5.3 the MAPP film former started to degrade between 200 °C and 250 °C. However, the weight loss and degradation of the MAPP film former in Figure 5.5 appears to be less rapid than the degradation of the glass fibre sizings in Figure 5.3. This might be explained with

the surface/volume ratio as well. The shape of the particles resembled rather the shape of a sphere than of a cylinder. The average diameter of the powderised film former particles was measured to be 395 µm using the FASEP fibre length measurement system that is described in Chapter 3. The fibres had a cylindrical shape and the thickness of the glass fibre sizings is less than 1 µm [7]. Thus, the surface/volume ratio of the glass fibre sizing was larger than the surface/volume ratio of the powderised film former particles. The DTG curves in Figure 5.6 show that the degradation of the pellets and film former were less rapid in a nitrogen rich atmosphere than in air. The peaks of the DTG curves are shifted to higher temperatures. In addition, the peaks of the DTG curves are both at approximately 460 °C. A comparison between Figure 5.6 and Figure 5.4 reveals that the DTG curves are similar. Thus, the glass fibre sizings, the MAPP pellets and the MAPP film former degraded in a similar manner in a nitrogen rich atmosphere. This agrees with the hypothesis that the glass fibre thermoplastic compatible sizings degraded more rapidly in air than the MAPP film former because of the larger surface area that was in contact with oxygen.

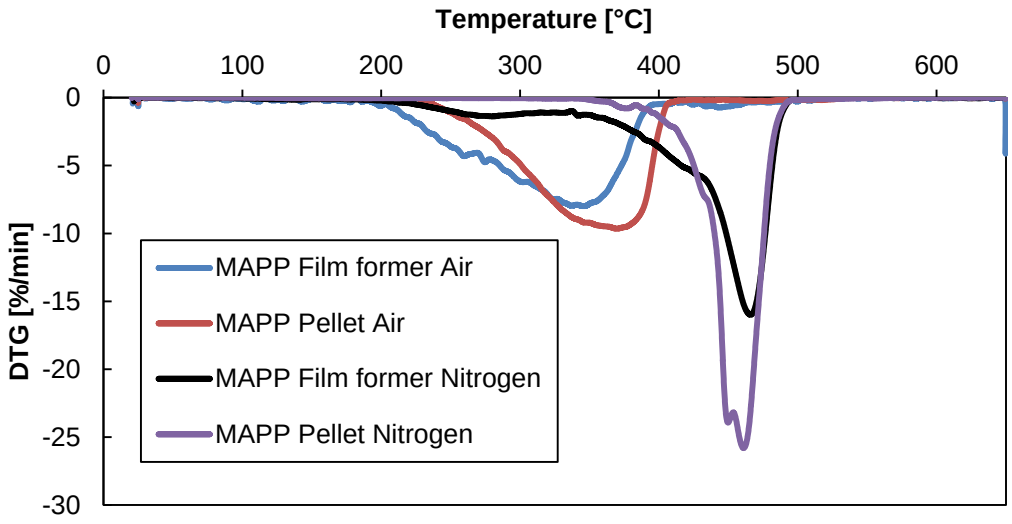

Figure 5.6. DTG curves of PP compatible sizings

In addition to the surface/volume ratios, interactions between the different compounds of the sizing cannot be excluded. Further work is required to identify the compounds that cause the degradation of the PP compatible sizings but this is not in the scope of this thesis. However, the data in Figure 5.3 shows that glass fibres with a PP compatible sizing can degrade in the range of thermoplastic processing temperatures when they are exposed to air. In hot melt processes, most of the glass

fibres will be embedded in the PP matrix during composite processing and the TGA data in Figure 5.3 does therefore not represent processing conditions. However, processing temperatures are often increased to up to 300 °C to increase the production throughput and even short exposure to these temperatures under air (e.g. when the molten composite exits the extruder) might cause a severe degradation of the glass fibre sizing. Similar to the thermoset compatible sizings (Figure 5.1 and Figure 5.2), the weight loss curves suggest that thermoplastic compatible sizings cannot resist thermal recycling temperatures of 500 °C. Microbond tests were performed to assess the effect of the sizing degradation on the interfacial adhesion between glass fibres and PP.

5.1.3 Effect of sizing degradation on interfacial adhesion

Microbond tests as described in Chapter 3 were performed to measure the apparent IFSS between thermally conditioned DS2200-13P chopped glass fibres and PP. The results are plotted in Figure 5.7.

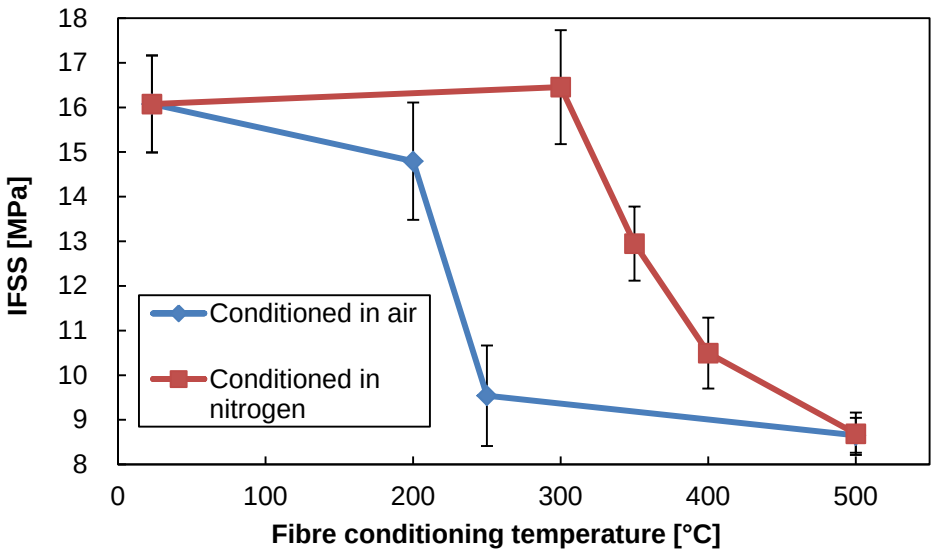

Figure 5.7. Drop of the microbond IFSS between glass fibres and PP with fibre conditioning temperature

Similar to the weight loss curves in Figure 5.3, the IFSS dropped in Figure 5.7 between 200 °C and 250 °C fibre conditioning temperature when the conditioning was performed in air. Higher conditioning temperatures did not cause a further significant drop when the error bars are considered. The thermal conditioning of the glass fibres in nitrogen rich atmosphere did not cause a reduction of the IFSS up to 300 °C. The IFSS decreased between 300 °C and 500 °C fibre conditioning temperature when the samples were conditioned in nitrogen rich atmosphere. At

500 °C fibre conditioning temperature the IFSS was independent from the atmosphere. The data in Figure 5.7 agrees with the conclusion in Chapter 2 that commercial glass fibre sizings lose their functionality when they are exposed to thermal recycling temperatures. In addition, the data of this section might be relevant for the recycling of glass fibre PP (GF/PP) composites. Thermoplastics like PP are intrinsically recyclable but it is well known that the tensile strength of GF/PP composites drops when they are recycled by melting and reprocessing. Previous studies explained the reduced strength of reprocessed GF/PP composites with glass fibre length degradation and chain scission of the PP matrix [8–10]. Bourmaud and Baley [8] suggested based on fracture surface analysis that the adhesion between glass fibres and PP matrix was also reduced by reprocessing. The data in this section supports their argument and shows that the degradation of PP compatible sizings at processing temperatures might be relevant for the recycling of GF/PP composites.

5.2 Effect of glass fibre degradation on composite performance

The data in Section 5.1 suggests that glass fibres lose their sizing during thermal recycling processes independently from the atmosphere. In this section, the 3B DS2200-13P glass fibres were thermally degraded in air by conditioning before composite processing at different temperatures using a Carbolite CWF 12/13 furnace as described in Chapter 3. All composites had a nominal fibre content of 12.8 vol%. Measurements as described in Chapter 3 confirmed the actual fibre content to be between 12.2 vol% and 12.8 vol%. 1 % MAPP was added to the composites in this section.

5.2.1 Residual fibre length after composite processing

Figure 5.8 shows the residual length of the glass fibres in the injection moulded composites as a function of the fibre conditioning temperature. The mean fibre length is compared with the weighted mean fibre length. A description of the procedure to determine the fibre length can be found in Chapter 3. The data in Figure 5.8 is complemented by Table 5.1, which shows the standard deviations of the fibre length distributions itself and the standard deviations between the arithmetic means of at least four repeat measurements. The standard deviations of the fibre length distributions are relatively large compared to the arithmetic mean values. As discussed in Chapter 4, the standard deviations of the fibre length

distributions describe the shape of the length distribution rather than the precision of the measurements. A comparison between Figure 5.8 and Table 5.1 also shows that the standard deviations between the repeat measurements were lower than the differences between the arithmetic means of the fibre length. Thus, the fibre length measurements were sufficiently precise to assess the effect of fibre conditioning temperatures on the residual fibre length in the injection moulded composites.

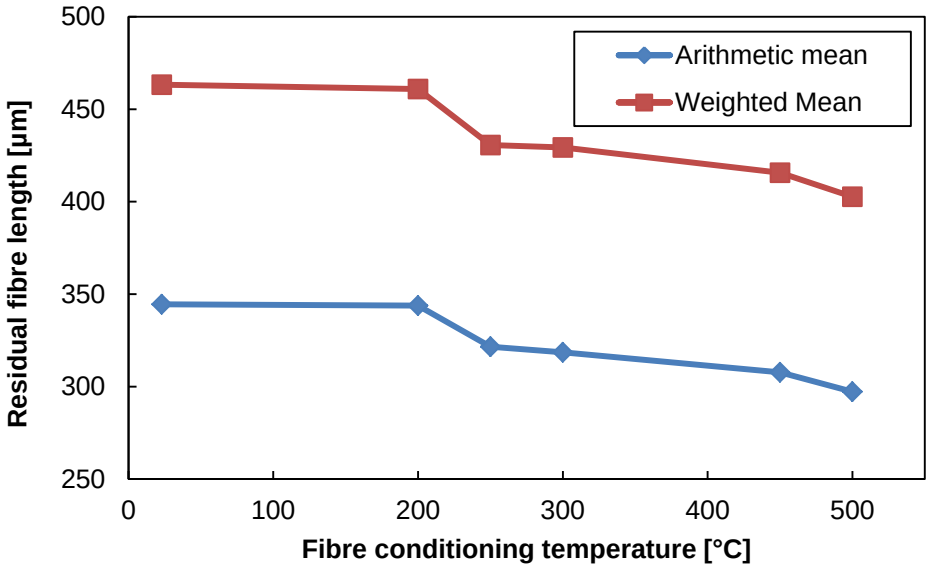

Figure 5.8. Reduction of the residual fibre length with fibre conditioning temperature

Table 5.1. Comparison between standard deviations of repeated fibre length measurements and standard deviations of fibre length distributions

Fibre conditioning temperature	Standard deviation of fibre length distribution	Standard deviation between repeat measurements
As received	209 µm	3 µm
200°C	200 µm	3 µm
250°C	191 µm	7 µm
300°C	194 µm	5 µm
450°C	190 µm	11 µm
500°C	189 µm	6 µm

The values of the weighted mean fibre length and the arithmetic mean fibre length in Figure 5.8 dropped when the fibres were thermally conditioned as described in Chapter 3. Figure 5.8 also shows that the weighted mean fibre length is larger than the arithmetic mean fibre length. This phenomenon was observed in Chapter 4 and

can be explained with the skewness of the fibre length distribution. As already discussed in Chapter 2 the length degradation of glass fibres in PP composites and other thermoplastic composites during melt processing has been reported in numerous studies [11–18]. Fibres are broken during melt processing of thermoplastic composites due to fibre-polymer interactions, fibre-fibre interactions and fibre-processor surface interactions [11,19]. The fibre-polymer interactions cause fibre buckling and breakage due to forces between the fibres and the polymer melt. The glass fibres in a polymer melt can be described as thin rods with a critical buckling radius inversely proportional to their tensile strength [15,18]. Research agrees [2,20–27] that the exposure of glass fibres to elevated temperatures leads to a reduction of the tensile fibre strength. A more detailed discussion can be found in Chapter 2. Thus, the additional length degradation of thermally conditioned glass fibres in the present study might partially be explained by a reduction of the fibre strength. The reduction of the fibre strength might also have enhanced the fibre length degradation of the thermally conditioned fibres due to fibre-fibre interactions and fibre processor surface interactions.

The glass fibres were received as chopped bundles. The thermally conditioned glass fibre bundles were not broken up during the thermal conditioning or during handling. However, thermally conditioned fibre bundles showed a strong tendency to form a fluffy mat before reaching the melting zone in the extruder. Figure 5.9 shows thermally conditioned fibres arranged in bundles and thermally conditioned glass fibres that were taken out of the feeding zone of the extruder.

Figure 5.9. Thermally conditioned fibres arranged in bundles after thermal conditioning (left) and thermally conditioned fibres taken from the barrel of the extruder (right)

The tendency of the thermally conditioned fibres to form a fluffy mat can be explained by the degradation of the glass fibre sizing. The TGA data in the Section 5.1 (Figure 5.3) indicates that the sizing of the 3B DS 2200-13P glass fibres started to degrade between 200 °C and 250 °C in air. Thus, the thermally conditioned glass

fibres were not held together in bundles before they reached the melting zone of the extruder. In contrast, the as received fibres were held together in bundles by the glass fibre sizing. Thus, the thermally conditioned fibres might have been less protected against length degradation than the as received fibres which might have contributed to the additional length reduction of the thermally conditioned fibres. The decrease of the residual fibre length between 200 °C and 250 °C indicated that the integrity of the bundles played an important role because the strength of glass fibres is hardly affected in that temperature range. Similar observations on the effect of the fibre arrangement were reported by Thomason [13] when he compared glass fibres that were pre-compounded via a wire coating process with pultrusion pre-compounded fibres.

5.2.2 Composite tensile strength

The tensile strength of the injection moulded composites is plotted in Figure 5.10 as a function of the fibre conditioning temperature in air. The composite tensile strength dropped sharply between 200 °C and 250 °C fibre conditioning temperature. Higher fibre conditioning temperatures caused a further reduction of the composite strength. After fibre conditioning at 500 °C the composite strength dropped to 37.7 ± 0.5 MPa which is barely higher than the tensile strength of the unreinforced PP (35.8 ± 0.2 MPa).

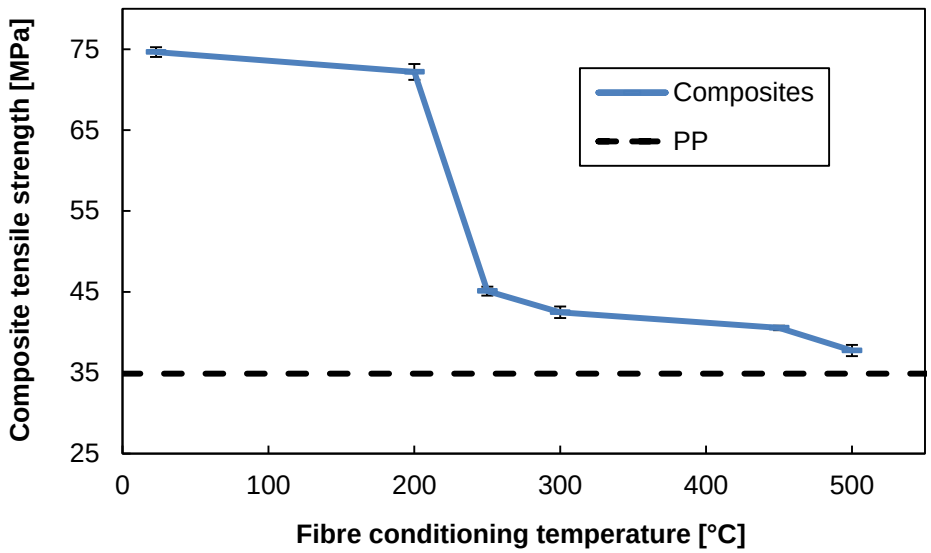

Figure 5.10. Reduction of the composite tensile strength with fibre conditioning temperature

Influence of the interfacial shear strength

The residual fibre length, fibre strength and the adhesion between fibre and matrix changed when the fibres were thermally conditioned. The residual fibre length dropped slightly between 200 °C and 250 °C fibre treatment temperature. However, the drop of the residual fibre length is relatively small and Thomason et al. [13] showed that the tensile strength of GF/PP composites does not increase sharply with the residual fibre length when the fibre length is less than 0.5 mm. Thus, the sharp drop of the composite tensile strength cannot be explained by the reduced residual fibre length. The microbond test results in Figure 5.11 show the IFSS between fibres that were thermally conditioned in air and PP with 1 % added MAPP. The initial values of the IFSS are higher than in Figure 5.7 because of the added MAPP. However, in both cases the IFSS dropped sharply between 200 °C and 250 °C conditioning temperature. The sharp drop of the IFSS and the composite tensile strength shows that it might be worth investigating the degradation of PP compatible glass fibre sizings during composite processing. Between 250 °C and 500 °C fibre conditioning temperature the apparent IFSS dropped only slightly. Figure 5.11 also shows the IFSS between PP with 1 % MAPP and boron free E-glass fibres that were received unsized from Owens Corning. The value of the IFSS between unsized fibres and PP with 1 % added MAPP is similar to the value of 3B DS 2200-13P fibres that were thermally conditioned at 500 °C. Thus, the sizing was probably completely degraded when the fibres were exposed to 500 °C in air.

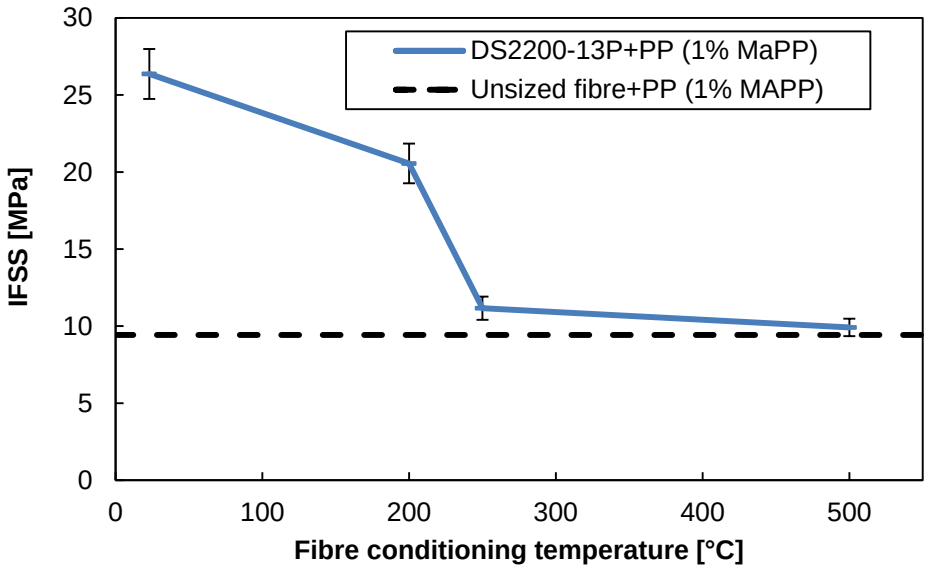

Figure 5.11. Reduction of the microbond IFSS with fibre conditioning temperature

The fracture surface of the composites also indicated a reduction of the IFSS when the glass fibres were thermally conditioned. Figure 5.12 shows the fracture surfaces of tensile tested composites reinforced with as received glass fibres and fibres that were conditioned at 200 °C. Figure 5.13 shows the fracture surfaces of composites reinforced with fibres that were conditioned at 250 °C and 500 °C.

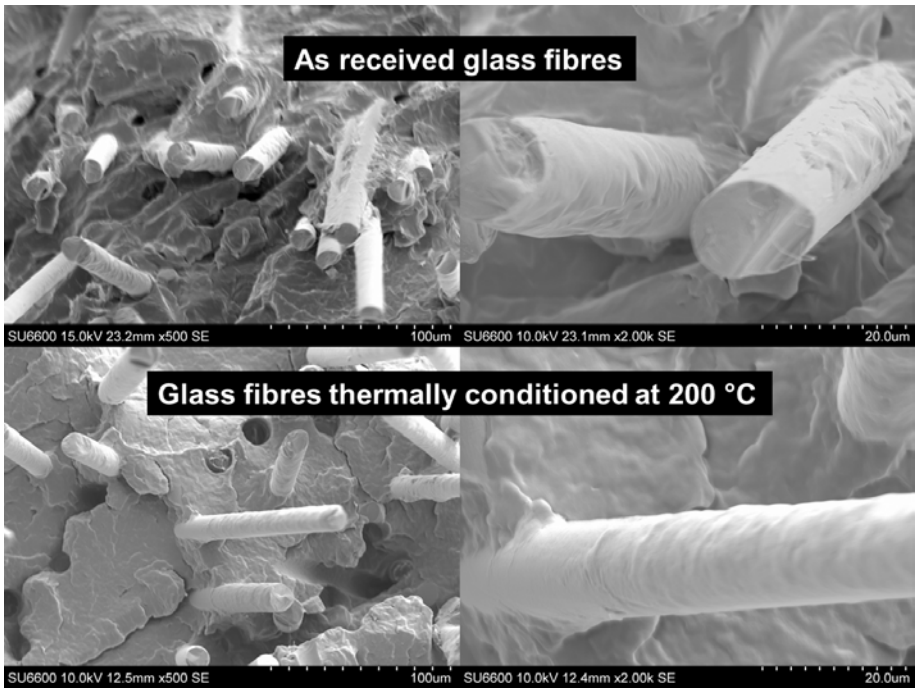

Figure 5.12. Fracture surfaces of composites based on as received fibres and thermally conditioned fibres

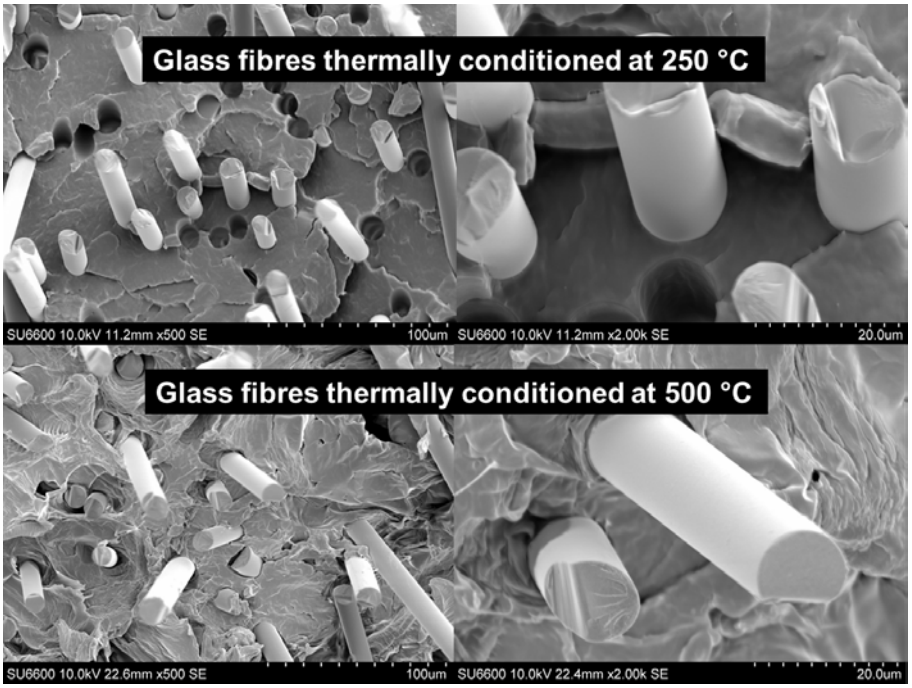

Figure 5.13. Fracture surfaces of composites based on thermally conditioned fibres

The fibres in Figure 5.13 are relatively clean while the fibres in Figure 5.12 are partially covered with PP. These types of SEM are often interpreted in terms of the level of fibre-matrix adhesion in the composite although it has been shown that such conclusions can be misleading [28]. In any case the SEM evidence is not inconsistent with the suggestion that the composites based on as received glass fibres had a higher interfacial adhesion than the composites based on fibres that were conditioned at 250 °C or higher temperatures. SEM micrographs of composite fracture surfaces did not reveal any clear differences between 250 °C and 500 °C fibre \conditioning temperature. The strength degradation of glass fibres due to exposure to elevated temperatures is well documented but only little strength loss was observed due to fibre treatment in the range of 200 °C to 300 °C for a period of time similar to that used in this thesis [2,24,26]. Consequently, it can be concluded that the sharp drop of the composite tensile strength between 200 °C and 250 °C fibre conditioning temperature was caused mainly by a degradation of the IFSS. Thus, the results presented in this chapter are in agreement with the results of other studies that were reviewed in Chapter 2. Recycled glass fibres cannot act as an effective reinforcement in injection moulded PP composites when the surface functionality has been degraded by thermal conditioning because the IFSS between fibres and matrix is low.

Influence of the fibre strength and fibre orientation

As discussed in Chapter 2 the exposure of glass fibres to temperatures higher than 300 °C causes a reduction of the fibre strength. The Bowyer-Bader analysis [14,29,30] as described in Chapter 2 was used to determine the fibre stress at maximum composite tensile stress, the IFSS and the fibre orientation factor from macromechanical tensile test data. The input parameters of the Bowyer-Bader analysis are summarised in Table 5.2. The results of the Bowyer-Bader analysis are plotted in Figure 5.14 and Figure 5.15 as a function of the fibre conditioning temperature. For comparison, the results of the microbond tests on thermally conditioned fibres and PP with 1% MAPP are also plotted in Figure 5.14.

Table 5.2. Input parameter Bowyer-Bader analysis - PP composites based on thermally conditioned fibres

Fibre volume fraction V_f	12.8 % Calculated from fibre weight content (see Chapter 4)
Fibre modulus E_f	78.7 GPa as received fibres [31] changed after thermal conditioning according to [32] to 78.9 GPa (250 °C), 80.1 (300 °C), 83.7 (450 °C), 88.9 (500 °C)
Average fibre radius r_f	6.4 µm (measured)
Composite strain 1 ε_1	1/3 of strain at break
Composite strain 2 ε_1	2/3 of strain at break
Composite tensile stress 1 σ_1	Composite tensile stress at ε_1
Composite tensile stress 2 σ_2	Composite tensile stress at ε_1
Composite tensile strength σ_{cMax}	Measured (see Figure 5.10)
Fibre length distribution	Measured as described in Chapter 3
Matrix stress Z	Calculated from strain using a polynomial fitting curve (see Chapter 4) and [14]
Polynomial fitting curve parameter x_1	0.68 obtained from tensile tests
Polynomial fitting curve parameter x_2	-5.98 obtained from tensile tests
Polynomial fitting curve parameter x_3	19.79 obtained from tensile tests

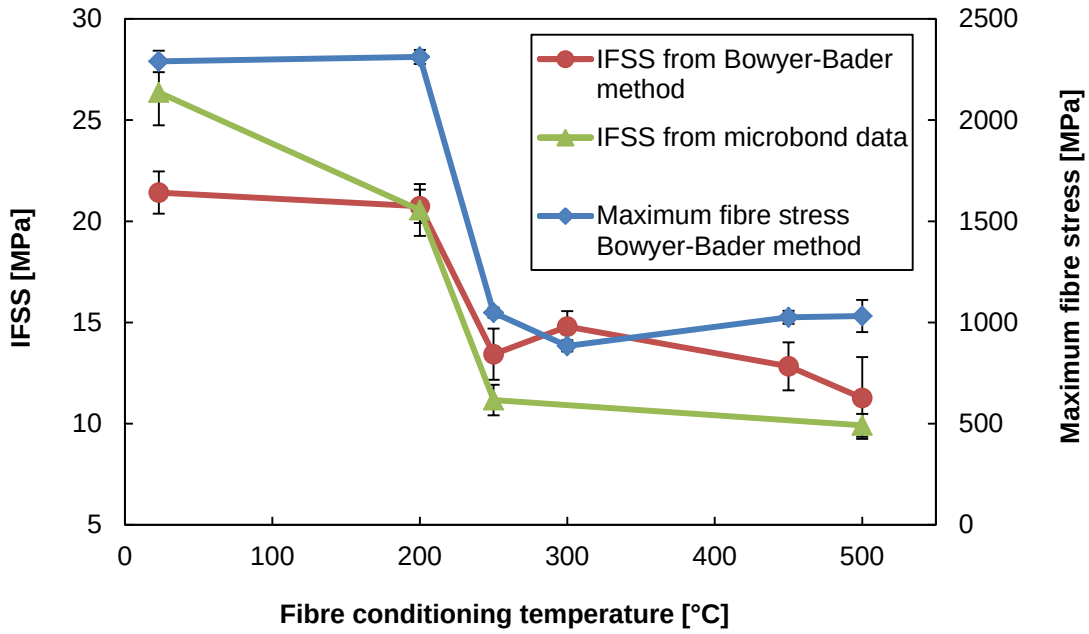

Figure 5.14. Reduction of the IFSS and the maximum fibre stress with fibre conditioning temperature

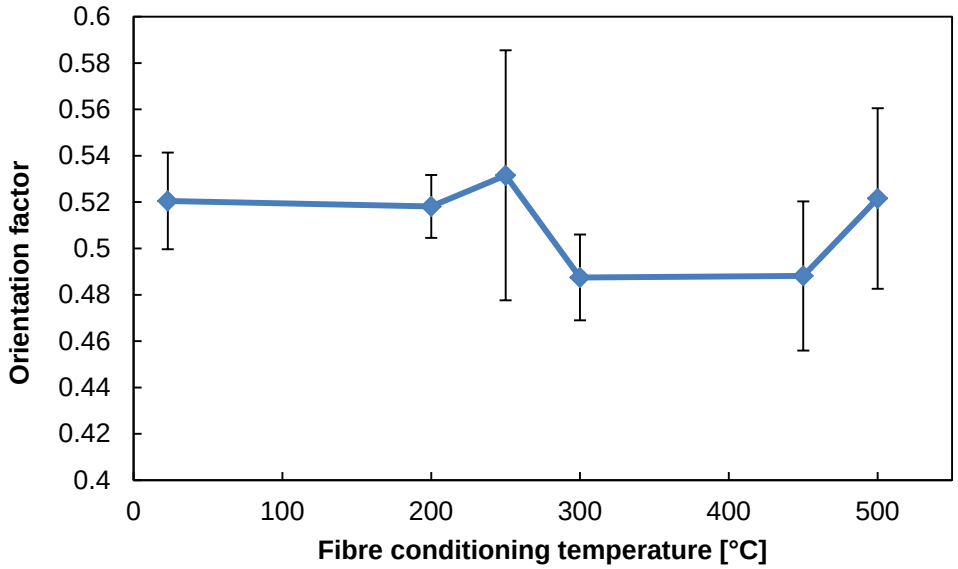

Figure 5.15. Absence of a correlation between the fibre orientation factor of Bowyer-Bader analysis and fibre conditioning temperature

T-tests showed that the fibre orientation factor in Figure 5.15 did not change significantly when the glass fibres were thermally conditioned. Similar to the microbond test results, the results of the Bowyer-Bader analysis in Figure 5.14 show that the IFSS dropped between 200 °C and 250 °C fibre treatment temperature and reached a value of around 10 MPa when the fibres were conditioned at 500 °C. As expected the maximum fibre stress also decreased with the thermal conditioning temperature. The sharp drop of maximum fibre stress between 200 °C and 250 °C

fibre conditioning temperature can be explained with the lack of stress transfer between fibres and matrix due to the reduction of the IFSS. Several studies showed that the strength of glass fibres is only slightly reduced when they are exposed to temperatures below 300 °C for 30 min for less time [2,24,26]. However, the values for the maximum fibre stress in Figure 5.14 do not follow a clear trend between 250 °C and 500 °C conditioning temperature. The reason for this behaviour will be discussed in the following paragraphs.

The measured composite strain at break, composite yield strain and the fibre strain at maximum fibre stress obtained from the Bowyer-Bader analysis are plotted in Figure 5.16 as a function of the fibre conditioning temperature.

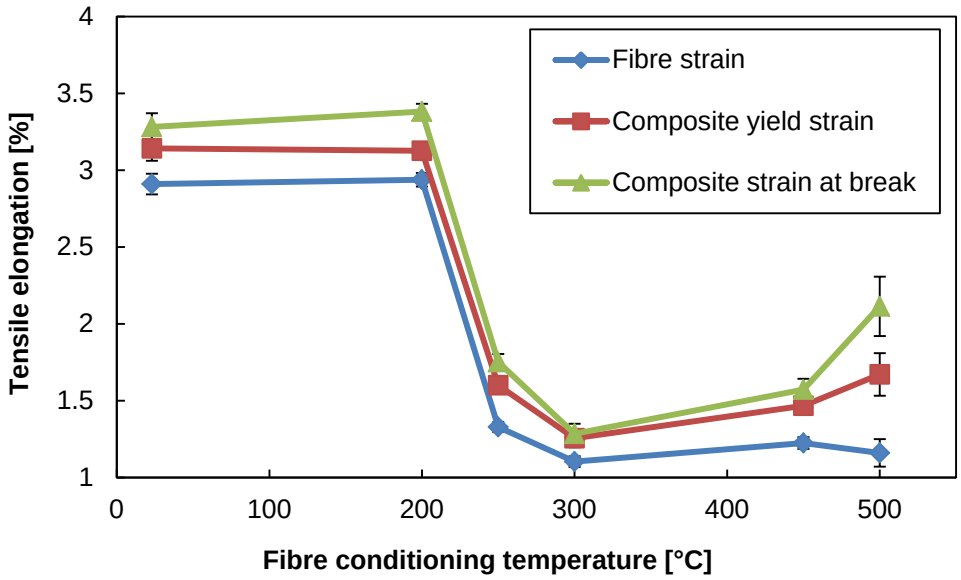

Figure 5.16. Effect of fibre conditioning temperature on the fibre strain (Bowyer-Bader analysis), the composite yield strain and the composite strain at break

Thomason [14] reported an agreement between fibre strain of the Bowyer-Bader analysis and the measured composite strain at break. Similar to Chapter 4, the Bowyer-Bader analysis was used to calculate the fibre stress at maximum composite tensile stress. The fibre strain was calculated from the maximum fibre stress assuming a linear stress-strain relationship. The maximum tensile stress was always observed at composite yield strain which was slightly lower than the composite strain at break. The data of injection moulded GF/PP composites with different MAPP contents in Chapter 4 showed a qualitative agreement between composite yield strain and fibre strain of the Bowyer-Bader analysis. In addition, the composite yield strain was observed to follow the same trends as the composite

strain at break. Thus, the fibre strain of the Bowyer-Bader analysis also followed the trend of the strain at break. In contrast, the data in Figure 5.16 shows some disagreement between the fibre strains of the Bowyer-Bader analysis and the composite strains. While the fibre strain decreased slightly between 250 °C and 500 °C fibre conditioning temperature the measured composite strains partially recovered.

The data in Figure 5.14 is based on the assumption that the fibre strain is equal to the average matrix strain. However, the different trends of the measured composite strains and fibre strain in Figure 5.16 suggest that this assumption is not valid when the fibres were thermally conditioned. Thus, a too low value for the matrix strain might have been assumed in the Bowyer-Bader analysis. The effect of the underestimation of the matrix strain in the Bowyer-Bader method is illustrated in Figure 5.17.

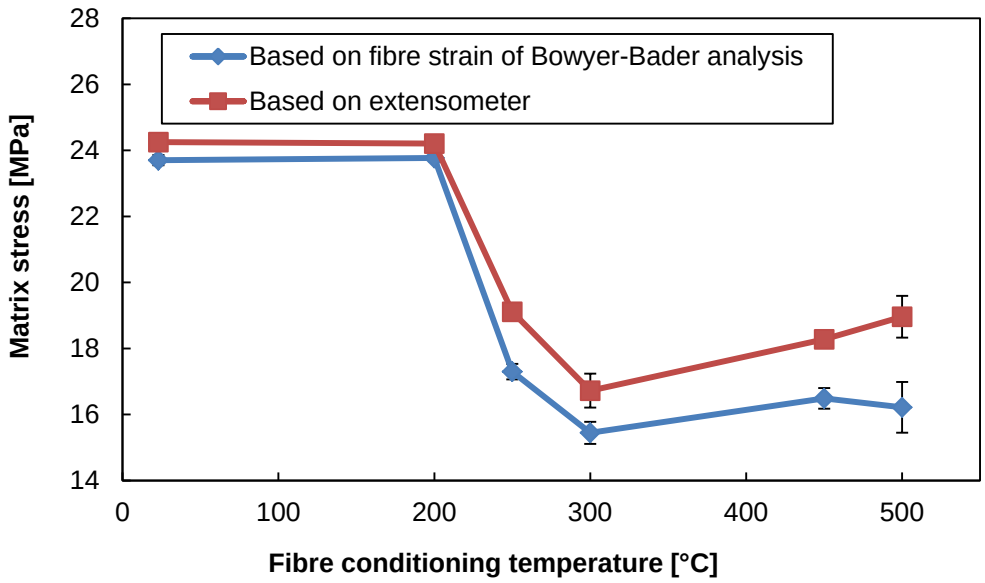

Figure 5.17. Effect of fibre conditioning temperature on the stresses in PP matrix calculated from the Bowyer-Bader analysis and video extensometer data

Figure 5.17 shows the stress of the PP matrix when the composites were subjected to maximum tensile stress. Two different values were calculated for the matrix stress. Both values were calculated from the polynomial fitting curve as described in Chapter 4 using the factors x_1, x_2 and x_3 that are listed in Table 5.2. One value is based on the Bowyer-Bader fibre strain and the other value is based on the composite yield strain that was recorded by a video extensometer during the tensile tests. Both methods provided similar values for as received fibre composites and

composites based on fibres that were conditioned at 200 °C. However, the values diverged when the fibres were conditioned at higher temperatures. Thus, the contribution of the matrix to the composite stress might have been underestimated and the contribution of the fibres might have been overestimated by the Bowyer-Bader analysis.

Based on the modified values for the matrix stress the maximum fibre stress was re-calculated. Figure 5.18 shows the maximum fibre stresses that were obtained from the Bowyer-Bader analysis. One set of data is based on the original matrix strain and apparently too low matrix contribution to the composite stress. The other set of data was also obtained from the Bowyer-Bader method. In contrast to the first set of data, the measured yield strain was used to determine the matrix contribution. The fibre contribution was calculated as the difference between the composite stress and the matrix contribution.

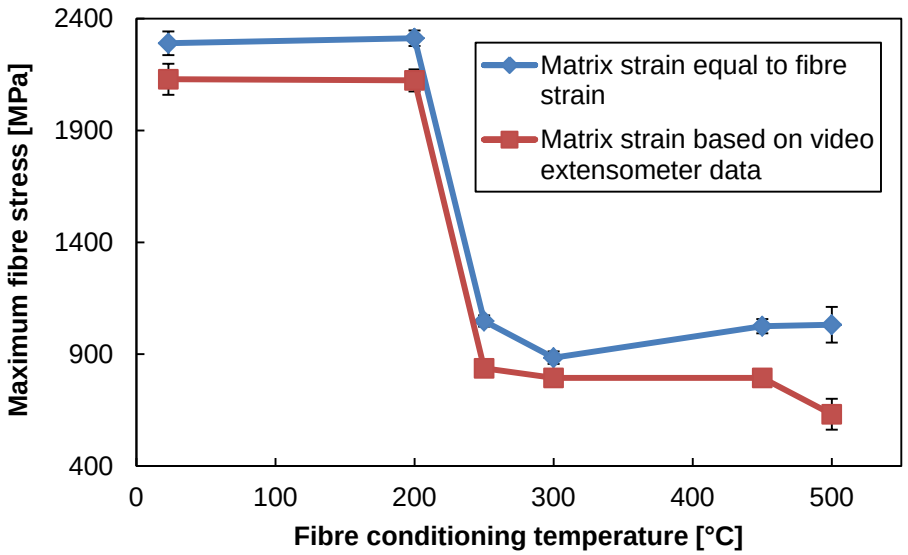

Figure 5.18. Reduction of the maximum fibre stress (Bowyer Bader analysis) with fibre conditioning temperature

Figure 5.18 suggests that the fibre stress at maximum composite tensile stress might have been overestimated when the average matrix strain was assumed to be equal to the fibre strain. The fibre stress at maximum composite tensile stress decreased between 250 °C and 500 °C fibre conditioning temperature when the average matrix strain was assumed to be equal to the video extensometer data. This would be in agreement with data on the tensile strength of thermally conditioned fibres. Several studies [2,20–27] were reviewed in Chapter 2 that

reported a reduction of the glass fibre strength when the fibres were conditioned at temperatures above 250 °C.

In conclusion, the reduction of the fibre stress at composite yield strain in Figure 5.18 and the reduction of the composite tensile strength in Figure 5.10 might be attributed to two mechanisms. Between room temperature and 250 °C fibre conditioning temperature the composite strength loss and reduction of the fibres stress was mainly caused by a drop of the IFSS. Above 250 °C the IFSS decreased only marginally but the composite tensile strength dropped further. One possible explanation for the additional reduction of the maximum fibres stress is the degradation of the fibre strength.

Critical fibre length for fibre failure

Similar to Chapter 4, the fraction of fibres was calculated that is longer than the critical length for fibre failure (supercritical fibres). The microbond IFSS in Figure 5.14 was used as input parameter. The strength of the chopped 3B DS 2200-13P glass fibres was not tested. Table 5.3 shows two different sets of data for the fibre strength. The second column shows the results of a study on the strength loss of continuous glass fibres at 20 mm gauge length [26]. The data of the continuous fibres was used to estimate the strength of the chopped fibres in the fourth column. It was assumed that the relative retained strength of the chopped fibres is similar to the relative retained strength of continuous fibres (third column). The strength of the as received chopped fibres was assumed to be 2 GPa [33].

Table 5.3. Estimated strength loss of glass fibres as a function of conditioning temperature

Temperature	Retained strength measured (20 mm gauge length) [26]		Retained strength estimated (180 μm - 380 μm gauge length) [33]
[°C]	[GPa]	[%]	[GPa]
As received	2.2	100	2
200	2	91	1.8
250	2	88	1.8
300	1.8	79	1.6
450	0.7	31	0.6
500	0.7	30	0.6

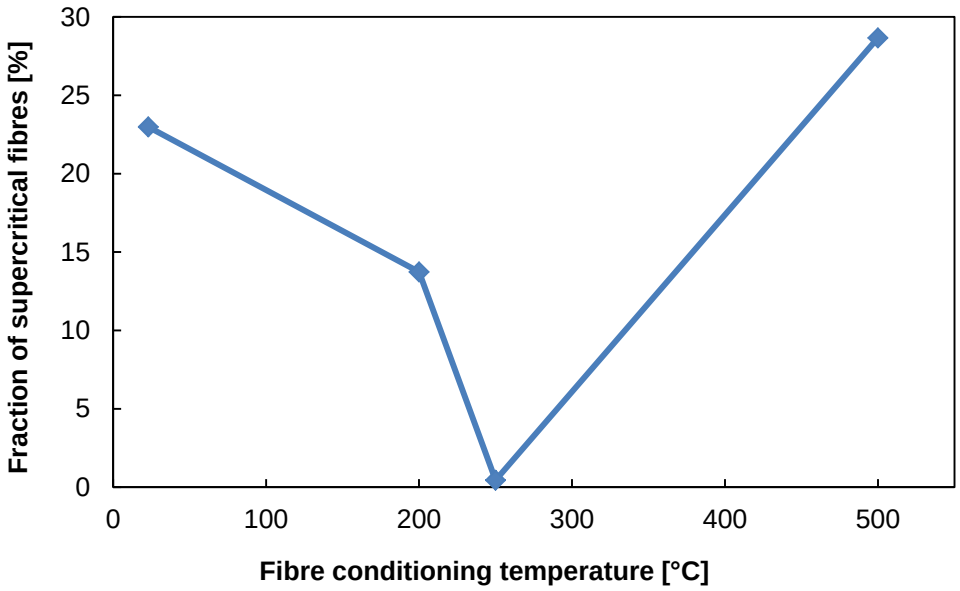

Figure 5.19. Effect of fibre conditioning temperature on the percentage of supercritical fibres

Several conclusions can be drawn from Figure 5.19 despite some uncertainty about the fibre strength. In all composites most of the fibres were shorter than the critical fibre length for fibre failure. Thus, fibre pull-out and interfacial failure were more likely than fibre fracture even when the fibres were thermally conditioned. The percentage of supercritical fibres reached a minimum at around 250 °C fibre

conditioning temperature because of the low IFSS and relatively high fibre strength. At higher conditioning temperatures the percentage of supercritical fibres increased. Thus, fibre failure was more likely when the fibres were conditioned at temperatures higher than 250 °C. The data in Figure 5.19 therefore agrees with the conclusion that the drop of the composite tensile strength above 250 °C was at least partially caused by a reduction of the fibre strength.

5.2.3 Composite strain at break, yield strain and impact strength

The stress strain curves in Figure 5.20 and the data in Figure 5.16 show that the yield strain and the strain at break followed similar trends. As already mentioned above the composite yield strain and the composite strain at break decreased between 200 °C and 300 °C fibre treatment temperature but recovered partially when the fibres were conditioned at higher temperatures. The fibre content, fibre length, fibre orientation and IFSS were identified in Chapter 2 as parameters that influence the strain at break of discontinuous GF/PP composites. From these parameters, only the fibre length and the IFSS were changed when the fibres were thermally conditioned. In addition, the fibre strength was reduced when the fibres were conditioned above 250 °C. As discussed in section 5.2.2 the fibre stress probably did not reach the fibre strength when the fibres were conditioned at 250 °C or 300 °C. Thus, the drop of the composite strain at break and composite yield strain between 200 °C and 300 °C can be attributed to a reduction of the IFSS. This would agree with observations reported by Thomason [14] and Bikiaris et al. [34] on injection moulded GF/PP composites. They observed that the composite strain at break increased with the IFSS. When the IFSS is low the fibres might debond from the matrix at lower stresses. The IFSS cannot explain the partial recovery of the composite strain at break and composite yield strain at higher fibre conditioning temperatures. It also appears unlikely that the additional reduction of the fibre length can explain the recovery of the composite strain at break. The arithmetic mean value of residual fibre length decreased by 24 µm when the fibre conditioning temperature was increased from 250 °C to 500 °C. Changes of that magnitude are unlikely to affect the composite strain at break. Other researchers [35,36] reported changes of the composite strain at break when the residual fibre length was changed by 1 mm or more.

The stress strain curves in Figure 5.20 show a relatively long ductile region when the fibres were conditioned at 500 °C. After conditioning at 250 °C most of the fibres

were strong enough to withstand the stresses in the composites until the composite failed. The failure might have been caused by the growth of cracks at the fibre ends as described in [37]. When the fibres were conditioned at 500 °C part of the longer fibres might have failed before composite failure. Thus, lower stresses were developed at the fibre ends and the composites failed at higher strains. Further work such as in situ tensile tests in an SEM [37] are required to confirm this speculation.

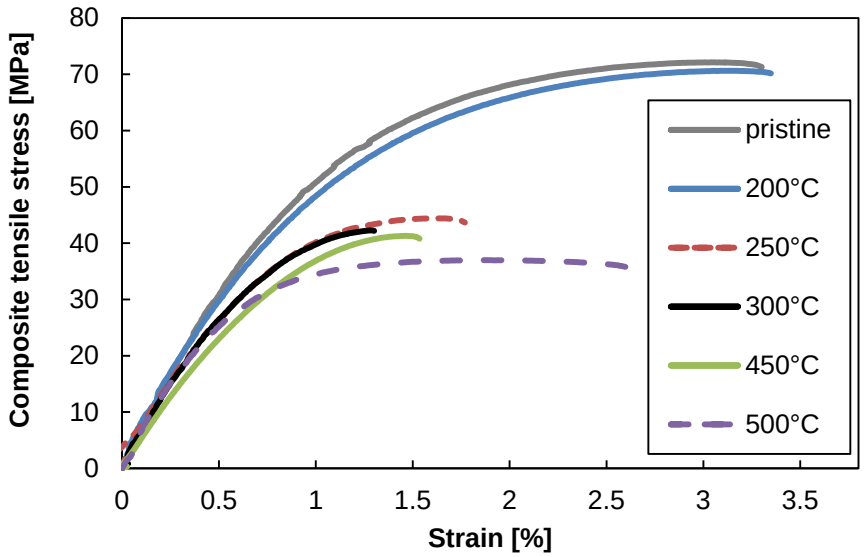

Figure 5.20. Stress strain curves of composites based thermally conditioned glass fibres

The unnotched charpy impact strength of the composites in Figure 5.21 exhibited a sharp drop between 200 °C and 250 °C fibre conditioning temperature. As shown in Figure 5.19 more than 75 % of the as received fibres were shorter than the critical fibre length. When the fibres were thermally conditioned at 250 °C more than 99 % of the fibres were shorter than the critical fibre length. It is therefore likely that fibre debond and fibre debond/pull-out were the predominant energy dissipation mechanisms [38,39]. The work of fracture correlates with the IFSS [40]. Less work was needed to debond the thermally conditioned fibres because of the lower IFSS. The sharp reduction of the impact strength can therefore be attributed to a reduction of the IFSS.

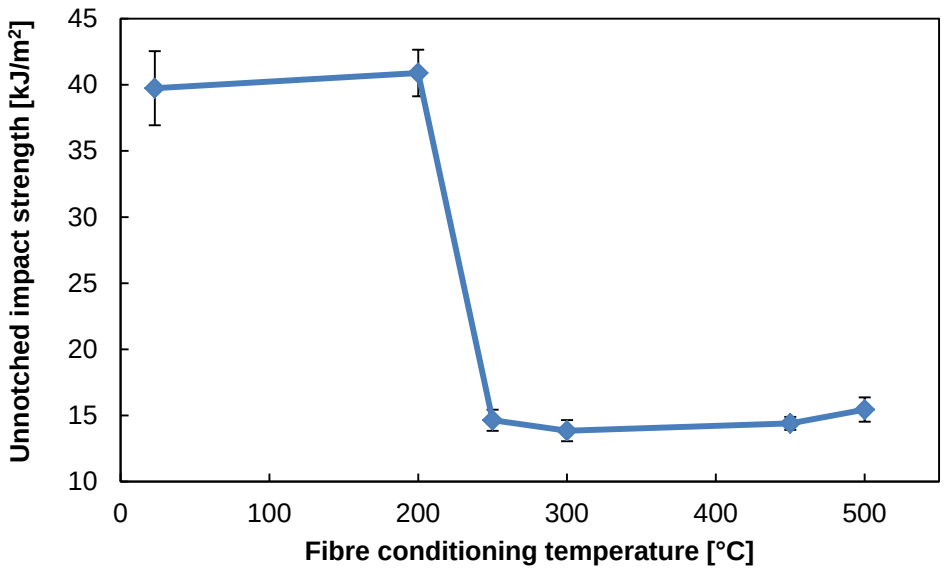

Figure 5.21. Reduction of the unnotched charpy impact strength with fibre conditioning temperature

T-tests showed that the increase of the impact strength between 300 °C and 500 °C fibre conditioning temperature was significant. The reason for the increase of the impact strength is not clear. The tensile strain at break also increased above 300 °C fibre conditioning temperature which was attributed to a matrix dominated composite behaviour. The weak fibres might have failed at low stresses which reduced the stress concentrations at the fibre ends and allowed the composites to be strained further without catastrophic composite failure. The increase of the impact strength might be explained in a similar way. Figure 5.19 shows that the fraction of supercritical fibres increased above 250 °C fibre conditioning temperature. Thus, energy dissipation by fibre fracture became more likely. The fibre fracture did not lead to composite failure. Thus, additional energy might have been dissipated when the fractured fibres debonded and pulled-out of the PP matrix. Further work is needed to understand the reasons for the increase of the impact strength between 300 °C and 500 °C fibre conditioning temperature. The impact strength seems to behave similar to the composite tensile strain at break. In situ tensile tests in an SEM [37] would therefore be useful to understand the failure mechanisms of these composites in more detail.

5.2.4 Composite modulus

Figure 5.22 suggests that the mean values of the composite modulus decreased with fibre conditioning temperature. However, the error bars are partly overlapping. Further statistical analysis was conducted to investigate the differences between the

arithmetic means of the modulus. T-tests showed that the modulus of the composites was significantly reduced when the fibres were conditioned at 300 °C, 450 °C and 500 °C. It was concluded in Chapter 2 that the modulus of discontinuous GF/PP composites is influenced by the fibre content, fibre length and fibre orientation. The fibre content was confirmed to be between 12.2 vol% and 12.8 vol% by ashing of the polymer matrix and weighting the fibres. All composites had a similar fibre orientation distribution because all processing parameters were kept constant. The fibre orientation distribution is also dependent on the fibre length or aspect ratio but in the present study the changes of the fibre length or aspect ratio were relatively small compared to studies by Spahr et al. [35] and Thomason [41]. The assumption of a constant fibre orientation distribution is also supported by the Bowyer-Bader analysis in Figure 5.15. The residual length of the fibres changed when the fibres were thermally conditioned.

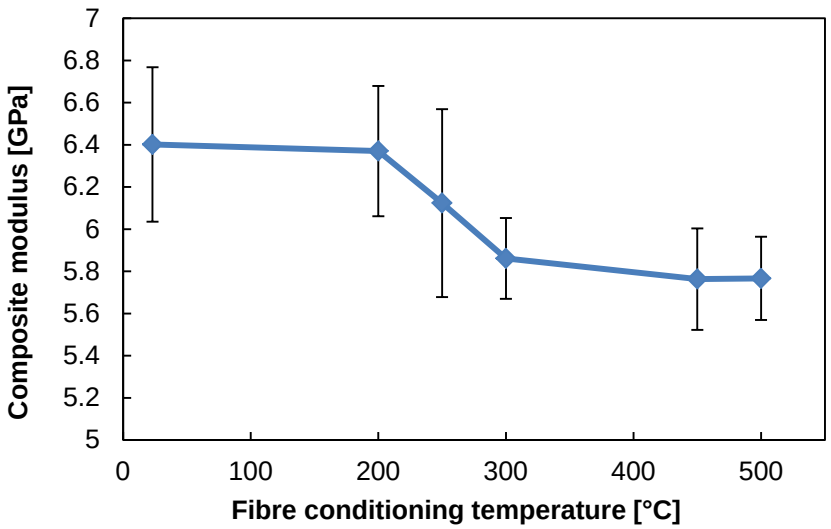

Figure 5.22. Reduction of the composite modulus with fibre conditioning temperature

The Cox model [42–44] as described in Chapter 2 was used to estimate the influence of the fibre length reduction on the composite modulus. The input parameters are listed in Table 5.4.

Table 5.4. Input parameter Cox model

Fibre volume fraction V_f	Calculated from fibre weight fraction [45] density of glass fibres 2.62 g/cm^3 [46], density of PP 0.905 g/cm^3 (manufacturer data)
Poisson's ratio υ	Calculated using rule of mixture, Poisons ratio of glass fibre 0.2 and PP 0.4 [47]
Packing factor X_i	4 [44]
E_M	1.71 GPa (measured)
E_f	78.7 GPa as received fibres [31] changed after thermal conditioning according to [32] to 78.9 GPa (250 °C), 80.1 GPa (300 °C), 83.7 GPa (450 °C), 88.9 GPa (500 °C)
Fibre orientation factor η_{oC}	0.62 (calculated as described above)
Aritmetic mean fibre length l	Measured (see Figure 5.8)

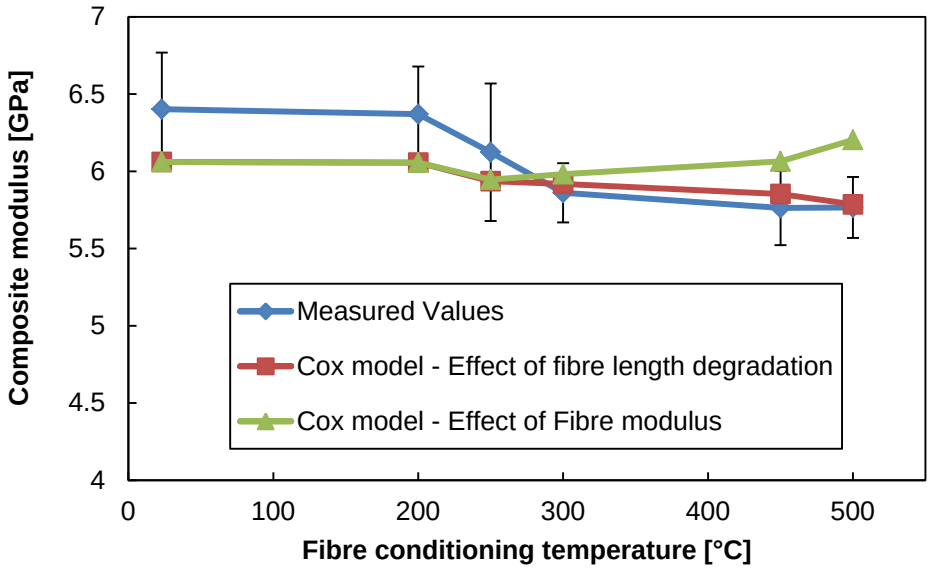

Figure 5.23. Cox model data to estimate effect of fibre length and fibre modulus on the composite modulus

The data in Figure 5.23 suggests that the behaviour of the the composite modulus could be explained with a reduction of the residual fibre length when the error bars are considered. The Cox model predicted an increase of the composite modulus at

450 °C and 500 °C fibre conditioning temperature when the fibre modulus increases as described by Yang and Thomason [32]. The measurement data in Figure 5.23 does not show an increase of the composite modulus. Thus, the present data does not allow drawing a final conclusion regarding the changes of the fibre modulus and its effect on the composite modulus.

5.3 Matrix modification to optimize composite performance

Similar to the previous section, a Carbolite CWF 12/13 furnace was used to thermally condition 3B DS 2200-13P glass fibres before extrusion compounding and injection moulding. In contrast to the previous section, the conditioning temperature was kept constant at 500 °C but the MAPP content of the composites was varied. For comparison, several plots in this section show data from Chapter 4 of as received fibre composites. The error bars of the as received fibre composite data were omitted for the sake of clarity.

5.3.1 Residual fibre length after composite processing

Figure 5.24 shows the arithmetic mean and weighted mean of the residual fibre length as a function of the MAPP content. Table 5.5 compares the standard deviations between the repeat measurements of the arithmetic mean values with the standard deviations of the fibre length distributions. As already mentioned in Chapter 4 and section 5.2.1 the standard deviations between the repeat measurements were small compared to the standard deviations of the fibre length distributions.

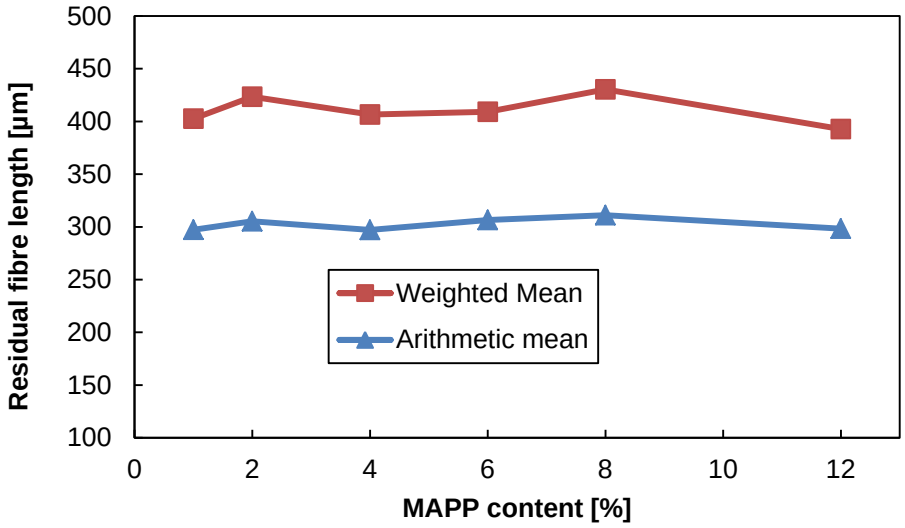

Figure 5.24. Absence of a correlation between the residual fibre length and MAPP content

Table 5.5. Comparison between standard deviations of repeated fibre length measurements and standard deviations of fibre length distributions

Added MAPP	Standard deviation of length distribution	Standard deviation between repeat measurements
1 %	181 µm	6 µm
2 %	191 µm	6 µm
4 %	190 µm	3 µm
6 %	178 µm	10 µm
8 %	194 µm	11 µm
12 %	168 µm	2 µm

The data in Figure 5.24 does not show a correlation between the residual fibre length and the added MAPP content. This observation is in agreement with the results that were presented in Chapter 4 and conflicting with data presented by Thomason [14] and Roux et al. [48]. The processing parameters, the injection moulder design and the relatively short residual fibre lengths in Figure 5.24 could have masked the effect of the MAPP in the present study. A more detailed discussion can be found in Chapter 4.

5.3.2 Composite modulus

Figure 5.25 shows the composite modulus as a function of the MAPP content. For comparison, the modulus of the as received fibre composites (Chapter 4) is also plotted in Figure 5.25. The modulus of the thermally conditioned fibre composites did not change between 1 % MAPP and 6 % MAPP but the values decreased between 6 % MAPP and 12 % MAPP. T-tests showed that the modulus of the thermally conditioned fibre composites decreased significantly between 2 % MAPP and 12 % MAPP. In addition, Figure 5.25 also shows the values for the fibre orientation factor. The values for the fibre orientation factor of the as received fibre composites were taken from Chapter 4. The values for the thermally conditioned fibre composites were calculated in the same way as the values for the as received fibre composites using the Cox model which is described in Chapter 2 and in different publications [42–44]. The input parameters to calculate the fibre orientation factor of the thermally conditioned fibre composites are listed in Table 5.6.

Table 5.6. Input parameters to calculate the fibre orientation factor from the composite modulus

Fibre volume fraction V_f	Calculated from fibre weight fraction [45] density of glass fibres 2.62 g/cm^3 [46], density of PP 0.905 g/cm^3 (manufacturer data)
Poison's ratio υ	Calculated using rule of mixture, Poisons ratio of glass fibre 0.2 and PP 0.4 [47]
Packing factor X_i	4 [44]
E_M	1.71 GPa (measured)
E_f	88.91 GPa [31,32]
Fibre length l	Measured (see Figure 5.24)
Composite modulus E_C	Measured (see Figure 5.25)

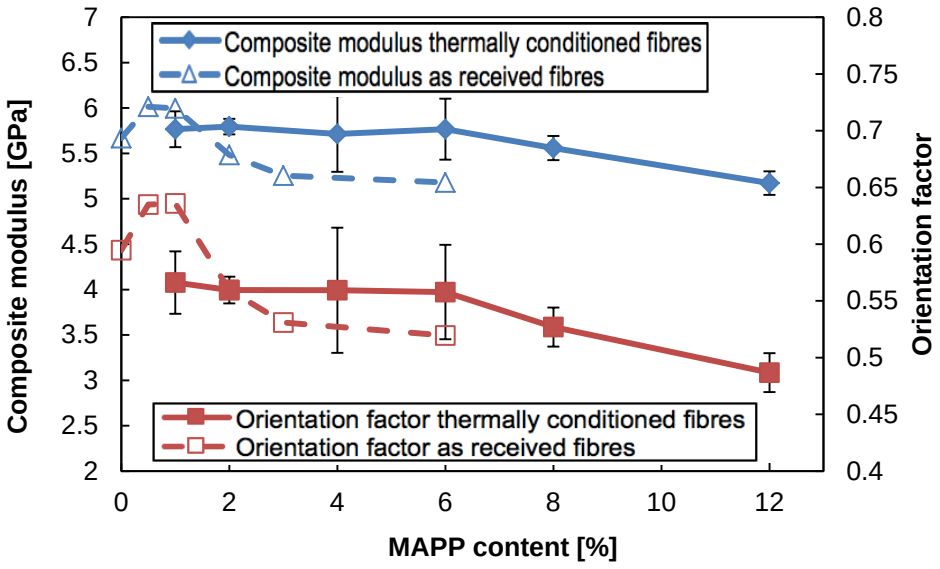

Figure 5.25. Reduction of the composite modulus and fibre orientation factor with MAPP content

The fibre length distribution and the fibre content were almost constant. The data in Chapter 4 showed that the modulus of the unreinforced PP was not influenced by the addition of MAPP. Similar to the as received fibre composites, the behaviour of the modulus of the thermally conditioned fibre composites in Figure 5.25 might be explained by changes in the fibre orientation. The data in Figure 5.25 suggests that the fibre orientation factor of the thermally conditioned fibre composites decreased with the MAPP content. Compared to the as received fibre composites, the fibre

orientation factor of the thermally conditioned fibre composites appears to drop at higher MAPP contents. However, Figure 5.25 shows only the added MAPP content. The actual MAPP content of the as received fibre composites was probably higher than shown in Figure 5.25 because the sizing of the as received fibres contained MAPP. In addition, random measurements errors and the resulting error bars might have masked a decrease of the composite modulus and fibre orientation factor between 2 % MAPP and 6 % MAPP.

5.3.3 Composite tensile strength

Similar to the as received fibre composites in Chapter 4, the tensile strength of the composites based on thermally conditioned glass fibres increased with the addition of MAPP. The data in Figure 5.26 shows that the tensile strength of the thermally conditioned fibre composites reached a plateau between 4 % MAPP and 8 % MAPP and decreased between 8 % and 12 % MAPP. A t-test confirmed that the tensile strength decreased significantly between 8 % and 12 % MAPP. Despite the increase of the composite tensile strength with increased MAPP content the composites based on thermally conditioned fibres were clearly weaker than composites based on as received fibres.

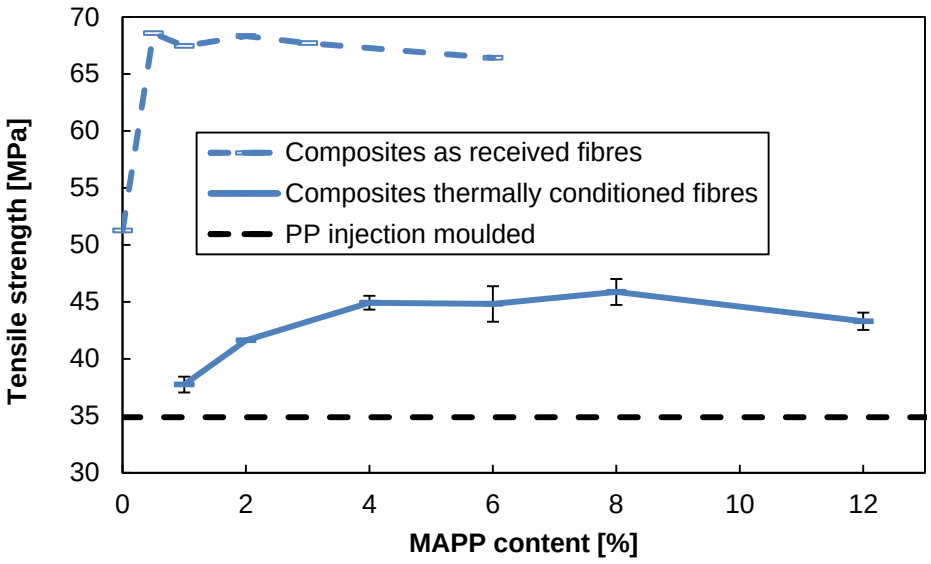

Figure 5.26. Effect of MAPP on the composite tensile strength

Influence of the IFSS

The tensile strength of the thermally conditioned fibre composites increased with the addition of MAPP to the composites. Comparable data on PP composites reinforced with thermally conditioned fibres was published by Roux et al. [48] and Zheng et al.

[49]. The optimum MAPP content of the thermally conditioned fibre composites in Figure 5.26 is higher than the optimum MAPP content for composites based on as received fibres which can be explained with the lack of the PP compatible sizing after thermal conditioning of the fibres. Figure 5.27 and Figure 5.28 show fracture surfaces of thermally conditioned fibre composites with 1 % MAPP and 8 % MAPP.

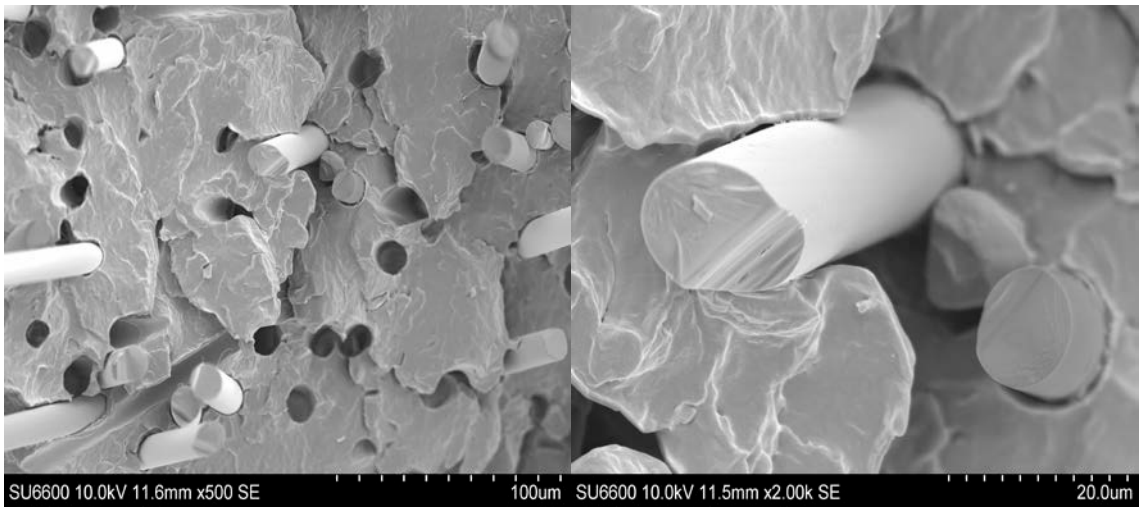

Figure 5.27. Fracture surface of composite based on thermally conditioned fibres, 1 % MAPP

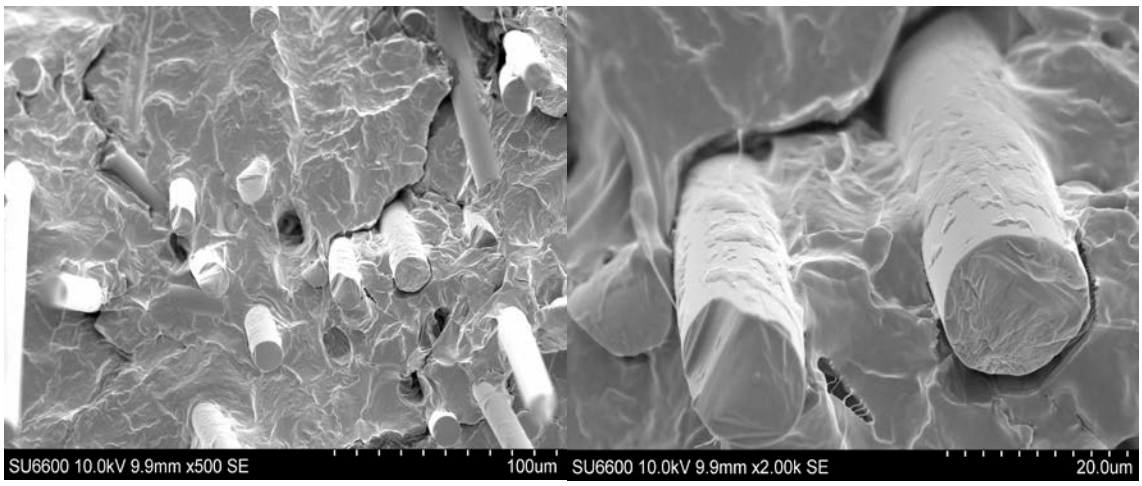

Figure 5.28. Fracture surface of composite based on thermally conditioned fibres, 8% MAPP

The fibres in Figure 5.27 are clean compared to the fibres in Figure 5.28 which are partially covered in PP. This could be interpreted as a proof for low interfacial adhesion at 1 % MAPP and higher interfacial adhesion at 8 % MAPP. No obvious differences were found between the fracture surfaces of composites with 8 % MAPP and fracture surfaces of composites with 12 % MAPP. In addition, the amount of resin on fibres of fracture surfaces might not always correlate with the IFSS [28].

Microbond tests were performed to obtain more robust information about the IFSS. The results of the microbond tests are plotted in Figure 5.29.

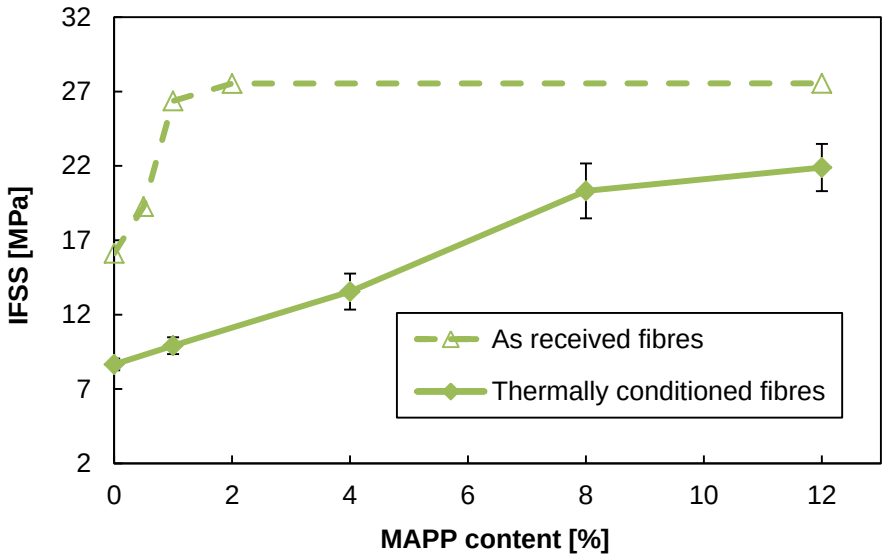

Figure 5.29. Increase of the microbond IFSS with MAPP content

The data in Figure 5.29 shows that the adhesion between thermally conditioned fibres and PP is less sensitive to the addition of MAPP than the adhesion between as received fibres and PP. The maximum level of adhesion was also lower when the fibres were thermally conditioned which can be explained with the sizing degradation during the thermal conditioning of the fibres. Similar to other studies [48,50–52] the data in Figure 5.29 shows that MAPP can increase the IFSS between unsized fibres (thermally conditioned fibres) and PP. Thus, the effect of MAPP on the IFSS between glass fibres and PP cannot solely be explained by acid basic interactions. Future work is required to understand the interaction between MAPP and unsized glass fibres. In contrast to the IFSS, the tensile strength of the thermally conditioned fibre composites did not increase between 4 % MAPP and 8 % MAPP. One explanation for such a plateau is that the glass fibre surfaces were saturated with maleic anhydride groups. The increase of the number of maleic anhydride groups did not lead to an increase of the IFSS or composite tensile strength [53]. However, the microbond data in Figure 5.29 suggests that the IFSS of the thermally conditioned fibre samples increased further between 4 % MAPP and 8 % MAPP. Thus, the tensile strength of the thermally conditioned fibre composites in Figure 5.26 might not have been limited by the IFSS. It was speculated in Chapter 4 that high MAPP contents led to a reduction of the degree of fibre alignment and an embrittlement of the composites. To further investigate the microstructural properties

of the thermally conditioned fibre composites, the Bader-Bowyer analysis as described in Chapter 2 was performed. The calculated values for the IFSS are plotted in Figure 5.30 together with the microbond test data and the data of the as received fibre composites. The input parameter of the Bader-Bowyer analysis are summarised in Table 5.2 in the previous section.

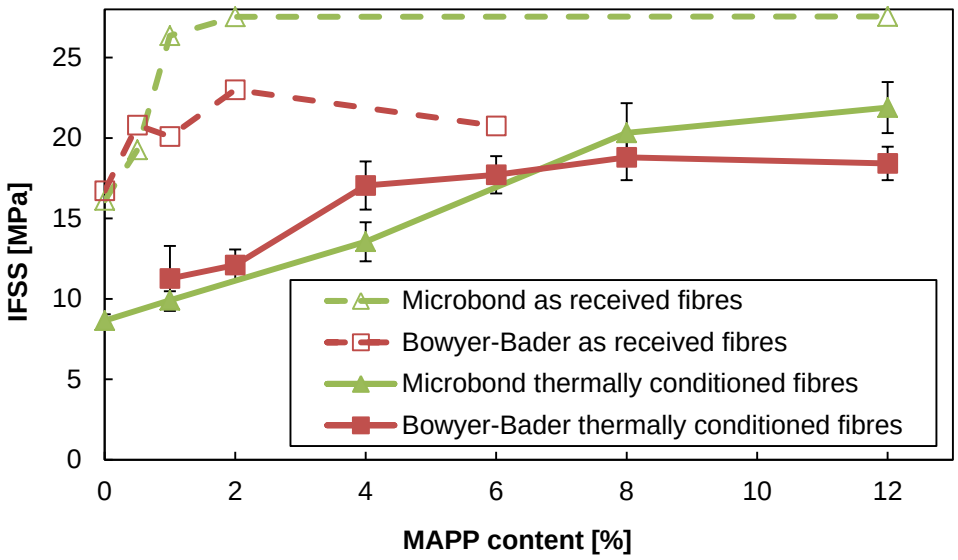

Figure 5.30. Comparison between the Bowyer-Bader IFSS and the microbond IFSS

Similar to the microbond test results, the Bowyer-Bader analysis predicted an increase of the IFSS of the thermally conditioned fibre composites with the addition of MAPP. In contrast to the microbond data, the IFSS obtained from the Bowyer-Bader analysis reached a plateau at 4 % MAPP while the microbond IFSS continued to increase. The as received fibre composites exhibited a similar behaviour. The Bowyer-Bader IFSS did not increase significantly above 0.5 % MAPP but the microbond IFSS increased up to 1 % MAPP. It is likely that the Bowyer-Bader IFSS of the thermally conditioned fibre composites and the Bowyer-Bader IFSS of the as received fibre composites were affected by the mechanisms that also affected the composite tensile strength. The trend of the Bowyer-Bader IFSS might therefore not be accurate.

Influence of fibre strength and critical fibre length for fibre failure

The values for the maximum stress of the thermally conditioned fibres obtained from the Bowyer-Bader analysis are plotted in Figure 5.31 as a function of the added MAPP content. The data in Figure 5.31 shows that the maximum stress of the

thermally conditioned fibres was lower than the maximum stress of the as received fibres which indicates a strength loss of the fibres due to thermal conditioning.

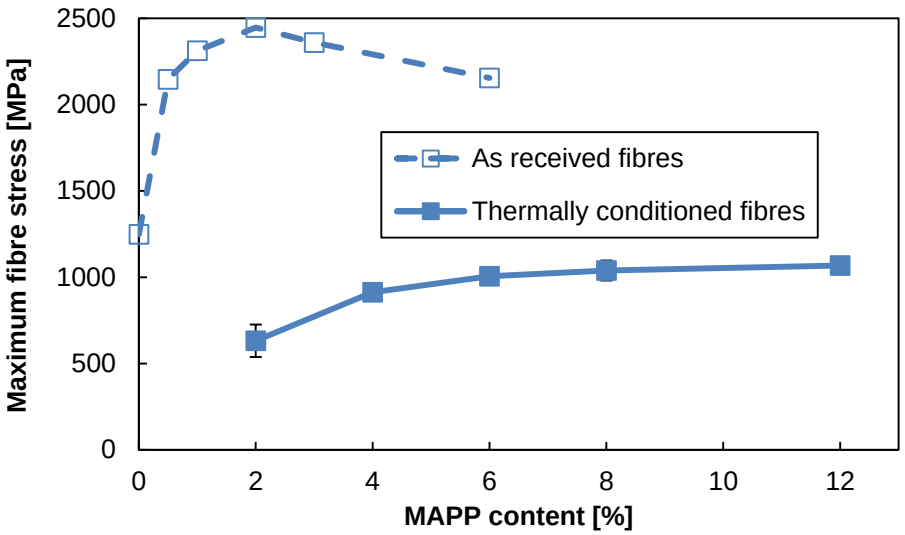

Figure 5.31. Increase of the maximum stress of thermally conditioned fibre with MAPP content

The data in Figure 5.31 shows that the maximum stress of the thermally conditioned fibres increased due to the addition of MAPP to the composites. This behaviour can be explained with an enhanced stress transfer between fibre and matrix. The as received fibre composites in Chapter 4 exhibited a similar behaviour. At higher MAPP contents the maximum fibre stress levelled off. A t-test confirmed that the stress of the thermally conditioned fibres did not increase significantly between 8 % MAPP and 12 % MAPP. The IFSS obtained from microbond tests in Figure 5.29 also levelled off between 8 % and 12 % MAPP. One possible explanation is the embrittlement of the composites as suggested by Zheng et al. [49]. A high MAPP content and a high IFSS cause a reduction of the energy that is dissipated by fibre pull-out. When one fibre fails a crevice is developed, surrounding fibres fail as well and a crack is formed which leads to composite failure. The behaviour of the as received fibre composites in Chapter 4 was explained with the same failure mechanisms. The low strength of the thermally conditioned fibres might have further promoted this failure mechanism. The maximum stress of the thermally conditioned fibres in Figure 5.31 is 956 MPa. It was speculated in Section 5.2 that the composite tensile strength and maximum fibre stress decreased between 250 °C and 500 °C because of a degradation of the fibre strength. The maximum fibre stress decreased from 786 MPa (250 °C) to 554 MPa (500 °C). The maximum stress of the thermally conditioned fibres in Figure 5.31 is significantly higher. Thus, the results of Section

5.2 and this section are apparently conflicting. One potential explanation is the critical fibre length. The addition of MAPP increased the IFSS and decreased the critical fibre length. Figure 5.32 shows the critical fibre length for fibre failure of the thermally conditioned fibres based on the values in Table 5.3 and the microbond IFSS in Figure 5.29.

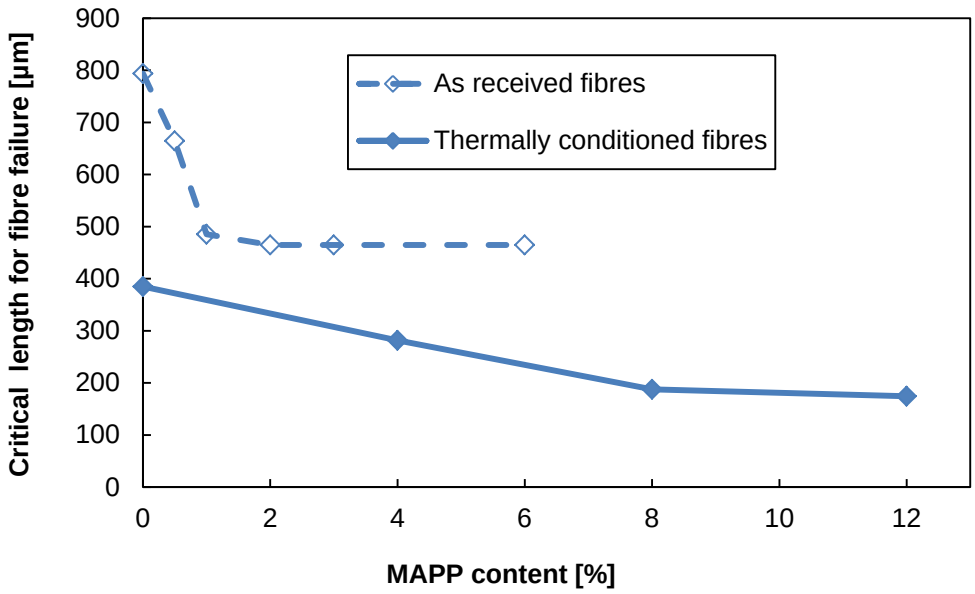

Figure 5.32. Reduction of the critical fibre length for fibre failure with MAPP content

The critical length for failure of the thermally conditioned fibres is shorter than the critical length for failure of the as received fibres because of the reduction of the fibre strength. The data in Figure 5.32 suggests that the critical fibre length for fibre failure in the thermally conditioned fibre composites might have been reduced by more than 50 % when the MAPP content was increased from 1 % to 12 %. Due to the reduction of the critical fibre length shorter fibres could contribute to the composite tensile stress. It is well known that the tensile strength of glass fibres increases when the length is reduced [31,49]. The larger contribution of shorter and stronger fibres to the composite tensile stress might explain the higher fibre stresses in this section compared to Section 5.2.

The data in Figure 5.33 is based on the measured fibre length distribution and the data in Figure 5.32. It shows that the fraction of supercritical fibres increased when more MAPP was added to the composites.

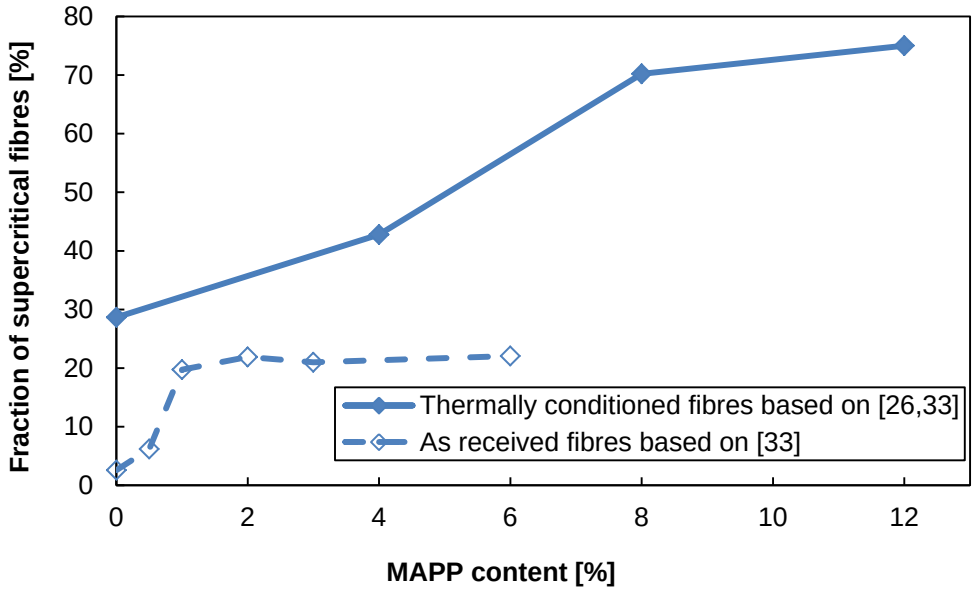

Figure 5.33. Increase of the fraction of supercritical fibres with MAPP content

Figure 5.33 suggests that the probability of fibre failure increased with the addition of MAPP and the increase of the IFSS. In addition, the thermally conditioned fibres were more likely to fail than the as received fibres. It should be noted that the data in Figure 5.33 depends strongly on the estimated value for the fibre strength and does not consider the length dependence of the fibre strength. Further work like single fibre tensile tests on chopped fibre extracted composites might be required to improve the accuracy of the data in Figure 5.33.

Influence of fibre orientation

In addition to the fibre strength, the composite tensile strength and the maximum fibre stress might also have been affected by the orientation factor. It was discussed in Chapter 4 and section 5.3.2 that high MAPP contents seem to affect the orientation of the glass fibres in the composites. Figure 5.34 shows the orientation factor of the Bowyer-Bader analysis as a function of the MAPP content.

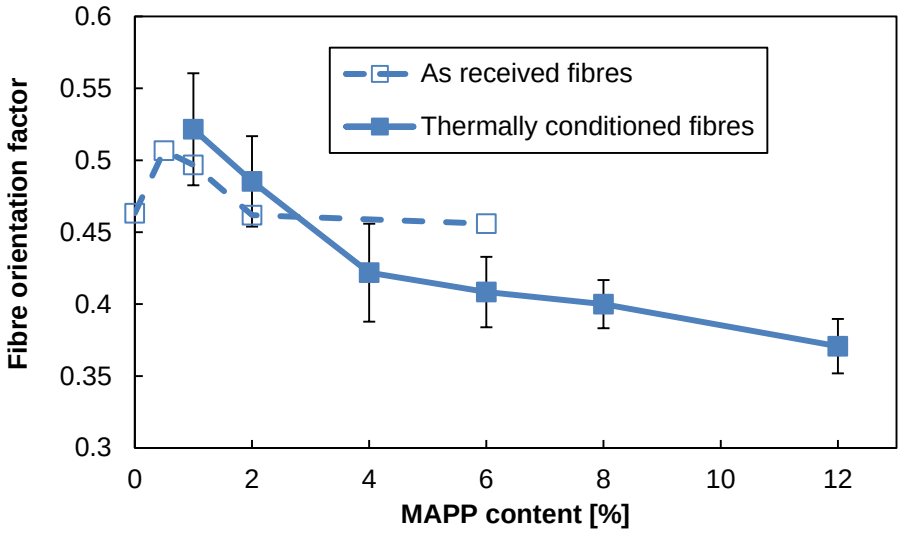

Figure 5.34. Reduction of the Bowyer-Bader fibre orientation factor with MAPP content

Similar to Figure 5.25, the data in Figure 5.34 suggests that high MAPP contents affected the orientation of fibres in as received fibre composites and thermally conditioned fibre composites. The data in Figure 5.34 suggests that the fibre orientation factor of the thermally conditioned fibre composites started to drop between 2 % and 4 % MAPP. Figure 5.25 suggests that the fibre orientation factor of the thermally conditioned composites was constant up to 6 % MAPP and dropped when the MAPP content was further increased. However, the error bars in Figure 5.25 might have masked a drop of the fibre orientation factor between 2 % and 4 % MAPP. Both figures indicate a reduction of the fibre orientation factor between 2 % and 12 % MAPP. Thus, the tensile properties of the thermally conditioned fibre composites might have been affected by changes of the fibre orientation similar to the as received fibre composites in Chapter 4. The question arises to which extend the orientation factor limited the composite tensile strength and to which extend the fibre strength limited the composite tensile strength. The present data cannot provide a final answer to that question but it is probably a combination of both.

5.3.4 Composite strain at break and yield strain

Figure 5.35 shows the strain at break and yield strain of the thermally conditioned fibre composites and as received fibre composites. The decrease of the strain at break of the thermally conditioned fibre composites between 1 % MAPP and 8 % MAPP and the increase of the strain at break between 8 % MAPP and 12 % MAPP were both confirmed to be significant by t-tests. The composite yield strain followed the composite strain at break.

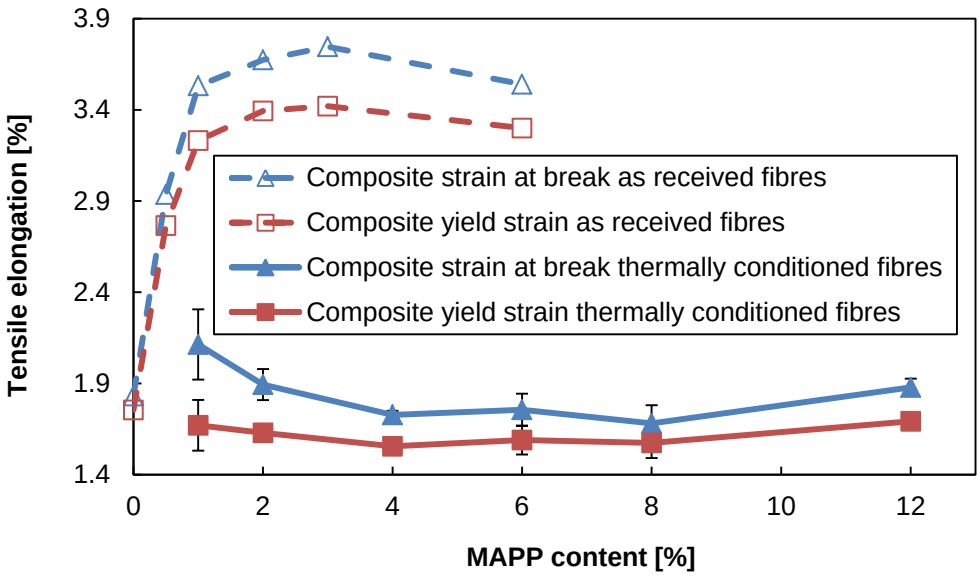

Figure 5.35. Effect of MAPP content on the composite strain at break and the yield strain

It was concluded in section 5.2.3 that the strain at break and the yield strain of the composites decreased when the fibres were conditioned at 250 °C because of the lack of interfacial adhesion. Several authors [14,34] observed that the improvement of the IFSS due to the addition of functionalised PP to the composites can lead to an increase of the composite strain at break. It might therefore be expected that the strain at break of the thermally conditioned fibre composites increases with the addition of MAPP similar to the as received fibre composites up to 3 % MAPP. However, the strain at break of the thermally conditioned fibres decreased initially with the addition of MAPP which might be explained with the failure of the thermally conditioned fibre at low stresses. When the MAPP content of the thermally conditioned fibre composites was increased from 1 % to 8 % more load was transferred to the weak fibres and the composite failure behaviour became progressively brittle and fibre dominated. Above 8 % MAPP the IFSS levelled off but the fibre orientation factor as shown in Figure 5.25 and in Figure 5.34 decreased further. Thus, less fibres were aligned in load direction and the composite behaviour became progressively matrix dominated. The increase of the composite strain at break when the fibre orientation decreased was also observed by other researchers [35,54]. The stress-strain curves in Figure 5.36 show that at low MAPP contents the composites exhibited a ductile behaviour. Composites with high MAPP contents showed a shorter ductile region and a fibre dominated fracture behaviour.

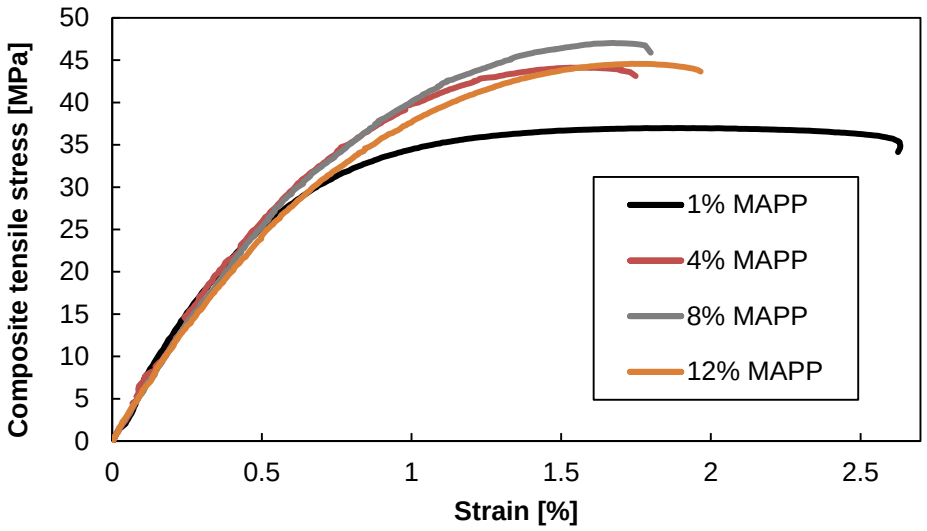

Figure 5.36. Stress-strain curves of composites with different MAPP contents

5.4 Summary and Conclusions

The investigation of the reinforcement potential of thermally recycled glass fibres in injection moulded PP was reported in this chapter. TGA showed that thermoset compatible glass fibre sizings and thermoplastic compatible glass fibre sizings degrade at temperatures that are used in thermal recycling processes. The sizing degradation occurred in both air and inert atmospheres. Microbond tests showed that the sizing degradation correlated with a reduction of the IFSS between fibres and PP. It was found that PP compatible sizings lost most of their functionality in the range of composite processing temperatures when they were exposed to air. The tensile strength and strain at break of injection moulded PP composites also dropped sharply when the fibres were thermally conditioned at 250 °C in air before composite processing. Although the thermal conditioning is different to processing conditions, the results in this chapter show that PP compatible sizing are highly susceptible to degradation in air. Further research is required to assess if PP compatible sizings are also thermally degraded during hot melt processing which might be highly relevant for the recycling of GF/PP composites.

The reduction of the IFSS obtained from microbond tests correlated with a drop of the composite tensile strength and strain at break. The Bader-Bowyer analysis was used to investigate the maximum stresses that the glass fibres experienced in the composites. It was hypothesized that the composite tensile strength was at least partially affected by a degradation of the glass fibre strength when the glass fibres

were conditioned at temperatures higher than 300 °C. The addition of MAPP to composites based on thermally conditioned fibres increased the IFSS and the composite tensile strength. However, the composites based on thermally conditioned fibres still had a significantly lower tensile strength than composites based on as received fibres which was attributed to the low strength of thermally conditioned fibres. In addition, micromechanical analysis suggested that the fibres were less aligned when more MAPP was added to the composites.

Thus, the data in this chapter shows that thermally recycled glass fibres need a post treatment to regenerate both the fibre strength and fibre surface functionality. The improvement of the IFSS by the addition of MAPP is not sufficient to regenerate the composite tensile strength. In addition, high MAPP contents appear to affect the fibre orientation and might also not be economically viable because of the higher material costs of MAPP compared to PP.

5.5 References

[1] Thomason JL. Glass fibre sizing: A review of size formulation patents. 2015.

[2] Feih S, Boiocchi E, Mathys G, Mathys Z, Gibson AG, Mouritz AP. Mechanical properties of thermally-treated and recycled glass fibres. Compos Part B Eng 2011;42:350–8.

[3] Yang L, Thomason JL, Zhu W. The influence of thermo-oxidative degradation on the measured interface strength of glass fibre-polypropylene. Compos Part A Appl Sci Manuf 2011;42:1293–300.

[4] Beyler CL, Hirschler MM. Thermal Decomposition of Polymers. In: DiNenno PJ, editor. SPE Handb. Fire Prot. Eng. 3rd ed., Quincy (Massachusetts): 2001, p. 110–31.

[5] Roberts D, Constable RC. Chemical Coupling Agents for Filled and Grafted Polypropylene Composites. In: Karian HG, editor. Handb. Polypropyl. Polypropyl. Compos., Marcel Dekker Inc.; 2003, p. 49–94.

[6] British Standards Institutions. ISO 11358-1:2014 Plastics — Thermogravimetry (TG) of polymers Part 1: General principles 2014.

[7] Thomason JL, Dwight D. The use of XPS for characterisation of glass fibre coatings. Compos Part A Appl Sci Manuf 1999;30:1401–13.

[8] Bourmaud A, Baley C. Investigations on the recycling of hemp and sisal fibre reinforced polypropylene composites. Polym Degrad Stab 2007;92:1034–45.

[9] Dickson AR, Even D, Warnes JM, Fernyhough A. The effect of reprocessing on the mechanical properties of polypropylene reinforced with wood pulp, flax or glass fibre. Compos Part A Appl Sci Manuf 2014;61:258–67.

[10] Otheguy ME, Gibson AG, Findon E, Cripps RM, Mendoza AO, Castro MTA. Recycling of end-of-life thermoplastic composite boats. Plast Rubber Compos 2009;38:406–11.

[11] Fisa B. Mechanical degradation of glass fibers during compounding with polypropylene. Polym Compos 1985;6:232–41.

[12] Gupta VB, Mittal RK, Sharma PK, Mennig G, Wolters J. Some studies on glass fiber-reinforced polypropylene. Part 1: Reduction in fiber length during processing. Polym Compos 1989;10:8–15.

[13] Thomason JL. The influence of fibre length and concentration on the properties of glass fibre reinforced polypropylene: 5. Injection moulded long and short fibre PP. Compos Part A Appl Sci Manuf 2002;33:1641–52.

[14] Thomason JL. Micromechanical parameters from macromechanical measurements on glass reinforced polypropylene. Compos Sci Technol 2002;62:1455–68.

[15] Mittal RK, Gupta VB, Sharma PK. Theoretical and experimental study of fibre attrition during extrusion of glass-fibre-reinforced polypropylene. Compos Sci Technol 1988;31:295–313.

[16] Fu S-Y, Lauke B, Mäder E, Yue C-Y, Hu X. Tensile properties of short-glass-fiber- and short-carbon-fiber-reinforced polypropylene composites. Compos Part A Appl Sci Manuf 2000;31:1117–25.

[17] Thomason JL. The influence of fibre length and concentration on the properties of glass fibre reinforced polypropylene. 6. The properties of injection moulded long fibre PP at high fibre content. Compos Part A Appl Sci Manuf 2005;36:995–1003.

[18] Phelps JH, Abd El-Rahman AI, Kunc V, Tucker CL. A model for fiber length attrition in injection-molded long-fiber composites. Compos Part A Appl Sci Manuf 2013;51:11–21.

[19] Turkovich R, Erwin L. Fiber fracture in reinforced thermoplastic processing. Polym Eng Sci 1983;23:743–9.

[20] Akesson D, Foltynowicz Z, Christeen J, Skrifvars M. Microwave pyrolysis as a method of recycling glass fibre from used blades of wind turbines. J Reinf Plast Compos 2012;31:1136–42.

[21] Kennerley JR, Fenwick NJ, Pickering SJ, Rudd CD. The properties of glass fibers recycled from the thermal processing of scrap thermoset composites. J Vinyl Addit Technol 1997;3:58–63.

[22] Kennerley JR, Kelly RM, Fenwick NJ, Pickering SJ, Rudd CD. The characterisation and reuse of glass fibres recycled from scrap composites by the action of a fluidised bed process. Compos Part A Appl Sci Manuf 1998;29:839–45.

[23] Yang L, Sáez Rodríguez E, Nagel U, Thomason JL. Can thermally degraded glass fibre be regenerated for closed-loop recycling of thermosetting composites? Compos Part A Appl Sci Manuf 2015;72:167–74.

[24] Jenkins PG, Yang L, Liggat J., Thomason JL. Investigation of the strength loss of glass fibre after thermal conditioning. J Mater Sci 2014;50:1050–7.

[25] Thomason JL, Kao CC, Ure J, Yang L. The strength of glass fibre reinforcement after exposure to elevated composite processing temperatures. J Mater Sci 2013;49:153–62.

[26] Thomason JL, Yang L, Meier R. The properties of glass fibres after conditioning at composite recycling temperatures. Compos Part A Appl Sci Manuf 2014;61:201–8.

[27] Lund MD, Yue Y. Impact of drawing stress on the tensile strength of oxide glass fibers. J Am Ceram Soc 2010;93:3236–43.

[28] Fu SY, Lauke B, Zhang YH, Mai Y-W. On the post-mortem fracture surface morphology of short fiber reinforced thermoplastics. Compos Part A Appl Sci Manuf 2005;36:987–94.

[29] Bowyer WH, Bader MG. On the re-inforcement of thermoplastics by imperfectly aligned discontinuous fibres. J Mater Sci 1972;7:1315–21.

[30] Thomason JL. The influence of fibre length and concentration on the properties of glass fibre reinforced polypropylene: 7. Interface strength and fibre strain in injection moulded long fibre PP at high fibre content. Compos Part A Appl Sci Manuf 2007;38:210–6.

[31] Yang L, Thomason JL. Effect of silane coupling agent on mechanical performance of glass fibre. J Mater Sci 2012;48:1947–54.

[32] Yang L, Thomason JL. The thermal behaviour of glass fibre investigated by thermomechanical analysis. J Mater Sci 2013;48:5768–75.

[33] Thomason JL, Kalinka G. Technique for the measurement of reinforcement fibre tensile strength at sub-millimetre gauge lengths. Compos Part A Appl Sci Manuf 2001;32:85–90.

[34] Bikiaris D, Matzinos P, Larena A, Flaris V, Panayiotou C. Use of silane agents and poly(propylene-g-maleic anhydride) copolymer as adhesion promoters in glass fiber/polypropylene composites. J Appl Polym Sci 2001;81:701–9.

[35] Spahr DE, Friedrich K, Schultz JM, Bailey RS. Microstructure and fracture behaviour of short and long fibre-reinforced polypropylene composites. J Mater Sci 1990;25:4427–39.

[36] Thomason JL, Vlug MA, Schipper G, Krikort HGLT. Influence of fibre length and concentration on the properties of glass fibre-reinforced polypropylene Part 3 Strength and strain at failure. Compos Part A Appl Sci Manuf 1996;27A:1075–84.

[37] Sato N, Kurauchi T, Sato S, Kamigaito O. Microfailure behaviour of randomly dispersed short fibre reinforced thermoplastic composites obtained by direct SEM observation. J Mater Sci 1991;26:3891–8.

[38] Thomason JL, A. VM. Influence of fibre length and concentration on the properties of glass fibre reinforced polypropylene: 4. Impact properties. Compos Part A Appl Sci Manuf 1997;28A:277–88.

[39] Cottrell AH. Strong Solids. Proc. R. Soc. London. Ser. A, London: 1964, p. 2–9.

[40] Friedrich K. Microstructural efficiency and fracture toughness of short fiber/thermoplastic matrix composites. Compos Sci Technol 1985;22:43–74.

[41] Thomason JL. The influence of fibre properties of the performance of glass-fibre-reinforced polyamide 6 ,6. Compos Sci Technol 1999;59:2315–28.

[42] Cox HL. The elasticity and strength of paper and other fibrous materials. Br J Appl Phys 2002;3:72–9.

[43] Ericson M, Berglund L. Deformation and fracture of glass-mat- reinforced polypropylene. Compos Sci Technol 1992;43:269–81.

[44] Thomason JL, Vlug MA. The influence of fibre length and concentration on the properties of glass fibres reinforced polypropylene: 1. Tensile and flexural modulus. Compos Part A Appl Sci Manuf 1996;27:477–84.

[45] Thomason JL. The interface region in glass fibre-reinforced epoxy resin composites : 1 . Sample preparation , void content and interfacial strength. Composites 1995;26:467–75.

[46] Wallenberger FT, Watson JC, Hong L. Glass Fibers. ASM Handb 2001;21:27–34.

[47] Lee N-J, Jang J. The effect of fibre-content gradient on the mechanical properties of glass-fibre-mat/polypropylene composite. Compos Sci Technol 2000;60:209–17.

[48] Roux C, Denault J, Champagne MF. Parameters regulating interfacial and mechanical properties of short glass fiber reinforced polypropylene. J Appl Polym Sci 2000;78:2047–60.

[49] Zheng A, Wang H, Zhu X, Masuda S. Studies on the interface of glass fiber-reinforced polypropylene composite. Compos Interfaces 2002;9:319–33.

[50] Mäder E, Pisanova E. Characterization and design of interphases in glass fiber reinforced polyproplyene. Polym Compos 2000;21:361–8.

[51] Mäder E, Freitag K-H. Interface properties and their influence on short fibre composites. Composites 1990;21:397–402.

[52] Mäder E, Jacobasch HJ, Grundke K, Gietzelt T. Influence of an optimized interphase on the properties of polypropylene/glass fibre composites. Compos Part A Appl Sci Manuf 1996;27:907–12.

[53] Bowland C. A formulation study of long fiber thermoplastic polypropylene (Part 2): The effects of coupling agent type and properties. Automot. Compos. Conf. Expo., 2009.

[54] Mittal RK, Gupta VB, Sharma P. The effect of fibre orientation on the interfacial shear stress in short fibre-reinforced polypropylene. J Mater Sci 1987;22:1949–55.

6. Polypropylene composites based on regenerated glass fibres

It was concluded in the previous chapter that thermally recycled fibres are unlikely to be able to compete with new (as received) fibres as reinforcement phase in Polypropylene (PP) because of their very low strength. Despite the addition of maleic anhydride grafted Polypropylene (MAPP) to the PP matrix and an optimised interfacial shear strength (IFSS), composites based on thermally degraded fibres had lower mechanical properties than composites based on as received fibres. Consequently, in this chapter a different approach was chosen to optimise the performance of composites based on thermally degraded glass fibres. The thermally degraded glass fibres were subject to different post treatments before composite processing to optimise their reinforcement potential in glass fibre PP (GF/PP) composites. The aim was to demonstrate whether composites based on thermally recycled glass fibres could compete with composites based on as received fibres.

Similar to Chapter 5, the glass fibres were thermally degraded by thermal conditioning before composite processing in a Carbolite CWF 12/13 furnace to imitate a thermal recycling process. Tensile tests and unnotched charpy impact tests were performed to assess the mechanical performance of the composites. Fibre length measurements, microbond tests and single fibre tensile tests were performed to investigate the microstructural properties of the composites. The error bars in all plots represent 95 % confidence intervals and t-tests (p=0.05) were conducted to further study the significance of observed trends. All composites had a nominal fibre content of 12.8 vol%. The composites were either processed via extrusion compounding and injection moulding or via a glass mat thermoplastic (GMT) process that was developed over the course of this PhD project.

6.1 Injection moulded composites based on regenerated fibres

Several studies reviewed in Chapter 2 correlated an increase of the glass fibre strength to the application of silane on the fibre surface [1–3]. This effect was explained with the ‘healing’ of surface flaws by silane. Feih et al. [4] correlated the strength of thermally degraded fibres with surface flaws. Thus, silanes should also increase the strength of thermally degraded fibres. However, there is a lack of clear evidence based on single fibre tensile tests for this hypothesis. Sáez et al. [5] and

Thomason et al. [6] stated that the post treatment of thermally degraded fibres with AminoPropyltriethoxySilane (APS) did not lead to a significant increase of the single fibre tensile strength. On the other hand, in both studies the average value of the fibre strength increased when the thermally degraded fibres were post treated with APS. Similar observations were reported by Yang et al. [7]. The strength of glass fibres depends on the fibre length because the probability for the presence of severe flaws increases with the fibre length [8,9]. Shorter fibres might be less likely to suffer from severe flaws caused by exposure of the fibres to elevated temperatures. Assuming that APS can heal some of the flaws of the thermally degraded glass fibres it might be speculated that APS has an effect on thermally degraded fibres when they are sufficiently short. In addition, the effect of APS on the strength of glass fibres might also be explained by a surface protection effect rather than the flaw healing theory [8]. Thus, the post treatment of thermally degraded fibres with APS might protect the fibres from additional damage when they are processed into composites.

It was decided to treat thermally degraded glass fibres with APS before processing them into injection moulded GF/PP. Details of the APS treatment are provided in Chapter 3. Composites based on fibres that were thermally degraded and post treated with APS (TD+APS) will be referred as APS treated fibre composites in this chapter. The mechanical properties of the APS treated fibre composites are compared with as received fibre composites and composites based on thermally degraded (TD) fibres with 1 % MAPP and 8 % MAPP (weight fraction of the PP matrix). Similar to Chapter 4 and Chapter 5, the actual MAPP content of the as received fibre composites might have been higher than 1 % because of MAPP in the glass fibre sizing.

6.1.1 Residual fibre length after composite processing

Roux et al. [10] reported an increase of the residual fibre length by 20 µm when they treated thermally degraded fibres with APS before composite processing. However, Roux et al. did not provide information how many fibres they measured. Their data should therefore be regarded with caution. It was suggested in Chapter 5 that thermally degraded fibres might be more susceptible to length degradation during composite processing because of their lower tensile strength and because of the lower integrity of the fibre bundles. The fibre bundles are broken into individual fibres at an earlier stage of the processing. Individualised fibres might be more susceptible

to abrasion and bending than fibres that are arranged in bundles. Figure 6.1 shows the residual fibre length of composites based on as received fibres, thermally degraded fibres and APS treated fibres. The data in Figure 6.1 suggests that the post treatment of the thermally degraded fibres with APS did not lead to a clear increase of the residual fibre length in the injection moulded composites. Thus, the APS treatment did not lead to an improvement of the fibre strength. However, it is possible that mechanisms like the reduced integrity of the fibre bundles masked the effect of the fibre strength on the residual fibre length.

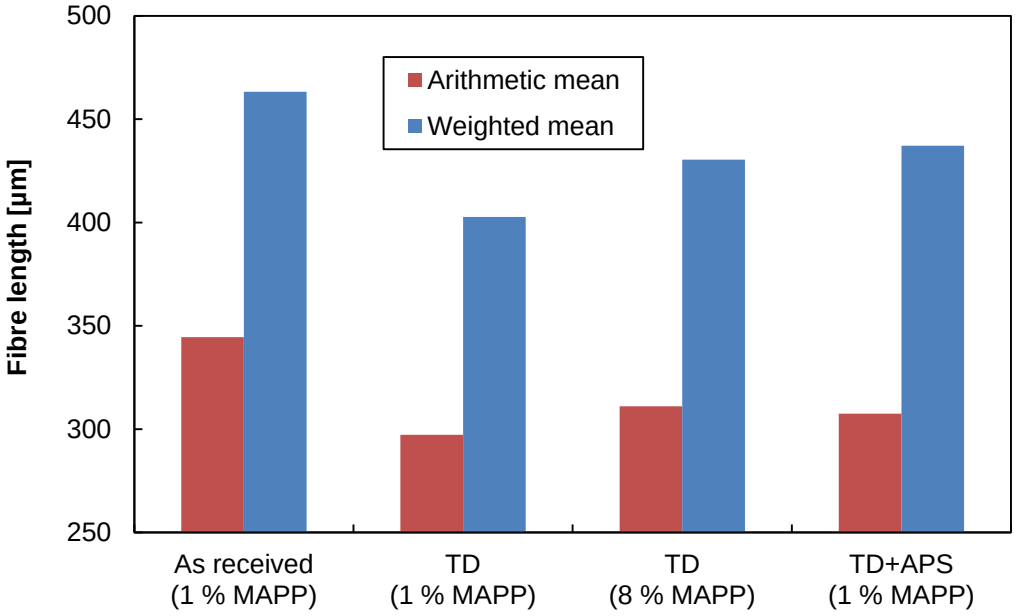

Figure 6.1. Effect of fibre regeneration and MAPP content on the residual fibre length of injection moulded GF/PP composites

6.1.2 Composite modulus

Figure 6.2 shows the modulus and the fibre orientation factor of the injection moulded composites. The composite modulus did not vary significantly between composites based on thermally degraded fibres with 1 % MAPP and APS treated fibre composites. The fibre modulus of the thermally degraded fibre composites decreased when 8 % MAPP were added to the PP matrix. Potential reasons for this effect were discussed in Chapter 5. The modulus of GF/PP composites depends mainly on the fibre length [11,12], fibre orientation [11,13] and fibre content [11,14–17,13,18]. The fibre content and the processing parameters were kept constant. The data in Figure 6.1 suggests that the APS treatment of the glass fibres did not lead to a large increase of the residual fibre length. Thus, the composite modulus was not expected to change when the thermally degraded fibres were post treated with APS.

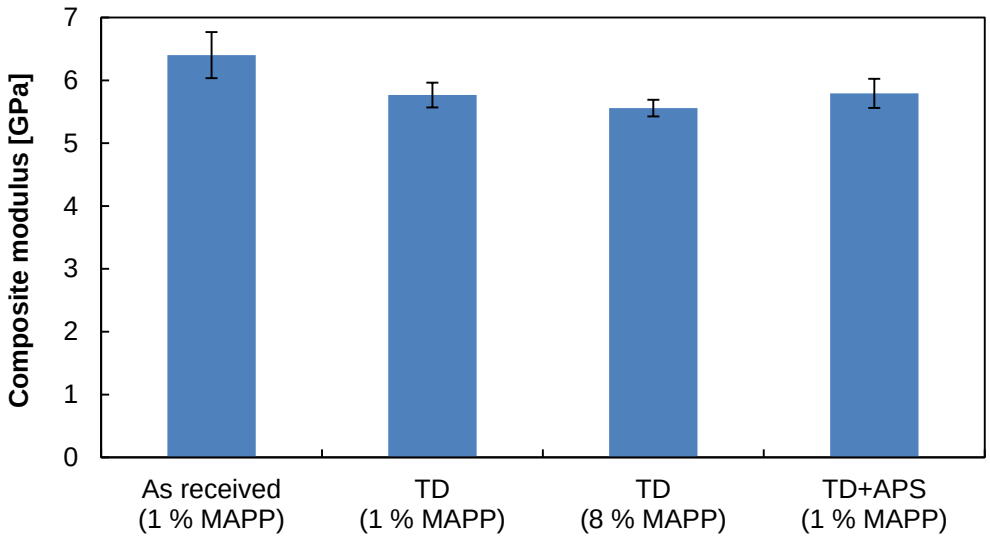

Figure 6.2. Effect of fibre regeneration and MAPP content on the modulus of injection moulded GF/PP composites

6.1.3 Composite tensile strength

The data in Figure 6.3 shows that the tensile strength of the composites was significantly improved by the post treatment of the thermally degraded fibres with APS. More than 50 % of the strength loss was recovered. The post treatment of the fibres with APS appears to be more effective in improving the composite tensile strength than the addition of MAPP to the matrix. Similar observations were reported by Roux et al. [10] but without a detailed discussion of the microstructural properties.

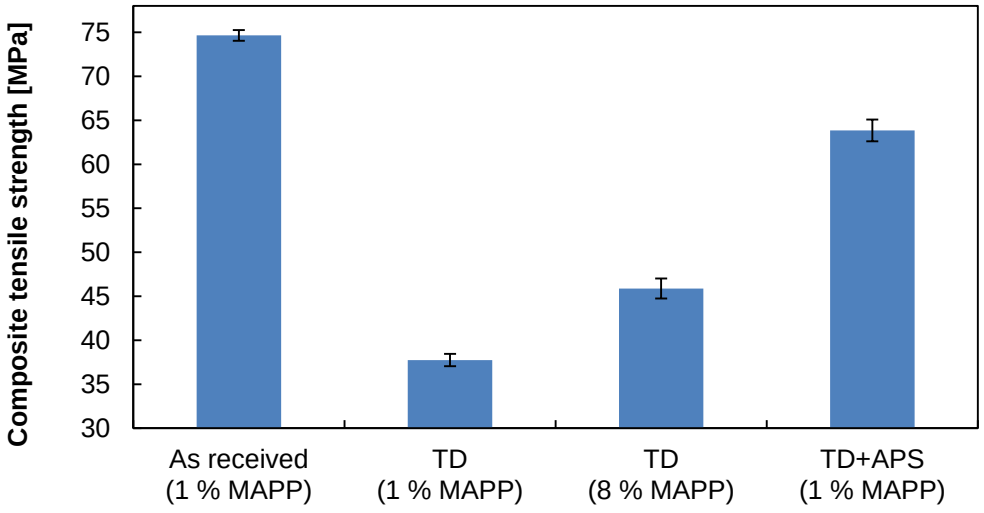

Figure 6.3. Effect of fibre regeneration and MAPP content on the tensile strength of injection moulded GF/PP composites

As already mentioned above, the post treatment of the thermally degraded fibres with APS did not lead to a large variation of the residual fibre length or fibre orientation and the fibre content was kept constant. It is therefore likely that the positive effect of the APS treatment on the composite tensile strength can be explained by changes of the IFSS or the fibre strength. It is well known that silanes like APS can enhance the IFSS of GF/PP composites [19–22]. To investigate the effect of APS on the IFSS, microbond tests and the Bowyer-Bader analysis were performed. The input parameters of the Bowyer-Bader analysis are summarised in Table 6.1. The results of the microbond tests and the Bowyer-Bader analysis are plotted in Figure 6.4.

Table 6.1. Input parameters for Bowyer-Bader analysis of injection moulded composites

Fibre volume fraction V_f	Calculated from fibre weight fraction [23] density of glass fibres 2.62 g/cm^3 [24], density of PP 0.905 g/cm^3 (manufacturer data)
Fibre modulus E_f	78.7 GPa as received fibres [8] changed after thermal conditioning according to [25] 88.9 GPa (500 °C)
Average fibre radius r_f	6.4 µm
Composite strain 1 ε_1	1/3 of strain at break
Composite strain 2 ε_1	2/3 of strain at break
Composite tensile stress 1 σ_1	Composite tensile stress at ε_1
Composite tensile stress 2 σ_2	Composite tensile stress at ε_1
Composite tensile strength σ_{cMax}	Measured (see Figure 6.3)
Fibre length distribution	Measured as described in Chapter 3
Matrix stress Z	Calculated from strain using a polynomial fitting curve [26]
Polynomial fitting curve parameter x_1	0.68 obtained from tensile tests
Polynomial fitting curve parameter x_2	-5.98 obtained from tensile tests
Polynomial fitting curve parameter x_3	19.79 obtained from tensile tests

The results of the microbond tests and the Bowyer-Bader analysis follow similar trends in Figure 6.4. The data shows that the post treatment of thermally degraded glass fibres with APS is beneficial for the IFSS of GF/PP composites which was also observed in other studies [7,10,27]. It was previously speculated that the surface of thermally degraded fibres might be dehydroxylated [6]. Thus, APS would not be able to bond well to the glass fibre surface. However, the results in Figure 6.4 disprove that speculation. The microbond test results indicate that the addition of 8 % MAPP to the PP matrix had the same effect on the IFSS as the post treatment of the thermally degraded fibres with APS. Thus, the higher tensile strength of APS treated fibre composites compared to composites based on thermally degraded fibres with 8 % MAPP was probably not caused by the IFSS.

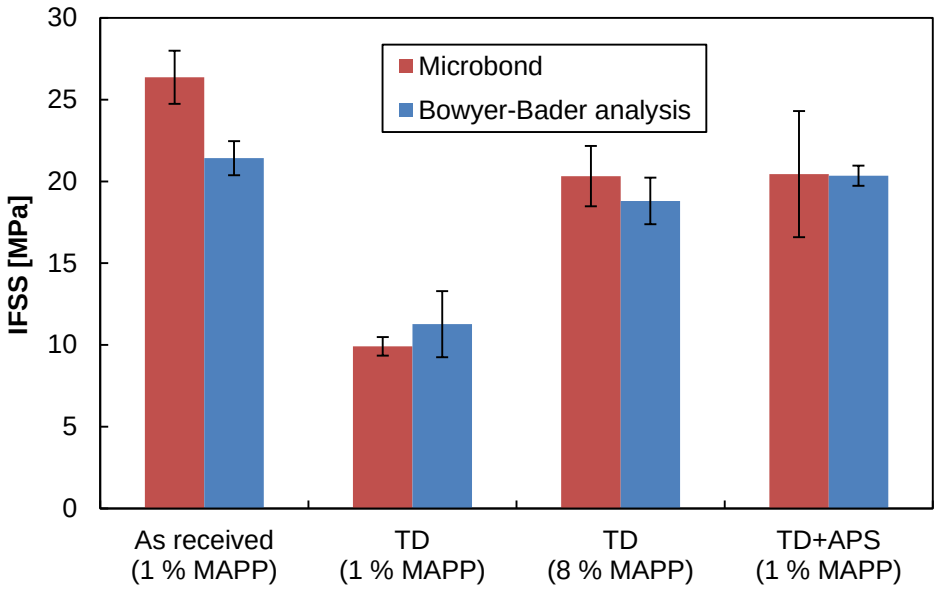

Figure 6.4. Effect of fibre regeneration and MAPP content on the IFSS

In addition to the IFSS, the Bowyer-Bader analysis was also used to calculate the stresses that the fibres experienced in the composites. Similar to Chapter 4 and Chapter 5, Figure 6.5 shows the maximum fibre stress that was reached at composite yield strain. Figure 6.6 compares the measured composite yield strain with the fibre strain that was obtained from the Bowyer-Bader analysis assuming a linear stress-strain relationship. The fibre strain and the composite strain follow the same trend which indicates an agreement between model and measurement data. The implications of the relatively large difference between the strain at break and the yield strain of composites based on thermally degraded fibre with 1 % MAPP were discussed in Chapter 5.

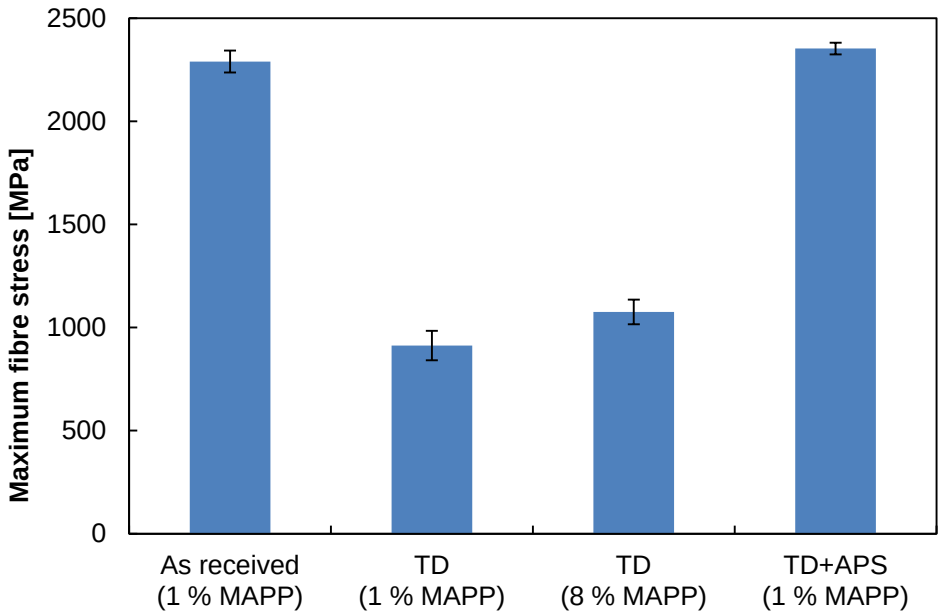

Figure 6.5. Effect of fibre regeneration and MAPP content on the maximum fibre stress in injection moulded GF/PP composites

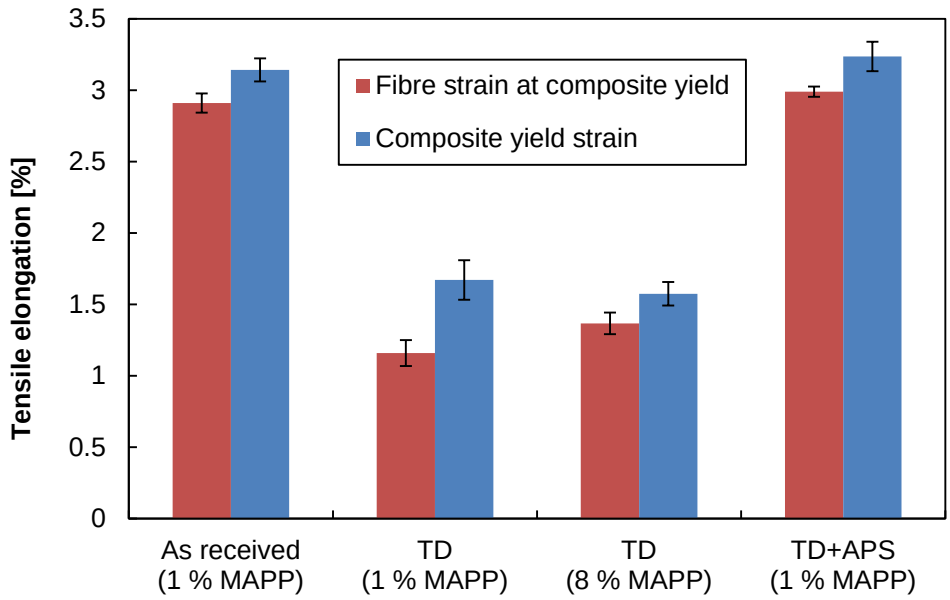

Figure 6.6. Effect of fibre regeneration and MAPP content on the fibre strain (Bowyer-Bader analysis) and the measured yield strain of injection moulded GF/PP composites

The data in Figure 6.6 suggests that the APS treated fibres were able to withstand similar stresses as the as received fibres. The APS treated fibres carried significantly more load than the thermally degraded fibres even when 8 % MAPP were added to the composites. The data in Figure 6.4 suggests that APS treated fibre composites and composites based on thermally degraded fibres with 8 %

added MAPP had a similar IFSS. It might be speculated that the increase of the maximum fibre stress and composite strength can be attributed to an improvement of the fibre strength. The present data therefore suggests that APS might regenerate the strength of chopped glass fibres. Yang et al. [7], Sáez et al. [5] and Thomason et al. [6] reported an increase of the average value of the single fibre tensile strength when thermally degraded fibres were treated with APS. However, the increase was regarded as not significant. Longer fibres might be more likely to suffer from severe flaws that cannot be 'repaired' by APS. While several researchers suggested that APS can 'repair' damaged glass fibre surfaces [1–3], Yang and Thomason [8] explained the higher strength of APS coated fibres compared to unsized fibres by the surface protection effect of APS. According to Yang and Thomason, APS prevents the formation of additional surface flaws rather than repairing existing ones. The data in Figure 6.6 might therefore at least partially be explained by the surface protection due to the APS coating. It might be speculated that the APS treated fibres were better protected from additional damage during processing than the unsized thermally degraded fibres. The present data does not allow a final conclusion regarding the effect of APS on the strength of thermally degraded glass fibres. As suggested in Chapter 7, tensile tests on chopped fibres and fibres extracted from moulded composites might help to elucidate the effect of APS on the strength of chopped fibres.

6.1.4 Composite strain at break

The data in Figure 6.7 suggests that the composite yield strain was completely recovered when the thermally degraded fibres were post treated with APS. The strain at break of the APS treated fibre composites was higher than the strain at break of the as received fibre composites. The reason for the higher strain at break of the APS treated fibre composites compared to the as received fibre composites is not clear and the exact compositions of the sizing of the as received fibres is unknown. The strain at break of GF/PP composites is governed by the fibre content [11,15,16,18,28], fibre orientation [11], residual fibre length [11,29] and the interphase/interface between fibre and matrix [26,27,30]. The fibre content and fibre orientation were similar for the as received fibre composites and the APS treated fibre composites. The IFSS and tensile strength of the as received fibre composites were higher than the IFSS and tensile strength of the APS treated fibre composites. This inverse correlation between IFSS and strain at break was also observed by other authors [3,28,30]. However, the data in Chapter 4 agrees with the data of

Thomason [26] and Bikiaris et al. [27] who observed an increase of the composite strain at break with the IFSS. The data in Chapter 4 showed that the composite strain at break increased with the IFSS between 0 % MAPP and 1 % MAPP. Thus, the APS treated fibre composites should have a lower strain at break than the as received fibre composites because of the lower IFSS. While the data in Figure 6.7 shows that there is no simple relationship between IFSS and composite strain at break it still appears likely that the higher strain at break of the APS treated fibre composites was caused by the interphase properties. All other factors were disregarded. Further work is necessary to elucidate the data in Figure 6.7.

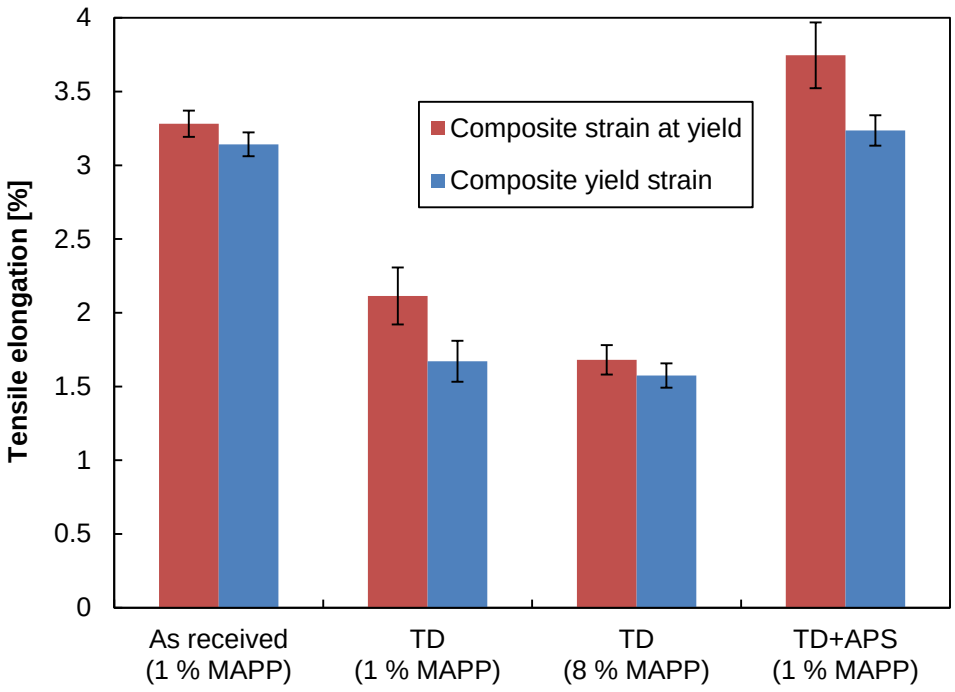

Figure 6.7. Effect of fibre regeneration and MAPP content on the strain at break and the yield strain of injection moulded GF/PP composites

6.2 Glass mat thermoplastic composites based on regenerated fibres

In this section, the effect of different fibre treatments on the performance of GMT composites is investigated. The following treatments were applied to PPG 8069 glass fibres before composite processing:

- Thermal conditioning/Thermal degradation (TD)
- Thermal degradation and resizing with APS (TD+APS)
- Thermal degradation and post treatment with sodium hydroxide (TD+NaOH)
- Thermal degradation and post treatment with sodium hydroxide and subsequent resizing with APS (TD+NaOH+APS)

A GMT process was chosen for the preparation of the composites because of the fibre length and the arrangement of the fibres. The GMT process allowed processing fibres that were long enough for single fibre tensile tests. Thus, the fibre, the matrix and the interface/interphase of the composites could be mechanically characterised. In addition, the GMT process does not require the fibres to be aligned in bundles. As already mentioned in Chapter 3, the fibre bundles disintegrated into single fibres when they were treated with sodium hydroxide (NaOH). The single fibres formed a fluffy mat that could not be fed into the extruder.

6.2.1 Single fibre tensile properties

Single fibre tensile tests were performed as described in Chapter 3 to determine the tensile properties of the glass fibres. The tensile tests were performed before the fibres were processed into composites.

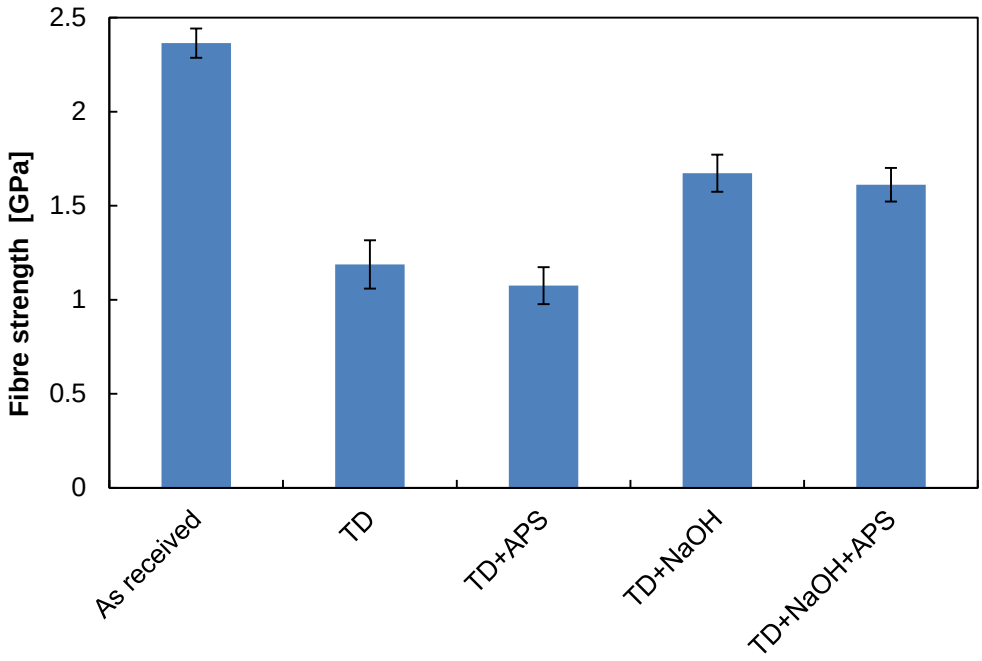

Figure 6.8. Single fibre tensile strength at 5 mm gauge length after different fibre treatments

The data in Figure 6.8 shows that the thermally degraded glass fibres had a lower tensile strength than the as received fibres. This reduction of the fibre strength was observed in several studies that were reviewed in Chapter 2 [6,7,31–37]. The true average strength of the thermally degraded fibres was probably lower than the value shown in Figure 6.8. The lowest measured value for the strength of a single fibre was 0.6 GPa. Extremely weak fibres are unlikely to survive the sample preparation process [38]. This hypothesis was supported by observations when the data in Figure 6.8 was generated. Around 35 % of the thermally degraded fibres failed before testing. In contrast, approximately 5 % of the as received fibres failed before testing. The data in Figure 6.8 suggests that the resizing of the thermally degraded fibres with APS did not lead to an improvement of the fibre strength. The data in Figure 6.8 therefore does not support the speculation of the previous section that APS might regenerate the strength of thermally degraded fibres. The treatment of the thermally degraded fibres with NaOH led to an increase of the fibre strength. The values for the strength of the NaOH treated fibres in Figure 6.8 are similar to data that was reported by Sáez [39].

The data of the fibre modulus in Figure 6.9 suggests an increase of the fibre modulus when the fibres were thermally degraded or thermally degraded and post treated. However, the error bars are overlapping. T-tests showed that only the modulus of thermally degraded fibres and TD+NaOH+APS treated fibres was significantly (p=0.05) higher than the modulus of the as received fibres. Yang and Thomason [25] observed in a more controlled experiment an increase of the fibre modulus by 13 % when the fibre were exposed to 500 °C. The relative increase of the fibre modulus in Figure 6.9 is lower which might at least partially be attributed to compliance effects. The shorter the gauge length the larger the compliance effect which leads to lower measurement values for the fibre modulus [8].

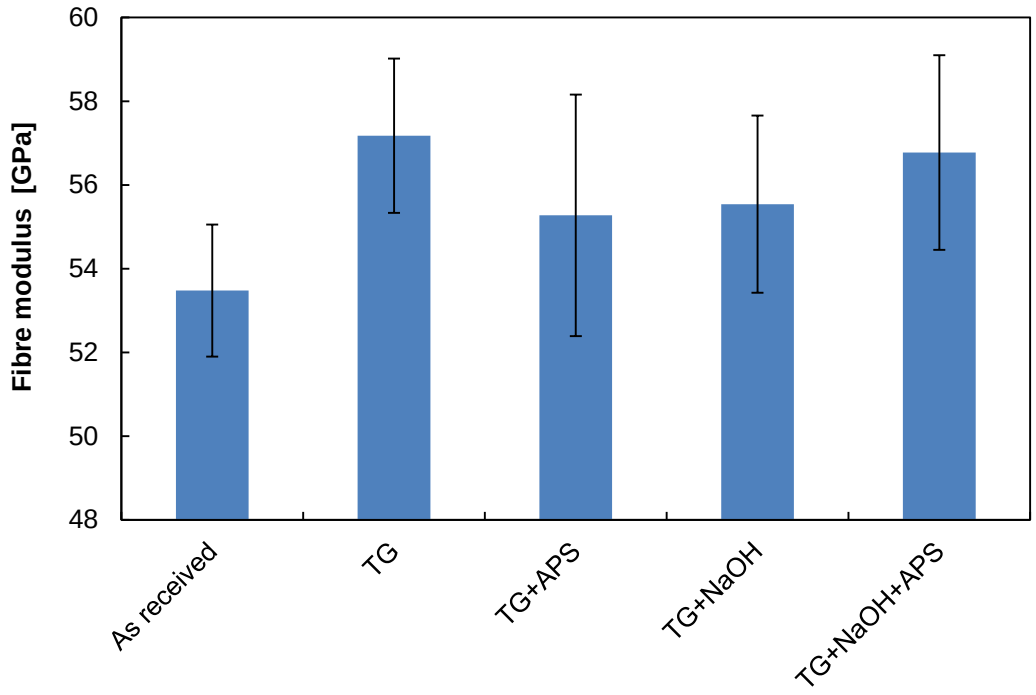

Figure 6.9. Fibre modulus at 5 mm gauge length after different fibre treatments

A detailed discussion of the mechanism how the NaOH regenerates the strength of thermally degraded fibres is out of the scope of this thesis. Yang et al. [7] explained the beneficial effect of hydrofluoric acid on the strength of thermally degraded fibres with an etching effect. The diameter of the fibres was reduced after the treatment with hydrofluoric acid. Surface flaws would either be modified or the layer with flaws would be etched away. In the present study, the average fibre diameter was measured to 10.5 ± 0.1 µm before NaOH treatment and to 10.4 ± 0.1 µm after NaOH treatment. However, such a difference is not significant considering that the diameter was determined using optical microcopy. The effect of NaOH on the

strength of thermally degraded fibres might therefore be explained with the modifications of surface flaws rather than the removal of damaged surface layers.

6.2.2 Residual fibre length after composite processing

The nominal length of the glass fibres that were processed into the GMT composites was 9 mm. Fibre length measurements as described in Chapter 3 showed that the actual length of the fibres was close to the nominal value. The arithmetic mean was measured to be 8.6 $\pm$ 0.5 mm and the weighted mean was measured to be 8.8 $\pm$ 0.5 mm. The residual fibre length of the GMT composites after different fibre treatments is plotted in Figure 6.10. The fibres were taken from the gripping region of the tensile test specimens. Figure 6.10 shows that the residual length of the fibres in the GMT composites was significantly shorter than the nominal length of the glass fibres. Part of the fibre length reduction was caused by the cutting of the tensile test specimens from the laminate. However, Figure 6.10 also suggests that the thermally degraded fibres were more susceptible to length degradation than as received fibres. The drop of the residual length of fibres in injection moulded composites in Chapter 5 was attributed to a reduction of the fibre strength and the bundle integrity/fibre arrangement. The fibre strength and arrangement of the fibres might also partially explain the drop of the residual fibre length between as received fibre composites and composites based on thermally degraded fibres in Figure 6.10. The fibres were prewashed before the thermal conditioning. During the prewash the fibre bundles already dispersed into single fibres. Thus, single fibres were fed into the sheet former when composites based on thermally degraded fibres were processed but fibre bundles were fed into the sheet former when as received fibre composites were prepared. The inner fibres of the as received fibre bundles might have been better protected than thermally degraded single fibres at the initial stage of the blending process in the sheet former. In addition to the fibre arrangement, the thermally degraded fibres might also have been affected by a reduction of the fibre strength. Thermally degraded fibres might have been more likely to break due to bending than as received fibres.

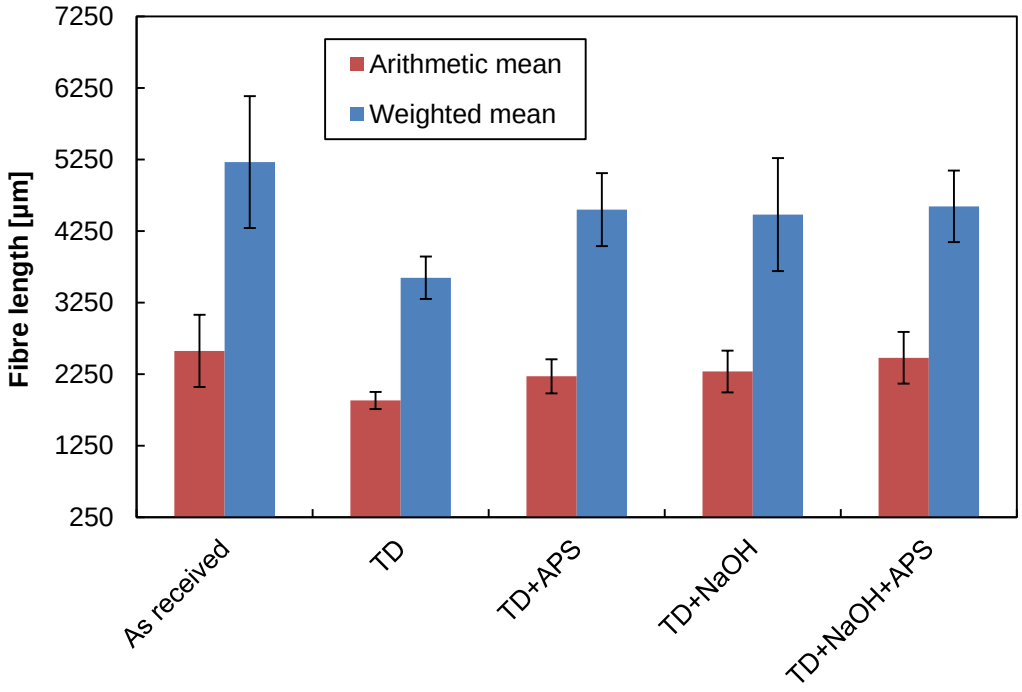

Figure 6.10. Residual fibre length of GMT composites after different fibre treatments

The data in Figure 6.10 also suggests that the post treatment of the thermally degraded fibres with APS, NaOH or a combination of both treatments correlated with an increase of the residual fibre length. The increase of the residual fibre length might partially be explained with increase of the fibre strength. Figure 6.11 suggests a correlation between the residual fibre length and the single fibre tensile strength. The residual fibre length increased with the single fibre tensile strength but the APS treated fibres did not agree with the other data. The APS treatment of the thermally degraded fibres resulted in an increase of the residual fibre length but the measured values of the single fibre tensile strength did not increase. Further work is required to investigate the reasons for the deviation of the APS treated fibres from the other data. It might be speculated that the measured single fibre strength did not represent the tensile strength of the APS treated fibres.

Single fibre tensile samples were prepared from the same batches of fibres that were processed into GF/PP composites. APS treated fibres tend to stick together when they are dried. The APS treated fibres were therefore blended with PP in the sheet former without prior drying. However, the fibres that were used for the single fibre tensile tests were dried in a plastic container before they were glued onto card frames. It was noticed during the preparation of the single fibre tensile test specimens that the dried fibres stuck to the walls of the plastic container as well as

to other fibres. Thus, the single fibres might have been damaged when they were separated from the other dried fibres and the plastic container. These difficulties were only experienced with APS treated fibres. The values for the tensile strength of APS treated fibres in Figure 6.8 might therefore be artificially low. Future work should include the tensile testing of fibres that are extracted from undried GF/PP mats.

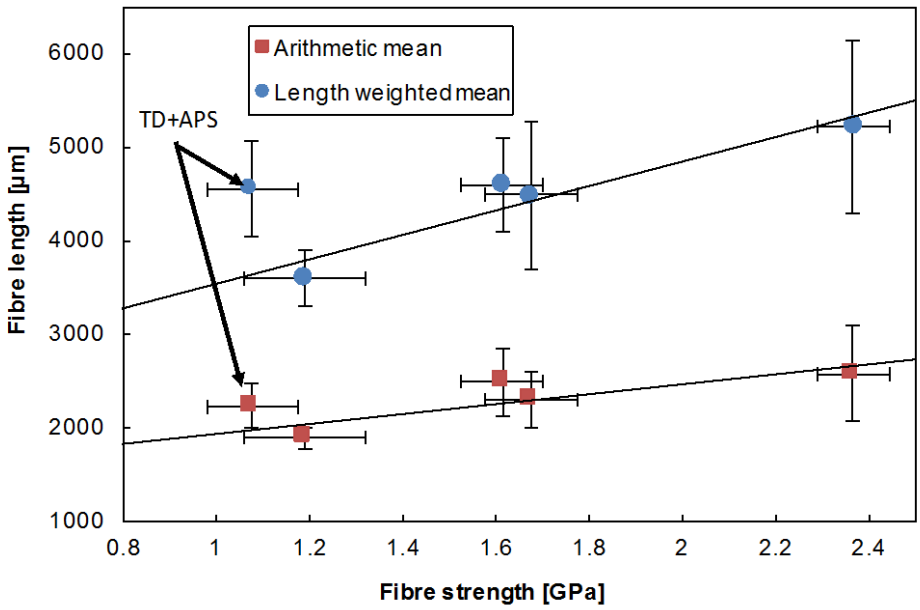

Figure 6.11. Increase of residual fibre length of GMT composites with single fibre strength

6.2.3 Composite modulus

Figure 6.12 suggests that the modulus of the GMT composites varied. T-tests showed that the variations in Figure 6.12 are not significant.

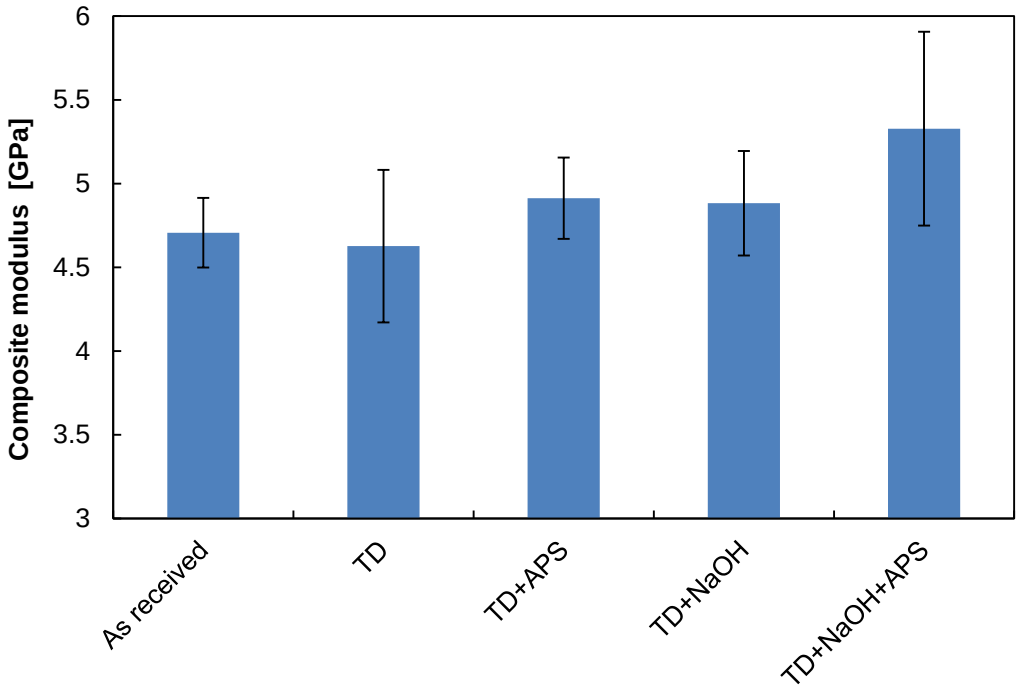

Figure 6.12. Modulus of GMT composites after different fibre treatments

It is well known that the modulus of GMT composites depends on the residual fibre length. Figure 6.10 showed that the residual length of the fibres in the GMT composites varied. However, these variations of the residual fibre length did not result in significant changes of the composite modulus. Ericson and Berglund [40] and Thomason and Vlug [12] demonstrated that the Cox model [41] can be used to predict the modulus of GMT composites. The Cox model was also used to obtain the data in Figure 6.13 which shows the predicted modulus of the GMT composites as a function of the residual fibre length. The input parameter are summarised in Table 6.2. The two graphs in Figure 6.13 show the predicted composite modulus based on two different assumptions for the fibre modulus. The modulus of the as received fibres was assumed to be 76 GPa [24]. It was assumed that the thermal conditioning of the fibres led to an increase of the fibre modulus by 13 % [25] from 76 GPa to 85.88 GPa. The orientation factor was calculated from the measured modulus of the as received fibre composites using the Cox model in reverse similar to Chapter 5. The obtained value of 0.335 is slightly lower than the theoretical value of 0.375 that was calculated by Krenchel [42]. This deviation might be explained with

out of plane misalignment of fibres or voids. The orientation factor was assumed to be constant for all composites because the processing parameters were kept constant.

Table 6.2. Input parameters for Cox model to predict modulus of GMT composites

Fibre volume fraction V_f	Calculated from fibre weight fraction [23] density of glass fibres 2.62 g/cm^3 [24], density of PP 0.905 g/cm^3 (manufacturer data)
Poison's ratio υ	Calculated using rule of mixture, Poisons ratio of glass fibre 0.2 and PP 0.4 [43]
Packing factor X_i	4 [12]
E_M	1.71 GPa (measured)
E_f	76 GPa before thermal conditioning [24] 85.88 GPa after thermal conditioning [25]
Average fibre length l	Measured arithmetic mean (Figure 6.10)
Average fibre radius r_f	Calculated from measured fibre diameter
Fibre packing factor X_i	4 [12]
Fibre orientation factor η_{oC}	0.335 (calculated from measured modulus of as received fibre composites)

The plot of the predicted composite modulus in Figure 6.13 illustrates that the effect of fibre length variations on the composite modulus was negligible when the fibres were longer than 1000 µm. In addition, the plot shows that the measured values of the composite modulus fell into the range of the values that were predicted by the Cox model.

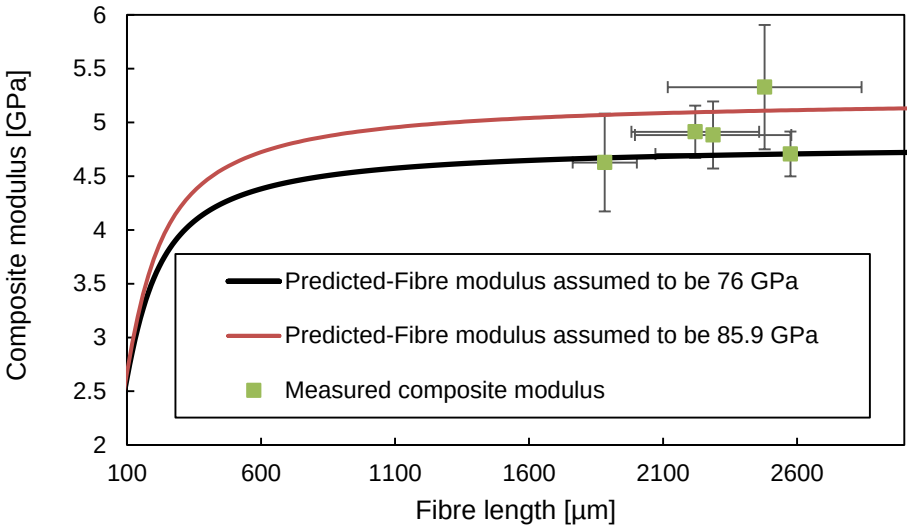

Figure 6.13. Influence of residual fibre length on the modulus of GMT composites

In addition to the fibre length, the actual fibre content of the composites was determined. The plot in Figure 6.14 shows the predicted composite modulus as a function of the fibre content. The residual fibre length was assumed to be constantly 2000 µm. All other input parameters were the same as in in Figure 6.13.

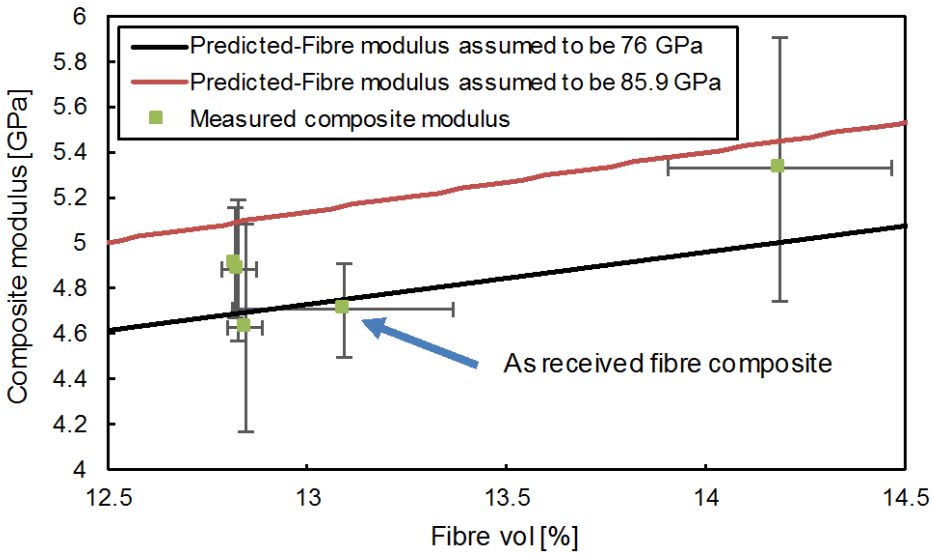

Figure 6.14. Influence of fibre content on the modulus of GMT composites

The model data in Figure 6.14 suggests that the composite modulus might have been affected by variations of the fibre content. However, measurement errors might have masked the the effect of the fibre content variations on the measured composite modulus.

6.2.4 Composite tensile strength

Similar to the injection moulded GF/PP composites, Figure 6.15 shows that tensile strength of the GMT composites decreased when the fibres were thermally degraded. The post treatment of the thermally degraded fibres with APS, NaOH and the combination of both treatments resulted in a significant increase of the composite tensile strength.

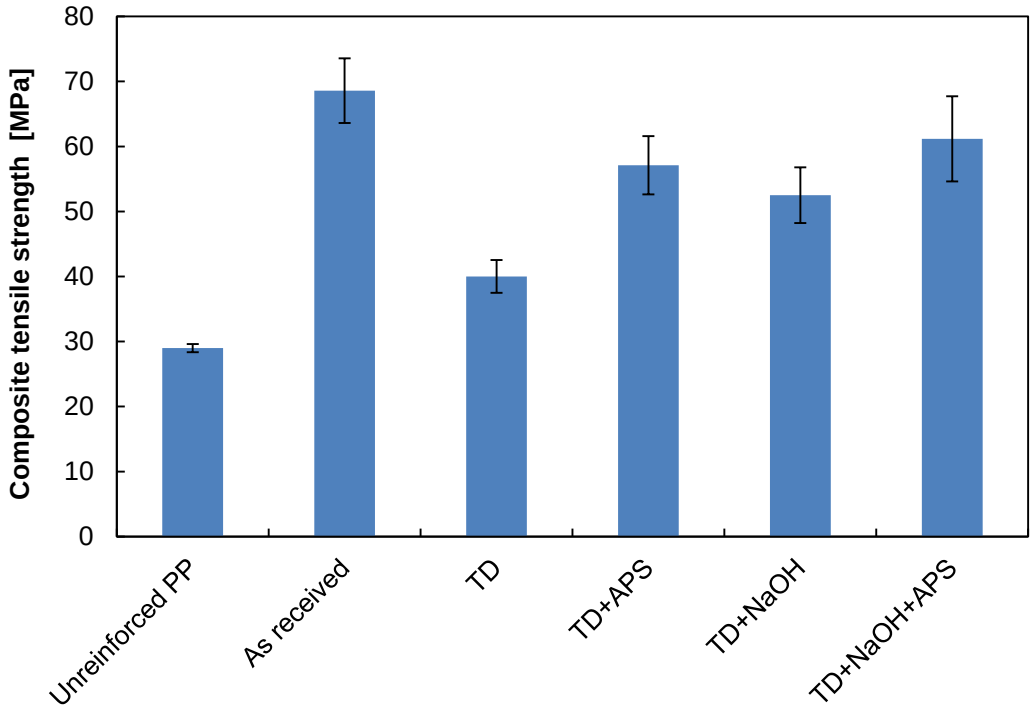

Figure 6.15. Tensile strength of GMT composites after different fibre treatments

Similar to Chapter 5 and the previous section, microbond tests and the Bowyer-Bader analysis were performed to further investigate the effects of the fibre treatments on the composite performance. The input parameters of the Bowyer-Bader analysis are summarised in Table 6.3. In the previous section, Chapter 5 and Chapter 4 the composite strains ε_1 and ε_2 were chosen to be 1/3 and 2/3 of the composite strain at break. Thomason [26,44] also chose ε_1 and ε_2 as a fraction of the composite strain at break. The yield strain of the injection moulded composites in Chapter 4 and Chapter 5 was almost equal to the strain at break. However, the strain at break of the GMT composites was significantly larger than the yield strain. Thus, when some of the GMT composites were strained to 2/3 of their strain at break they had already passed their yield strain and maximum load. The Bowyer-Bader analysis [45] and Kelly-Tyson model [46] only describe the behaviour of

composites below their yield strain. It was therefore decided to analyse the GMT composites in the range between 1/3 and 2/3 of the composite yield strain. For the sake of brevity, the IFSS obtained from the Bowyer-Bader analysis will be called Bowyer-Bader IFSS and the maximum fibre stress obtained from the Bowyer-Bader analysis will be called Bowyer-Bader fibre stress. The apparent IFSS obtained from microbond tests will be referred as microbond IFSS.

Table 6.3. Input parameters for Bowyer-Bader analysis of GMT composites

Fibre volume fraction V_f	Calculated from fibre weight fraction [23] density of glass fibres 2.62 g/cm^3 [24], density of PP 0.905 g/cm^3 (manufacturer data)
Fibre modulus E_f	76 GPa before thermal conditioning [24] 85.88 GPa after thermal conditioning [25]
Average fibre radius r_f	5.3 µm without NaOH treatment 5.2 µm after NaOH treatment (measured)
Composite strain 1 ε_1	1/3 of yield strain
Composite strain 2 ε_1	2/3 of yield strain
Composite tensile stress 1 σ_1	Composite tensile stress at ε_1
Composite tensile stress 2 σ_2	Composite tensile stress at ε_2
Composite tensile strength σ_{cMax}	Measured (see Figure 6.15)
Fibre length distribution	Measured as described in Chapter 3
Matrix stress Z	Calculated from strain using a polynomial fitting curve [26]
Polynomial fitting curve parameter x_1	0.69 obtained from tensile tests
Polynomial fitting curve parameter x_2	-6.06 obtained from tensile tests
Polynomial fitting curve parameter x_3	19.90 obtained from tensile tests

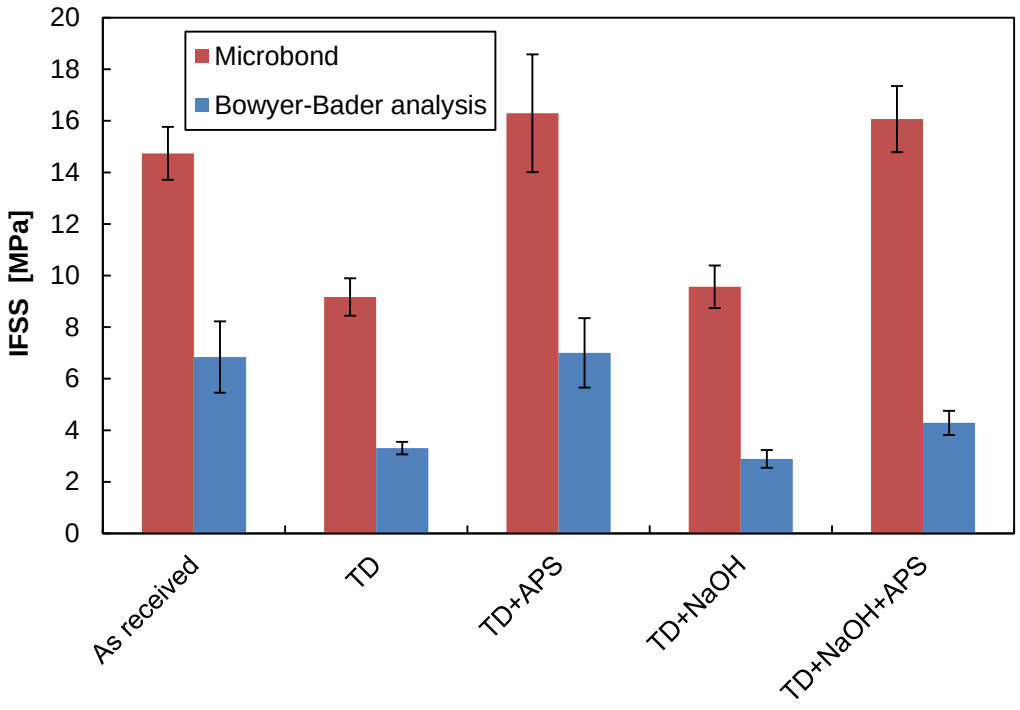

Figure 6.16. IFSS obtained from microbond tests and Bowyer-Bader analysis after different fibre treatments

Figure 6.16 compares the microbond IFSS with the Bowyer-Bader IFSS. The values provided by these two methods do not agree quantitatively but the trends are similar. The absolute differences between the microbond IFSS and the Bowyer Bader IFSS in Figure 6.16 are larger than the differences that were observed when the injection moulded composites were analysed in Chapter 4 and Chapter 5. Several authors [47–49] showed that the apparent IFSS of microbond tests and single fibre pull-out tests depends on the embedded length. The apparent IFSS decreased with the embedded fibre length which was attributed to an uneven stress distribution and an underestimation of the IFSS because of the averaging of the interfacial stress. The relatively low values of the Bowyer-Bader IFSS in Figure 6.16 compared to the microbond IFSS might be explained in a similar way. The fibres in the GMT composites were longer than than droplets of the microbond samples. Thus, the Bowyer-Bader analysis provided significantly lower values for the average IFSS than the microbond tests. This effect was not that obvious in Chapter 4 and Chapter 5 because the injection moulded composites had a relatively short residual fibre length. The effect of the embedded fibre length on the Bowyer-Bader IFSS was therefore limited. The thermal conditioning of the glass fibres led to a reduction of the IFSS. This indicates that the as received fibres were coated with a sizing that promoted the interaction with PP. Similar to the study by Yang et al. [7] on the

treatment of thermally degraded fibres with hydrogen fluoride (HF), the NaOH treatment led to an increase of the fibre strength but the surface functionality was not regenerated and the IFSS did not increase. In agreement with results in literature [7,10,27] and the data in the previous section, the results in Figure 6.16 confirm again that the surface functionality of thermally degraded fibres can be regenerated with APS. The microbond IFSS and the Bowyer Bader IFSS increased when the thermally degraded fibres were post treated with APS. Yang et al. [7] observed that the effect of the APS treatment on the IFSS was reduced when thermally degraded fibres were treated with HF before the application of APS. They explained their observations with residual nanoparticles on the fibre surface. In contrast to the HF treatment, the treatment of the fibres with NaOH did not seem to reduce the effectivity of the subsequent APS treatment. The microbond test results suggest that the combination of NaOH treatment and APS treatment improved the IFSS to the same extent as the APS only treatment. This indicates that the rinsing of the fibres in hydrochloric acid as part of the NaOH treatment was effective in washing away residues from the glass fibre surfaces. The SEM micrographs in Figure 6.17 illustrate the effect of the different treatments on the fibre surface. The fibre surfaces of the HF treated fibres is covered with particles while the surfaces of the NaOH treated fibres were relatively clean because of the rinsing in HCl.

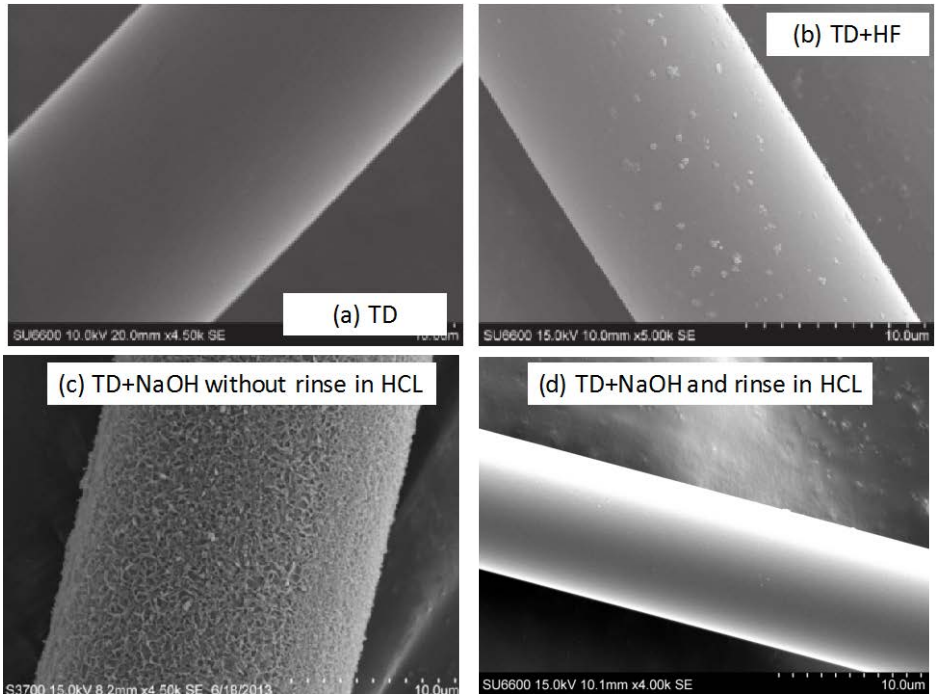

Figure 6.17. SEM fibre surfaces after different chemical treatments, micrograph (a) and (b) reproduced from [7] and (c) reproduced from [50]

A comparison between the IFSS in Figure 6.16 and the composite tensile strength in Figure 6.15 shows that the composite tensile strength correlated with the IFSS. The drop of the composite tensile strength when the fibres were thermally degraded can therefore partially be explained by a reduction of the IFSS. The APS treatment of the thermally degraded fibres led to an increase of the composite tensile strength which can at least partially be attributed to enhanced stress transfer between fibres and matrix. A further increase of the IFSS and composite tensile strength might be achievable by the addition of MAPP to the composite. Zheng et al. [9] demonstrated that the tensile strength and IFSS of GMT composites based on thermally degraded fibres can be increased with the addition of MAPP. The IFSS cannot explain the increase of the composite tensile strength when the thermally degraded fibres were treated with NaOH. Figure 6.18 shows that the treatment of the thermally degraded fibres with NaOH led to an increase of the single fibre strength and also an increase of the maximum fibre stress. Thus, the data in Figure 6.15 and Figure 6.18 shows that the tensile strength of the GMT composites was influenced by the fibre strength. The results of the Bowyer-Bader analysis suggest that the thermally degraded fibres experienced stresses in the composites that were similar to their single fibre tensile strength. Thus, it is likely that fibres failed when these composites were tensile tested. The Bowyer-Bader fibre stress increased when the thermally degraded fibres were treated with APS. In contrast to the injection moulded composites in the previous section, the Bowyer-Bader fibre stress of the GMT composites did not recover completely when the thermally degraded fibres were treated with APS. It might be speculated that the effect of the APS treatment on the fibre strength depends on the fibre length. The fibres of the GMT composites were longer than the fibres of the injection moulded composites. Longer fibres might be more likely to have flaws that cannot be modified or repaired by the APS. The maximum value of the Bowyer-Bader fibre stress was significantly higher than the single fibre tensile strength when the fibres were treated with APS. Similar to the data in Figure 6.10, the data in Figure 6.18 suggests that the actual strength of the APS treated fibres was higher than the value that was obtained from single fibre tensile tests. Possible reasons were already discussed above.

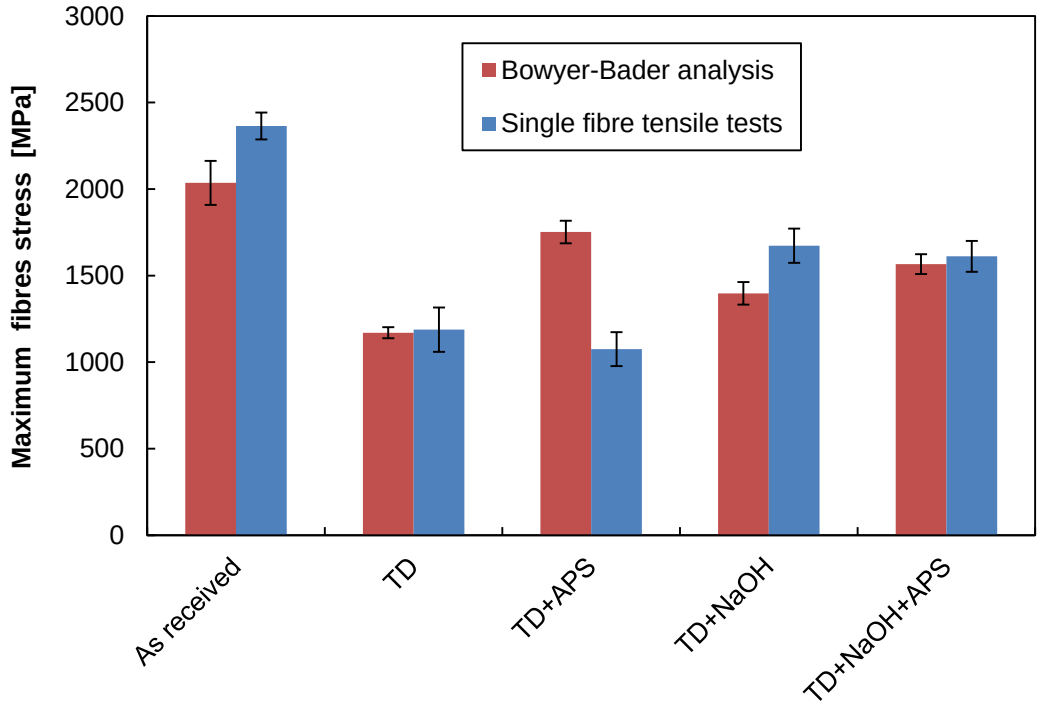

Figure 6.18. Maximum fibre stress obtained from Bowyer-Bader analysis and single fibre tensile strength after different fibre treatments

In contrast to the IFSS and the maximum fibre stress, the orientation factors of the Bowyer-Bader analysis remained almost constant (0.28 ± 0.02) which was expected because the processing conditions were kept constant.

Figure 6.19 shows the fibre strain that was calculated from the maximum fibre stress assuming a linear stress-strain relationship and a fibre modulus of 76 GPa [24] for the as received fibres and 85.88 GPa [25] for the thermally degraded and regenerated fibres. The fibre strain shows an agreement with the measured composite yield strain which indicates a match between model and experiment [26,44].

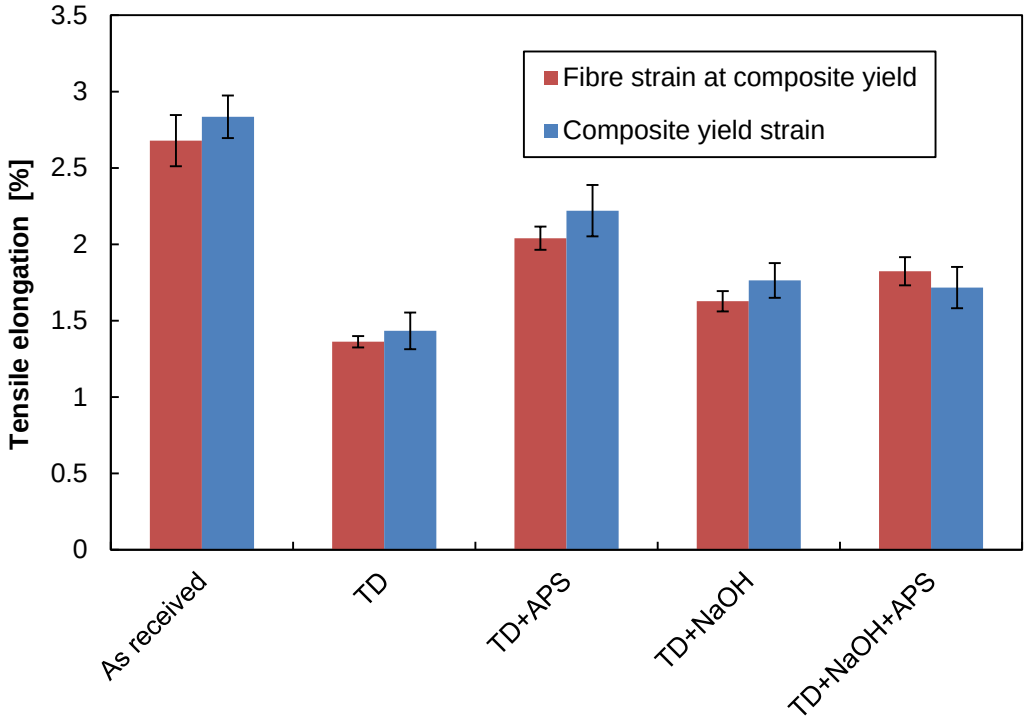

Figure 6.19. Fibre strain (Bowyer-Bader analysis) and measured GMT composite yield strain after different fibre treatments

6.2.5 Composite strain at break

The data in Figure 6.20 shows that the yield strain of the GMT composites was reduced when the fibres were thermally degraded. It is the consensus that fibre ends act as failure initiation sites in discontinuous fibre composites [16,28,29,51]. Stress concentrations at the fibre ends cause the growth of microvoids and the subsequent formation of cracks along the fibre matrix interfaces [52]. Following this hypothesis, the yield strain of the GMT composites in Figure 6.20 was reduced when the fibres were thermally degraded because of a reduction of the IFSS. The reduction of the residual fibre length did probably not cause a reduction of the yield strain. According to the Kelly-Tyson model [46] less stresses build up at the fibre ends when the residual fibre length is reduced. The reduction of the fibre strength is another factor that might have affected the yield strain. The data in Figure 6.18 suggests that the fibres in composites experienced stresses in the range of their tensile strength. Part of the fibres might therefore have been failed and caused a drop of the tensile stress. The treatment of the thermally degraded fibres with APS led to an increase of the composite yield strain. The yield strain of the injection moulded GF/PP composites in Section 6.1 exhibited a similar behaviour. It was suggested that the recovery of the strain at break can be explained with an

improvement of the IFSS due to the APS treatment of the fibres. The treatment of the thermally degraded fibres with NaOH also led to an increase of the composite yield strain. The treatment of the thermally degraded fibres only increased the fibre strength but did not regenerate the surface functionality of the fibres. Thus, the yield strain of the GMT composites was not solely controlled by the IFSS but also by the fibre strength. It might be speculated that long fibres bridged cracks in the matrix. After the NaOH treatment the thermally degraded fibres were able to withstand higher stresses when they bridged cracks in the composites.

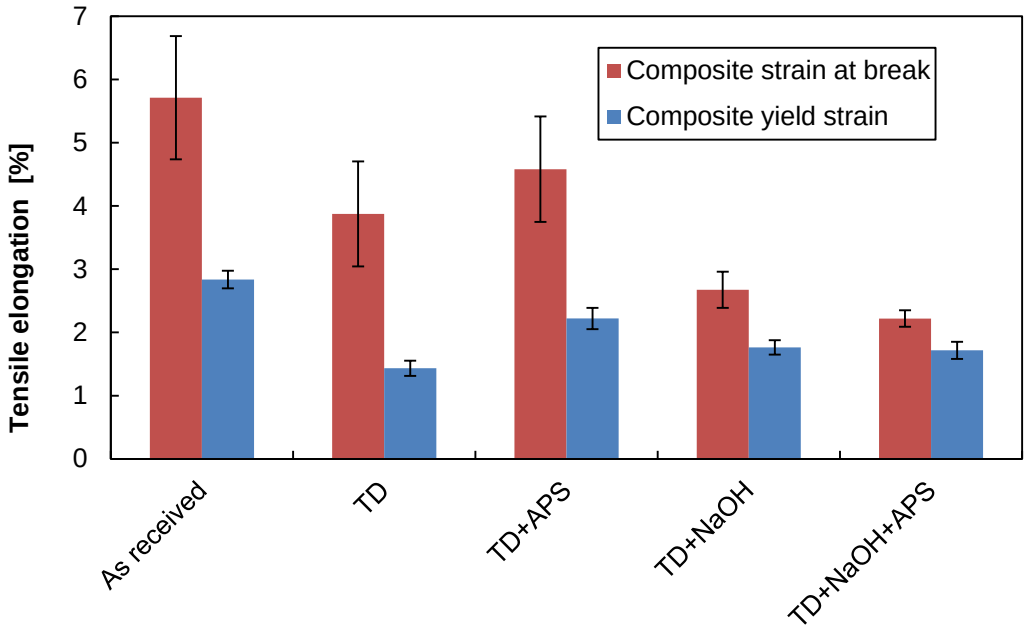

Figure 6.20. Strain at break and yield strain of GMT composites after different fibre treatments

The data in Figure 6.20 also suggests a reduction of the composite strain at break when the fibres were thermally degraded. The treatment of the thermally degraded fibres with APS led to an increase of the average value of the composite strain at break. Similar to the yield strain, the lower strain at break of the thermally degraded fibre composites might be explained by a reduction of the fibre strength and IFSS. The partial recovery of the composite strain at break when the fibres were treated with APS might be attributed to an improved IFSS. More energy might have been dissipated by fibre debond and fibre pull-out when the composite strain exceeded the yield strain. It was found in Chapter 2 that the results of studies on the strain at break of GF/PP composites are conflicting. The increase of the strain at break in Figure 6.20 is in agreement with a study by Thomason et al. [29] who observed an increase of the strain at break of similar GMT composites when the fibres were

coated with an optimised sizing. It should also be noticed that the difference between the strain at break of the APS treated fibre composites and the strain at break of the thermally degraded fibre composites is not significant at 95 % confidence.

The treatment of the thermally degraded fibres with NaOH led to a reduction of the composite strain at break. The stress strain curves in Figure 6.21 show that the as received fibre composites, thermally degraded fibre composites and the APS treated fibre composites were plastically deformed when they passed their yield strain. In contrast, the composites based on NaOH treated fibres failed almost immediately beyond the yield strain. The treatment of the NaOH treated fibres with APS did not lead to an improvement of the composite strain at break.

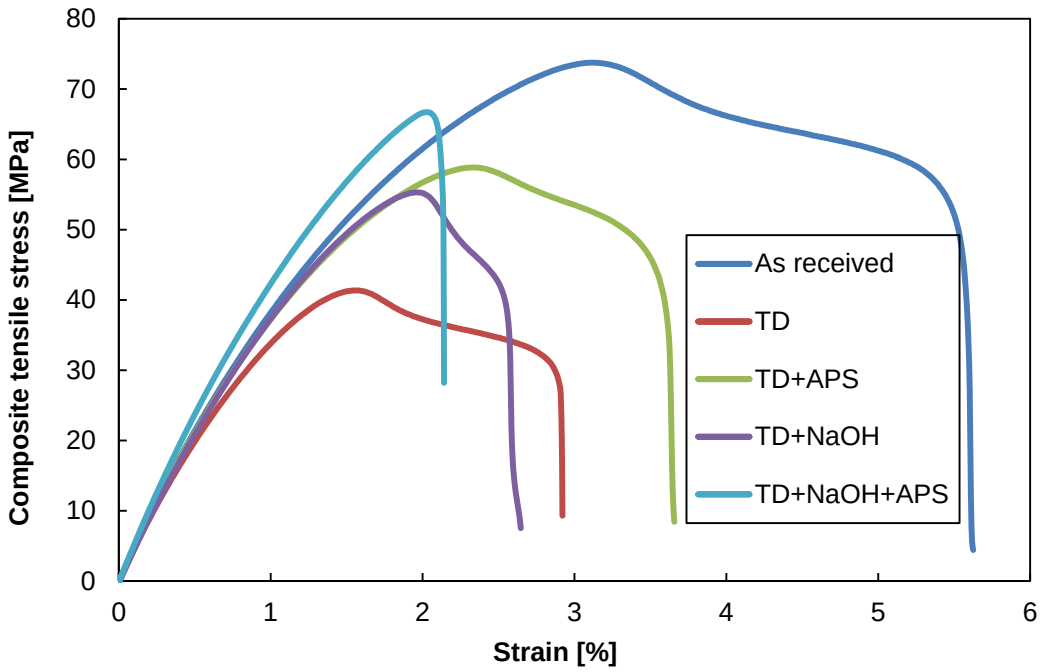

Figure 6.21. Typical stress-strain curves of GMT composites after different fibre treatments

The reason for the relatively low strain at break of the NaOH treated fibre composites is not clear. Table 6.4 shows that the NaOH+APS treated fibre composites had a slightly higher fibre content than the other composites. It is well known that the strain at break of GF/PP composites decreases with the fibre content [11,15,16,18,28] [29,40,51]. However, the NaOH treated fibres composites also exhibited a low strain at break and the measured fibre content was close to the nominal value. Thus, the fibre content is not an explanation for the low strain at

break of the NaOH treated fibre composites and the NaOH+APS treated fibre composites.

Table 6.4. Measured fibre contents of GMT composites

Fibre treatment	Fibre volume fraction [vol%]
As received	13.1 ± 0.28
TD	12.8 ± 0.04
TD+APS	12.8 ± 0.01
TD+NaOH	12.8 ± 0.04
TD+NaOH+APS	14.2 ± 0.28

The data in Figure 6.11 shows that the fibres in the NaOH treated fibre composites and the NaOH+APS treated fibre composites were longer than the fibres in the thermally degraded fibre composites. It was observed by Thomason et al. [29] and Spahr et al. [11] that the strain at break of GF/PP composites might decrease with the residual fibre length. However, the data in Figure 6.11 also shows that as received fibre composites had the largest residual fibre length of all GMT composites. In addition, the APS treated fibre composites had a similar fibre length like the NaOH treated fibre composites and did not suffer from a low strain at break. In conclusion, there is no obvious correlation between residual fibre length and the strain at break of the GMT composites. The strain at break of GF/PP composites is also affected by the fibre orientation. The strain at break decreases when more fibres are aligned in load direction [11,53]. It appears unlikely that the GMT composites in this thesis had largely different fibre orientations. The modulus of the GMT composites showed variations but these variations were explained with variations of the fibre content.

Several studies observed that the strain at break of GF/PP composites was influenced by the IFSS. An increase of the IFSS led to an increase [26,27] or decrease [3,28] of the composites strain at break. The drop of the composite strain at break in Figure 6.20 when the fibres were thermally degraded was partially explained by a reduction of the IFSS. The NaOH treated fibre composites had a similar IFSS as the thermally degraded fibre composites but the strain at break was

significantly lower. The NaOH+APS treated fibre composites had a similar IFSS as the as received fibre composites but the strain at break was also clearly lower than the strain at break of the thermally degraded fibre composites. The low strain at break of the NaOH treated fibre composites and NaOH+APS treated fibre composites can therefore not be explained by the IFSS data in Figure 6.16. Thus, the behaviour of the strain at break cannot be explained with fibre properties (fibre orientation, fibre content, fibre strength, residual fibre length) or the interface properties.

The only constituent that was not characterised is the matrix. It might be speculated that the PP matrix was degraded by residues of the NaOH treatment that were attached to the glass fibre surfaces. Salvador et al. [54] demonstrated that PP is resistant to hydrochloric acid and NaOH at room temperature. On the other hand, Baah and Baah [55] observed mass losses when PP was immersed in NaOH. The mass loss increased with time and temperature. As described in Chapter 3, the glass fibres were rinsed once in hydrochloric acid and three times in water after they were immersed in NaOH. It is therefore unlikely that any residues were left on the fibre surfaces. The microbond test results and the SEM micrographs also suggest that there were no residues of the chemical treatment left on the glass fibre surfaces. A thermal gravimetric analysis was performed to confirm that the properties of the PP matrix were not affected by the NaOH treatment of the glass fibres. Unprocessed PP fibres were analysed. NaOH treated glass fibres were placed at the bottom of the beaker of the TGA and the PP fibres were placed on top.

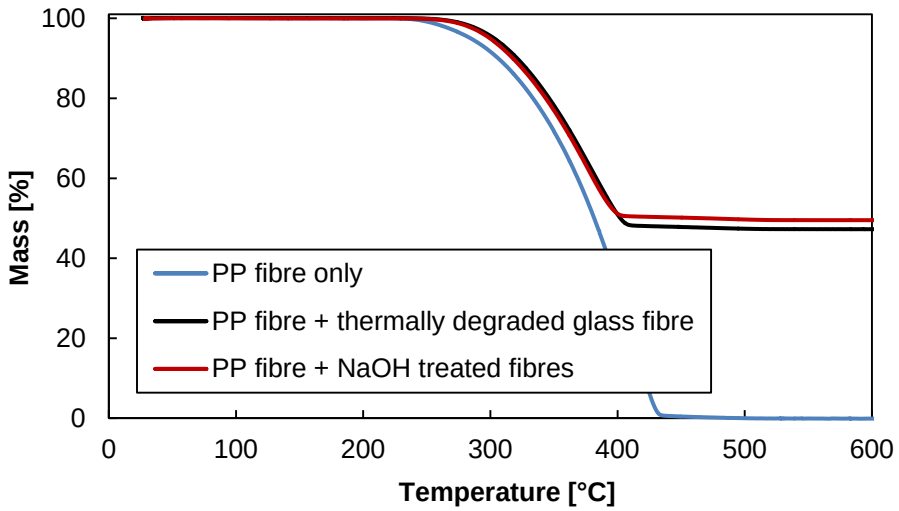

Figure 6.22. TGA (in air) of PP fibres in presence and absence of glass fibres

The mass loss curves in Figure 6.22 show that the thermal degradation of the PP was not accelerated by the presence of glass fibres. Thus, it is unlikely that the PP matrix of the GMT composites was degraded because of chemical residues on the glass fibre surfaces. Additional work is therefore required to explain the behaviour of the strain at break of the GMT composites. In situ tests of the GMT composites in an SEM might provide more information about the failure mechanisms.

6.3 Summary and Conclusion

The effect of APS and NaOH post treatments on the reinforcement potential of thermally degraded glass fibres was reported in this chapter. It was found that the post treatment of thermally degraded fibres with APS leads to an improvement of the performance of injection moulded GF/PP composites. This improvement of the composite performance was partially attributed to an increase of the IFSS. However, microbond data and a comparison with the data of Chapter 5 suggested that the effect of APS on the composite performance cannot exclusively be explained by an improvement of the IFSS. The results of the Bowyer-Bader analysis suggested that APS treated fibres and as received fibres experienced similar stress levels in the composites. It was hypothesized that the treatment of the thermally degraded fibres with APS also increased the strength of the fibres in the composites. APS might have ‘healed’ existing flaws or prevented the formation of new flaws.

When bundles of thermally degraded fibres were treated with NaOH the bundles disintegrated and the single fibres formed a fluffy mat that could not be fed into the extruder. A GMT process was set up as part of this PhD to overcome the processing problems of the NaOH treated glass fibres. Similar to the injection moulded composites, the tensile strength of the GMT composites dropped when the fibres were thermally degraded. The values of the fibre stress at composite yield strain obtained from the Bowyer-Bader analysis were similar to values of the fibre strength obtained from single fibre tensile tests. Thus, it is likely that thermally degraded fibres failed in the composites. The post treatment of the thermally degraded glass fibres with APS improved the tensile strength of the GMT composites. Microbond tests showed that the IFSS was completely recovered. The Bowyer-Bader analysis showed that the APS treatment of the thermally degraded fibres led to an increase of the fibre stress in the GMT composites but in contrast to the injection moulded composites the fibre stress did not reach the level of the as received fibres. It was

concluded that the APS treatment did not regenerate the strength of the fibres in the GMT composites to the same extent as the fibres of the injection moulded composites. One potential explanation is the residual fibre length. The injection moulded fibres had a shorter residual fibre length than the GMT composites. It was speculated that the APS treatment is more effective in the regeneration of the strength of short fibres. Longer fibres might be more likely to suffer from flaws that cannot be 'healed' by the APS treatment. Single fibre tensile tests at 5 mm gauge length did not show an increase of the fibre strength when the thermally degraded fibres were treated with APS. The absence of this effect might have been caused by problems related to sample preparation and handling. Single fibre tensile tests showed that the post treatment of thermally degraded fibres with NaOH improved the fibre strength. The increase of the fibre strength correlated with an increase of the composites tensile strength. When the NaOH and the APS treatment were combined the tensile strength of the GMT composites was almost completely recovered. Apart from composites based on NaOH treated fibres, the composite strain at break followed the trend of the composite tensile strength. The treatment of the thermally degraded fibres with NaOH led to a further reduction of the composite strain at break. Further work is required to understand the behaviour of the composite strain at break.

It can be concluded from this chapter that most of the reinforcement potential of thermally degraded fibres can be regenerated. A comparison between the data of Chapter 5 and this chapter revealed that the regeneration of thermally degraded fibres had a larger effect on the composite performance than the increase of the IFSS by the addition of coupling agent to the PP matrix. The optimum post treatment appears to depend on the residual fibre length of the composites. When the final length of the fibres is sufficiently short an APS treatment might regenerate most of their reinforcement potential. A combination of the NaOH treatment and the APS treatment might be required to regenerate the reinforcement potential of longer fibres.

6.4 References

[1] Zinck P, Pays MF, Rezakhanlou R, Gerard JF. Mechanical characterisation of glass fibres as an indirect analysis of the effect of surface treatment. J Mater Sci 1999;34:2121–33.

[2] Zinck P, Mäder E, Gerard JF. Role of silane coupling agent and polymeric film former for tailoring glass fiber sizings from tensile strength measurements. J Mater Sci 2001;36:5245–52.

[3] Mäder E, Moos E, Karger-Kocsis J. Role of film formers in glass fibre reinforced polypropylene - new insights and relation to mechanical properties. Compos Part A Appl Sci Manuf 2001;32:631–9.

[4] Feih S, Mouritz AP, Case SW. Determining the mechanism controlling glass fibre strength loss during thermal recycling of waste composites. Compos Part A Appl Sci Manuf 2015;76:255–61.

[5] Sáez Rodríguez E, Yang L, Thomason JL. IInvestigation of strength recovery of recycled heat treated glass fibres through chemical treatments. 19th Int. Conf. Compos. Mater., Montreal: 2013

[6] Thomason JL, Yang L, Meier R. The properties of glass fibres after conditioning at composite recycling temperatures. Compos Part A Appl Sci Manuf 2014;61:201–8.

[7] Yang L, Sáez Rodríguez E, Nagel U, Thomason JL. Can thermally degraded glass fibre be regenerated for closed-loop recycling of thermosetting composites? Compos Part A Appl Sci Manuf 2015;72:167–74.

[8] Yang L, Thomason JL. Effect of silane coupling agent on mechanical performance of glass fibre. J Mater Sci 2012;48:1947–54.

[9] Zheng A, Wang H, Zhu X, Masuda S. Studies on the interface of glass fiber-reinforced polypropylene composite. Compos Interfaces 2002;9:319–33.

[10] Roux C, Denault J, Champagne MF. Parameters regulating interfacial and mechanical properties of short glass fiber reinforced polypropylene. J Appl Polym Sci 2000;78:2047–60.

[11] Spahr DE, Friedrich K, Schultz JM, Bailey RS. Microstructure and fracture behaviour of short and long fibre-reinforced polypropylene composites. J Mater Sci 1990;25:4427–39.

[12] Thomason JL, Vlug MA. The influence of fibre length and concentration on the properties of glass fibres reinforced polypropylene: 1. Tensile and flexural modulus. Compos Part A Appl Sci Manuf 1996;27:477–84.

[13] Mittal RK, Gupta VB. The strength of the fibre-polymer interface in short glass fibre-reinforced polypropylene. J Mater Sci 1982;17:3179–88.

[14] Thomason JL. The influence of fibre length and concentration on the properties of glass fibre reinforced polypropylene: 5. Injection moulded long and short fibre PP. Compos Part A Appl Sci Manuf 2002;33:1641–52.

[15] Thomason JL. The influence of fibre length and concentration on the properties of glass fibre reinforced polypropylene. 6. The properties of injection moulded long fibre PP at high fibre content. Compos Part A Appl Sci Manuf 2005;36:995–1003.

[16] Fu S-Y, Lauke B, Mäder E, Yue C-Y, Hu X. Tensile properties of short-glass-fiber- and short-carbon-fiber-reinforced polypropylene composites. Compos Part A Appl Sci Manuf 2000;31:1117–25.

[17] Ota WN, Amico SC, Satyanarayana KG. Studies on the combined effect of injection temperature and fiber content on the properties of polypropylene-glass fiber composites. Compos Sci Technol 2005;65:873–81.

[18] Xavier SF, Misra A. Influence of glass fiber content on the morphology and mechanical properties in injection molded polypropylene composites. Polym Compos 1985;6:93–9.

[19] Mäder E, Freitag K-H. Interface properties and their influence on short fibre composites. Composites 1990;21:397–402.

[20] Mäder E, Jacobasch HJ, Grundke K, Gietzelt T. Influence of an optimized interphase on the properties of polypropylene/glass fibre composites. Compos Part A Appl Sci Manuf 1996;27:907–12.

[21] Mäder E, Pisanova E. Characterization and design of interphases in glass fiber reinforced polyproplyene. Polym Compos 2000;21:361–8.

[22] Nygård P, Redford K, Gustafson C-G. Interfacial strength in glass fibre-polypropylene composites: influence of chemical bonding and physical entanglement. Compos Interfaces 2002;9:365–88.

[23] Thomason JL. The interface region in glass fibre-reinforced epoxy resin composites : 1 . Sample preparation , void content and interfacial strength. Composites 1995;26:467–75.

[24] Wallenberger FT, Watson JC, Hong L. Glass Fibers. ASM Handb 2001;21:27–34.

[25] Yang L, Thomason JL. The thermal behaviour of glass fibre investigated by thermomechanical analysis. J Mater Sci 2013;48:5768–75.

[26] Thomason JL. Micromechanical parameters from macromechanical measurements on glass reinforced polypropylene. Compos Sci Technol 2002;62:1455–68.

[27] Bikiaris D, Matzinos P, Larena A, Flaris V, Panayiotou C. Use of silane agents and poly(propylene-g-maleic anhydride) copolymer as adhesion promoters in glass fiber/polypropylene composites. J Appl Polym Sci 2001;81:701–9.

[28] Hassan A, Rahman NA, Yahya R. Extrusion and injection-molding of glass fiber/MAPP/polypropylene: effect of coupling agent on DSC, DMA, and mechanical properties. J Reinf Plast Compos 2011;30:1223–32.

[29] Thomason JL, Vlug MA, Schipper G, Krikort HGLT. Influence of fibre length and concentration on the properties of glass fibre-reinforced polypropylene Part 3 Strength and strain at failure. Compos Part A Appl Sci Manuf 1996;27A:1075–84.

[30] Fu SY, Lauke B, Zhang YH, Mai Y-W. On the post-mortem fracture surface morphology of short fiber reinforced thermoplastics. Compos Part A Appl Sci Manuf 2005;36:987–94.

[31] Akesson D, Foltynowicz Z, Christeen J, Skrifvars M. Microwave pyrolysis as a method of recycling glass fibre from used blades of wind turbines. J Reinf Plast Compos 2012;31:1136–42.

[32] Kennerley JR, Fenwick NJ, Pickering SJ, Rudd CD. The properties of glass fibers recycled from the thermal processing of scrap thermoset composites. J Vinyl Addit Technol 1997;3:58–63.

[33] Kennerley JR, Kelly RM, Fenwick NJ, Pickering SJ, Rudd CD. The characterisation and reuse of glass fibres recycled from scrap composites by the action of a fluidised bed process. Compos Part A Appl Sci Manuf 1998;29:839–45.

[34] Feih S, Boiocchi E, Mathys G, Mathys Z, Gibson AG, Mouritz AP. Mechanical properties of thermally-treated and recycled glass fibres. Compos Part B Eng 2011;42:350–8.

[35] Jenkins PG, Yang L, Liggat J., Thomason JL. Investigation of the strength loss of glass fibre after thermal conditioning. J Mater Sci 2014;50:1050–7.

[36] Thomason JL, Kao CC, Ure J, Yang L. The strength of glass fibre reinforcement after exposure to elevated composite processing temperatures. J Mater Sci 2013;49:153–62.

[37] Lund MD, Yue Y. Impact of drawing stress on the tensile strength of oxide glass fibers. J Am Ceram Soc 2010;93:3236–43.

[38] Thomason JL. On the application of Weibull analysis to experimentally determined single fibre strength distributions. Compos Sci Technol 2013;77:74–80.

[39] Sáez Rodríguez E. Regenerating the strength of thermally recycled glass fibres using chemical treatments. PhD thesis. University of Strathclyde, 2016.

[40] Ericson M, Berglund L. Deformation and fracture of glass-mat- reinforced polypropylene. Compos Sci Technol 1992;43:269–81.

[41] Cox HL. The elasticity and strength of paper and other fibrous materials. Br J Appl Phys 2002;3:72–9.

[42] Krenchel H. Theoretical investigations of the elasticity and strength of fibre-cement. Fibre Reinf., Alademisk forlag; 1964, p. 11–38.

[43] Lee N-J, Jang J. The effect of fibre-content gradient on the mechanical properties of glass-fibre-mat/polypropylene composite. Compos Sci Technol 2000;60:209–17.

[44] Thomason JL. Interfacial strength in thermoplastic composites - at last an industry friendly measurement method? Compos Part A Appl Sci Manuf 2002;33:1283–8.

[45] Bowyer WH, Bader MG. On the re-inforcement of thermoplastics by imperfectly aligned discontinuous fibres. J Mater Sci 1972;7:1315–21.

[46] Kelly A, Tyson WR. Tensile properties of fibre-reinforced metals: Copper/tungsten and copper/molybdenum. J Mech Phys Solids 1965;13:329–50.

[47] Zhandarov S, Mäder E. Characterization of fiber/matrix interface strength: applicability of different tests, approaches and parameters. Compos Sci Technol 2005;65:149–60.

[48] Zhandarov S, Mader E, Yurkevich OR. Indirect estimation of fiber/polymer bond strength and interfacial friction from maximum load values recorded in the microbond and pull-out tests. Part 1: local bond strength. J Adhes Sci Technol 2002;16:1171–200.

[49] Gorbatkina YA. Correlation between the strength of fiber-reinforced plastics and the adhesive strength of fiber—Matrix joints. Mech Compos Mater 2000;36:169–76.

[50] Thomason JL, Nagel U, Sáez Rodríguez E, Yang L. Regenerating the strength of thermally recycled glass fibres using hot sodium hydroxide. Compos Part A Appl Sci Manuf 2016;87:220–7.

[51] Lee N-J, Jang J. The effect of fibre content on the mechanical properties of glass fibre mat/polypropylene composites. Compos Part A Appl Sci Manuf 1999;30:815–22.

[52] Sato N, Kurauchi T, Sato S, Kamigaito O. Microfailure behaviour of randomly dispersed short fibre reinforced thermoplastic composites obtained by direct SEM observation. J Mater Sci 1991;26:3891–8.

[53] Ericson ML, Berglund LA. Processing and mechanical properties of orientated preformed glass-mat-reinforced thermoplastics. Compos Sci Technol 1993;49:121–30.

[54] Salvador MD, Amigó V, Vidal MJ, Ribes A, Contat L. Evaluation of chemical degradation of commercial polypropylene. J Mater Process Technol 2003;143-144:693–7.

[55] Baah C a., Baah JI. Polypropylene degradation in NaOH environments. Mater Des 2002;23:341–3.

7. Conclusions and future work

This chapter is divided into two sections. The first section provides an overview of the conclusions that were drawn in this thesis. The second section suggests future research that can be performed based on the results and conclusions of this thesis.

7.1 Conclusions

The mechanical performance of composites based on thermally recycled glass fibres is usually inferior to composites based on as received glass fibres. This drop of the composite performance can be explained by a degradation of the fibre strength and fibre sizing when the glass fibres are exposed to elevated temperatures in the thermal recycling process. In this thesis the hypothesis was probed that the regeneration of the fibre strength and fibre surface functionality by the application of post treatments leads to an improvement of the composite performance. The main objective was to develop a composite based on thermally recycled fibres that can compete with composites based on new glass fibres. To achieve the main objective it was necessary to develop an understanding of the structure performance relationship of the composites and to study the effect of the glass fibre degradation on composite performance.

7.1.1 Structure performance relationship of glass fibre polypropylene composites

It was found in the literature review in Chapter 2 that the methods to characterise the microstructure of GF/PP composites are developed and the structure performance relationship of GF/PP composites is well researched. Only few studies reported the tensile properties of glass fibre Polypropylene (GF/PP) composites as a function of the fibre content and MAPP content. The experimental data in Chapter 4 showed that tensile strength of injection moulded GF/PP composites increases with the fibre content and MAPP content. The data also supports the hypothesis [1,2] that the optimum MAPP content depends on the fibre content. In addition, it was found that high MAPP contents can be detrimental to the composite tensile strength. It was concluded that high MAPP contents might reduce the degree of fibre alignment and embrittle the composites. Further work is suggested in Section 7.2.1 to confirm the effect of the MAPP content on the fibre orientation. The comparison of microbond data and data obtained from the Bowyer-Bader analysis confirmed that both methods can detect differences of the interfacial shear strength (IFSS). It was

also revealed that the results of the Bowyer-Bader analysis might be affected by other factor than the IFSS. For example, the Bowyer-Bader analysis suggested a reduction of the IFSS at high MAPP contents which correlated with a reduction of the composite tensile strength. Microbond tests did not show a reduction of the IFSS at high MAPP contents. Further analysis showed that the composite tensile strength and the results of the Bowyer-Bader analysis were affected by different mechanisms like the fibre orientation and the reduction of energy dissipated by fibre debond/pull-out. It was therefore concluded that the Bowyer-Bader analysis is a useful screening tool but cannot replace micromechanical tests like microbond tests.

7.1.2 Polypropylene composites based on thermally degraded glass fibres

The experimental data in Chapter 5 showed that the thermal degradation of glass fibres affects the performance of injection moulded GF/PP composites. The reduction of the composite tensile strength was dependent on the temperature that the fibres were exposed to before composite processing. The exposure of glass fibres to temperatures of around 250 °C in air caused a sharp drop of the composite tensile strength which was caused mainly by a reduction of the IFSS. Higher temperatures caused a further drop of the composite tensile strength which could be at least partially attributed to a drop of the fibre strength. The addition of MAPP to the composites led to an increase of the composite tensile strength. The increase of the composite tensile strength correlated with an increase of the IFSS obtained from microbond tests. The IFSS almost reached the value of the as received fibre composites. However, the sizing of the fibres was degraded. Thus the increase of the IFSS with the MAPP content cannot be explained by acid basic interactions as proposed by Mäder et al. [3,4]. Despite the recovery of the IFSS, the tensile strength of composites based on thermally degraded fibres was clearly lower than the tensile strength of composites based on as received fibres which indicates a low fibre strength. Similar to Chapter 4 it was observed that at high MAPP contents the composite tensile strength dropped while the IFSS increased and levelled off. It was concluded from the data in Chapter 5 that thermally recycled fibres need a post treatment to act as an effective reinforcement in injection moulded GF/PP composites. The post treatment needs to regenerate the fibre strength and the compatibility between fibre and matrix. The optimization of the IFSS by the addition of MAPP to the composites leads to only a partial recovery of the composite tensile strength and might also economically not viable because MAPP is the most expensive component of GF/PP composites.

7.1.3 Polypropylene composites based on regenerated fibres

The reinforcement potential of thermally degraded fibres was increased by a post treatment with AminoPropyltriethoxySilane (APS) and sodium hydroxide (NaOH). Approximately 70 % of the tensile strength of the injection moulded composites was recovered when the thermally degraded fibres were treated with APS. The effect of the APS treatment on the tensile strength of the injection moulded composites could not solely be explained by the effect of APS on the IFSS. It was concluded that the strength of the thermally degraded fibres in the composites was increased by the APS treatment. NaOH treated fibres could not be processed via extrusion compounding and injection moulding. The NaOH treated fibres formed a fluffy mat that could not be fed into the extruder. A glass mat thermoplastic (GMT) process was set up to process glass fibres that were treated with NaOH. The NaOH treatment of the thermally degraded fibres led to a partial recovery of the GMT tensile strength. The effect of the NaOH treatment on the composite tensile strength was correlated with an increase of the single fibre tensile strength. The post treatment of thermally degraded fibres with APS also led to an increase of the GMT composite tensile strength. Compared to the injection moulded composites, a lower percentage of the GMT composite tensile strength was recovered when the thermally degraded fibres were treated with APS. It was concluded that the APS post treatment might be more suitable for short fibres in injection moulded composites while a combination of NaOH and APS treatment is required for longer fibres that are processed into GMT composites.

Thus, the data of this thesis shows that the regeneration of thermally recycled glass fibres can result in an improvement of the composite mechanical performance. The optimum treatment of the thermally recycled fibres might depend on the final fibre length in the composite. No hydrogen fluoride was required to regenerate the glass fibres and common processing routes were used to process the composites. The results of this thesis are therefore a step forward to the development of a drop-in product based on recycled glass fibres.

7.2 Future work

7.2.1 Structure performance relationship of glass fibre polypropylene composites

Further work is required to confirm that the addition of MAPP to the PP matrix affected the orientation of the fibres in the composites. One common method to assess the orientation of glass fibres in thermoplastic composites is the microscopy of polished cross sections. The cross-section of fibres appears to be an ellipse when they are not aligned perpendicular to the flow direction. The measurement of the minor axis and major axis of the ellipses allows to quantify the fibre alignment [5–8]. One problem of the method described above is that it becomes imprecise when fibres are aligned almost perpendicular to the sample cross-section. Mlekusch [9] demonstrated that this effect can be minimised by the analysis of cross-sections that are inclined to the main fibre orientation. Another weakness of the analysis of polished cross-sections is the orientation duality. Polished cross-sections do not provide information about the sign of the angle between fibre axis and sample cross-section. Two fibres appear to be identical even when their alignment differs by 180° from each other. Zak et al. [10] developed a method that involves the analysis of two parallel consecutive cross-sections and allows to determine the sign of the angle between fibre axis and sample cross-section. Apart from the microscopy of polished cross-sections, X-ray radiography [11], confocal laser scanning microscopy [12] and computer tomography [13] can also be used to characterise the orientation of glass fibres in thermoplastics. Considering the high investment costs of X-ray radiography, laser scanning microscopy and computer tomography, the microscopy of polished cross-sections appears to be the most suitable method to analyse the materials of this thesis.

7.2.2 Polypropylene composites based on thermally degraded glass fibres

The fact that PP compatible sizings degrade in the range of PP composite processing temperatures when they are exposed to air deserves further investigation. During composite processing the fibres are mostly covered with the PP matrix. However, it cannot be excluded that the fibres are exposed to air and high temperatures in the feeding zone or compression of the extruder before they are completely compounded with PP. Air might also be trapped in extruded composite and form voids at the fibre ends [14]. Natural fibres like cellulose fibres were observed to suffer from thermo-oxidative degradation during extrusion

compounding with thermoplastics. The products of the oxidation led to colour changes of the composites [15]. The thermal degradation of cellulose fibres was also related to results of Fourier transform infrared spectroscopy analysis [16]. However, there are no comparable studies on the degradation of the glass fibre sizings during processing. The PP compatible sizing was observed to change its colour from white to brown when it was thermally degraded. Thus, it might be speculated that the extrusion compounding of the GF/PP composites at different temperatures might lead to colour changes caused by the degraded fibre sizing. Unfortunately, higher processing temperatures would also lead to a degradation and colour changes of the PP matrix. Another option to observe colour changes of the glass fibres would be to replace the PP with an amorphous thermoplastic like Poly(methyl methacrylate) or Polycarbonate that would be transparent and allow to detect colour changes of the glass fibres. If the PP compatible sizings are actually degraded during the processing of PP composites it might be worth developing more heat resistant sizings. Sizings with a better heat resistance might lead to an increase of the composite performance and improve the recyclability of GF/PP composites by reprocessing. Further work is also required to understand the effect of MAPP on the IFSS between unsized glass fibres and PP. Mäder et al. [4] already performed wetting experiments on glass fibres and molten PP. Unfortunately they did not present data on unsized fibres and MAPP. Such an experiment would help to investigate how maleic anhydride groups affect the wetting of unsized fibres and if there is a correlation with the IFSS.

7.2.3 Polypropylene composites based on regenerated fibres

Over the course of this thesis it was not possible to process NaOH treated fibres into injection moulded composites because of the fibre arrangement. The regenerated fibres formed a fluffy mat that could not be fed into the extruder. Glass fibres have the tendency to align themselves into bundles when they are tumbled in a humid environment. A tumbling process and the subsequent application of sizing as described in several patents [17,18] would allow to process NaOH regenerated fibres via extrusion compounding and injection moulding.

Further work is also required to understand the failure behaviour of the GMT composites. In this thesis, the composite strain at break usually followed the trend of the composite tensile strength. However, the GMT composites failed in a brittle manner when the glass fibres were regenerated with NaOH. Tensile tests in an SEM

similar to the work of Sato et al. [19] would help to investigate the failure behaviour of the GMT composites.

It was suggested that APS increases the strength of thermally degraded fibres in composites. A gauge length study on the tensile strength of thermally degraded glass fibres would help to asses if the effect of APS on the fibre strength depends on the fibre length. The extraction and testing of fibres from processed composites would allow to study how APS protects fibres during processing from strength loss. Boiling xylene could be used to dissolve the PP matrix of the composites [20] without using high temperatures that would be required to ash the matrix. A method developed by Thomason and Kalinka [21] could be used to test fibres shorter than 1 mm.

The data of this thesis is based on the assumption that the conditions of thermal recycling processes can be masked by a thermal conditioning of the glass fibres in a furnace before composite processing. It was shown that the properties of thermally recycled and thermally conditioned fibres are similar. However, thermal recycling processes like the fluidized bed process might lead to additional fibre degradation because of mechanical interaction between glass fibres. Future work should therefore also include the regeneration of thermally recycled fibres and the preparation of composites based on these fibres.

The principle goal of this thesis was to develop composites based on thermally recycled glass fibres that can compete with composites based on new or as received fibres. That goal has been achieved in terms of mechanical properties but the thermal recycling and regeneration of the fibres need to be cost effective. The recycling and regeneration of glass fibres should also consume less energy than the production of new glass fibres. The energy balance and costs are reviewed in the appendix but more experimental work is required for a comprehensive technology assessment. Future work needs to focus on the question of the optimum ratio between the volume of the sodium hydroxide solution and the volume/surface area of the glass fibres. The reusability of the sodium hydroxide solution needs to be investigated as well. Both aspects would determine the amount of sodium hydroxide that is consumed for the glass fibre regeneration. The amount of consumed sodium hydroxide would affect the financial viability and energy balance of a glass fibre recycling and regeneration plant.

7.3 References

[1] Bowland C. A formulation study of long fiber thermoplastic polypropylene (Part 2): The effects of coupling agent type and properties. Automot. Compos. Conf. Expo., 2009.

[2] Thomason JL. The influence of fibre length and concentration on the properties of glass fibre reinforced polypropylene: 7. Interface strength and fibre strain in injection moulded long fibre PP at high fibre content. Compos Part A Appl Sci Manuf 2007;38:210–6.

[3] Mäder E, Pisanova E. Characterization and design of interphases in glass fiber reinforced polyproplyene. Polym Compos 2000;21:361–8.

[4] Mäder E, Jacobasch HJ, Grundke K, Gietzelt T. Influence of an optimized interphase on the properties of polypropylene/glass fibre composites. Compos Part A Appl Sci Manuf 1996;27:907–12.

[5] Thomason JL. Micromechanical parameters from macromechanical measurements on glass reinforced polypropylene. Compos Sci Technol 2002;62:1455–68.

[6] Spahr DE, Friedrich K, Schultz JM, Bailey RS. Microstructure and fracture behaviour of short and long fibre-reinforced polypropylene composites. J Mater Sci 1990;25:4427–39.

[7] Haddout A, Villoutreix G. An experimental study of fibre orientation in injection moulded short glass fibre-reinforced polypropylene/polyarylamide composites. Composites 1994;25:147–53.

[8] Mlekusch B, Lehner EA, Geymayer W. Fibre orientation in short-fbre-reinforced thermoplastics I . Contrast enhancement for image analysis. Compos Sci Technol 1999;59:543–5.

[9] Mlekusch B. Fibre orientation in short- fibre-reinforced thermoplastics II . Quantitative measurements by image analysis. Compos Sci Technol 1999;59:547–60.

[10] Zak G, Park CB, Benhabib B. Estimation of three-dimensional fibre-orientation distribution in short-fibre composites by a two-section method. J Compos Mater 2001;35:316–39.

[11] Bright PF, Crowson RJ, Folkes MJ. A study of the effect of injection speed on fibre orientation in simple mouldings of short glass fibre-filled polypropylene. J Mater Sci 1978;13:2497–506.

[12] Eberhardt C, Clarke A. Fibre-orientation measurements in short-glass-fibre composites. Part I: automated, high-angular-resolution measurement by confocal microscopy. Compos Sci Technol 2001;61:1389–400.

[13] Bernasconi A, Cosmi F, Hine PJ. Analysis of fibre orientation distribution in short fibre reinforced polymers: A comparison between optical and tomographic methods. Compos Sci Technol 2012;72:2002–8.

[14] Vaxman A, Narkis M, Siegmann A, Kenig S. Void formation in short-fiber thermoplastic composites. Polym Compos 1989;10:449–53.

[15] Le Baillif M, Oksman K. The effect of processing on fiber dispersion, fiber length, and thermal degradation of bleached sulfite cellulose fiber polypropylene composites. J Thermoplast Compos Mater 2009;22:115–33.

[16] Sapieha S, Pupo JF, Schreiber HP. Thermal degradation of cellulose-containing composites during processing. J Appl Polym Sci 1989;37:233–40.

[17] Hill HG, Adzima LJ. Reinforcing fiber pellets. 5578535, 1996.

[18] Strait MA, Hill HG, Schweizer RA, Seng S. System for preparing glass fibre pellets. 5868982, 1999.

[19] Sato N, Kurauchi T, Sato S, Kamigaito O. Microfailure behaviour of randomly dispersed short fibre reinforced thermoplastic composites obtained by direct SEM observation. J Mater Sci 1991;26:3891–8.

[20] Lee N-J, Jang J. The effect of fibre-content gradient on the mechanical properties of glass-fibre-mat/polypropylene composite. Compos Sci Technol 2000;60:209–17.

[21] Thomason JL, Kalinka G. Technique for the measurement of reinforcement fibre tensile strength at sub-millimetre gauge lengths. Compos Part A Appl Sci Manuf 2001;32:85–90.

A. Appendix

In the following sections the technology of thermal glass fibre recycling and fibre regeneration is assessed. This technology assessment reviews and extends the work of Pickering et al. [1] who assessed the economic viability of a fluidised bed process to thermally recycle glass fibre composites.

Economics of fluidised bed process and fibre regeneration

Pickering et al. [1] modelled the economics of a fluidised bed pilot plant to thermally recycle glass fibre reinforced polymer (GFRP) waste and concluded that the break even point would be reached at a throughput of 9000 t/year. They assumed that the recycled glass fibres can be sold for 80 % of the price of new glass fibres which is equivalent to 700 $/t. This assumption is questionable because of the low reinforcement potential of recycled fibres. The strength of composites based on thermally degraded fibres is lower than the strength of composites based on new fibres. For example, Roux et al. [2] did not observe any increase of the composite tensile strength when thermally degraded glass fibres were added to PP (without added maleic anhydride). The results of this thesis also demonstrated that the reinforcement potential of thermally degraded glass fibres is low. Thus, thermally recycled glass fibres might need to compete with mineral fillers like calcium carbonate instead of reinforcement grade glass fibres. Calcium carbonate can be purchased for less than 500 $/t [3,4]. The assumed price of 700 $/t for recycled glass fibre might therefore not be competitive. However, a reduction of the selling price to 500 $/t would mean that the break even point will not be reached. Thus, the thermal recycling of glass fibres using the fluidised bed process does not appear to be economically viable because of the low value of the recycled fibres.

The regeneration of thermally recycled glass fibres could help to increase the economic value of recycled fibres. It was demonstrated in this thesis that composites based on regenerated fibres can reach almost 90 % of the tensile strength of as received fibre composites. Thus, the regenerated fibres might be sold for up to 90 % of the price of new glass fibres. The analysis by Pickering et al. [1] is based on the assumption that the recycled fibres can be sold for 80 % of the price of new glass fibres. In order to reach the break even point as calculated by Pickering et al. the costs for the regeneration of the recycled fibres should therefore not exceed 10 % of the price of new glass fibres. Otherwise the break even point as calculated

by Pickering et al. would not be reached. It might be reasonable to assume that the glass fibres are recycled and regenerated in the same plant. Thus, the additional overhead costs would be limited. The main expense factors might be operational labour costs to operate the plant and electricity costs to heat the sodium hydroxide (NaOH) solutions. Other expense factors would be chemicals like NaOH and hydrochloric acid. The quantification of the expense factors would require data that is not available yet. For example, the optimum ratio between the volume of NaOH solution and the volume/surface area of the glass fibres has not been established and it is unknown how often the same NaOH solution can be reused to regenerate glass fibres. Both factors would substantially alter the electricity costs and the costs for the NaOH. In addition, fixed capital would be needed for equipment like reaction vessels and ovens. The process of glass fibre regeneration is less researched than the fluidised bed process. In contrast to the fluidised bed process, there is currently no fibre regeneration process in place that could simply be scaled up. Thus, the type of the required equipment cannot be quantified at this stage.

Energy balance of the fluidised bed process and fibre regeneration

Pickering et al. [1] have modelled the economics of a fluidised bed pilot plant to thermally recycle GFRP waste but they have not commented on ecological aspects like the energy balance. Thermal recycling processes like the fluidised bed process also require an energy input but the oxidation of the organic residues of the thermoset resin in a secondary chamber in the presence of methane is exothermic. An important question is whether thermal recycling processes like the fluidised bed process would help to save energy. Table A.1 presents how much energy would be needed to produce 1 kg of recycled glass fibre using the fluidised bed plant that was modelled by Pickering et al. [1].

Table A.1. Energy required to produce 1 kg of recycled glass fibre after [1]

Process or fuel	Energy per 1 kg recycled glass fibre
Electrical energy to process GFRP waste	+19.4 MJ
Energy recovered from oxidation of organic composite components	- 41.6 MJ
Methane needed for oxidation of organic composite components	+ 26.7 MJ
Σ	4.6 MJ

The energy required to produce 1 kg of new reinforcement grade glass fibres varies between 12.6 MJ and 32 MJ depending on the plant size and furnace design [5]. Thus, the use of recycled glass fibres instead of new glass fibre would allow to save at least $12.6\ \mathrm{MJ/kg} - 4.6\ \mathrm{MJ/kg} = 8\ \mathrm{MJ/kg}$.

It was shown that up to 50 % of the global demand for reinforcement grade glass fibres could be covered by recycled fibres [6]. The demand for reinforcement grade glass fibres has reached almost 5 million tonnes in 2015 [7]. $2.5 \times 10^9\ \mathrm{kg} \times 8\ \mathrm{MJ/kg} = 2 \times 10^{10}\ \mathrm{MJ}$ could be saved when half of the global demand for glass fibres would be met by thermally recycled fibres. The average energy consumption per household in UK excluding transport was 16,405 kWh (59,058 MJ) in 2014 [8]. It can be concluded that the energy saving due to the thermal recycling of glass fibres would be equivalent to the energy consumption of $2 \times 10^{10}\ \mathrm{MJ} / 59{,}058\ \mathrm{MJ/household} = 344{,}000\ \mathrm{households}$.

Considering that most glass fibre manufacturing plants consume more than 12.6 MJ to produce one kilogramme of glass fibre [5] the actual energy saving would be higher and the energy savings calculated above are minimum values. The thermal recycling of GFRP waste might therefore be environmentally friendlier than the landfilling of GFRP waste and the production of new glass fibres. However, this statement would only apply if thermally recycled fibres could be used to replace new fibres. The energy balance above does not consider the energy that is needed to regenerate the recycled glass fibres. Further experimental work is required to answer the following two questions. What is the optimum ratio between volume of

NaOH solution and volume/surface area of the glass fibres? How often can the same NaOH solution be reused to effectively regenerate glass fibres? The energy required to produce 1 kg of NaOH is approximately 22 MJ [9] which is in the same range as glass fibres. Thus, the energy balance would be affected by the two questions that were raised above and future research will need to address them.

Items of the energy balance

Electrical energy required to process GFRP waste in fluidised bed

Pickering et al. [1] estimated that approximately 13125 GWh of electrical energy are required to process 9000 t of GFRP waste in a fluidised bed plant. In addition, their model is based on composites with a fibre content of 40 wt% and fibre yield rate of 67.5 %. Thus, 2430 t recycled glass fibre could be extracted from 9000 t GFRP waste. The energy consumption required to produce 1 t of thermally recycled fibre would be $13125\ \mathrm{GWh}\ /\ 2430\ \mathrm{t} = 19400\ \mathrm{MJ/t}$ which is equivalent 19.4 MJ per 1 kg recycled glass fibre.

Energy recovered from oxidation of organic composite components

Thermoset resins release energy during combustion [10]. A boiler could be used to recover part of the energy that is released in the fluidised bed process when organic components of the composites are oxidised. Pickering et al. [1] estimated that such a boiler could provide 4680 kW when the fluidised bed plant processes 9000 t GFRP waste per year (250 working days/year). The energy recovered from the boiler within one year would be $4680\ \mathrm{kW\ x\ 250\ x\ 24\ h} = 28{,}080\ \mathrm{GWh}$. 2430 t could be extracted from 9000 t GFRP waste. Thus $28080\ \mathrm{GWh}\ /\ 2430\ \mathrm{t} = 41600\ \mathrm{MJ/t}$ could be recovered for each tonne of glass fibre which is equivalent to 41.6 MJ/kg glass fibre.

Methane needed for oxidation of organic composite residues

The oxidation of the organic composite components is an exothermic reaction but it requires methane. Pickering et al. [1] assumed that 144 kg methane are needed for the processing of 1 t GFRP waste. 1 t x 0.4 x 0.675 = 270 kg of recycled glass fibre can be obtained from 1 t of GFRP waste with 40 wt% fibre content. The production of 1 kg recycled glass fibres involves therefore $144\ \mathrm{kg}\ /\ 270\ \mathrm{kg} = 0.533\ \mathrm{kg}$ methane. The caloric value of methane is approximately 50 MJ/kg [11]. Thus,

$0.533\ \text{kg x}\ 50\ \text{MJ/kg} = 26.7\ \text{MJ}$ are consumed for each kilogramme of recycled glass fibre.

References

[1] Pickering SJ, Kelly RM, Kennerley JR, Rudd CD, Fenwick NJ. A fluidised-bed process for the recovery of glass fibres from scrap thermoset composites bundles. Compos Sci Technol 2000;60:509–23.

[2] Roux C, Denault J, Champagne MF. Parameters regulating interfacial and mechanical properties of short glass fiber reinforced polypropylene. J Appl Polym Sci 2000;78:2047–60.

[3] Job S. Recycling glass fibre reinforced composites – history and progress. ReinforcedPlastics 2013;57:19–23.

[4] Stratton P. An overview of the north american calcium carbonate market. Québec City: 2012.

[5] Stiller H. Material intensity of advanced composite materials. Wuppertal Pap 1999.

[6] Thomason JL, Nagel U, Sáez Rodríguez E, Yang L. Regenerating the strength of thermally recycled glass fibres using hot sodium hydroxide. Compos Part A Appl Sci Manuf 2016;87:220–7.

[7] Owens Corning Investor Presentation 2015. http://s1.q4cdn.com/942908807/files/doc_presentations/2015/Q3/Q3-Presentation-v9.pdf (accessed April 3, 2016).

[8] Waters L, Wilkes E;, Goodright V. Chapter 3: Domestic energy consumption in the UK between 1970 and 2014. Energy Consum. UK, Department of Energy & Climate Change; 2015.

[9] Boustead I. Sodium hydroxide 2005. http://www.inference.phy.cam.ac.uk/sustainable/LCA/elcd/external_docs/naoh_31116f0a-fabd-11da-974d-0800200c9a66.pdf (accessed August 11, 2016).

[10] Pickering S, Benson M. The recycling of thermosetting plastics. Second Int. Conf. Plast. Recycl., London: Plastics and rubber institute; 1991, p. 1–10.

[11] Sikdar DC. Caloric value of fuels. Chem. Process Calc., 2013, p. 237.